Functionalized Dipyrrins as Ligands for Photoactive Coordination Complexes

Inaugural-Dissertation

to obtain the academic degree

Doctor rerum naturalium (Dr. rer. nat.)

submitted to the Department of Biology, Chemistry, Pharmacy

of Freie Universität Berlin

by

Benjamin Florian Hohlfeld

Berlin, 2021

The submitted doctoral thesis has been performed in the time period of November 2016 to April 2021 at the Institute of Chemistry and Biochemistry, Freie Universität Berlin, under the supervision of Prof. Dr. Nora Kulak (Freie Universität Berlin; present affiliation: Otto-von-Guericke-Universität Magdeburg) in collaboration with Dr. Arno Wiehe (biolitec research GmbH).

My doctoral thesis entitled “Functionalized Dipyrrins as Ligands for Photoactive Coordination Complexes” has been composed by myself and is based on my own work; the work of others has been specifically acknowledged in the text. Furthermore, I assure that this doctoral thesis had not been submitted for any other degree.

1. Reviewer:	Prof. Dr. Nora Kulak, Otto-von-Guericke-Universität Magdeburg
2. Reviewer:	Prof. Dr. Mathias Christmann, Freie Universität Berlin
Disputation:	September 13, 2021

The work of this dissertation has resulted so far in a number of publications, presentations and a patent:

Publications:

1. Benjamin F. Hohlfeld, Keith J. Flanagan, Nora Kulak, Mathias O. Senge, Mathias Christmann, and Arno Wiehe, ***"Synthesis of Porphyrinoids, BODIPYs and (Dipyrrinato)ruthenium(II) Complexes from Pre-functionalized Dipyrromethanes"***, *Eur. J. Org. Chem.* **2019**, 4020-4033. DOI: 10.1002/ejoc.201900530
2. Benjamin F. Hohlfeld, Burkhard Gitter, Keith J. Flanagan, Christopher J. Kingsbury, Nora Kulak, Mathias O. Senge and Arno Wiehe, ***"Exploring the relationship between structure and activity in BODIPYs designed for antimicrobial phototherapy",*** *Org. Biomol. Chem.* **2020**, *18*, 2416-2431. DOI: 10.1039/d0ob00188k
3. Benjamin F. Hohlfeld, Burkhard Gitter, Christopher J. Kingsbury, Keith J. Flanagan, Dorika Steen, Gerhard D. Wieland, Nora Kulak, Mathias O. Senge and Arno Wiehe, ***"Dipyrrinato-Iridium(III) Complexes for an Application in Photodynamic Therapy and Antimicrobial Photodynamic Inactivation"***, *Chem. J. Eur.* **2021**, in press. DOI: 10.1002/ chem.202004776
4. **Co-authorship:** Claudia S. Gutsche, Benjamin F. Hohlfeld, Keith J. Flanagan, Mathias O. Senge, Nora Kulak, and Arno Wiehe, ***"Sequential Nucleophilic Substitution of the α-Pyrrole and p-Aryl Positions of meso-Pentafluorophenyl-Substituted BODIPYs"***, *Eur. J. Org. Chem*. **2017**, 3187-3196. DOI: 10.1002/ejoc.201700264

Presentations:

1. Claudia S. Gutsche, Benjamin F. Hohlfeld, Susanna Gräfe, Burkhard Gitter, Keith J. Flanagan, Mathias O. Senge, Nora Kulak and Arno Wiehe, ***Pre- and Post-Functionalization in Dipyrrin Metal Complexes – Synthesis and Biological Evaluation***, Presentation given at the '10th International Conference on Porphyrins and Phthalocyanines, 1.-6.7.2018, Munich, Germany.
2. Claudia S. Gutsche, Benjamin F. Hohlfeld, Susanne Gräfe, Burkhard Gitter, Keith J. Flanagan, Mathias O. Senge, Nora Kulak and Arno Wiehe, ***Development of new photosensitizers for the photodynamic inactivation of bacteria***, Presentation given at the 'Photodynamic Therapy and Photodiagnosis Update 'Conference, 19.-22.09.2018, Kochel am See, Germany.

3. Benjamin F. Hohlfeld, Burkhard Gitter, Keith J. Flanagan, Christopher J. Kingsbury, Nora Kulak, Mathias O. Senge and Arno Wiehe, ***Structure and Activity of BODIPYs Designed for Antibacterial and Antitumor Phototherapy***, Poster presentation at the 'Photodynamic Therapy and Photodiagnosis Update' Conference, 5.-6.11.2020. (Online conference)

Patent:

Claudia S. Gutsche, Arno Wiehe, Benjamin F. Hohlfeld, Burkhard Gitter, Volker Albrecht, *"**Application of metal complexes in anti-tumor and anti-bacterial therapy**"*, US application No. 62625411.

Acknowledgments

First and foremost, I sincerely thank Dr. Arno Wiehe for his support, as well as for his constant advice, availability and for sharing his experience.

I particularly like to thank Prof. Dr. Nora Kulak for the possibility to join her working group, which finally made this work possible and for her constant advice and availability during the thesis.

I would particularly like to thank Prof. Dr. Mathias Christmann for evaluating my thesis and for his cooperation during the compilation of my first manuscript.

My grateful thanks go to Prof. Dr. Mathias Senge, Dr. Keith Flanagan, and Dr. Christopher Kingsbury, all of Trinity College University, Dublin, for performing and evaluating the x-ray structure analyses and the great cooperation in the production of the manuscripts.

I thank Burkhard Gitter, Dorika Steen, Sandra Heinig and all other employees of the biolitec research GmbH for the performing of the tumor cell and bacterial testing.

I also thank Prof. Dr. Volker Albrecht of biolitec research GmbH for provision of the required work materials and chemicals.

I would like to thank Corinna Schattschneider, from the working group of Prof. Nora Kulak, for providing the cyclen for my research.

Dr. Katharina Achazi and Elisa Quaas from Freie Universität Berlin I would like to thank for performing cellular uptake studies.

I thank all members of the NMR core facility and mass spectrometry for the rapid and conscientious measuring of numerous spectra.

I gratefully acknowledge Marcel Zastrow, Robert Walter, John Selent, Victoria Chua, and Annelie Puhlmann for their experimental support.

Finally, I gratefully thank my family and friends for their support and patience during my research.

Abbreviations

ATR	attenuated total reflectance
COSY	correlation spectroscopy
cyclen	1,4,7,10-tetraazacyclododecane
DCM	dichloromethane
DDQ	2,3-dichloro-5,6-dicyano-*p*-benzoquinone
DIPEA	*N*,*N*-diisopropylethylamine
DMF	*N*,*N*-dimethylformamide
DMSO	dimethyl sulfoxide
ε	molar extinction coefficient
EI	electron ionization
ESI	electrospray ionization
EtOAc	ethyl acetate
HFIP	1,1,1,3,3,3-hexafluoro-2-propanol, hexafluoroisopropanol
HMBC	heteronuclear multiple-bond correlation
HMQC	heteronuclear multiple-quantum correlation
HRMS	high-resolution mass spectrometry
Hz	hertz
IR	infrared
MOF	metal-organic framework
NBS	*N*-bromosuccinimide
NMR	nuclear magnetic resonance
OLED	organic light-emitting diode
PDT	photodynamic therapy
PBS	phosphate-buffered saline
R_f	retardation factor
ROS	reactive oxygen species
rt	room temperature
S_NAr	nucleophilic aromatic substitution
THF	tetrahydrofuran
TOF	time-of-flight
$\tilde{\nu}$	wavenumber
UV/vis	ultraviolet-visible

Table of Contents

Kurzzusammenfassung

Die vorliegende Dissertation umfasst ein Konzept für die Darstellung von Metall- und Borkomplexen auf Basis der Dipyrromethenstruktur. *meso*-Substituierte Dipyrromethane und Dipyrromethene (Dipyrrine) dienten hierbei zur Herstellung der verschiedenen Komplexverbindungen. Die Pentafluorphenyl- und die 4-Fluor-3-nitrophenylgruppe ermöglichten eine selektive Funktionalisierung der jeweiligen *para*-Position mit diversen Nucleophilen (Amine, Alkohole oder Thiozucker) mittels der nucleophilen aromatischen Substitution. Durch Oxidation wurden die substituierten Dipyrromethane in ihre dazugehörigen Dipyrrine überführt und ermöglichten die zielgerichtete Synthese von entsprechenden heteroleptischen und homoleptischen Dipyrrinato-komplexen. Gleichzeitig erlaubten die funktionalisierten Dipyrromethane auch eine Herstellung von entsprechenden Bor-Dipyrromethenkomplexen (BODIPY). Die in den verschiedenen Kapiteln dargestellten Dipyrrinatoverbindungen sind von Interesse für die Entwicklung neuer Photosensibilisatoren für die photodynamische Therapie (PDT). Weiterhin wurden die synthetisierten Komplexe von Mitarbeitern der biolitec research GmbH in Jena auf ihre Dunkel- und Phototoxizität gegen Zellen und Bakterien hin untersucht.

1. meso-Substituierte Dipyrromethane als Bausteine für die Darstellung von BODIPYs und (Dipyrrinato)ruthenium(II)-Komplexen

Dipyrromethane sind bedeutende Ausgangsverbindungen für die Synthese von Porphyrinen, Corrolen und weiteren makrozyklischen Verbindungen. Gleichzeitig bilden die Dipyrromethane auch die Ausgangsverbindungen für BODIPYs und Dipyrrinatokomplexe. In diesem Projekt wurde untersucht, inwiefern *meso*-(4-amino-3-nitrophenyl)-substituierte Dipyrromethane sich für die Herstellung von BODIPYs und (Dipyrrinato)ruthenium(II)-Komplexen eignen.

Mittels der nucleophilen aromatischen Substitution wurde das 5-(4-Fluor-3-nitrophenyl)-dipyrromethan mit einem breiten Spektrum an verschiedensten Aminen effizient funktionalisiert. Auch konnte das Spektrum der möglichen Nucleophile auf einen Azido-Substituenten erweitert werden. Ausgehend von diesen funktionalisierten Dipyrromethanen wurden die entsprechenden BODIPYs durch Oxidation der Dipyrromethane zu den Dipyrromethenen und anschließende Komplexierung mit Bortrifluorid erfolgreich dargestellt. Des Weiteren konnten die Dipyrromethane auch zur gezielten Herstellung von funktionalisierten Dipyrrinen herangezogen werden. Die Umsetzung zu den (Dipyrrinato)(*p*-cymol)ruthenium(II)-Komplexen erfolgte schließlich durch die Komplexierung der Dipyrrine mit einen Chlorido(*p*-cymol)ruthenium(II)-Halbsandwich-Komplex. Ausgehend von den (*p*-Cymol)(dipyrrinato)ruthenium(II)-Komplexen lieferte der Austausch der

Liganden gegen 2,2´-Bipyridin schließlich die entsprechenden Bis(2,2‘-bipyridyl)(dipyrrinato)-ruthenium(II)-Komplexe.

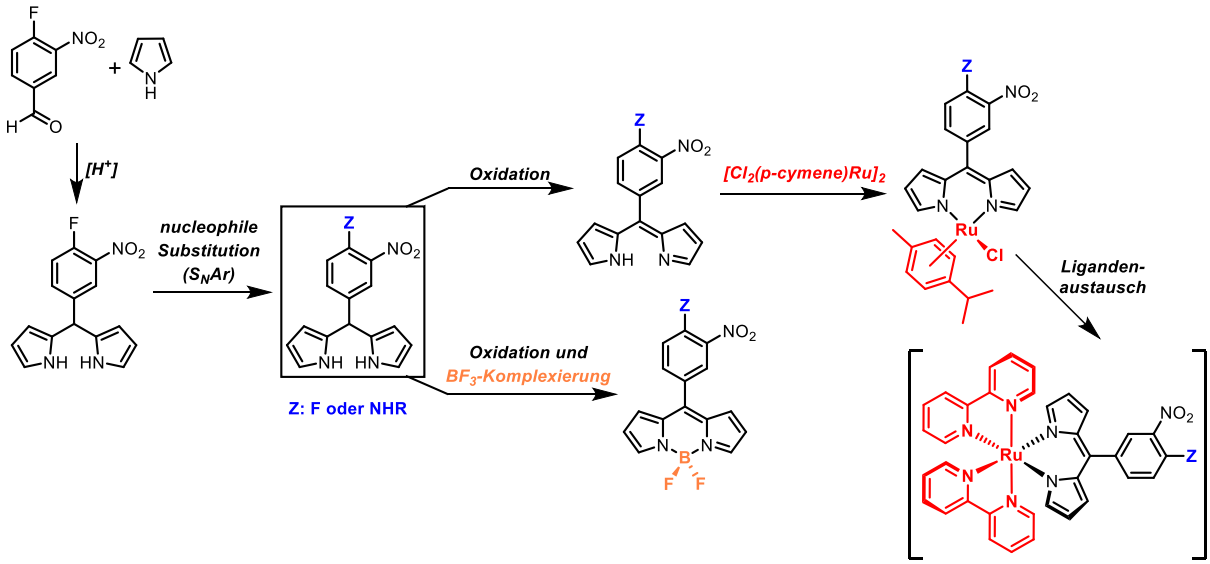

2. Modifikation der BODIPY-Struktur durch die selektive Substitution mit NBS, in Kombination mit der Einführung zusätzlicher funktioneller Gruppen über die aromatische nucleophile Substitution

Im Rahmen dieses Projektes wurde das Konzept der BODIPY-Kernsubstitution mit der Einführung funktioneller Gruppen über die nucleophile Substitution, an der 4-Fluor-3-nitrophenyl- und der Pentafluorphenylgruppe, kombiniert. Durch diese Modifizierungen sollten die Eigenschaften der BODIPYs verändert werden, um eine Anwendung als Photosensibilisatoren zu ermöglichen. Hierzu wurden zunächst funktionalisierte BODIPYs mit *N*-Bromsuccinimid (NBS) umgesetzt. Die selektive Substitution der 2- und 6-Positionen der BODIPY gelang allerdings nur bedingt, da neben der gewünschten Disubstitution auch eine Polysubstitution mit Brom beobachtet wurde. Dennoch gelang es *mono*-bromierte Verbindungen mit ausgewählten funktionalisierten BODIPYs zu erhalten. Die Verwendung von funktionalisierten 1,3,5,7-Tetramethyl-BODIPYs ermöglichte schließlich eine effektive Kombination der beiden Konzepte (selektive Bromierung der BODIPY-Kernstruktur und die nucleophile Substitution).

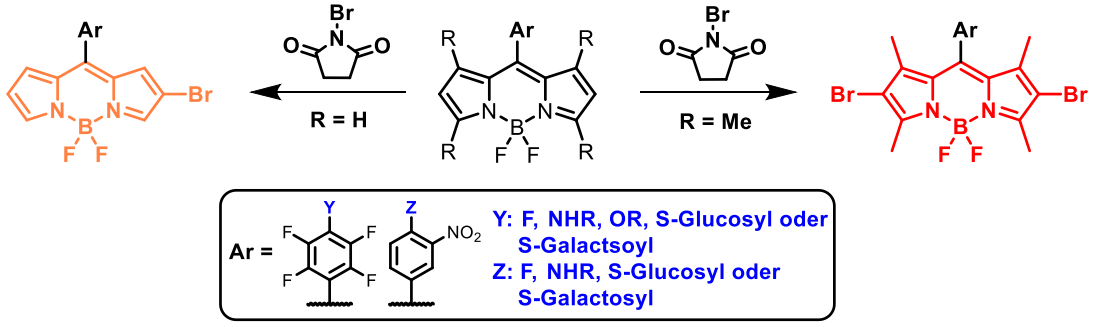

Weiterhin wurde das Spektrum an möglichen Nucleophilen auf Thiozucker erweitert. Eine Substitution der BODIPYs mit Thio-Glucose und Thio-Galactose sollte zur Verbesserung der Bioverfügbarkeit beitragen. Schließlich gelang es, modifizierte BODIPYs zu erhalten, bei denen schon in geringer Konzentration eine deutliche phototoxische Aktivität gegenüber Bakterien beobachtet wurde. Auch unter realistischeren Bedingungen (Zugabe von Serum) zeigten ausgewählte Verbindungen noch eine deutliche Phototoxizität.

3. meso-Substituierte Dipyrrine als Bausteine für die Darstellung von photoaktiven (Dipyrrinato)iridium(III)-Komplexen

In diesem Projekt wurden heteroleptische (Dipyrrinato)iridium(III)-Komplexe synthetisiert. Die Synthese der (Dipyrrinato)iridium(III)-Komplexe erfolgte unter Verwendung von *meso*-substituierten Dipyrrinen. Diese wiederum wurden aus den entsprechenden substituierten Dipyrromethanen durch Oxidation erhalten. Ausgangspunkt waren erneut das Pentafluorphenyl- und das 4-Fluor-3-nitrophenyl-substituierte Dipyrromethan, die mittels nucleophiler Substitution an der *para*-Position des Phenyl-Restes modifiziert wurden. Ausgehend von diesen funktionalisierten Dipyrrinen wurden zunächst (Dipyrrinato)iridium(III)-Komplexe mit einem Pentamethylcyclopentadienylliganden hergestellt. Ein Ligandenaustausch mit 2-Phenylpyridin an ausgewählten (Dipyrrinato)(pentamethyl-cyclopentadienyl)iridium(III)-Komplexen gelang jedoch nicht. Die Darstellung der (Dipyrrinato)-bis(2-phenylpyridyl)iridium(III)-Komplexe war nur durch Umsetzung entsprechender Dipyrrine mit einem cyclometallierten (2-Phenylpyridyl)iridium(III)-Komplex möglich.

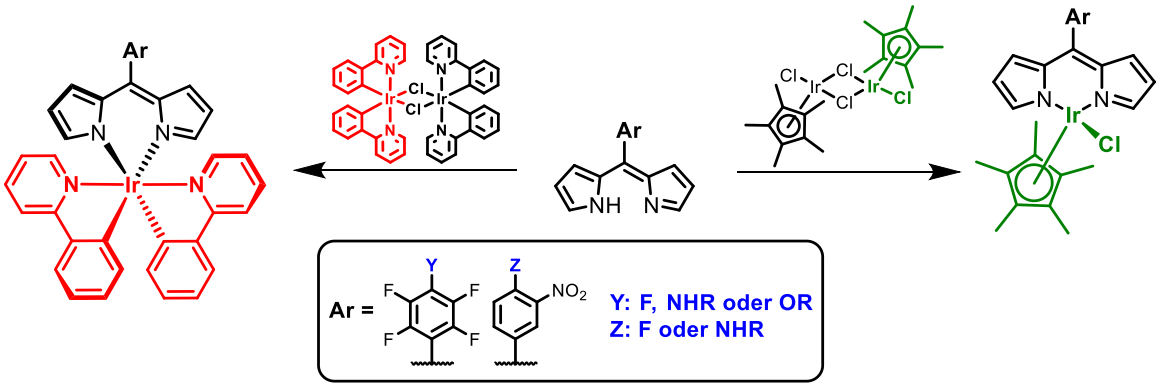

Weiterhin wurden auch (Dipyrrinato)bis(2-phenylpyridyl)iridium(III)-Komplexe mit *para*-Fluoratomen mit Thiozuckern funktionalisiert. Auch hier sollte die Glykosylierung mit Thio-Glucose bzw. Thio-Galactose, die Bioverfügbarkeit der Komplexe verbessern.

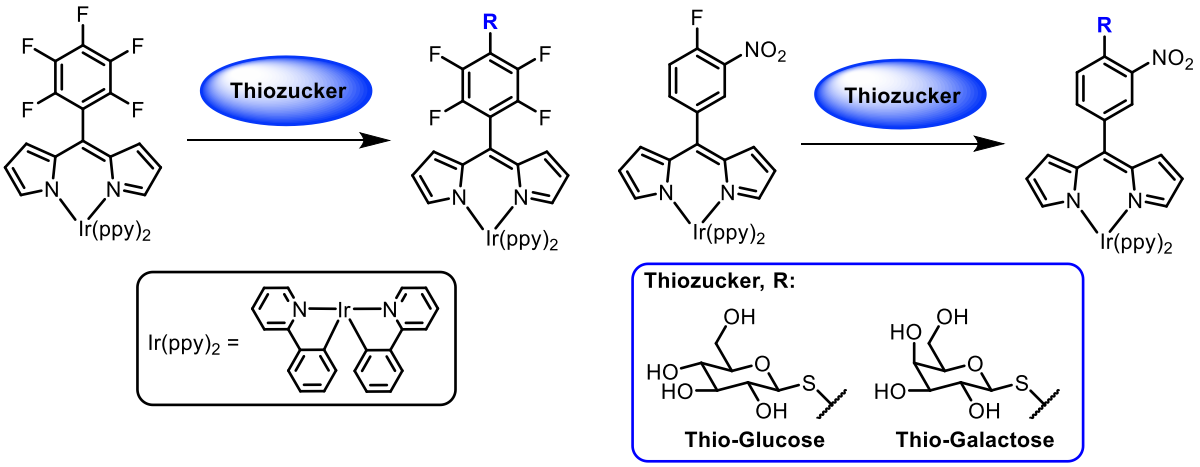

In den Zell- und Bakterientests konnte in vielen Fällen eine starke phototoxische Aktivität der (Dipyrrinato)iridium(III)-Komplexe festgestellt werden. In Gegenwart von Licht war bereits eine geringe Konzentration ausreichend, um eine deutliche Reduktion der Zellviabilität bzw. eine deutliche Reduktion der Anzahl der Bakterienkolonien zu erreichen. Insbesondere traf dies auf (Dipyrrinato)-bis(2-phenylpyridyl)iridium(III)-Komplexe mit endständigen Hydroxygruppen sowie auf die glykosylierten Derivate zu. Weiterhin zeigten auch die (Dipyrrinato)(pentamethylcyclopentadienyl)-iridium(III)-Komplexe eine deutliche Wirkung gegen Bakterien, sowohl unter Belichtung als auch bei Abwesenheit von Licht.

4. Darstellung homoleptischer Dipyrrinatokomplexe

In diesem Teilprojekt wurde die Darstellung von homoleptischen Bis(dipyrrinato)- und Tris(dipyrrinato)-Komplexen mittels *meso*-(3-Nitrophenyl)-substituierter Dipyrrine untersucht. Im Gegensatz zur Darstellung der heteroleptischen (Dipyrrinato)ruthenium(II)- und -iridium(III)-Komplexe erforderte die Herstellung der homoleptischen Bis(dipyrrinato)- und Tris(dipyrrinato)-Komplexe nur die direkte Umsetzung der entsprechenden Metallsalze mit dem jeweiligen Dipyrrin. Die Synthese der Bis(dipyrrinato)- und Tris(dipyrrinato)-Komplexe war allerdings nur mit einer begrenzten Anzahl der Dipyrrine erfolgreich. Auch war eine Dunkel- oder Phototoxizität der hergestellten Dipyrrinato-komplexe gegenüber Zellen und Bakterien nicht festzustellen.

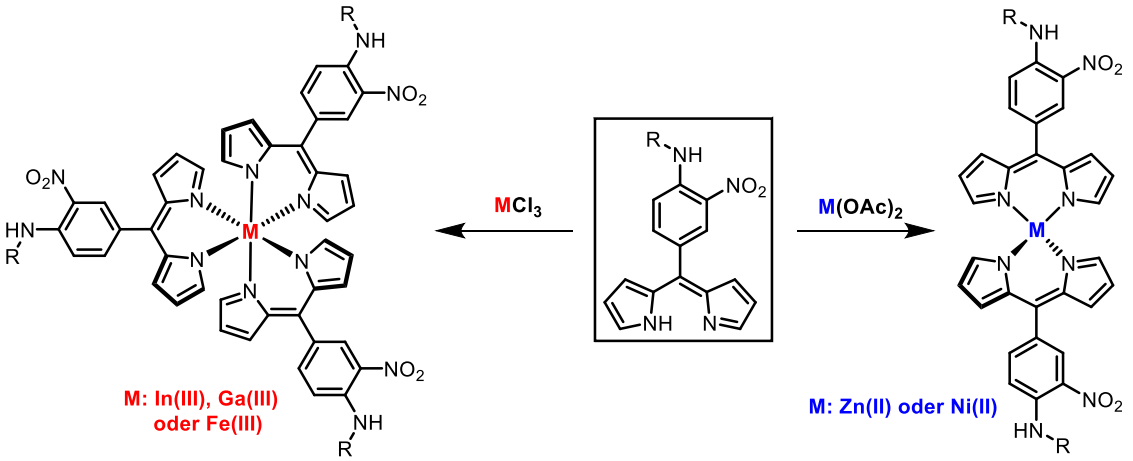

5. Darstellung eines BODIPY-Cyclen Derivates

BODIPYs werden als Fluoreszenzfarbstoffe in bildgebenden Verfahren oder für die Markierung von (Bio-)Molekülen eingesetzt. Auch sind die Metallkomplexe des 1,4,7,10-Tetraazacylcododecanes (Cyclens) in der Lage Proteine oder DNA zu spalten, was diese Metallkomplexe für eine potenzielle therapeutische Anwendung Interessant macht.

In diesem Projekt wurde ein Konjugat aus einem BODIPY und einem Cyclen hergestellt. Die Verknüpfung der beiden Moleküle sollte über die Kupfer(I)-katalysierte 1,3-dipolare Cycloaddition mit einem Azido-BODIPY und einem Propargyl-substituierten Cyclen erfolgen.

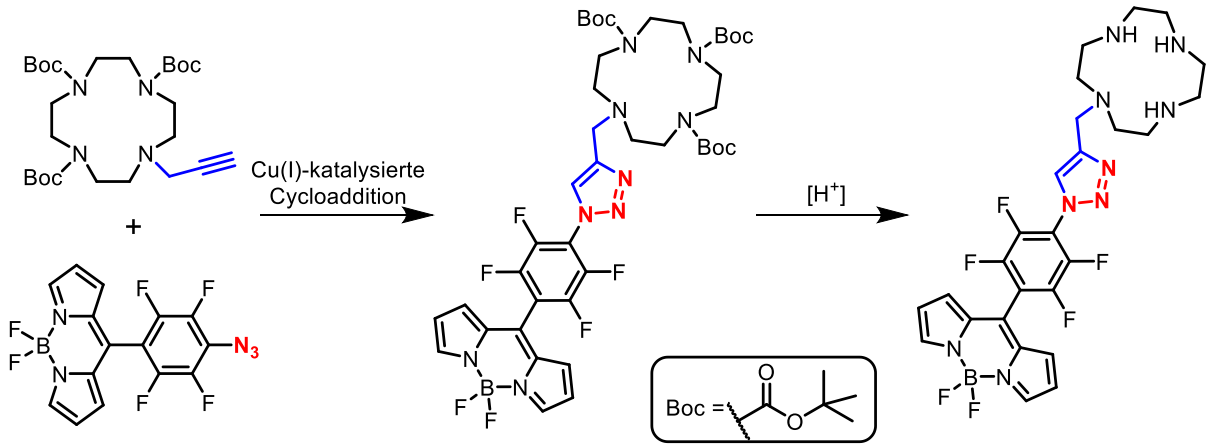

Abstract

In this thesis a concept for the synthesis of metal and boron complexes, based on the dipyrromethene structure, is presented. Specifically, *meso*-substituted dipyrromethanes and dipyrromethenes (dipyrrins) have been used for the synthesis of these complexes. The pentafluorophenyl and the 4-fluoro-3-nitrophenyl moiety enabled the selective functionalization of the related *para*-fluorine position with various nucleophiles (amines, alcohols, or thiocarbohydrates) *via* nucleophilic aromatic substitution (S_NAr). Dipyrromethanes were oxidized into the dipyrrins and enabled a targeted synthesis of the corresponding heteroleptic and homoleptic dipyrrinato complexes. Starting from the *meso*-substituted dipyrromethanes, a targeted synthesis of the respective boron-dipyrromethenes (BODIPYs) was also successful. The dipyrrinato compounds presented in these projects are relevant for the development of photosensitizers for photodynamic therapy (PDT). To investigate the (photo)toxic potential of the dipyrrinato complexes, the compounds were evaluated for their dark and phototoxicity in tumor cell and bacterial assays by employees of the biolitec research GmbH.

Dipyrromethanes are important starting materials for the preparation of porphyrins, corroles, or other macrocyclic compounds. As well, dipyrromethanes are applied in the synthesis of BODIPYs and dipyrrinato metal complexes. In one project, *meso*-(4-amino-3-nitrophenyl)-substituted dipyrromethanes were investigated as suitable building blocks for the development of BODIPYs and dipyrrinato ruthenium(II) complexes. An efficient substitution of the *para*-fluorine of the 4-fluoro-3-nitrophenyl moiety was achieved with various amines *via* S_NAr. The scope of suitable nucleophiles has also been extended to an azido group.

Starting from these functionalized dipyrromethanes the corresponding BODIPYs were prepared. Furthermore, the pre-functionalized dipyrromethanes were oxidized to their respective dipyrrins and the subsequent synthesis of (*p*-cymene)(dipyrrinato)ruthenium(II) complexes was carried out *via* reaction with a chlorido(*p*-cymene)ruthenium(II) half-sandwich precursor. Finally, the exchange of the *p*-cymene ligand with 2,2'-bipyridine led to the bis(2,2'-bipyridyl)(dipyrrinato)ruthenium(II) complexes.

In another BODIPY-related project, the concept of the BODIPY core substitution with bromine was combined with the introduction of functional groups *via* the nucleophilic substitution in the *para*-position of the 4-fluoro-3-nitrophenyl and pentafluorophenyl moiety at the respective *meso*-position of the BODIPYs, to adapt the properties of the BODIPY towards an application as photosensitizers. For this, pre-functionalized BODIPYs were reacted with *N*-bromosuccinimide (NBS). However, on modifying the BODIPY core structure with NBS, multiple brominations were observed and only the corresponding mono-brominated BODIPYs could be isolated in pure form in some cases. The application of 1,3,5,7-tetramethyl-substituted BODIPYs on the other hand enabled an effective

combination of these concepts (selective bromination of the BODIPY core structure and the nucleophilic aromatic substitution). The scope of suitable nucleophiles was also extended to thiocarbohydrates. This functionalization with thioglucose and thiogalactose intended to contribute to an improvement of bioavailability. A phototoxicity against bacteria was observed already at low concentrations for certain BODIPYs. Notably, a high phototoxic activity was still found under more realistic testing conditions, i.e., on repeating the bacterial assays with the addition of 10% of serum.

In a third project, the preparation of the dipyrrinato iridium(III) complexes was carried out with *meso*-substituted dipyrrins, again starting from dipyrromethanes carrying the pentafluorophenyl and the 4-fluoro-3-nitrophenyl moiety, respectively. A wide scope of functionalized dipyrrins was synthesized *via* the nucleophilic substitution on these two dipyrromethanes followed by oxidation to the corresponding dipyrrins. Starting from these pre-functionalized dipyrrins, heteroleptic dipyrrinato iridium(III) complexes with an additional pentamethylcyclopentadienyl ligand were synthesized. However, the synthesis of (dipyrrinato)bis(2-phenylpyridyl)iridium(III) complexes could only be achieved *via* the reaction of the functionalized dipyrrins with a cyclometalated chlorido-(2-phenylpyridyl)iridium(III) precursor. In the course of these investigations (dipyrrinato)-bis(2-phenylpyridyl)iridium(III) complexes with free *para*-fluorine position were also prepared and reacted with thiocarbohydrates. Again, the glycosylation was performed to improve the bioavailability. In the tumor cell and bacterial assays, the (dipyrrinato)bis(2-phenylpyridyl)iridium(III) complexes with terminal hydroxy groups and the glycosylated derivatives exhibited a high phototoxicity even at low concentrations. Also, certain (dipyrrinato)(cyclopentadienyl)iridium(III) complexes showed a pronounced activity against bacteria under irradiation as well as without light.

In a side project, the preparation of homoleptic bis(dipyrrinato) and tris(dipyrrinato) complexes with *meso*-(3-nitrophenyl)-based dipyrrins was investigated. The syntheses of the corresponding complexes were carried by a direct complexation of the dipyrrins with the metal salts. However, only a limited number of the homoleptic dipyrrinato complexes could be synthesized with the tested dipyrrins. The tumor cell and bacterial assays indicated no significant dark or phototoxicity for the bis(dipyrrinato) and tris(dipyrrinato) complexes.

BODIPYs are used as fluorescence dyes in imaging and as markers. Metal complexes of the 1,4,7,10-tetraazacyclododecane (cyclen) can cleave protein structures or DNA, making this type of metal complexes interesting for therapeutic applications. In a last project, a conjugate between a cyclen and a BODIPY was prepared. The coupling of these molecules was realized *via* a copper(I)-mediated 1,3-dipolar cycloaddition with an azido-BODIPY and a propargyl-substituted cyclen. Moreover, a subsequent complexation of the BODIPY-cyclen conjugate with copper(II) was investigated.

1. Introduction

1.1 Importance of metal complexes for biology, medicine, and industry

Currently, various enzymes and proteins are known where small non-protein structures (cofactors) are required for an activity as catalyst. Within metalloenzymes different metal ions or metal ion clusters operate as cofactors in the catalytic active centers and, as well, metal ions are important cofactors for biologically active metalloproteins.[1] Beyond metal ions, organic compounds and coordination complexes can also serve as cofactors for enzymes and proteins. In this context, metal complexes based on the tetrapyrrole scaffold represent the most widespread complex-dependent cofactors in cells and bacteria. Enzymes containing tetrapyrrole-based cofactors are involved in essential biological processes, e.g., biosynthesis, transport of oxygen, and further fields of the cell metabolism.[2] Hemes (complexes of iron with porphyrin derivatives, Fig. 1) are an integral part of the cellular respiration, the transport of oxygen, the protein biosynthesis, and other important biological functions.[2a,b] Hemes are often part of large protein structures, e.g., hemoglobin or cytochrome P450 enzymes.[2a,2c,3] Another example for tetrapyrrole-based cofactors in cells are represented by the cobalamins (coordination complexes of cobalt with corrin derivatives, Fig. 1). As biologically active cobalamins the methyl- and 5'-deoxyadenosyl-cobalamine are known. These two cobalamins (coenzymes B_{12}) are important cofactors for enzymes within the amino acid metabolism. The cyanocobalamin is produced exclusively industrially, however, these types of cobalamins differ only in one of the axial ligands (Fig. 1; red highlighted structures).[2a,4]

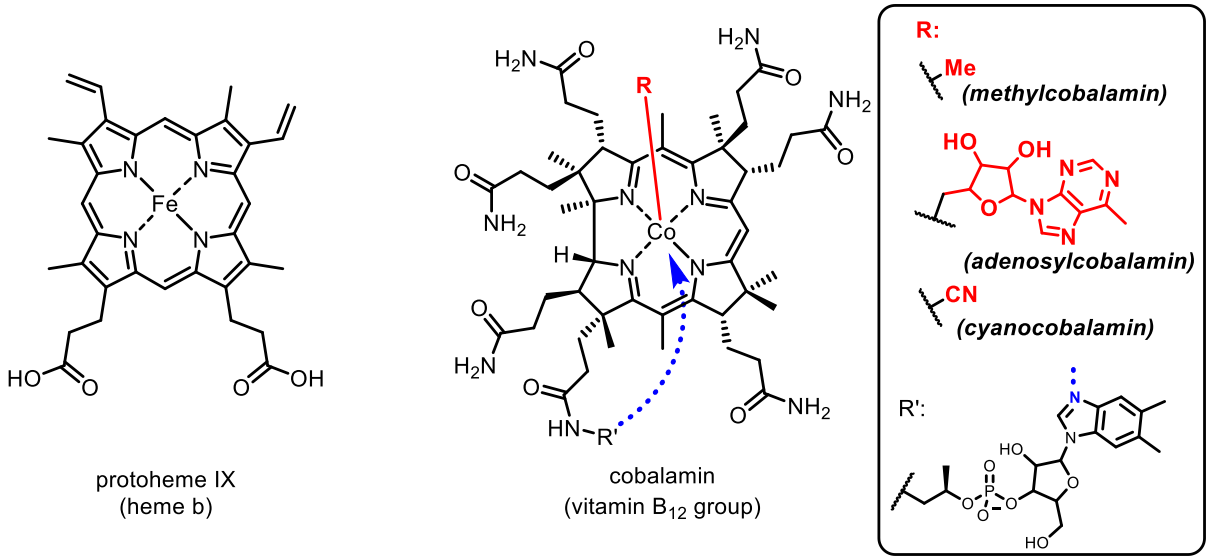

Figure 1: Structures of protoheme IX (heme b) and cyanocobalamins (vitamin B_{12} group).

Metal tetrapyrrolic complexes are also fundamental parts in metabolic processes of plants. In photosynthesis, chlorophylls (complexes of magnesium with chlorin derivatives, Fig. 2) act as light

acceptors in light harvesting arrays or are involved as electron donors in the photosynthetic reaction centers.[2a,2b,5] As well, metal tetrapyrrole complexes are involved in metabolic processes within bacteria. Specific bacteria species are able perform photosynthesis *via* bacteriochlorophylls. Bacteriochlorophylls lack a double bond compared to the chlorophylls found in plant cells (Fig. 2).[2a,6]

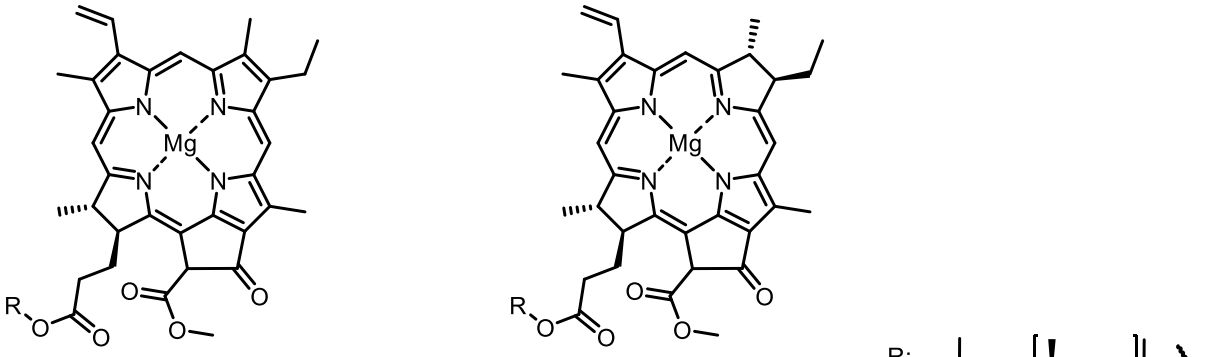

chlorophyll a **bacteriochlorophyll a**

Figure 2: Structure of chlorophyll a and bacteriochlorophyll a.

Furthermore, a complex-based cofactor is known whose structure is not related to the tetrapyrrole scaffold. The molybdenum cofactor (coordination complex of molybdenum and the molybdopterin, Fig. 3) is also widespread in bacteria and cells. Similar to hemes, the molybdenum cofactor is an essential part of certain molybdoenzymes, e.g., sulfite oxidases or xanthine oxidases. The molybdenum cofactor is mainly involved in the nitrogen and sulfur metabolism of cells and bacteria.[7] In addition, within bacteria the tungsten cofactor was discovered. The tungsten cofactor is as well based on the molybdopterin scaffold, however, in this case, the molybdenum is replaced by tungsten.[8]

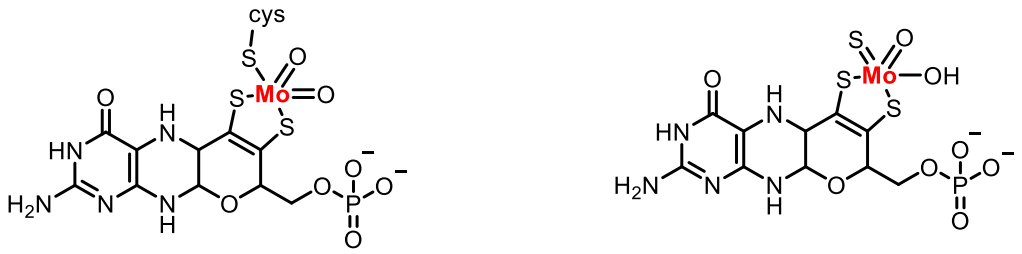

molybdenium cofactor from sulfite oxidase ***molybdenium cofactor from xanthine oxidase***

Figure 3: Examples for the structure of the molybdenum-cofactor in sulfite and xanthine oxidases.

Metal complexes are also important as therapeutic agents in medical treatments. Especially, metal complexes found attention for the treatment of malignant diseases. *Cis*-diammine-dichloridoplatinum(II) (cisplatin) is a well-known chemotherapeutic agent. Cisplatin is a neutral and square planar platinum(II)-based metal complex. The two chlorido and two ammonia ligands are arranged in a *cis*-geometry (Fig. 4). Due to its specific properties, cisplatin is able to interact with the nucleobases of the DNA, forming respective cisplatin-DNA adducts. These cisplatin-DNA adducts finally lead to an inhibition of DNA replication and DNA transcription.[9] However, cisplatin also shows serious

side effects, e.g., nephrotoxicity and neurotoxicity.[9a,10] As well, a significant resistance formation of cells against cisplatin has been observed.[11] To reduce the side effects and to increase the effectiveness against cancer cells, other platinum analogues have been investigated. Based on the cisplatin structure, additional platinum(II) complexes have been developed for the treatment against cancer, e.g., carboplatin and oxaliplatin (Fig. 4). These types of cisplatin analogues show lower side effects, while preserving their anticancer activity against the tumor cells.[9a,12]

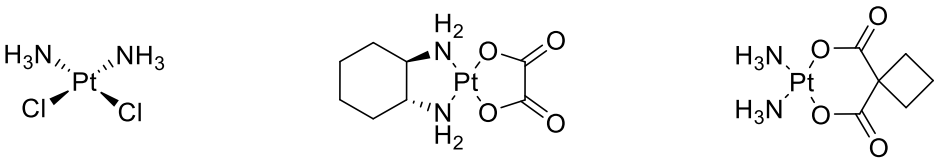

cisplatin oxaliplatin carboplatin

Figure 4: Structure of cisplatin, oxaliplatin, and carboplatin.

Beside platinum-based complexes, other metal complexes find interest as therapeutically active compounds as well. For example, ferrocene derivatives of tamoxifen (ferrrocifen) and chloroquine (ferroquine) show high potential as antiproliferative compounds (Fig. 5).[13] Coordination complexes of gold are known as therapeutic agents against rheumatoid arthritis, e.g., auranofin and aurothiomalate (Fig. 5). For auranofin, also an anticancer activity has been reported.[13a,14] Coordination complexes containing platinum, gold, and ferrocene, represent only a small number of compounds with promising antiproliferative properties. In the literature, numerous examples for metal complexes are also investigated for a possible treatment of cancer.[13a,15]

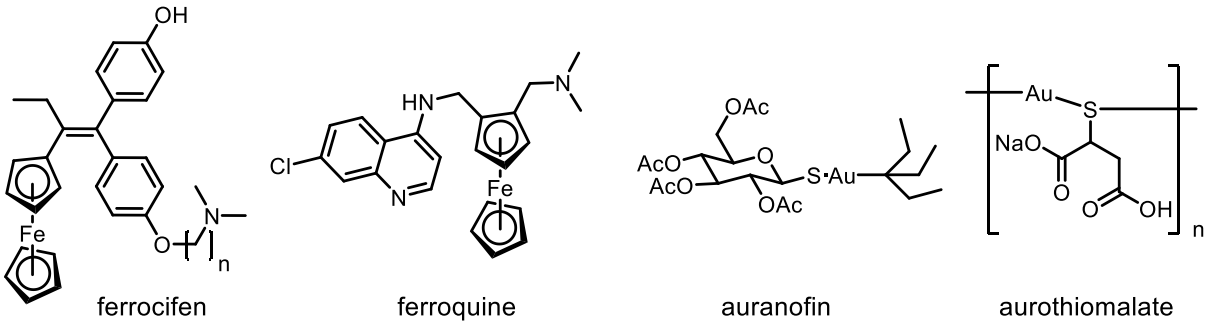

ferrocifen ferroquine auranofin aurothiomalate

Figure 5: Examples for metal complexes based on ferrocene and gold investigated for an application in anticancer therapy.

In the recent years, iridium, ruthenium, and rhodium caught interest as well for the preparation of therapeutically active complexes. In this context, specifically iridium and ruthenium complexes have shown potential for an application as chemotherapeutic agents.[16] The ruthenium complexes NAMI-A und KP1019 and the cyclometalated ruthenium complex TLD1433 are investigated in clinical trials for their possible use as chemotherapeutic agents (Fig. 6.).[16d,16e,17]

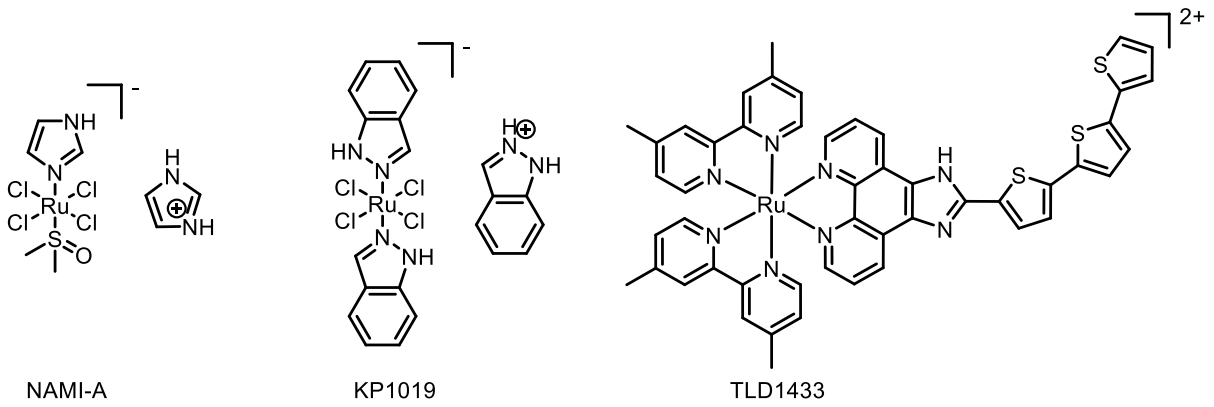

Figure 6: Ruthenium complexes currently investigated in clinical trials.

Moreover, some ruthenium(II) complexes show an increased uptake into cells, resulting in an enhanced anticancer activity. The high antiproliferative effect of these ruthenium complexes is a result of the interaction with the serum protein transferrrin. This protein usually has the task of transporting iron cations into the cells *via* binding these iron cations and interaction with the transferrin receptor. In this context, some ruthenium complexes exhibit as well a significant binding affinity to transferrin, resulting into an improved cellular uptake.[18] In addition, iridium(III) complexes show also a high affinity to specific cellular targets, e.g., mitochondria, DNA, or protein structures.[16d,19]

Metal complexes also show high potential for an application against bacterial infections.[13a,20] First antimicrobial agents based on metal complexes have already been described at the beginning of the 20th century. The arsenic complexes contained in arsphenamine (Fig. 7) enabled the treatment of syphilis, even before the discovery of penicillin.[13a,21] As well, for mercury in form of the Merbromin (Fig. 7) an antiseptic activity is known.[13a,22]

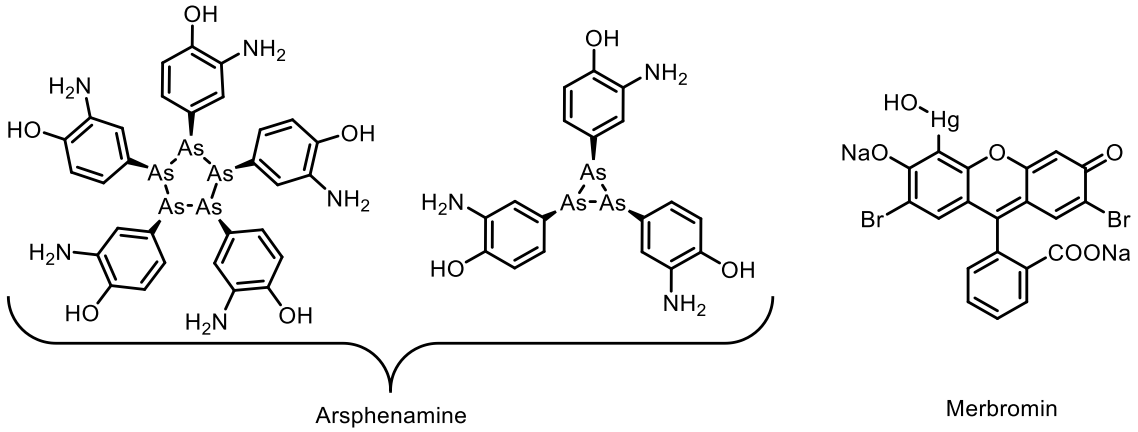

Figure 7: Arsenic and mercury complexes for antibacterial treatment.

Presently, a large number of metal complexes find attention for an application as antimicrobial agents. Various metal complexes are investigated for their antimicrobial properties, e.g., complexes of tin, silver, gold, iron, copper, palladium, or ruthenium. Typically, different organic ligands are reported to

form the respective antimicrobial complexes, e.g., *N*-heteroleptic carbenes, Schiff bases, as well as ligands based on known antibiotics.[23] Currently, ruthenium complexes and iridium complexes with phenanthroline and cyclopentadienyl ligands (Fig. 8) are intensively studied for their antimicrobial activity.[20,24]

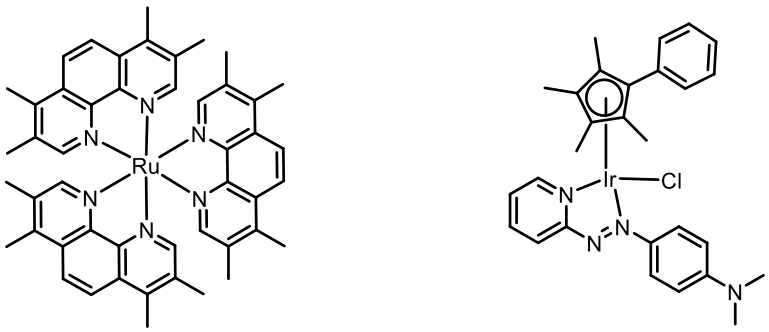

Figure 8: Examples for ruthenium and iridium complexes with phenanthroline and cyclopentadienyl ligands.

Beyond an application as chemotherapeutic agents, metal complexes are also showing increasing promise for an alternative to the well-established tetrapyrrole-based photosensitizers in PDT. Iridium and ruthenium complexes are of specific interest in this respect (see chapter 1.2.; Photodynamic therapy).[20,25]

Next to an application as chemotherapeutic agents or photosensitizers, metal complexes are also well established in medical imaging. For example, gadolinium complexes find application as contrast agents in magnetic resonance imaging. Complexes of technetium and copper are used as contrast agents in positron emission tomography (Fig. 9).[26]

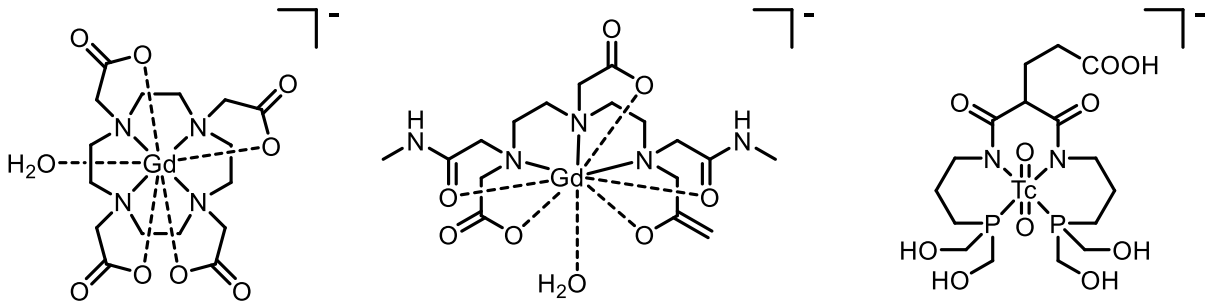

Figure 9: Examples for metal complexes as contrast agents in medical diagnostics.

Furthermore, complexes with metalloids find also high interest for medical diagnostics, e.g., boron-dipyrromethenes (BODIPYs).[27]

Beside the therapeutic and diagnostic applications, metal complexes are also widespread in chemical reactions. For example, metal complexes catalyze many chemical reactions or facilitate the stereoselective control of reactions.[28] Palladium-based complexes are widespread catalysts (Fig. 10)

in cross coupling reactions and frequently used in the well-known Heck-Reaction and Suzuki-Reaction.[28b,29]

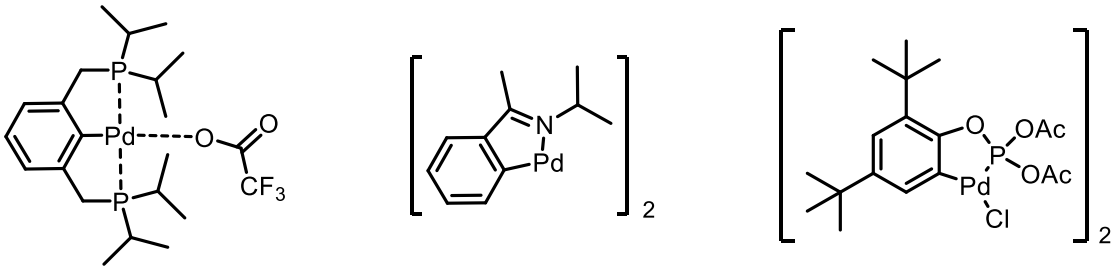

Figure 10: Examples for palladium-based catalysts in cross coupling reactions.

As well, metal complexes are employed in the epoxidation of olefins[30] or are used to control the stereoselectivity during reactions. Specifically, chiral complexes are often chosen for controlling the stereoselectivity. For example, chiral metal complexes are established in cyclopropanation of alkenes.[30a,31] In olefin metathesis or olefination, metal complexes are also involved. Here, ruthenium complexes are well established in these types of reactions, alternatively, molybdenum or titanium complexes have been described as catalysts.[32] The well-known Grubbs catalysts, as well as the Tebbe's reagent, are prominent complexes for metathesis reactions (Fig. 11).[33]

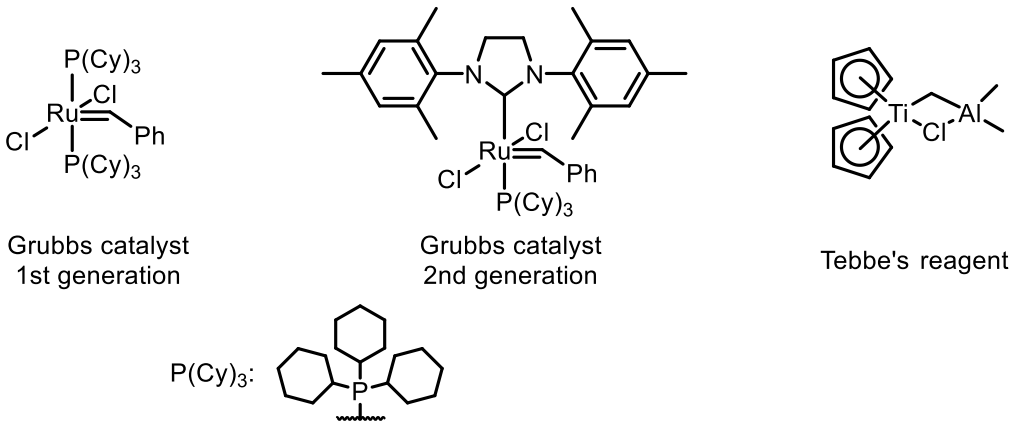

Figure 11: Structure of Grubbs catalyst und Tebbe's reagent.

Due to their special optical properties, metal complexes are of high relevance for industrial applications. For example, metal complexes are important parts of dye-sensitized solar cells,[34] of (chemo-)sensors,[35] or of OLED (organic light-emitting diode) technology.[34c,36] Furthermore, large three-dimensional arrangements of metal ions and organic ligands (metal-organic frameworks, MOFs) are important materials for the storage of hydrogen or methane.[37]

1.2 Photodynamic therapy

The use of light as therapeutic agent for different diseases had already been described in antiquity. At the beginning of the 20th century, the combination of light and chemicals to induce cell death was discovered. Finally, in the following decades, the discovery of the phototoxic activity of hematoporphyrin and the related hematoporphyrin derivatives gave the initial impulse for the development of PDT.[38] Since then, PDT has been established for an effective treatment against malignant diseases.[39] Moreover, PDT is not limited to cancer, but has also shown potential for the treatment of bacterial, viral, and parasitic infections.[40] PDT can also be applied to the treatment of non-malignant inflammatory skin diseases, like psoriasis or *acne vulgaris*.[39a,41] In addition, the preparation of antimicrobial surfaces based on photosensitizers is currently investigated.[42]

As described above, this therapy uses light (of an appropriate wavelength) to activate a light-sensitive molecule (photosensitizer). Visible light or light in the infrared region is commonly used for PDT.[43] Especially, light near the infrared region (600 – 1200 nm) is preferred for PDT, as the highest penetration depth into organic tissue is achieved in this range. Therefore, this region is usually named as the optical therapeutic window of the tissue.[43a,43d] For an application in PDT an ideal photosensitizer should show no toxic activity in the ground state, only by excitation with light photochemical processes should be initiated.[43a,43d,44e] By light excitation, the photosensitizer is transferred from the ground state into an excited singlet state. From this excited state, the photosensitizer can pass through intersystem crossing (ISC) into an excited triplet state. Finally, the excited photosensitizer (triplet state) can produce reactive oxygen species (ROS) *via* two possible reaction pathways. On the one hand, the excited photosensitizer can interact directly with surrounding molecules or biomolecules *via* the transfer of electrons to form radicals (type-I mechanism, Fig. 12).

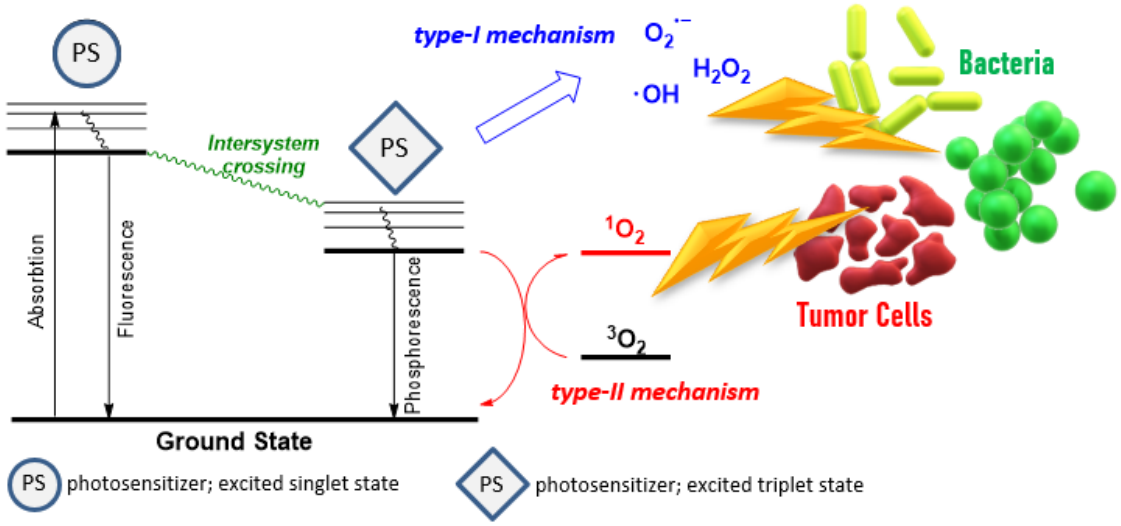

Figure 12: Modified Jablonski-diagram for the mechanism of PDT.

Other ROS are produced by further interaction of these generated species with oxygen, e.g., hydroxyl radicals, hydrogen peroxide, superoxide radical anions, or hydroperoxyl radicals. Finally, these ROS damage target structures (tumor cells and bacteria, respectively; Fig. 12). In addition to this type-I mechanism, the excited photosensitizer (in the exited triplet state), can as well interact directly with dioxygen (also in a triplet state) that is present in all cells. The energy of the excited photosensitizer is transferred to oxygen. In this process, the ground state triplet oxygen is converted into highly reactive singlet oxygen *via* energy transfer from the exited photosensitizer (type-II mechanism, Fig. 12). The photosensitizer itself returns to its ground state (Fig. 12) and can be irradiated again to form more singlet oxygen.[43a,43c-e] These ROS (including singlet oxygen) can irreparably damage, e.g., tumor cells, resulting in destruction of the cells *via* apoptosis or necrosis. [43a,43c-e] The antimicrobial effect on bacteria, viruses, and other microorganisms is also caused *via* critical damage by ROS.[44]

PDT has different advantages in comparison to chemotherapeutic agents or surgery. For example, PDT enables a selective treatment of the tissue by only local irradiation and a targeted destruction of the tumor without damaging the entire organism. In addition, less side effects are expected, as an ideal photosensitizer is not toxic in its ground state.[19,38b,43c,43e] The targeted treatment of PDT against cancer is also supported by the relatively short lifetime of singlet oxygen and other ROS within the tissue. Therefore, only cells are destroyed which are directly in the surroundings of the irradiated surface decreasing the damage to the healthy tissue.[19,45] However, the usable wavelength for PDT has an upper limit at 800 to 900 nm. On the one hand, the absorption capacity of water increases significantly at higher wavelengths (> 900 nm), so that water is in direct competition to the photosensitizer. At the same time, light with a longer wavelength (>800 nm) does not provide enough energy to generate the required singlet oxygen.[16d,43a]

Various photosensitizers, based on the tetrapyrrole structure, are reported for an application in PDT, e.g., porphyrins, phthalocyanines, (bacterio-)chlorins, or related metal complexes of these tetrapyrrole structures (Fig. 13).[25a,45c,46]

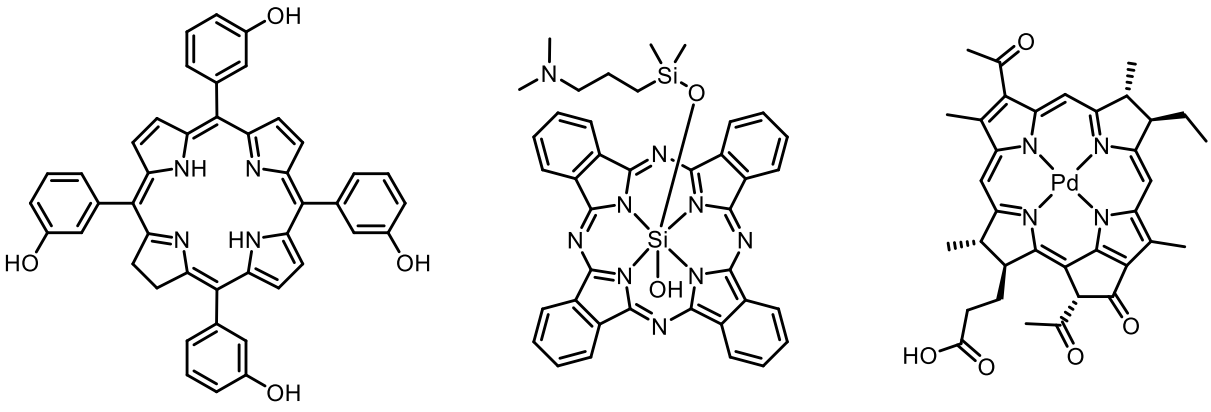

Temoporfin | Silicon Phthalocyanine 4 | Padaporfin

Figure 13: Examples for tetrapyrrole-based photosensitizers in the PDT.

Next to porphyrins and related tetrapyrroles, aromatic hydrocarbons show pronounced potential for an application in PDT. Phenothiazine-based (such as methylene blue) and xanthene-based (such as rose bengal or eosin) photosensitizers show high singlet oxygen quantum yields. Also for the naturally occurring hypericin phototoxic properties have long been known (Fig. 14).[45c,46] Furthermore, anthracene or naphthalene-based compounds are investigated for potential use as photoactive substances.[45c,47]

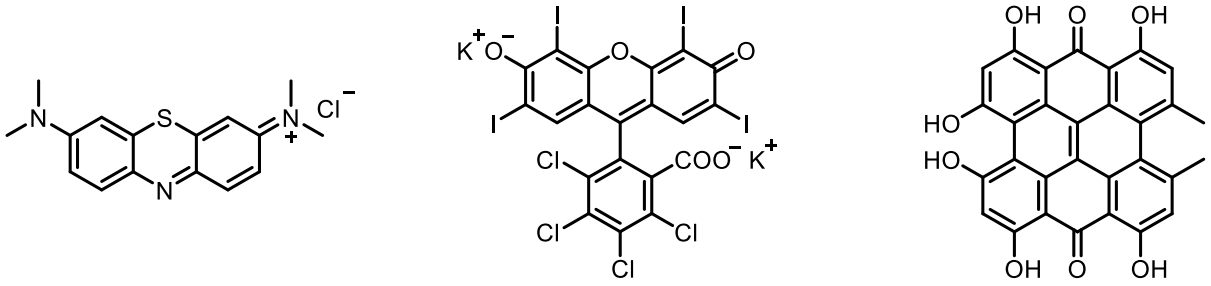

Figure 14: Examples for photosensitizers based on aromatic hydrocarbons.

In the last years, the importance of metal complexes as possible photosensitizers for PDT steadily increased. Specifically, cyclometalated ruthenium and iridium complexes show a high potential as photoactive compounds (Fig. 15).[16d,19,25a,48] Especially, for iridium(III) complexes after light irradiation an increased conversion to the triplet state with high singlet oxygen quantum yields are found.[19,49]

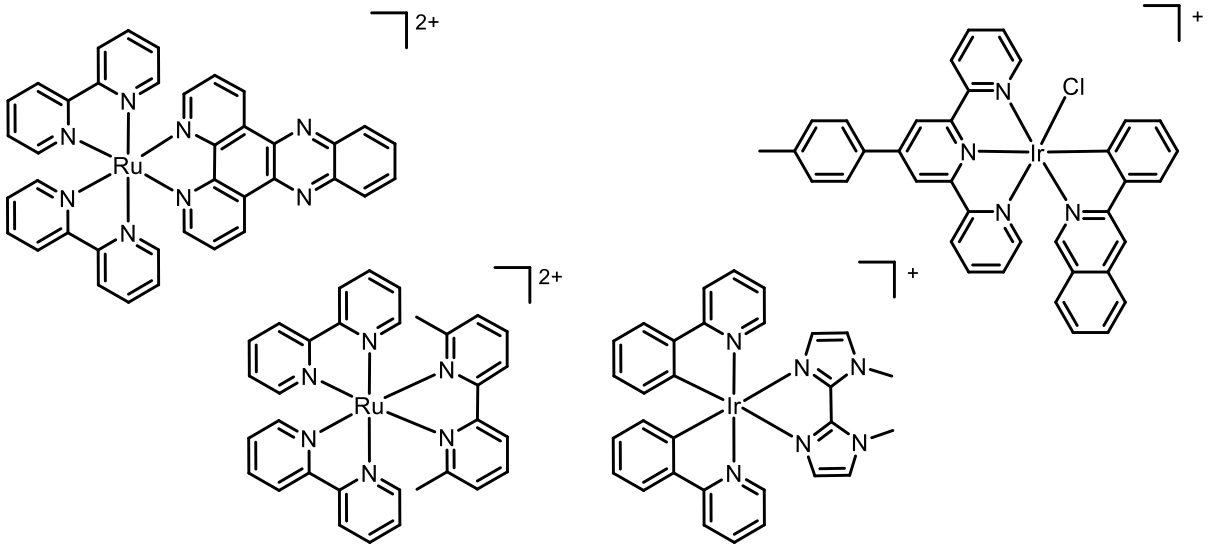

Figure 15: Examples for cylometalated ruthenium and iridium complexes as potential photosensitizers.

In this context, dipyrrinato metal complexes are also intensively discussed as new types of photoactive coordination complexes for PDT (see chapter 1.4, dipyrrins as ligands for dipyrrinato metal complexes).[50]

1.3 *meso*-Substituted dipyrromethanes

Dipyrromethanes are essential building blocks for the preparation of tetrapyrrolic compounds and other pyrrole-based macrocyclic structures, e.g., porphyrins, corroles, hexaphyrins, and calixpyrroles.[51] In addition, an effective synthesis of boron-dipyrromethenes and related dipyrrinato metal complexes is also possible starting from dipyrromethanes.[27a,50b,52] Dipyrromethanes with additional substituents at their *meso*-position are also well established for the preparation of porphyrinoids and dipyrrinato complexes.[27a,50b,51c,52]

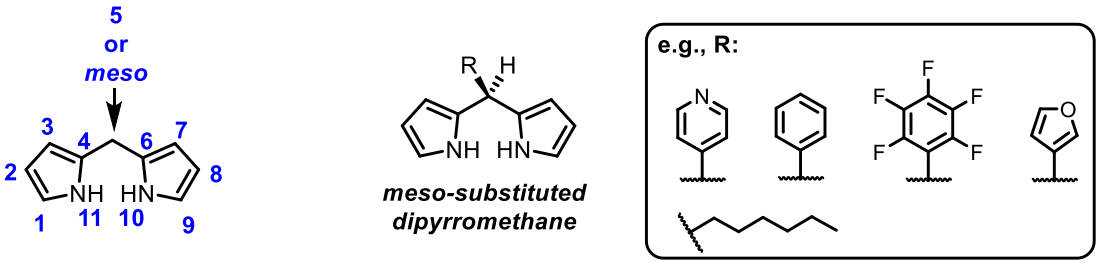

Figure 16: The dipyrromethane scaffold and examples for *meso*-substituted dipyrromethanes.

In general, dipyrromethanes are synthesized *via* the condensation of pyrrole with an aldehyde or a ketone by addition of a suitable acidic catalyst (Scheme 1). First synthetic procedures were already described in the 1970s, where pyrrole was reacted with 4-piperidine-carboxyaldehyde in methanol and hydrochloric acid as catalyst to form the corresponding dipyrromethane.[53]

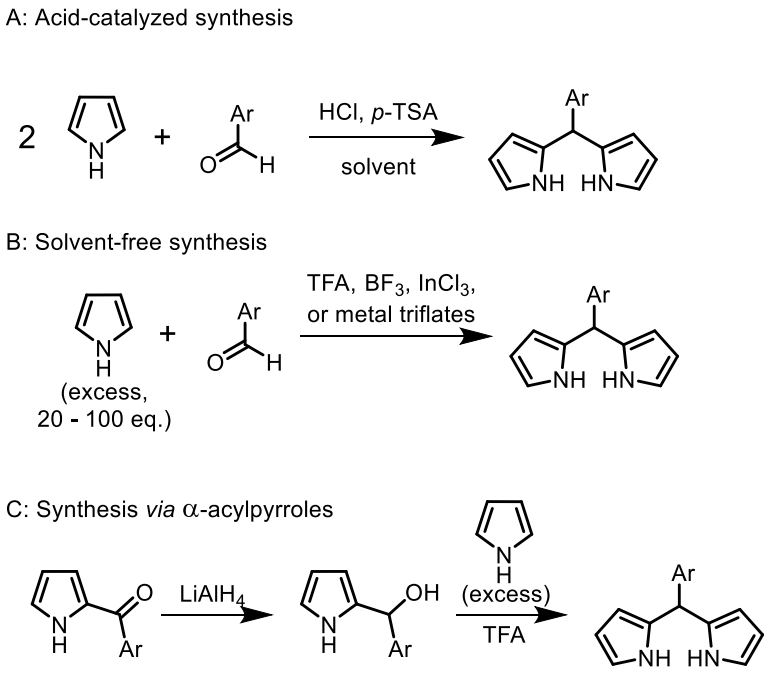

Scheme 1: Synthetic procedures for *meso*-substituted dipyrromethanes.

As an alternative to hydrochloric acid, *para*-toluene sulfonic acid or trifluoroacetic acid are used for the preparation of dipyrromethanes.[51a,54] Significant improvements in the synthesis of dipyrromethanes were achieved by Lindsey in 1994; aldehydes were now directly reacted with an excess of pyrrole, instead of using an additional solvent.[51c,55] Trifluoroacetic acid, indium(III) chloride, or metal triflates are described as suitable catalysts for this synthetic procedure (Scheme 1).[56] The modifications of the reaction conditions by Lindsey accounted for significantly higher yields of the corresponding dipyrromethanes. In addition to the classical acid-catalyzed condensation of pyrrole with aldehydes, alternative synthetic methods have also been developed, e.g., the direct coupling of *α*-acylpyrroles with pyrroles (Scheme 1).[51c] Alkynes, nitrosoalkenes, and azoalkenes are also suitable starting materials for a condensation with pyrroles to form the respective dipyrromethanes.[51a,54,56b] The use of cation exchange resins for the condensation of aldehydes and pyrroles has also been discussed.[57]

As described above, the synthesis of *meso*-substituted dipyrromethanes can be performed *via* the condensation of pyrrole with benzaldehydes under acidic conditions, according to the descriptions by J. Lindsey and co-workers.[51c,55] The mechanism for the preparation of *meso*-substituted dipyrromethanes is described through an electrophilic aromatic substitution of the *α*-carbon position of the pyrrole. In addition, the mechanism of the dipyrromethane synthesis is similar to the mechanism of porphyrin formation. However, the large excess of pyrrole prevents further oligomerization of the dipyrromethane once it has formed.[51b,51c,55] In the synthesis, a suitable acid is used as catalyst for the condensation of the benzaldehyde with two pyrroles. The mechanism for the acid-catalyzed condensation of pyrrole and an aldehyde is presented in Scheme 2. In the initial step, the carbonyl group is protonated by the acid to improve the reactivity in the following step (Scheme 2, **A**). In the next step, the attack of the pyrrole on the protonated carbonyl group follows. In this case, the attack of the pyrrole occurs *via* the *α*-position of the pyrrole to form the respective adduct (Scheme 2, **B**). The resulting positive charge is stabilized within the pyrrole ring by resonance. Finally, the aromatic system on the pyrrole is restored *via* the abstraction of a proton. In this intermediate step, one pyrrole molecule is linked to the benzaldehyde and a hydroxy group is formed (Scheme 2, **C**). In the next step, the hydroxy group is protonated and under the removal of one water molecule an additional pyrrole molecule is again attacking *via* the corresponding *α*-position (Scheme 2, **D**). A positive charge is resulting from the attack of the pyrrole (Scheme 2, **E**) and is again stabilized within the pyrrole ring by resonance. In the final step, a proton is removed to restore the aromaticity, resulting in the desired dipyrromethane (Scheme 2, **F**).[51b,58]

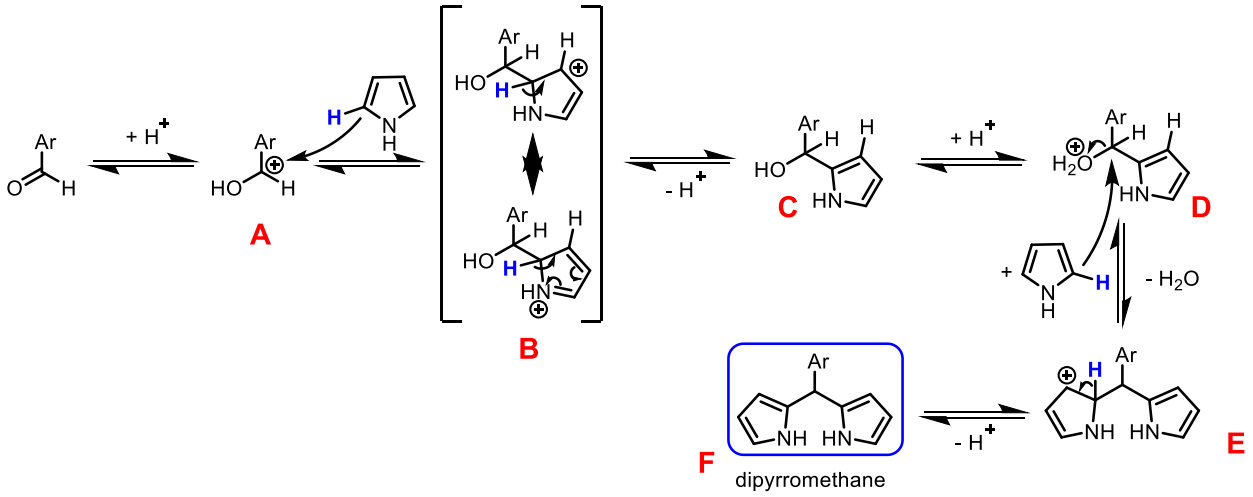

Scheme 2: Mechanism for the synthesis of dipyrromethanes.

As described above, the large excess of pyrrole shifts the equilibrium towards the dipyrromethane and further oligomerization of the dipyrromethane is prevented. However, the formation of oligomers is not excluded, i.e., corresponding oligomers between pyrrole and aldehydes can be observed, e.g., the tripyrrane. In addition, an attack of the *β*-carbon position of the pyrrole is also possible (Scheme 3). In this case, the related *N*-confused dipyrromethane can be observed. The mechanism for the formation of the *N*-confused dipyrromethane is equivalent to the formation of dipyrromethane. However, the attack over the *α*-position of the pyrrole is preferred, due to the enhanced resonance stabilization.[51b,55] Under the reaction conditions according to Lindsey, the formation of the described by-products is to be expected only to a very small extent.[51b,55,56b,59]

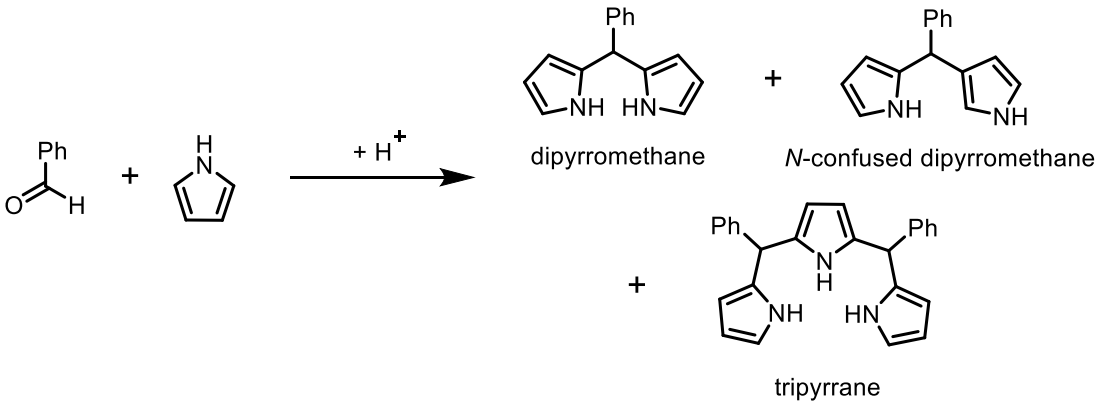

Scheme 3: Products of the dipyrromethane synthesis.

1.4 Dipyrrins as ligands for dipyrrinato metal complexes

Dipyrrins (dipyrromethenes) show high similarities to dipyrromethanes, however, within the dipyrrin molecule the pyrrole units are linked *via* a methine bridge. Therefore, dipyrrins have a planar structure

with a conjugated π-electron system.[60] Due to its bis-pyrrolic geometry and the similarity to the porphin structure, dipyrrins are often named as semi-porphyrins (Fig. 17).[60c,61]

Figure 17: Porphin scaffold with highlighted dipyrrin substructure and nomenclature for the dipyrrin scaffold.

For the preparation of dipyrrins several synthetic pathways are described. A direct synthesis can be performed *via* an acid-catalyzed condensation of 2-formylpyrrole with an additional (substituted) pyrrole. Alternatively, the synthesis of dipyrrins can be carried out by the condensation of two 2-carboxy-pyrroles (Scheme 4). However, the preparation of *meso*-substituted dipyrrins is not possible *via* these methods.[62] For the synthesis of *meso*-substituted dipyrrins alternative methods have been described. *meso*-Substituted dipyrrins can be synthesized using pyrrole and carboxylic acids or acyl chlorides. As well, (*meso*-substituted) dipyrrins can be prepared *via* the oxidation of respective dipyrromethanes with suitable oxidation agents, e.g., 2,3-dichloro-5,6-dicyano-*p*-benzoquinone (DDQ) or *p*-chloranil (Scheme 4).[60b,62a,63]

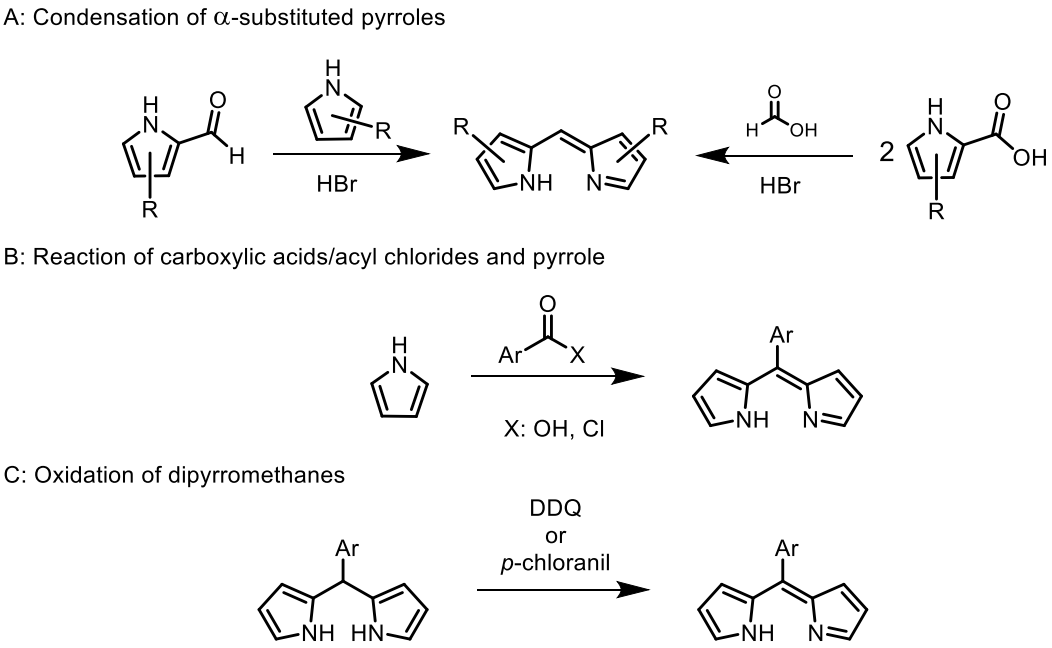

Scheme 4: Synthetic pathways for (*meso*-substituted) dipyrrins.

The oxidation of dipyrromethanes with quinones (DDQ or *p*-chloranil) is a common method for the synthesis of dipyrrins. The driving force for this oxidation is caused by the formation of two conjugated

systems (dipyrromethenes and hydroquinone). In general, a quinone can be easily reduced by uptake of electrons to the corresponding hydroquinone. Additional electron-withdrawing substituents, as they are present in DDQ or in *p*-chloranil, enhance the absorption of the electrons and facilitate the reduction of the quinone.[64] However, the exact mechanism for the oxidation of dipyrromethanes by DDQ is not known. Based on studies of the reaction behavior in the oxidation of different molecules with quinones (DDQ), two mechanisms are discussed: (1) The hydride shift and (2) the single-electron transfer (SET) in combination with the transfer of protons (Scheme 5).[64b-d, 65]

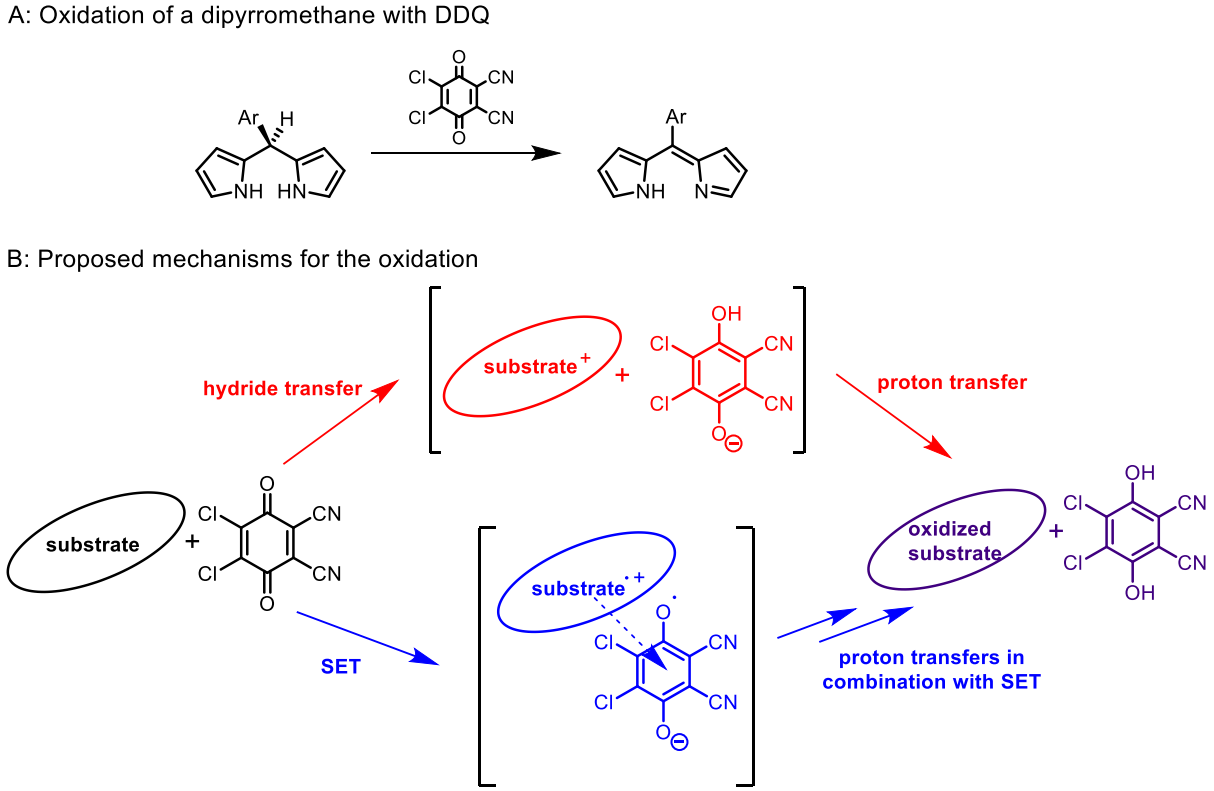

Scheme 5: Oxidation of a dipyrromethane with DDQ (A) and schematic mechanisms for the oxidation with DDQ (B).

Dipyrrins are of high interest for an application as ligands in coordination chemistry. First bis(dipyrrinato) complexes had already been described at the beginning of the 20th century by Hans Fischer.[66] This type of organic ligand is known to coordinate various metals. Furthermore, complexes with boron or with elements of the alkaline metal group are also well known.[60c,62a,67] Dipyrrinato metal complexes can exclusively consist of dipyrrin ligands (homoleptic complexes, Fig. 18). Depending on the employed metal ion, complexes with two or three dipyrrin ligands are possible. Thus, zinc(II), nickel(II), or copper(II) were reported to form bis(dipyrrinato)metal complexes with dipyrrins.[62a,66,68] While iron(III), indium(III), or gallium(III) form respective tris(dipyrrinato)metal complexes.[67a,50b,69] Interestingly, for bis(dipyrrinato)copper(II) complexes a pseudo tetrahedral geometry was found.[68c]

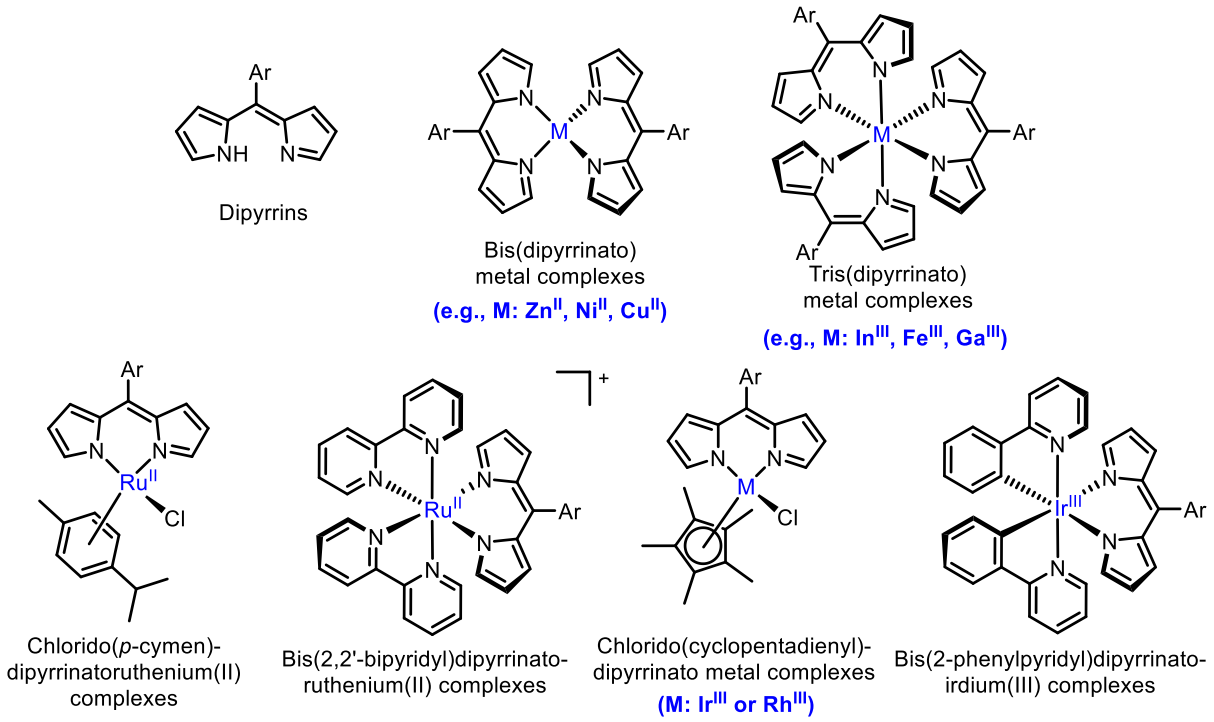

Figure 18: Examples for homoleptic and heteroleptic dipyrrinato metal complexes.

Furthermore, dipyrrinato complexes with a combination of dipyrrins and additional aromatic ligands are also known (heteroleptic complexes, Fig. 18). Typically, iridium(III), ruthenium(II), or rhodium(III) are employed to form heteroleptic dipyrrinato complexes. Cyclopentadienyl, *p*-cymene, 2,2-bipyridyl, and 2-phenylpyridyl moieties are reported as additional aromatic ligands.[67b,67c,70]

For the synthesis of homoleptic dipyrrinato complexes, the corresponding metal salts are simply reacted with dipyrrins under basic conditions (Scheme 6).[50b,60b,62a,67a,69] In addition, the preparation of asymmetric bis(dipyrrinato) metal complexes with two different dipyrrin ligands is known.[71]

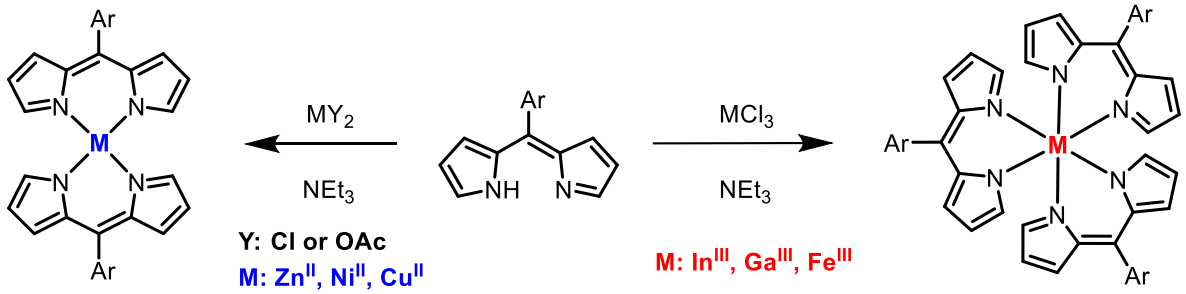

Scheme 6: Synthesis of homoleptic bis- and tris(dipyrrinato) metal complexes.

In contrast, syntheses of heteroleptic dipyrrinato complexes are generally performed *via* the reaction of dipyrrins with (dichlorido-bridged) metal half-sandwich complexes. Here, dipyrrins are reacted under basic conditions with these half-sandwich precursors to form the corresponding heteroleptic dipyrrinato complexes, e.g., chlorido(*p*-cymene)(dipyrrinato)ruthenium(II) complexes or chlorido-(cylopentadienyl)(dipyrrinato)iridium(III) complexes. Cyclometalated dipyrrinato complexes are

synthesized by a similar protocol. In this case, (dichlorido-bridged) 2-phenylpyridyl or 2,2'-bipyridyl metal precursors are used for the synthesis of respective heteroleptic dipyrrinato complexes, e.g., bis(2,2'-bipyridyl)(dipyrrinato)ruthenium(II) complexes or (dipyrrinato)bis(2-phenylpyridyl)iridium(III) complexes (Scheme 7).[67a,67c,70b-d] Alternatively, bis(2,2'-bipyridyl)(dipyrrinato)ruthenium(II) complexes can be also prepared from related chlorido(*p*-cymene)(dipyrrinato)ruthenium(II) complexes *via* a ligand exchange with 2,2'-bipyridine (Scheme 7).[50b,72]

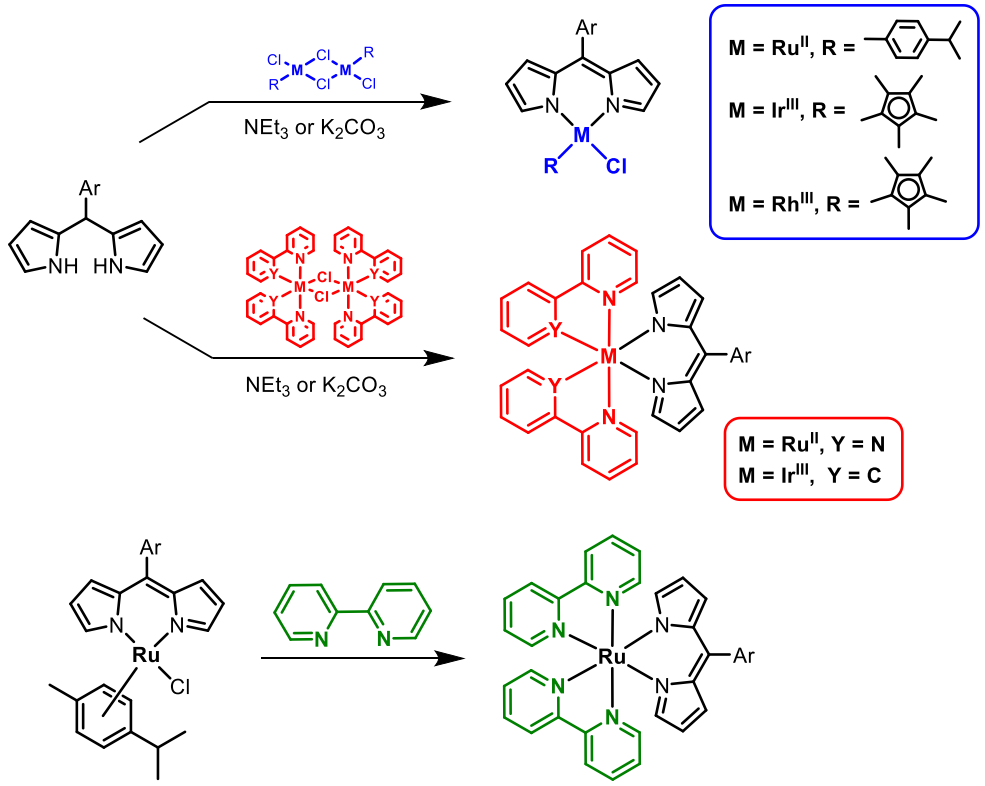

Scheme 7: Preparation of heteroleptic dipyrrinato complexes.

Besides homoleptic and heteroleptic dipyrrinato complexes, coordination complexes are known, where only a single dipyrrin ligand coordinates to the metal center. For example, specific mono-dipyrrinato complexes are described with manganese, iron, cobalt, or aluminum (Fig. 19).[73] Furthermore, dipyrrinato complexes coordinating to alkali metals[63b,60c] and complexes of dipyrrin ligands with metalloids are known, e.g., complexes with sodium, lithium, silicon, germanium, or boron, the latter representing the prominent boron-dipyrromethenes or BODIPYs, see below chapter 1.5 (Fig. 19).[67d,74]

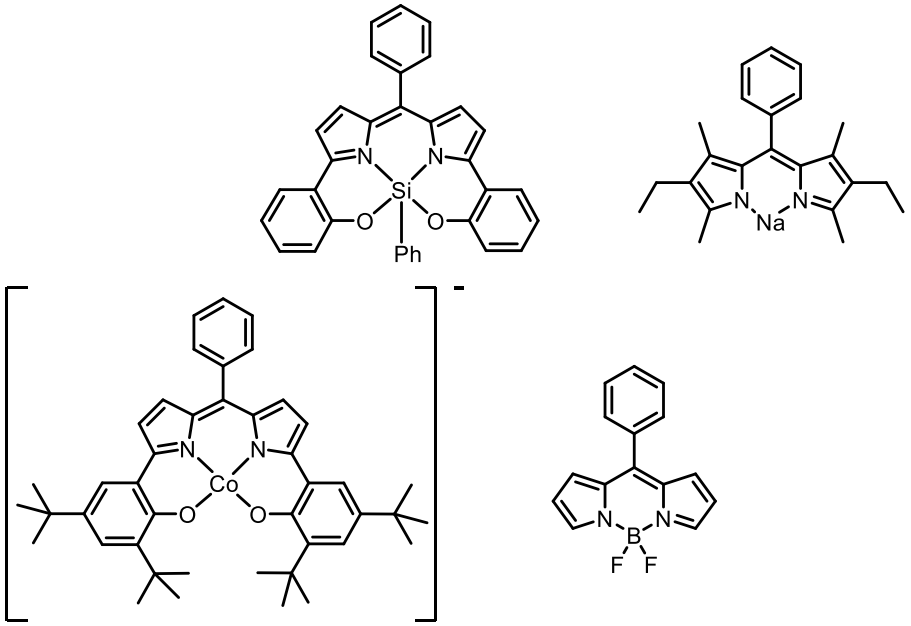

Figure 19: Examples for mono-dipyrrinato complexes.

Dipyrrinato complexes find application in various fields. For example, dipyrrinato complexes with cobalt, nickel, manganese or iron are important as catalysts for chemical reactions.[73a-d] As well, dipyrrinato complexes are suitable starting materials for the development of MOFs, supramolecular arrays, or nanoparticles.[60c,75] Bis(2,2'-bipyridyl)(dipyrrinato)ruthenium(II) complexes and (dipyrrinato)bis(2-phenylpyridyl)iridium(III) complexes find application as light harvesting arrays in photovoltaics.[72,76] In recent years, dipyrrinato complexes have also become a focus of inorganic medicinal chemistry. Dipyrrinato metal complexes show promising properties for an application as chemotherapeutics. Specifically, for some dipyrrinato complexes an interaction with DNA is found, resulting in a reduction of cell growth (Fig. 20).[16b,67a,77]

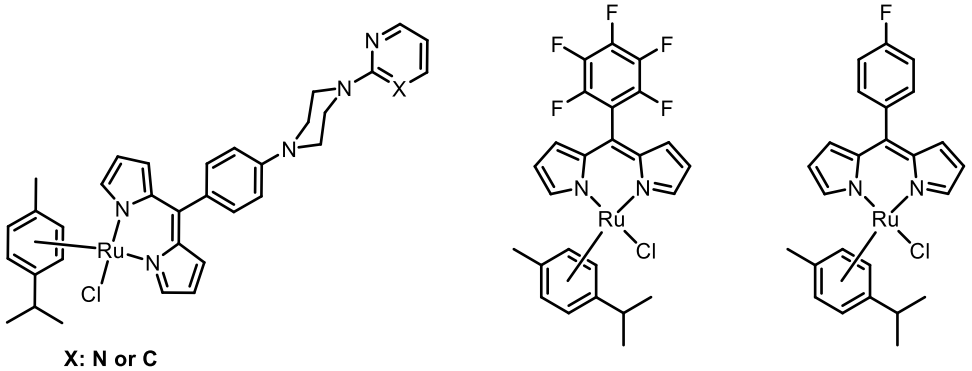

Figure 20: Examples for dipyrrinato ruthenium(II) complexes as potential chemotherapeutic agents.

The application of dipyrrinato complexes is not limited to chemotherapeutic agents. Recently, some dipyrrinato metal complexes have been described with potential for an application as photosensitizers in PDT.[50a,50b,78] Specifically, the glycosylated gallium complex, which was synthesized in a collaboration of biolitec and Freie Universität Berlin, proved to be effective in antibacterial PDT (Fig. 21).[50b]

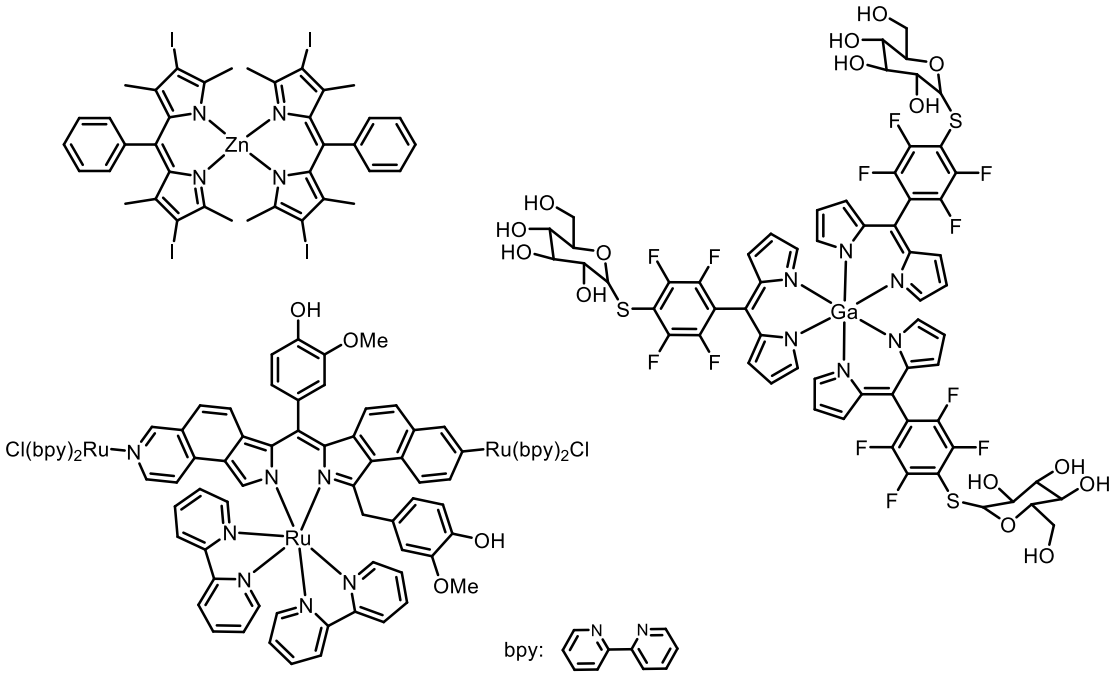

Figure 21: Examples for dipyrrinato metal complexes as potential photosensitizers.

1.5 Boron-dipyrromethenes (BODIPYs)

As discussed above, dipyrromethenes are known for the coordination of many different elements, e.g., sodium, lithium, calcium, ruthenium, or indium.[60c] As well, coordination complexes with metalloids are well known. The most famous dipyrrinato metalloid complex is represented by the boron-dipyrromethenes (BODIPYs). In the case of BODIPYs, the boron is coordinated in form of a boron difluoride to the corresponding dipyrrin ligand. The commonly used abbreviation BODIPY is derived from the term **bo**ron-**dipy**rromethene. Furthermore, the BODIPY framework is also referred to as 4,4-difluoro-4-bora-3a,4a-diaza-*s*-indacene, due to the high structural similarity with *s*-indacene. The 8-position is also termed *meso*-position, the 3- and 5-positions are referred to as α-positions, and the 1-, 2-, 6-, and 7-positions of the BODIPY structure is referred to as β-positions (Fig. 22).[27a,67d,79]

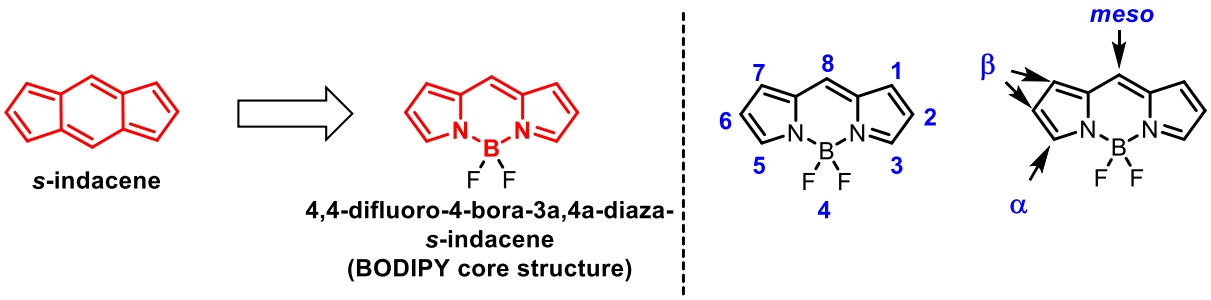

Figure 22: Comparison of the structures of *s*-indacene and BODIPY (red), and nomenclature for the BODIPY core structure (blue).

The BODIPY can be formally described as a complex of a negatively charged dipyrrinato ligand and an electron-deficient boron difluoride. However, calculations show that the actual negative charge is located on the boron difluoride part, specifically at the fluorine atoms. The respective positive charge is delocalized *via* the ring structure of the dipyrrinato ligand.[62d] Within the BODIPY structure, only the π-electron system of the dipyrrinato ligand is delocalized and the BODIPYs exhibit a nearly planar structure.[62d,80] Typically, BODIPYs show an intensive absorption at approx. 500 nm and an additional weaker absorption at approx. 350 nm. The intensive band results from the excitation into the S_1 excited state. On the other hand, the less intense band results from the excitation to the S_2 excited state. In this case, this state relaxes exclusively by internal conversion into the S_1 state, since no fluorescence can be detected from this S_2 excited state.[79,81]

First, *meso*-substituted BODIPYs were described by Treibs and Kreuzer in 1968,[82] and later developed by other authors, e.g., Lindsey and Wagner.[83] BODIPYs can be prepared *via* the condensation of pyrrole with acyl chlorides, followed by deprotonation and complexation with boron trifluoride (Scheme 8).[27a,62d,84] This method has already been established for BODIPYs prepared from substituted pyrroles with sterically demanding substituents.[85]

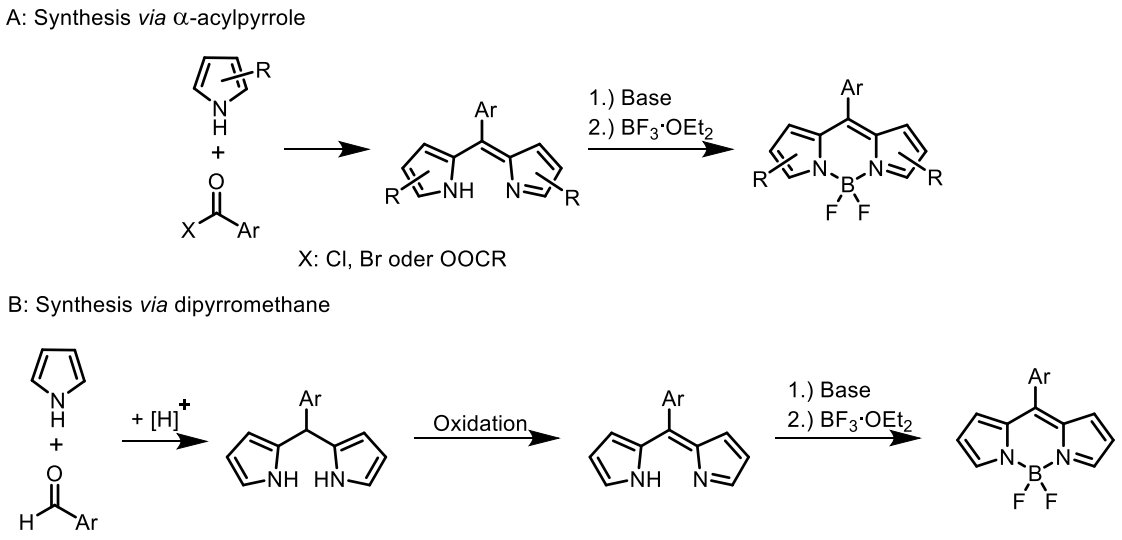

Scheme 8: Synthetic procedures for the preparation of BODIPYs.

Alternatively, BODIPYs can be prepared *via* an oxidation-complexation sequence (Schemes 8 and 9). According to the synthetic procedure described by Lindsey and Wagner, the corresponding *meso*-substituted dipyrromethanes are oxidized with a suitable oxidation agent, e.g., DDQ. In the synthesis, the dipyrrin is deprotonated by a base, e.g., triethylamine or *N*,*N*-diisopropylethylamine. Finally, the substrate is treated with the boron trifluoride-diethyl ether complex to form the corresponding BODIPY (Scheme 9). This synthesis is often performed in a one-pot multi-step reaction.[27a,67d,82,83] The BODIPYs synthesized in this thesis were also prepared according to this procedure which was originally described by Lindsey and Wagner.[83]

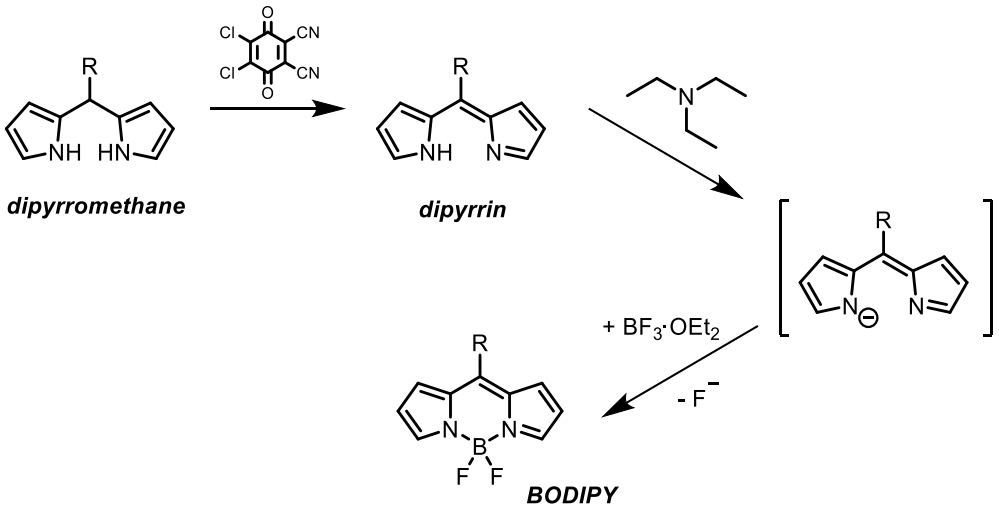

Scheme 9: Preparation of BODIPYs *via* dipyrromethanes.

Due to their excellent fluorescence properties, BODIPYs are well established as markers in medical imaging in diagnostics.[27] Furthermore, BODIPYs have found application in MOF,[86] as part of chemo sensors, in organic photovoltaics,[87] or energy-transfer cassettes.[88]

In the past decade, interest in new potential photosensitizers based on the BODIPY structure has constantly increased.[89] BODIPYs show promising properties for an application in PDT. For example, BODIPYs have high extinction coefficients and high resistance against photobleaching (decreasing of the fluorescence during prolonged irradiation times with light near the absorption maximum).[89] However, for the application as photosensitizers in PDT, the BODIPY structure must be modified. On the one hand, the absorption must be shifted to higher wavelength ranges (red-infrared range) and the BODIPY core structure must be as well modified to enhance intersystem crossing. The intersystem crossing allows the molecule to enter into the excited triplet state and enables the generation of ROS.[82d,90] The improvement of the BODIPY core structure towards an application as a photosensitizer can be achieved *via* the introduction of heavy atoms, e.g., bromine or iodine (Fig. 23). The heavy atom effect causes a shift of the absorption maximum towards higher wavelengths, stabilizes the triplet state, and increases the intersystem crossing rate.[89,91]

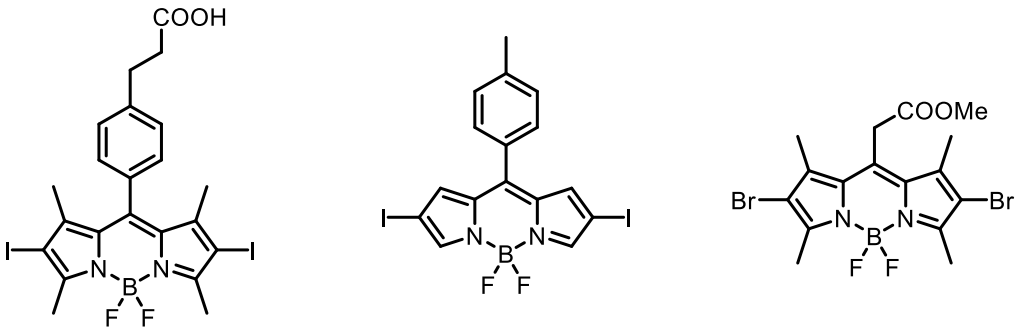

Figure 23: Examples for BODIPY core substitution with halogens.

The absorption properties, as well as the singlet oxygen generation, can be also influenced by various phenyl, alkenyl or alkenyl substituents at the respective *meso*-, *α*-, and *β*-positions. The concepts of core-substitution with halogens and aromatic hydrocarbons are often combined (Fig. 24).[85,89b,90b,92]

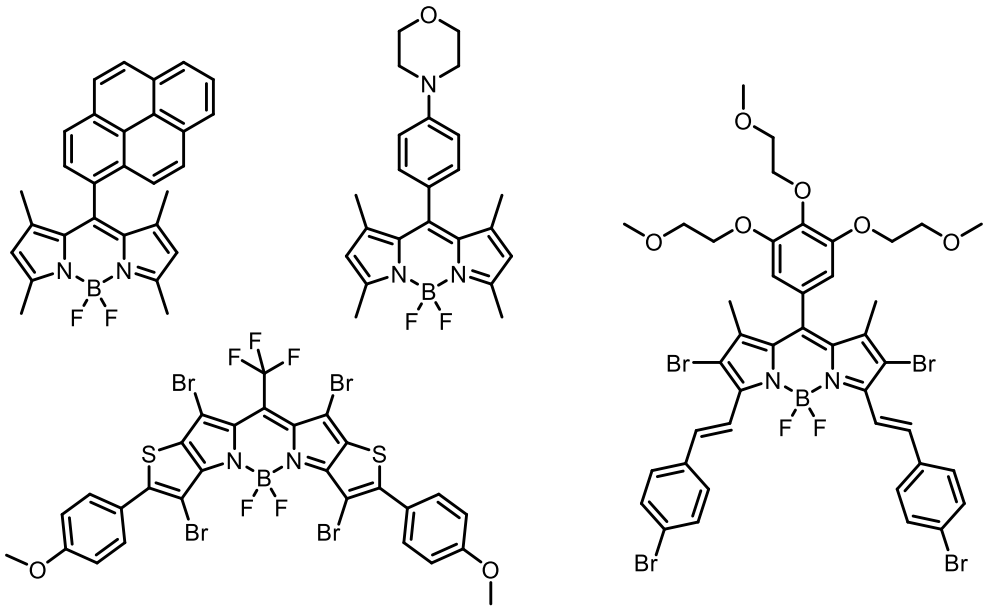

Figure 24: Examples for core-substitution of BODIPYs *via* halogens and aromatic hydrocarbons.

1.6 The nucleophilic aromatic substitution

For the functionalization of arenes two possible substitution reactions are described: (1) The electrophilic and (2) the nucleophilic aromatic substitution. The electrophilic aromatic substitution enables the direct functionalization of aromatic compounds with suitable electrophiles. After coupling to the related arene the resulting positive charge is delocalized *via* resonance. Finally, the aromaticity can be restored by abstraction of a proton. In comparison, the nucleophilic aromatic substitution requires more specific conditions. Here, a negative charge is resulting from the attack of a nucleophile. In this case, a formal abstraction of a hydride anion is required for the restorage of the aromatic system (Scheme 10).[93] The hydride anion represents a weak leaving group and only under certain conditions a removal of the hydride is described.[94]

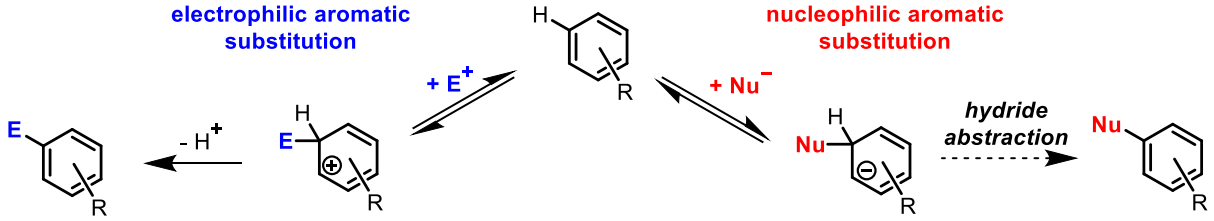

Scheme 10: Comparison of the electrophilic and the nucleophilic aromatic substitution.

Therefore, an additional leaving group is necessary, which will remove the negative charge during the separation. As well, an electron-withdrawing group supports the attack of the nucleophile. The negative inductive effect of this group removes electron density from the aromatic system and at the same time stabilizes the intermediate stage resulting from the attack of the nucleophile. These two concepts enable the nucleophilic substitution of arenes (Scheme 11).[93,95]

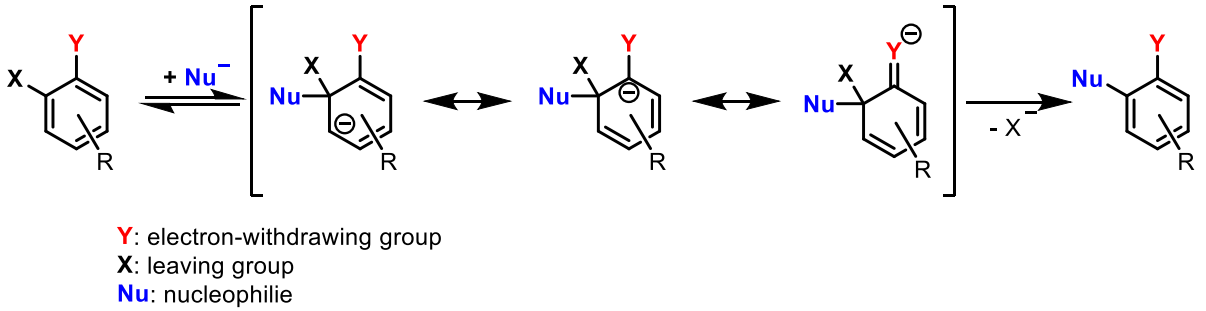

Scheme 11: Mechanism for the S_NAr with involvement of an electron-withdrawing group and a suitable leaving group.

In this thesis, dipyrromethanes, dipyrrins, and related dipyrrinato complexes with a pentafluorophenyl and a 4-fluoro-3-nitrophenyl group were functionalized *via* S_NAr. In the literature, various nucleophiles, e.g., amines, alcohols, and thiols, are reported for a substitution of the pentafluorophenyl group.[50b,52,96] Also, the nucleophilic substitution of the 4-fluoro-3-nitrophenyl group has been reported with a limited number of amines.[97] Within the pentafluorophenyl group, the fluorine atoms generate the required electron-withdrawing effect, due to their high electronegativity. In the 4-fluoro-3-nitrophenyl moiety the nitro group serves as the required electron-withdrawing group.

The nucleophilic substitution of the pentafluorophenyl group begins with the attack of the nucleophile (Scheme 12, **A**). In general, the attack of the nucleophile can occur *via* the *para*-, *meta*-, or *ortho*-position. In all cases, the resulting negative charge can be distributed over the aromatic ring in the intermediate state (Scheme 12, **B**).

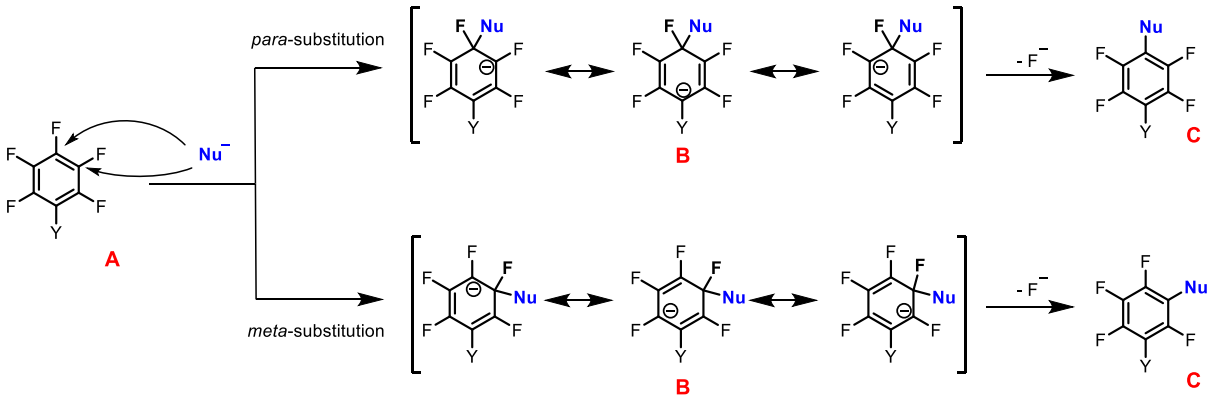

Scheme 12: Mechanism for the S_NAr at the pentafluorophenyl group.

During the nucleophilic substitution of the *para*-position, the negative charge, resulting from the attack of the nucleophile, can be partially transferred to the *ipso*-position and to the respective *ortho*-positions *via* resonance. The same applies to the substitution of the *ortho*-position. However, a negative charge from the *meta*-position cannot be transferred to the *ipso*-position, due to the specific arrangement of the *ipso*-position (Scheme 12, **B**). In addition, the substitution of the *ortho*-position is often sterically hindered. For these reasons, the substitution of the *para*-position is often preferred for the pentafluorophenyl moiety. Finally, the aromaticity is restored by abstraction of a fluorine (Scheme 12, **C**).[95] The high regioselectivity towards the *para*-position is also influenced by the substituent (Y) at the *ipso*-position. Substituents with electron-donating and electron-withdrawing effects have a significant influence on the substitution pattern (*meta*- and/ or *para*-substitution). The electron-donating and electron-withdrawing character of a substituent can be described by the Hammett substituent constant (σ). Substituents (Y) with a negative value for σ support a substitution of the *meta*-position. This is, because substituents with a negative value for σ cause a destabilization of the transition state (in case of the attack of the nucleophile at the *para*-position), due to the electron-donating character of these substituents. On the other hand, substituents (Y) with a positive value for σ support an attack of the nucleophile at the *para*-position, due to a stabilization of the transition state by an electron-withdrawing effect. For example, fluorine or pentafluorophenyl substituents show a positive value for σ. For methoxy or amino groups (as substituent Y) the substitution of the corresponding *meta*-position is favored.[95]

For the nucleophilic substitution of 1-fluoro-2,4-dinitrobenzene and 1-bromo-2,4-dinitrobenzene a stepwise reaction with appearance of an intermediate state was found, similar to Meisenheimer complexes.[98] Due to the high similarity, the substitution of the 4-fluoro-3-nitrophenyl group should also progress *via* a comparable mechanism. The nucleophilic substitution exclusively takes place at the *para*-position, since only this position carries a fluorine atom as potential leaving group (Scheme 13).

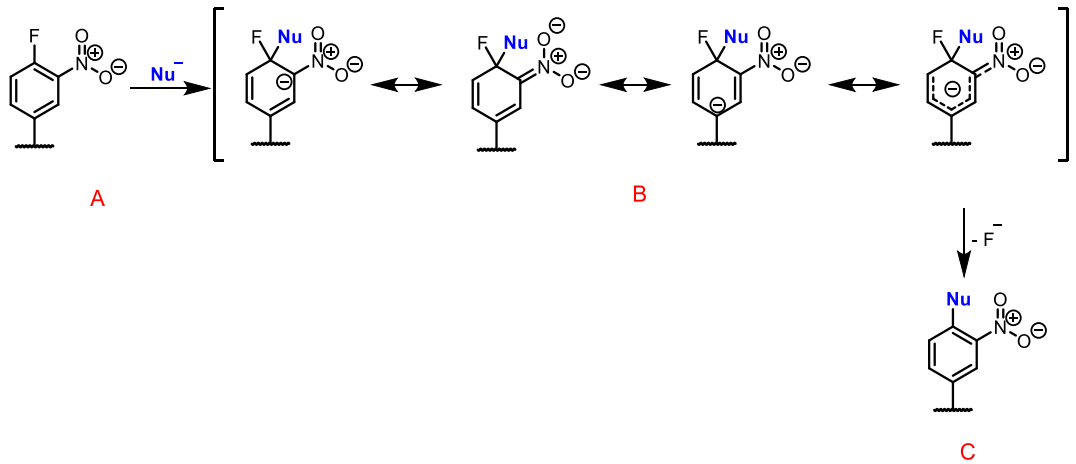

Scheme 13: Proposed mechanism for the substitution of the 4-fluoro-3-nitrophenyl moiety.

In the first step, the nucleophile attacks at the *para*-position of the phenyl ring. As a result of the attack a negative charge is generated (Scheme 13, **A**). Again, this negative charge can be distributed in the aromatic system *via* resonance. As well, the negative charge is stabilized through the nitro group (Scheme 13, **B**). Finally, the aromatic system is restored by the abstraction of a fluoride (Scheme 13, **C**).

1.7 Aim of the work

In recent years, the attention in dipyrrinato complexes for various applications has steadily increased. Dipyrrinato metal complexes are gaining promising potential as chemotherapeutically active compounds.[16b,67a77] Recently, some dipyrrinato complexes also attracted interest as potential photosensitizers for PDT,[50,78] however, so far, only a limited number of dipyrrinato complexes have been described and evaluated as therapeutically active compounds.

The main objective for this thesis was the development of photoactive compounds based on dipyrrinato metal complexes and boron-dipyrromethenes (BODIPYs). The synthesized coordination complexes presented in this thesis are relevant in the context of potential photosensitizers for an application in PDT and for antimicrobial photodynamic inactivation.

First, synthesis focused on *meso*-substituted dipyrromethanes as building blocks for the related homoleptic and heteroleptic dipyrrinato metal complexes, as well as for *meso*-substituted BODIPYs (Scheme 14).

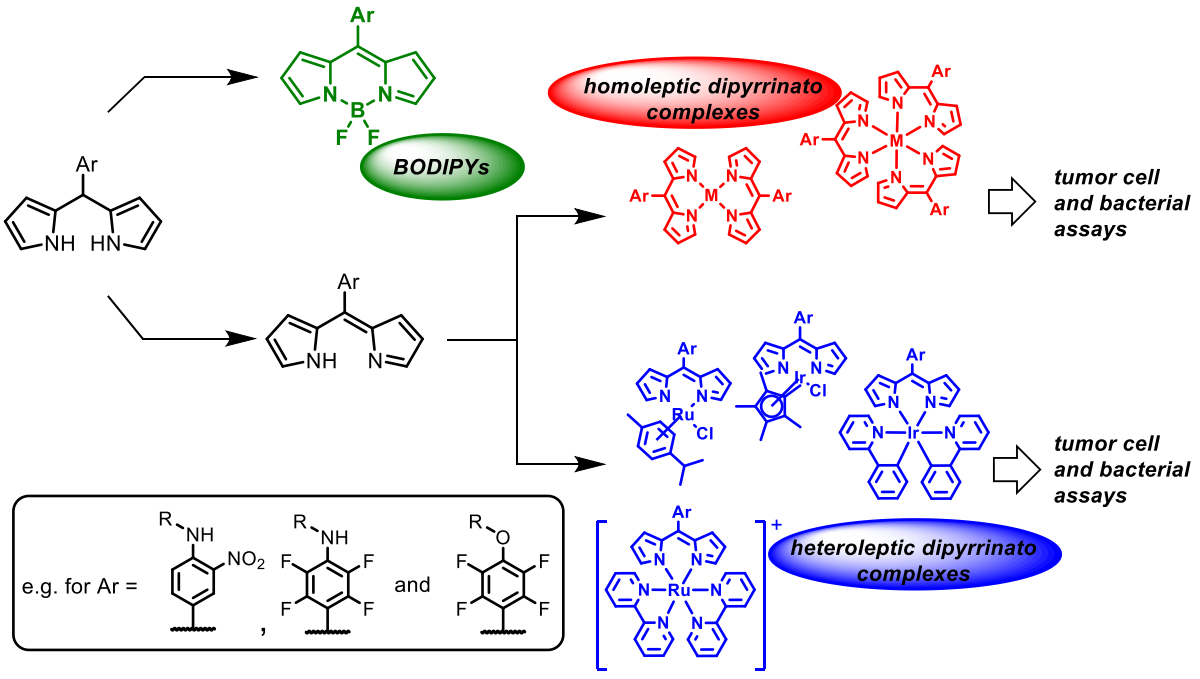

Scheme 14: Schematic presentation for the preparation of *meso*-substituted dipyrrinato metal complexes and *meso*-substituted BODIPYs *via* pre-functionalized dipyrromethanes.

In this context, the introduction of 4-fluoro-3-nitrophenyl and pentafluorophenyl moieties to the respective *meso*-position enable diverse synthetic modifications for an adjustment of the properties of the target compounds, e.g., solubility in polar solvents, preparation of conjugates, or improvement of the bioavailability. 5-Pentafluorophenyldipyrromethanes served as starting materials for subsequent nucleophilic substitutions, to achieve a wide range of differently functionalized target compounds. The pentafluorophenyl group had already been proven particularly useful for subsequent substitution with various nucleophiles, e.g., amines, alcohols, or thiols.[50b,52,96] In the context of nucleophilic substitution, the 4-fluoro-3-nitrophenyl moiety was also to be investigated as an alternative structure for the target compounds. In addition, the concept of the nucleophilic substitution should be extended to carbohydrates, to increase the bioavailability and adjust the solubility in polar solvents. Therefore, the aim was also extended to the *post*-functionalization of *meso*-(4-fluoro-3-nitrophenyl) and *meso*-pentafluorophenyl-substituted dipyrrinato complexes with thiocarbohydrates.

The alteration of the photophysical properties of corresponding BODIPYs *via* the modification of the BODIPY core structure with bromine enabled the generation of ROS. Moreover, the objective was to combine the concept of a BODIPY core modification with the nucleophilic substitution of the 4-fluoro-3-nitrophenyl and the 5-pentafluorophenyl moiety with diverse functional groups. These two concepts enable a possible application of the modified BODIPYs as photosensitizers in PDT and antimicrobial photodynamic inactivation (Scheme 15). Here, the aim was also to apply the functionalization with thiocarbohydrates to the brominated BODIPYs.

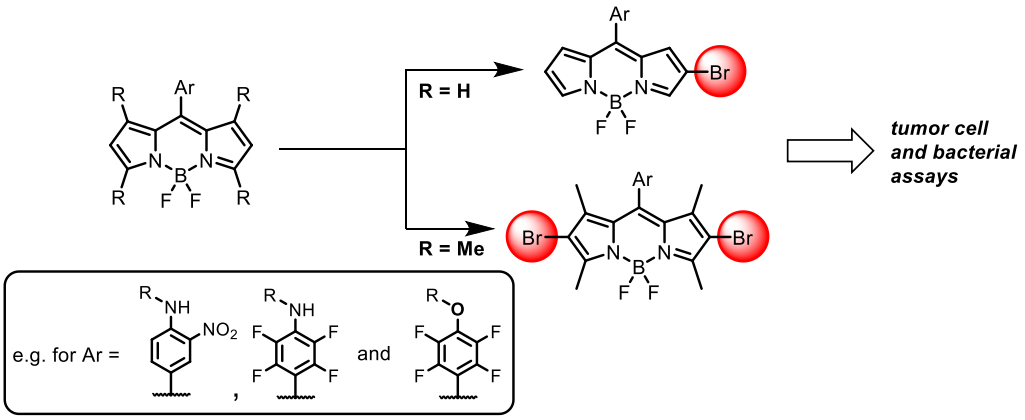

Scheme 15: Schematic representation of the modification of the BODIPY core structure.

In a proof-of-concept investigation, BODIPYs were also tested as building blocks for the synthesis of conjugates with a cyclen or a dipyrrinato complex (Scheme 16). The coupling of these structural components should be realized *via* the copper(I)-catalyzed azide-alkyne cycloaddition.

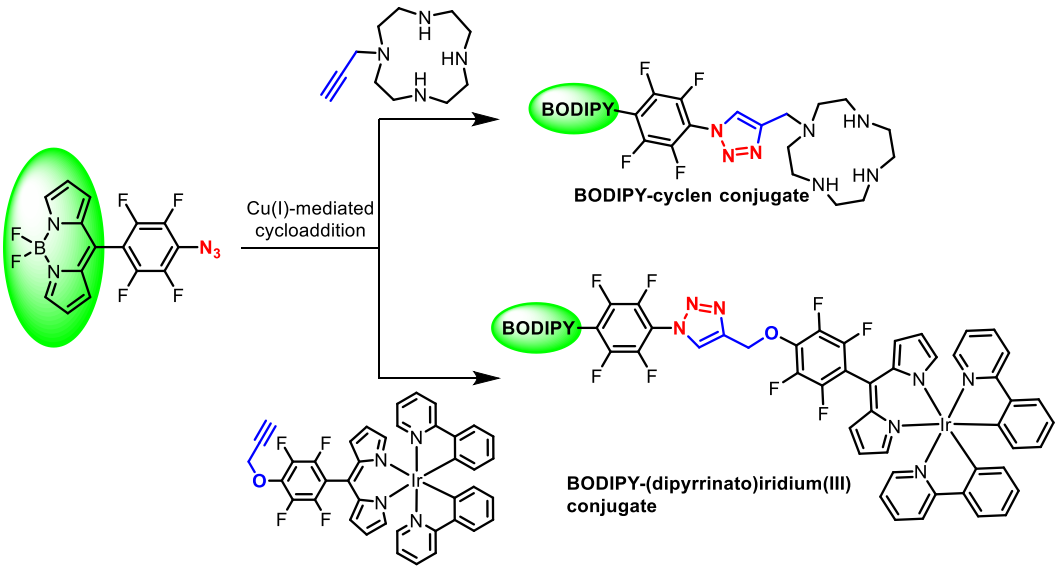

Scheme 16: Schematic representation of the preparation of BODIPY conjugates.

2. Summary of publications

2.1 *meso*-(4-Amino-3-nitrophenyl)-substituted dipyrromethanes as building blocks for BODIPYs and dipyrrinato ruthenium(II) complexes

In this publication 3-nitro-substituted dipyrromethanes were introduced as possible building blocks for porphyrins, corroles, BODIPYs, and dipyrrinato ruthenium(II) complexes. The 3,4,5-tetrafluorophenyl moiety was also investigated as an alternative substituent for *meso*-substituted dipyrromethanes, to form the related tetrapyrrole macrocycles and BODIPYs. Some of these compounds had been prepared in the context of the previous master thesis of B. Hohlfeld.[99] For the present thesis, the respective 3-nitrophenyl-based dipyrromethanes were employed as starting materials for the preparation of dipyrrins, BODIPYs, and dipyrrinato ruthenium(II) complexes. Specifically, the 4-fluoro-3-nitrophenyl group was investigated as an alternative to the pentaflourophenyl group, as the pentafluorophenyl moiety had already been established as a suitable structural element for *meso*-substituted dipyrromethanes. The electron-withdrawing effect of the pentafluorophenyl substituent stabilizes the dipyrromethane against decomposition and the *para*-fluorine enables efficient nucleophilic substitutions. The *para*-fluorine exchange can be performed with various nucleophiles, e.g., amines, alcohols, or thiols. *meso*-Substituted dipyrromethanes functionalized in this way were employed for the synthesis of the corresponding porphyrins, corroles, BODIPYs, or other tetrapyrroles. [50b,52,96] In the 4-fluoro-3-nitrophenyl moiety, the nitro group also exerts an electron-withdrawing effect, so that an application of the 4-fluoro-3-nitrophenyl moiety appeared to be applicable as a building block for *meso*-substituted dipyrromethanes. So far, only a limited number of amines were reported for the nucleophilic substitutions of the fluoro-3-nitrophenyl moiety.[97]

First, it was investigated whether the 4-fluoro-3-nitrobenzaldehyde is suitable for the synthesis of *meso*-substituted dipyrromethanes. For this, the corresponding 5-(4-fluoro-3-nitrophenyl)-dipyrromethane **1** was prepared from 4-fluoro-3-nitrobenzaldehyde und pyrrole (Scheme 17). Pyrrole was used in large excess, to suppress further polymerization of the resulting dipyrromethane and trifluoroacetic acid was used as the acid catalyst. Finally, the corresponding dipyrromethane **1** could be obtained as light-yellow solid with an excellent yield of 92%.

Dipyrromethane **1** served as starting material for the subsequent functionalization with nucleophiles. Starting form **1**, nucleophilic substitutions with several different amines were investigated. In addition to simple primary amines, e.g., *n*-butylamine, amines with additional functional groups were also tested, e.g., a hydroxy group or a terminal alkyne group. In many cases, an almost complete consumption of **1** could be observed within one hour.

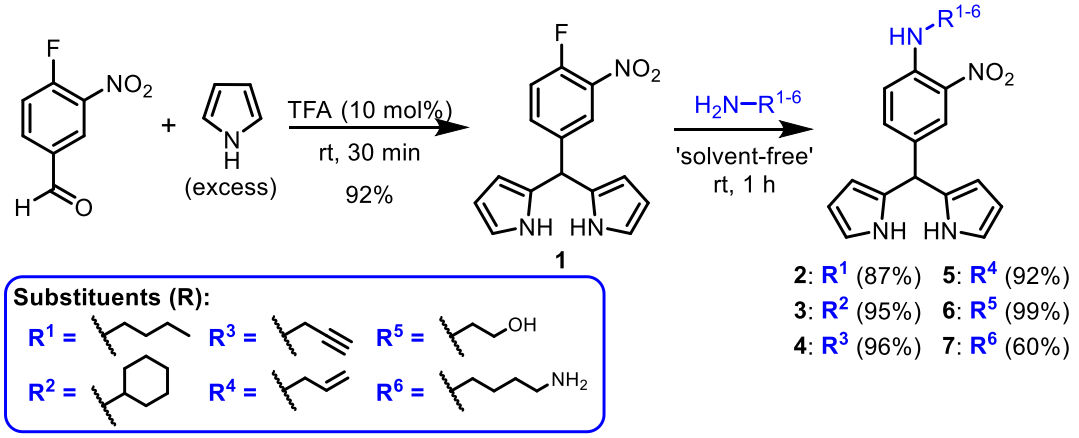

Scheme 17: Synthesis of dipyrromethane **1** und nucleophilic substitution with amines.

Furthermore, the reactions could be carried out under solvent-free conditions. Dipyrromethane **1** was simply dissolved in the amines tested and stirred without any heating. With all investigated amines high yields - in some cases nearly quantitative yields - could be achieved (Scheme 17).

In addition, a secondary amine and aniline were also tested for the nucleophilic substitution. For *N*,*N*-dibutylamine, a successful functionalization in high yield was achieved (Scheme 18). Also, in the case of aniline, substitution was successful, however, the product could not be completely separated from the unreacted aniline used in excess. Finally, also solid amines were tested with the substitution of **1** (6-methoxy-6-oxohexane amine and serinol, Scheme 18). In these cases, the amine and dipyrromethane **1** were dissolved in a suitable solvent. Significantly longer reaction times were required compared to the solvent-free variants. Nevertheless, the related products **10** and **11** were again obtained in excellent yields (Scheme 18).

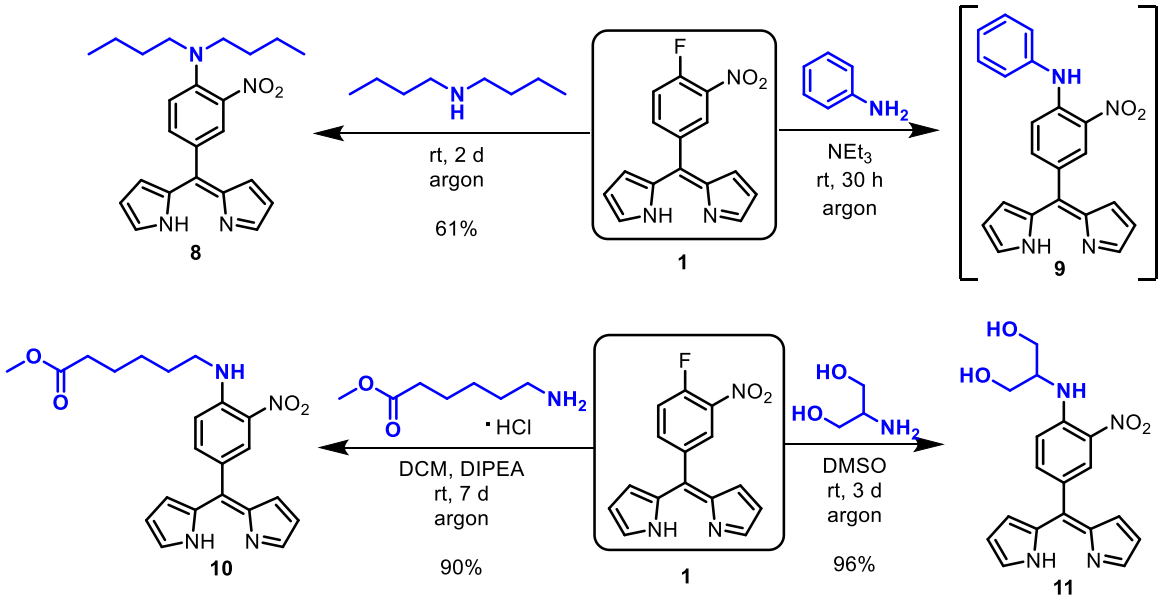

Scheme 18: Nucleophilic substitution of dipyrromethane **1** with amines. Product **9** contained aniline, which could not be completely removed.

The scope of possible nucleophiles was also extended to an azido group. In the substitution of **1** with sodium azide again a nearly quantitative yield was obtained (Scheme 19).

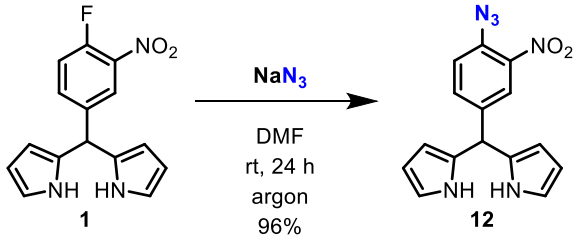

Scheme 19: Nucleophilic substitution of dipyrromethane **1** with sodium azide.

Beyond amines and an azide, alcohols are in principle also possible nucleophiles for the substitution of **1**. To test this, dipyrromethane **1** was reacted with butanol to obtain the corresponding butoxy-substituted product **13**. However, a successful substitution with butanol was not achieved. Instead, the formation of various compounds was observed. In this case, the occurrence of multiple compounds gave evidence for the decomposition of the dipyrromethane under the conditions for the substitution with alcohols.

In the following reactions, these *meso*-substituted dipyrromethanes served as building blocks for the subsequent preparation of BODIPYs and dipyrrins (Table 1 and Scheme 20). The BODIPYs were synthesized according to the well-known oxidation-complexation sequence.[27a,67b,82,83] Almost all syntheses were carried out in dichloromethane (DCM) and yielded in the desired BODIPYs (Table 1). Using the pre-functionalized dipyrromethanes, different BODIPYs with a wide range of functionalized groups could be synthesized, e.g., alkene group, alkyne group, hydroxy group, or azido group. However, the preparation of BODIPY **18** was only successful when using THF as solvent (Table 1).

Table 1: Preparation of BODIPYs from pre-functionalized dipyrromethanes.

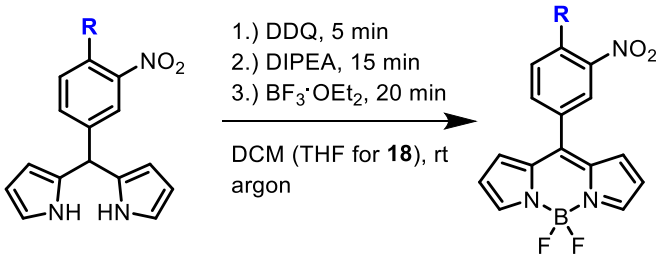

Entry	Starting material	Substituent (R)	Product	Yield [%]
1	**1**		**21**	25
2	**2**	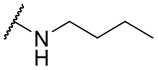	**14**	38
3	**3**	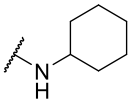	**15**	20
4	**4**	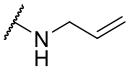	**16**	39
5	**5**	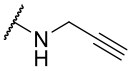	**17**	44
6	**6**	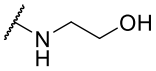	**18**	25
7	**8**	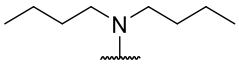	**19**	33
8	**10**	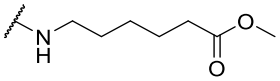	**20**	41
9	**12**		**22**	26

The pre-functionalized dipyrromethanes were as well applied for the synthesis of the related dipyrrins. For this, a selection of dipyrromethanes was treated with *p*-chloranil, to produce the desired dipyrrins. All oxidations led to the *meso*-substituted dipyrrins (Scheme 20).

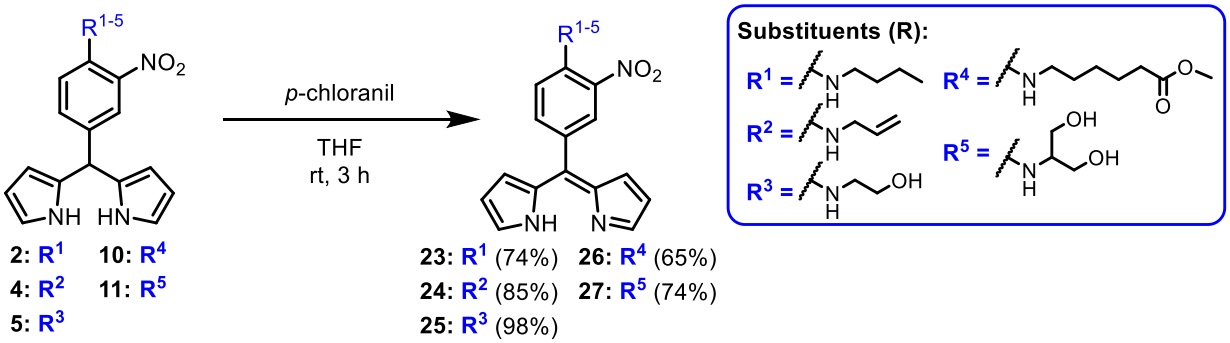

Scheme 20: Oxidation of pre-functionalized dipyrromethanes.

In the next part, the dipyrrins were investigated for their potential in the synthesis of heteroleptic dipyrrinato ruthenium(II) complexes. Hence, the dipyrrins were reacted with a dichlorido-bridged (*p*-cymene)ruthenium(II) half-sandwich complex and *N*,*N*-diisopropylethylamine (DIPEA) to form the

chlorido(*p*-cymene)(dipyrrinato)ruthenium(II) complexes. All tested dipyrrins were successfully transferred into the dipyrrinato ruthenium(II) complexes, with yields of at least 40% (Scheme 21).

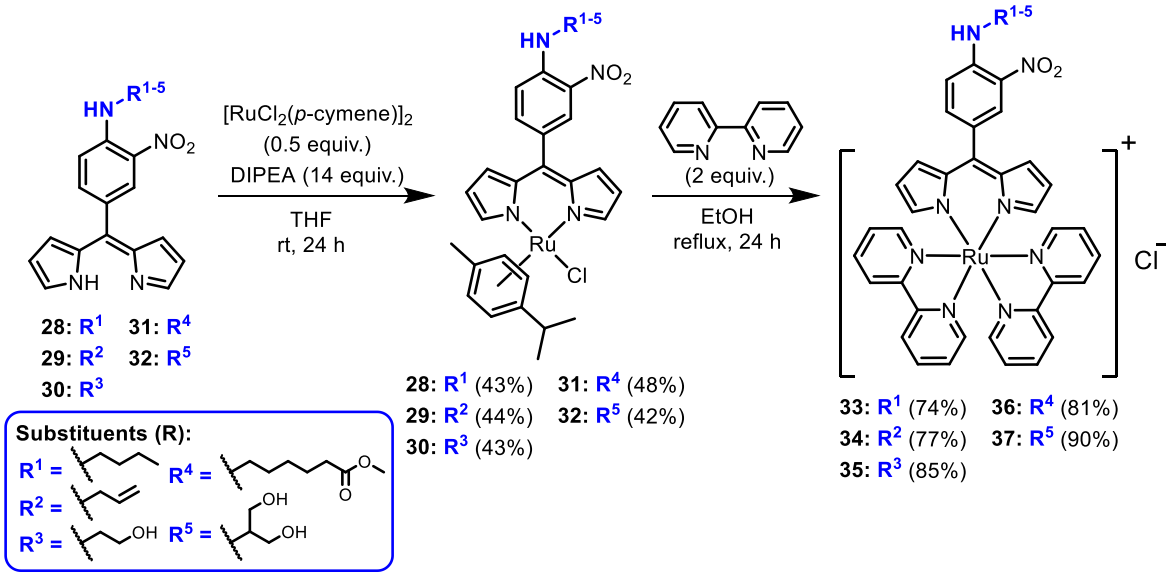

Scheme 21: Preparation of heteroleptic chlorido(*p*-cymene)(dipyrrinato)ruthenium(II) complexes and subsequent ligand exchange with 2,2‘-bipyridine.

Finally, the ligand exchange with the chlorido(*p*-cymene)(dipyrrinato)ruthenium(II) complexes and 2,2’-bipyridine was investigated. For this, the dipyrrinato ruthenium(II) complexes were dissolved together with 2,2’-bipyridine in ethanol and reacted under reflux. In this final step, the desired bis(2,2‘-bipyridyl)(dipyrrinato)ruthenium(II) complexes were obtained with high yields (Scheme 21).

The BODIPY core structure enables a variety of further modifications with different substituents.[100] Among other nucleophiles, derivatives of malonic acid are suitable for the functionalization of the BODIPY core structure *via* oxidative nucleophilic substitution of a hydrogen atom at one of the pyrrole rings.[101] Here, selected 8-(4-amino-3-nitrophenyl)-substituted BODIPYs were evaluated for the modification of the 3-position of the BODIPY with dimethyl malonate (Scheme 22).

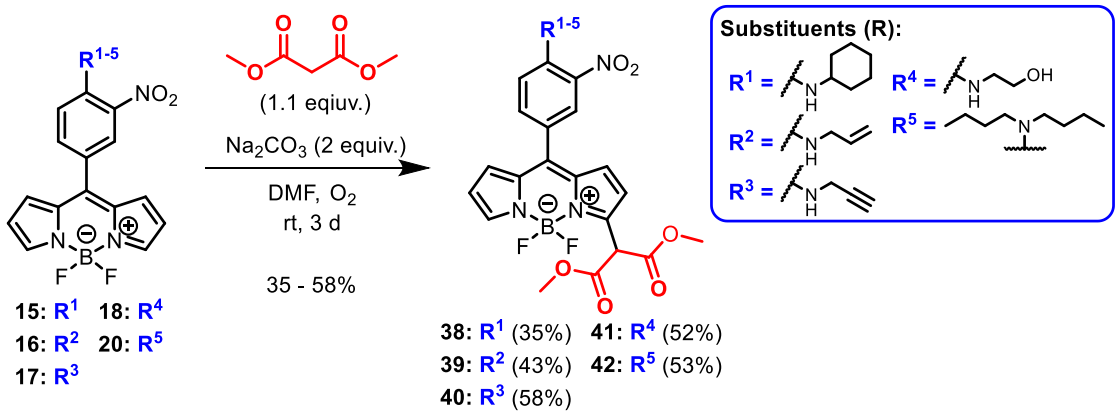

Scheme 22: Modification of the BODIPY core structure with dimethyl malonate.

For the substitution of the related 3-position, the BODIPYs were reacted with the dimethyl malonate under an oxygen-rich atmosphere. Finally, all core modified BODIPYs were formed with yields up to 58% (Scheme 22).

In addition, for BODIPY **14** and the dipyrrinato ruthenium(II) complex **28**, X-ray structure analyses could be performed confirming the structure in the solid state (Fig. 25). These molecular structures were measured, dissolved, and refined by Dr. Keith Flanagan from the group of Prof. Mathias O. Senge at Trinity College Dublin.

Remarkably, an intermolecular hydrogen bond between the hydrogen of the amine and the related nitro group was found for both compounds. This hydrogen bonds ensured, that the corresponding nitro group is arranged planar to the corresponding phenyl ring.

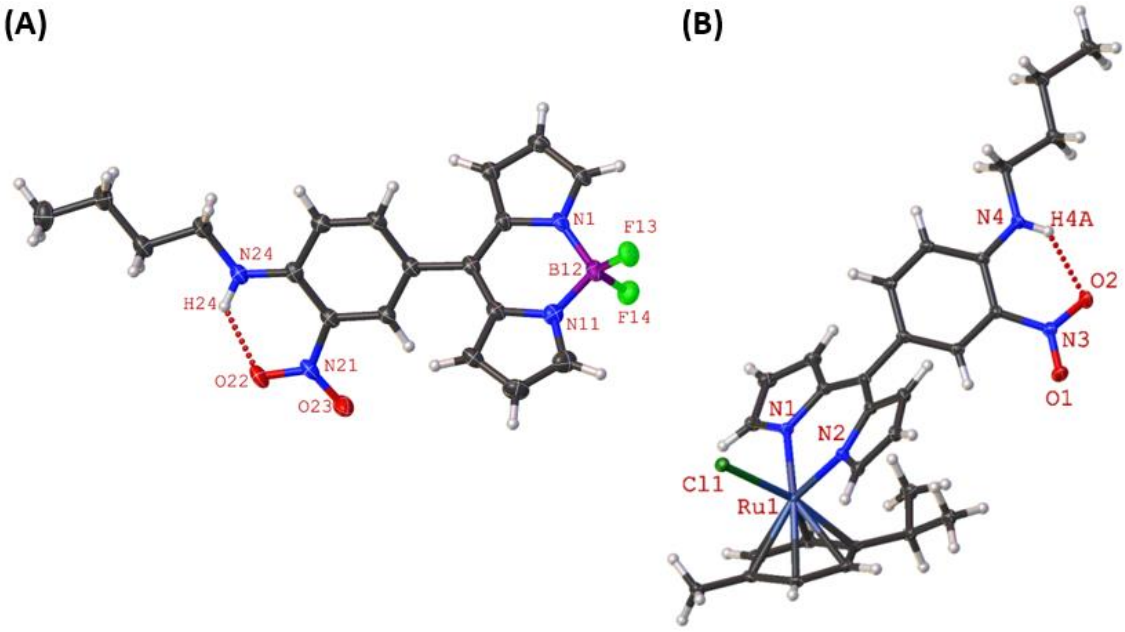

Figure 25: Molecular structures for BODIPY **14** (A) and (dipyrrinato)ruthenium(II) complex **28** (B) with indicated hydrogen bond.

In summary, a very efficient substitution of the 5-(4-fluoro-3-nitrophenyl)dipyrromethane with a wide range of amines under solvent-free conditions could be achieved. Furthermore, the scope of possible nucleophiles was not limited to simple amines, but also amines with additional functional groups and an azido group allowed an efficient substitution of the 4-fluoro-3-nitrophenyl substituent. These functionalized dipyrromethanes proved to be suitable building blocks for the further preparation of BODIPYs and dipyrrins. Moreover, the functionalized dipyrrins afforded the preparation of corresponding chlorido(*p*-cymene)(dipyrrinato)ruthenium(II) complexes. Finally, a ligand exchange in these chlorido(*p*-cymene)(dipyrrinato)ruthenium(II) complexes enabled the synthesis of the respective bis(2,2‘-bipyridyl)(dipyrrinato)ruthenium(II) complexes.

Starting from the 5-(4-fluoro-3-nitrophenyl)dipyrromethane, more than 30 new related dipyrromethanes, dipyrrins, BODIPYs, and heteroleptic dipyrrinato ruthenium(II) complexes, were synthesized. Thus, the 4-fluoro-3-nitrophenyl moiety turned out as a prominent substituent for the synthesis of *meso*-substituted dipyrromethanes, dipyrrins, and related dipyrrinato complexes.

2.2 Modification of the BODIPY structure *via* the targeted functionalization with bromine and the introduction with additional functional groups

In this project, the BODIPY structure was subject of modifications to adjust the properties towards improved photosensitizing abilities. As a result of the introduction of halogen atoms, the generation of singlet oxygen should be significantly improved enabling an application as photosensitizers in PDT. Moreover, BODIPYs carrying a pentafluorophenyl or a 4-fluoro-3-nitrophenyl moiety in the *meso*-position were subjected to the combination of targeted BODIPY core substitution with bromine and nucleophilic substitution. The nucleophilic substitution allowed the introduction of different functional groups, e.g., a terminal alkyne group, free hydroxy groups, or thiocarbohydrates.

In preparation for the following steps, the 5-pentafluorophenyldipyrromethane **43** was functionalized with *n*-butylamine and 1-butanol (Scheme 23). Having these two functionalized dipyrromethanes (**44** and **45**) at hand, the corresponding functionalized BODIPYs (**46** and **47**) were prepared (Scheme 23). The synthesis of the unsubstituted dipyrromethane **43** and the butoxy-substituted dipyrromethane **45** were carried out according to the literature.[52,55]

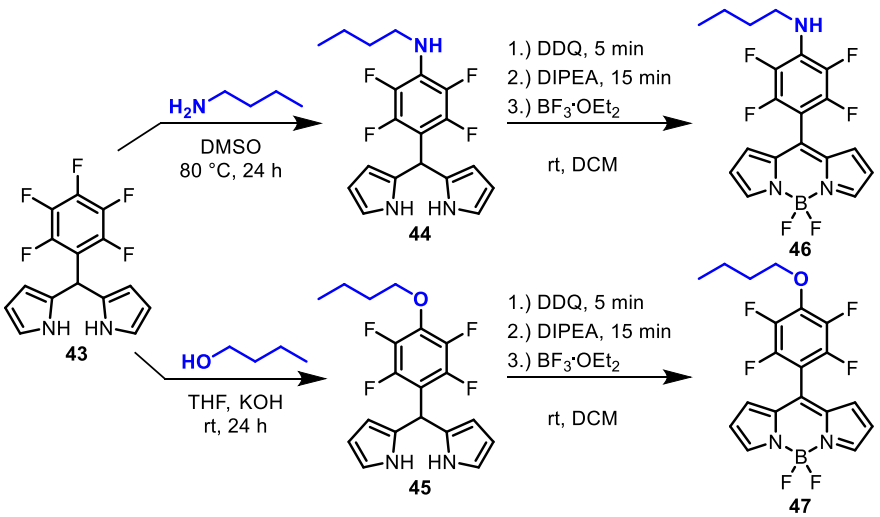

Scheme 23: Functionalization of BODIPY **43** with *n*-butylamine and 1-butanol, followed by subsequent transformation into BODIPYs **46** and **47**.

First, the targeted halogenation of the 2- and 6-positions at the BODIPY was investigated with selected BODIPYs. Starting from the 3-nitrophenyl-substituted BODIPYs **14** and **21**, the substitutions were performed with NBS in hexafluoroisopropanol (HFIP). Under these conditions (HFIP and NBS) an almost

instantaneous conversion was observed. However, halogenation of multiple positions of the BODIPY core structure occurred, resulting in a mixture of different (brominated) BODIPYs (Scheme 24, variant A). A complete separation of the different reaction products was not possible, after purifications still a mixture of BODIPYs was obtained. The same results were observed for the substitutions of the pentafluorophenyl BODIPY **48** and the 4-propargyloxy-tetrafluorophenyl BODIPY **49** (Scheme 24, variant A). The pentafluorophenyl-BODIPY **48** and the 4-propargyloxy-2,3,5,6-tetrafluorophenyl-BODIPY **49** had been prepared from their related dipyrromethanes according to the literature.[52]

To obtain the desired 2,6-dibrominated BODIPYs, the experiments were repeated with BODIPYs **21** and **48**, however, in this case, HFIP was replaced by DCM to achieve a slower and targeted halogenation of the BODIPY. In fact, a significantly longer reaction time was observed for the halogenation of the BODIPYs in DCM. Interestingly, the desired di-brominated BODIPYs **50** and **52** were only obtained in minor amounts. The major compounds were identified as the corresponding mono-brominated BODIPYs **54** and **55** (Scheme 24, variant B). Also, other brominated BODIPYs could be found, however, these BODIPYs were only detected in very low quantities.

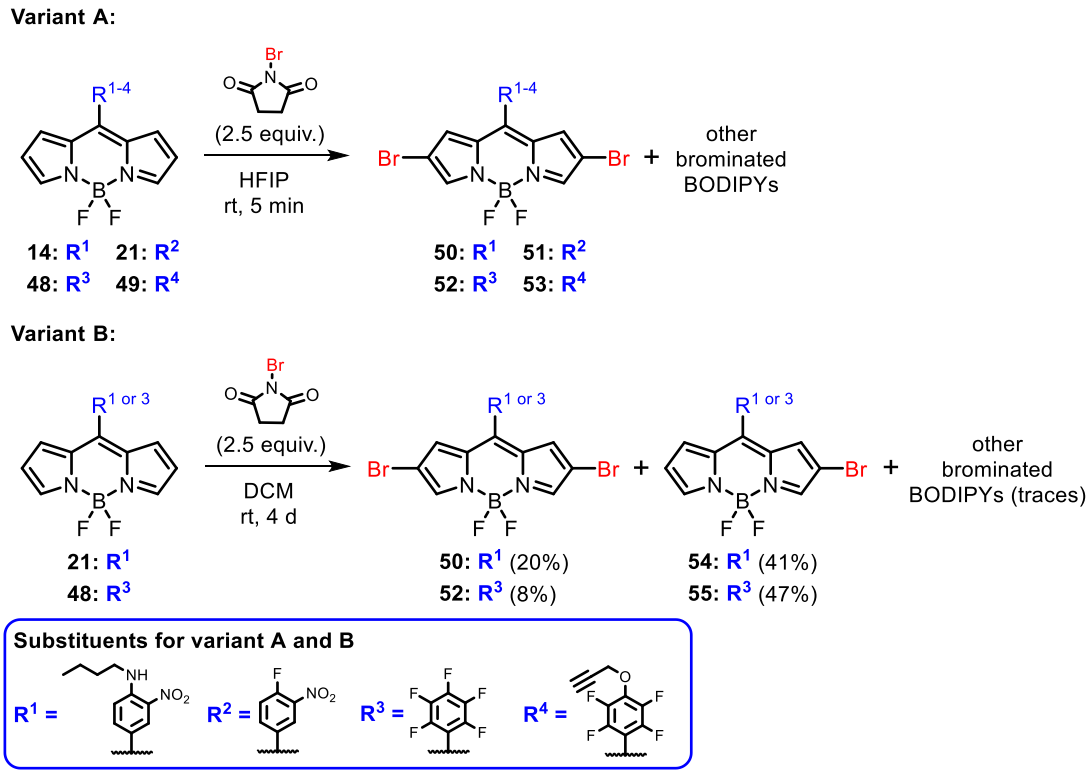

Scheme 24: Modification of the BODIPY core structure with NBS in HFIP and DCM (BODIPYs **48** and **49** had been prepared according to the literature).[52]

Finally, a selective bromination of the 2-position was possible by an adjusted reaction time with DCM as solvent. For the tested tetrafluorophenyl-substituted BODIPYs a reaction time between one and 2.5 hours was optimal to provide a targeted mono-bromination of the BODIPY core structure. The highest yield was achieved with the unsubstituted BODIPY **48**. The halogenation with the additional pre-

functionalized BODIPYs provided the respective mono-brominated products as well, in moderate to high yields (Scheme 25).

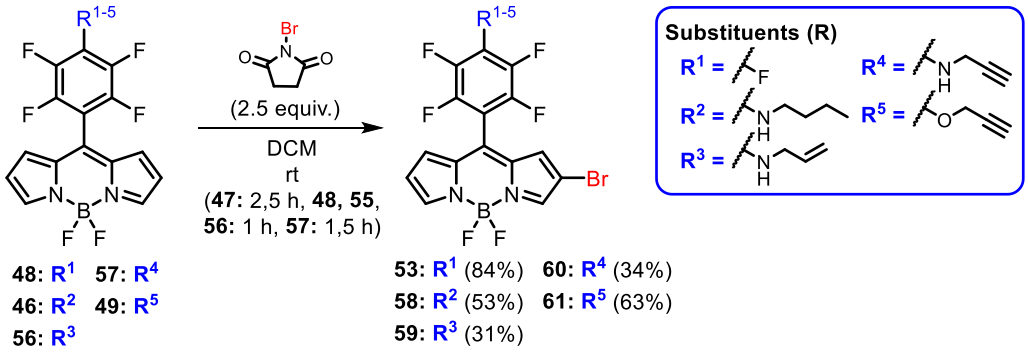

48: R^1 **57:** R^4
46: R^2 **49:** R^5
56: R^3

53: R^1 (84%) **60:** R^4 (34%)
58: R^2 (53%) **61:** R^5 (63%)
59: R^3 (31%)

Scheme 25: Targeted halogenation of tetrafluorophenyl-substituted BODIPYs (BODIPYs **56** and **57** had been prepared according to the literature[52]).

With the 3-nitrophenyl-substituted BODIPYs **14**, **17**, and **21** similar results were obtained for the halogenation in DCM. Here, a reaction time of three hours was required for a targeted mono-bromination of the 2-position. Again, the highest yield was achieved with the unsubstituted BODIPY **21**. Using the pre-functionalized BODIPYs, the respective products were also formed in moderate yields (Scheme 26). In comparison, there is a tendency that the tetrafluorophenyl-based BODIPYs provide higher yields.

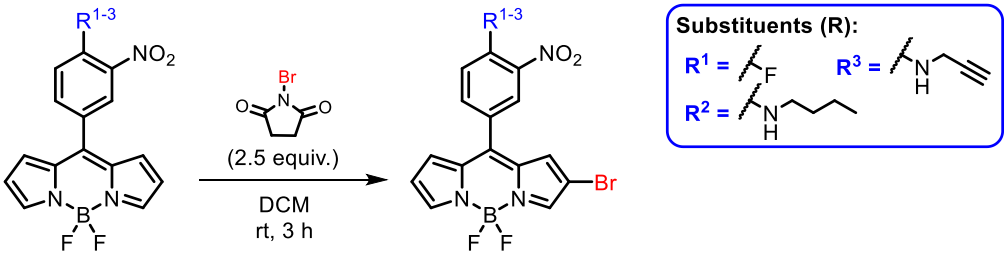

21: R^1 **17:** R^3
14: R^2

61: R^1 (64%) **64:** R^3 (30%)
63: R^2 (48%)

Scheme 26: Targeted halogenation of 3-nitrophenyl-substituted BODIPYs.

To achieve a selective halogenation of the 2- and 6-position, the investigations were continued with BODIPYs where specific positions of the core structure were blocked by methyl groups. For this, 1,3,5,7-tetramethyl-substituted BODIPYs were chosen for further halogenations. Again, these BODIPYs (**65** and **66**) were equipped with the pentafluorophenyl and the 4-fluoro-3-nitrophenyl moiety at the *meso*-position. The synthesis for BODIPY **65** had been performed according to the literature[102] and was expanded to the 4-fluoro-3-nitrophenyl benzaldehyde. In detail, the corresponding benzaldehydes were reacted with 2,4-dimethylpyrrole under trifluoroacetic acid-catalysis, followed by oxidation, deprotonation with DIPEA, and BF_3 complexation to form the desired BODIPYs **65** and **66** (Scheme 27).

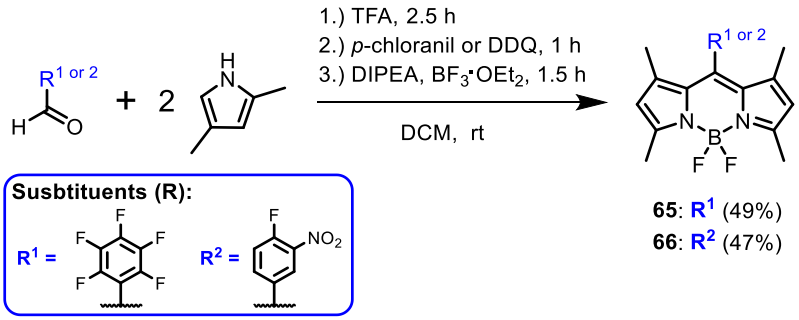

Scheme 27: Preparation of the 1,3,5,7-tetramethyl-substituted BODIPYs **65** und **66**.

In the next step, nucleophilic substitutions with different amines were performed using the BODIPYs **65** and **66**. A substitution of **65** had already been described, however, only *n*-butylamine was presented as an example for the functionalization.[102] Now, systematic nucleophilic substitutions of BODIPY **65** with different amines were carried out. Amines with additional functional groups were chosen, e.g., a terminal alkynyl group or free hydroxy groups. The reactions with the tested amines provided the respective functionalized BODIPYs, except for the case of serinol (R^4), where the related product could not be obtained (Scheme 28).

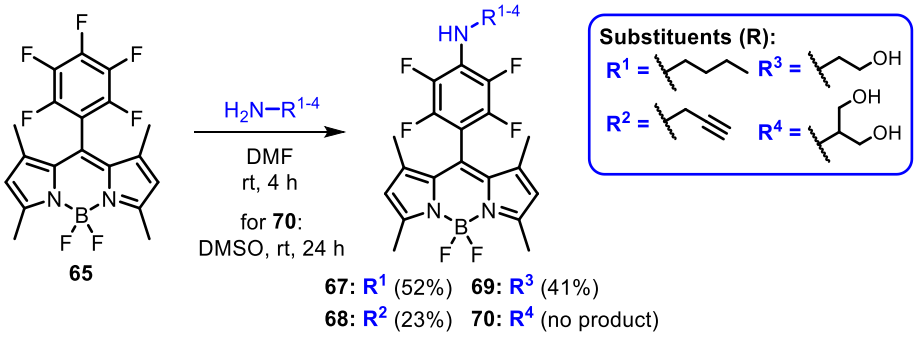

Scheme 28: Nucleophilic substitutions of BODIPY **65** with amines.

BODIPY **66** was also reacted with the same set of amines. In these cases, all substitutions led into the formation of the corresponding substituted BODIPYs. Serinol could be as well employed for the substitution of BODIPY **66** (Scheme 29). In comparison, the nucleophilic substitutions with BODIPY **66**, carrying the 4-fluoro-3-nitrophenyl moiety were more effective.

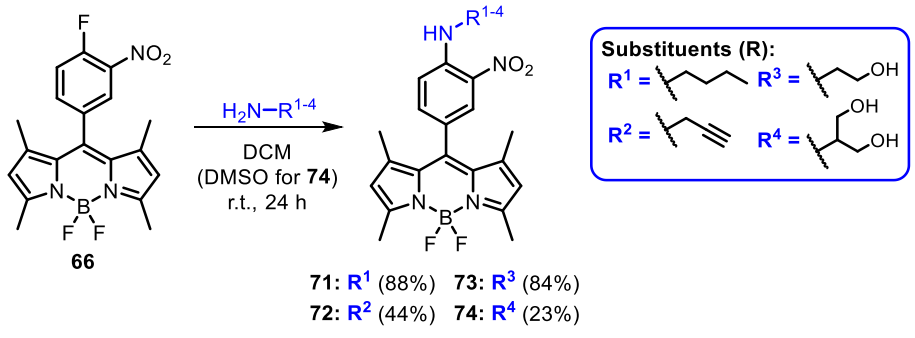

Scheme 29: Nucleophilic substitutions of BODIPY **66** with amines.

Finally, the modification of the BODIPY core structure was performed with these 1,3,5,7-tetramethyl BODIPYs. For this, the BODIPYs were dissolved in HFIP and treated with NBS. Again, a complete consumption of the starting materials could be detected after a very short reaction time. The selective halogenation finally succeeded with NBS, and a bromination of other positions than the desired 2- and 6- positions could not be found. All 2,6-dibromated tetrafluorophenyl-based BODIPYs were obtained in good yields (Scheme 30).

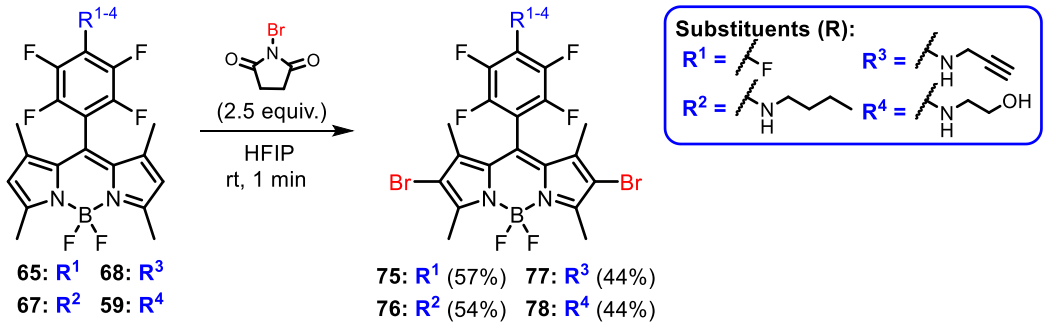

65: R^1 **68:** R^3
67: R^2 **59:** R^4

75: R^1 (57%) **77:** R^3 (44%)
76: R^2 (54%) **78:** R^4 (44%)

Scheme 30: Halogenation of the tetrafluorophenyl-substituted BODIPYs with NBS.

Similar results were found for the 3-nitrophenyl-based BODIPYs. Here, also, only a short reaction time was required for the targeted halogenation of the 2- and 6-position in HFIP. The corresponding products were obtained in good yields, without any evidence for a substitution of other positions of the core structure than the desired 2- and 6-position (Scheme 31).

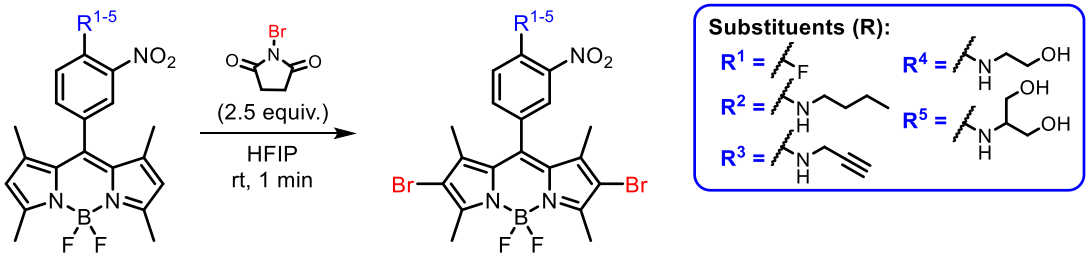

66: R^1 **73:** R^4
71: R^2 **74:** R^5
72: R^3

79: R^1 (57%) **82:** R^4 (54%)
80: R^2 (63%) **83:** R^5 (48%)
81: R^3 (44%)

Scheme 31: Halogenation of the 3-nitrophenyl-substituted BODIPYs with NBS.

Carbohydrates were also tested in the substitution of the 1,3,5,7-tetramethyl-BODIPYs **65** and **66**. Here, thio-*β*-D-carbohydrates had been used for direct substitution of the *para*-phenyl positions. The sodium salts of thioglucose and thiogalactose were reacted with the BODIPYs (**65** and **66**) to form the glycosylated derivatives (**84**, **85**, **88**, and **89**). The glycosylated BODIPYs could be obtained in high yields within 15 minutes (Scheme 32). Subsequently, the glycosylated BODIPYs were reacted with NBS to functionalize the 2- and 6-position of the BODIPY core structure with bromine. This halogenation of the glycosylated BODIPYs afforded the desired products in good yields (Scheme 32).

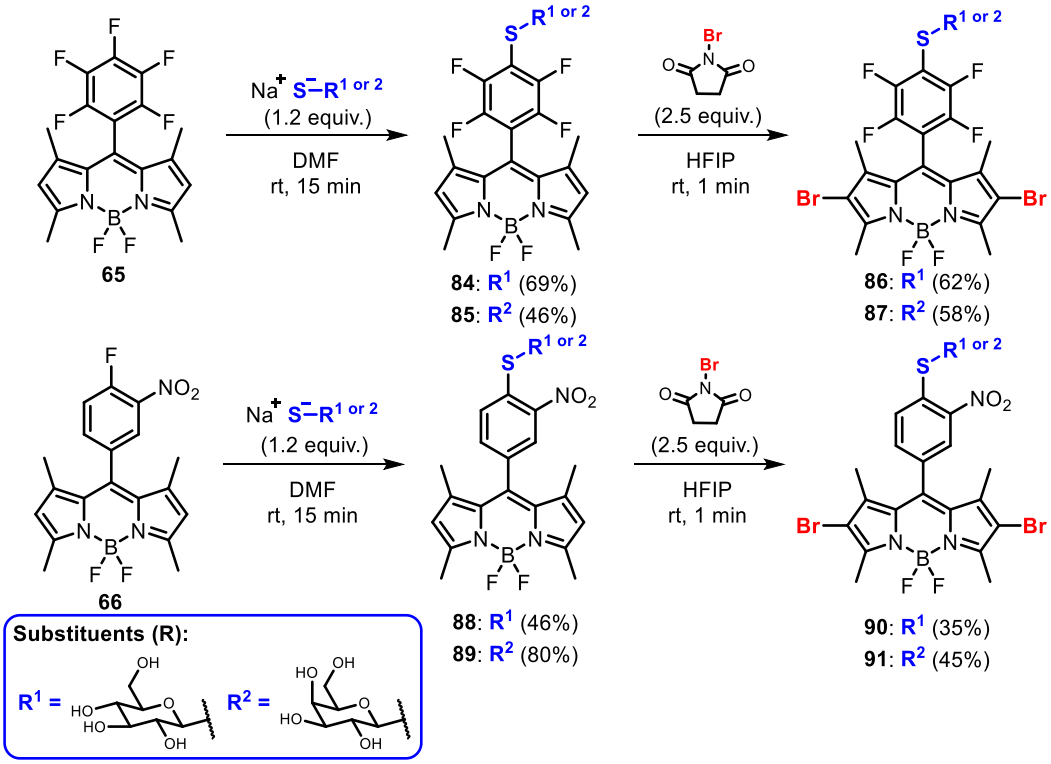

Scheme 32: Glycosylation and subsequent halogenation with NBS of BODIPYs **65** und **66**.

In addition, the glycosylation was also extended to the core-unsubstituted BODIPYs **21** and **48**. Using the synthetic procedure described above, the BODIPYs **21** and **48** were also successfully substituted with thioglucose and thiogalactose in high yields. (Scheme 33).

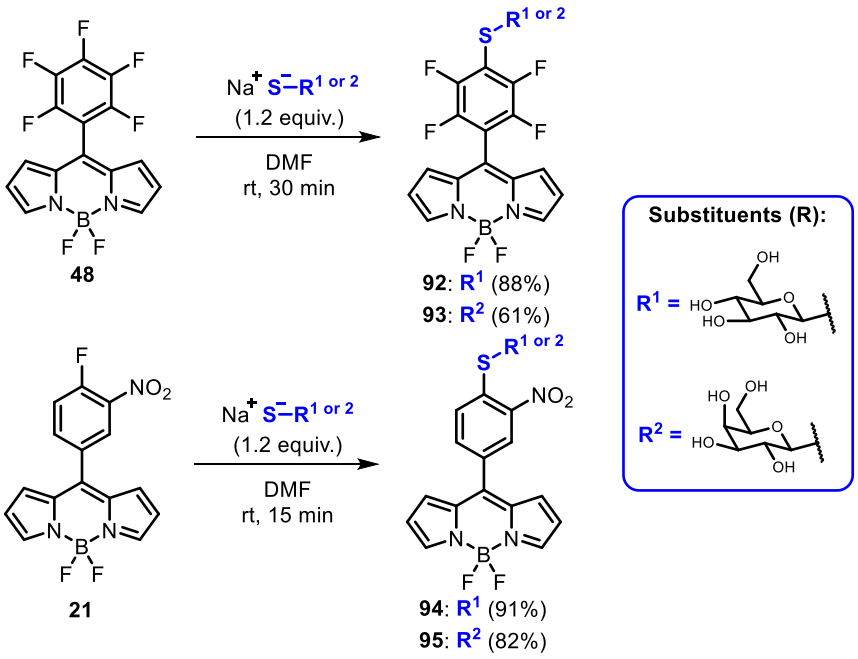

Scheme 33: Glycosylation of the core-unsubstituted BODIPYs **21** und **48**.

The dark and phototoxicity of the core-modified BODIPYs was evaluated in bacterial assays against *S. aureus* and *P. aeruginosa*. The antimicrobial activity was not only investigated in phosphate-buffered

saline (PBS), but additional experiments in the presence of blood serum were performed. The proteins present in serum or wounds can have significant effects on the effectiveness of therapeutic agents. These antimicrobial assays were carried out by the biolitec research GmbH.

In the bacterial assays, all tested 2,6-dibromo-1,3,5,7-tetramethyl-substituted BODIPYs proved to be highly effective compounds against *S. aureus*. The modified BODIPYs showed a significant dark toxicity at the highest concentration. Under light irradiation an inactivation of bacteria beyond the detection limit was achieved even at low concentrations. In the presence of serum, the dark and phototoxicity decreased. However, a significant phototoxic activity against *S. aureus* was still found for the 2,6-dibromo-1,3,5,7-tetramethyl-substituted BODIPYs, functionalized with thiocarbohydrates or free hydroxy groups. In addition, some mono-brominated BODIPYs also showed a phototoxic activity against *S. aureus* even in the presence of serum. Remarkably, some glycosylated BODIPYs even exhibited a notable phototoxic activity against the Gram-negative germ *P. aeruginosa* under irradiation.

In summary, the combination of the targeted bromination of the BODIPY core structure with the nucleophilic substitution of the 4-fluoro-3-nitrophenyl and the pentafluorophenyl moiety was successfully applied for the preparation of the desired modified BODIPYs. In the case of the targeted bromination of the 2- and 6-positions, the 1,3,5,7-tetramethyl-substitutued BODIPYs were more suitable since the halogenation of the core-unsubstituted BODIPYs yielded multiple substitutions with bromine. However, with the core-unsubstituted BODIPYs a selective halogenation of the 2-position proved to be possible. Using the synthetic procedures described above, brominated BODIPYs with a set of different functional groups were presented. Moreover, this protocol was also suitable for combining the substitution with bromine and the introduction of thiocarbohydrates. Especially, the combination of the 2,6-dibromo-1,3,5,7-tetramethyl-BODIPYs structure with thiocarbohydrates resulted in effective photosensitizers for a possible application against *S. aureus* and *P. aeruginosa*. Also, the mono-brominated derivatives showed promising potential as photoactive compounds.

2.3 meso-Substituted dipyrrins as building blocks for photoactive dipyrrinato iridium(III) complexes

In this project *meso*-substituted dipyrrins were used for the preparation of heteroleptic dipyrrinato iridium(III) complexes. In general, iridium complexes are of high interest as possible therapeutically active compounds against cancer. As well, for some cyclometalated iridium(III) complexes a generation of ROS has been reported, which highlights these types of complexes for an application in PDT. Here, dipyrrins based on the pentafluorophenyl and the 4-fluoro-3-nitrophenyl moiety were investigated as suitable ligands for the synthesis of dipyrrinato iridium(III) complexes. In addition, dipyrrins with additional functional groups, e.g., terminal alkene or alkyne groups, free hydroxy groups, and thiocarbohydrates, were applied for the synthesis of functionalized dipyrrinato iridium(III) complexes.

In analogy to the oxidation of *meso*-(4-amino-3-nitrophenyl)dipyrromethanes, the tetrafluorophenyl-substituted dipyrromethanes were oxidized in the same way. In preparation for this, the pre-functionalized dipyrromethanes **96** – **101** were synthesized according to the literature.[50b,52] *p*-Chloranil could be applied to transform all tetrafluorophenyl-based dipyrromethanes into the respective dipyrrins in good to excellent yields (Scheme 34). As an alternative to *p*-chloranil, DDQ was tested for the oxidation of the dipyrromethanes. In general, higher yields were found with *p*-chloranil for the oxidation of the dipyrromethanes, compared to DDQ as oxidation agent.

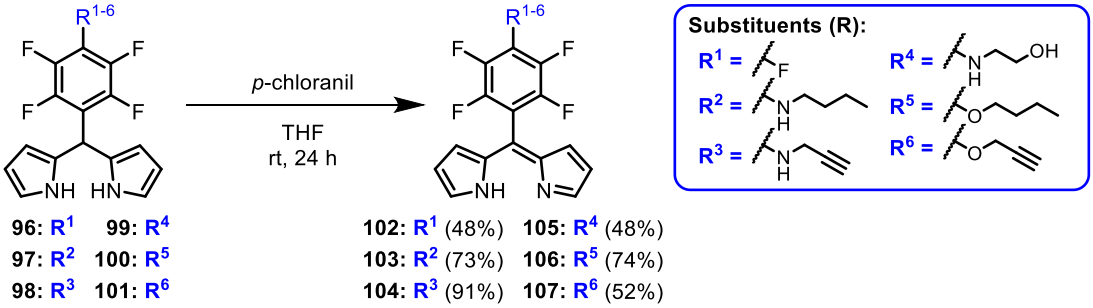

96: R^1 **99:** R^4
97: R^2 **100:** R^5
98: R^3 **101:** R^6

102: R^1 (48%) **105:** R^4 (48%)
103: R^2 (73%) **106:** R^5 (74%)
104: R^3 (91%) **107:** R^6 (52%)

Scheme 34: Preparation of tetrafluorophenyl-substituted dipyrrins *via* oxidation with *p*-chloranil.

The 3-nitrophenyl-based dipyrromethanes were oxidized to the corresponding dipyrrins. In addition to the already described 3-nitrophenyl-based dipyrrins (see chapter 2.1), the oxidation of the dipyrromethanes **1**, **4**, and **8** was carried out analogously with *p*-chloranil. Except for the unsubstituted dipyrromethane **1**, all tested dipyrromethanes were successfully transformed into the related dipyrrins. In the case of the unsubstituted dipyrromethane **1**, no reaction could be observed using *p*-chloranil (Scheme 35).

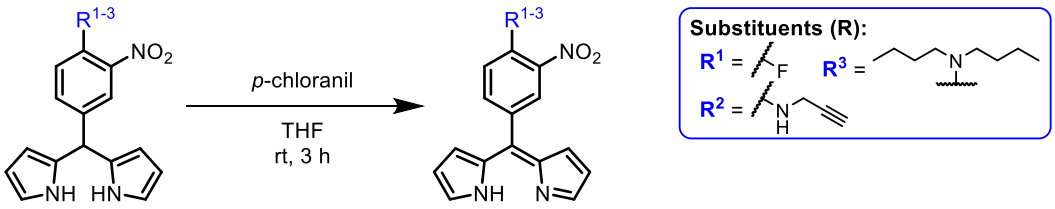

1: R^1 **8:** R^3
4: R^2

108: R^1 (no product) **110:** R^3 (71%)
109: R^2 (57%)

Scheme 35: Preparation of 3-nitrophenyl-subtitutued dipyrrins *via* oxidation with *p*-chloranil.

To obtain the unsubstituted dipyrrin **108**, the reaction was repeated with DDQ as the oxidation agent. With DDQ, the respective product **108** could be obtained in high yields (Scheme 36). In the oxidation of the 3-nitrophenyl-based dipyrromethanes, DDQ provided again lower yields.

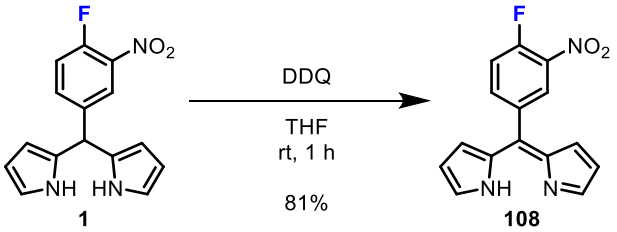

Scheme 36: Oxidation of dipyrromethane **1** with DDQ.

In the next step, the preparation of chlorido(dipyrrinato)(pentamethylcyclopentadienyl)iridium(III) complexes was performed. Tetrafluorophenyl-based dipyrrins were reacted with DIPEA and the dichlorido-bridged (pentamethylcyclopentadienyl)iridium(III) half-sandwich complex. Related dipyrrinato iridium(III) complexes were exclusively formed with dipyrrins carrying no terminal alkene or alkyne groups (Table 2).

Table 2: Preparation of chlorido(pentamethylcyclopentadienyl)(dipyrrinato)iridium(III) complexes from tetrafluorophenyl-based dipyrrins.

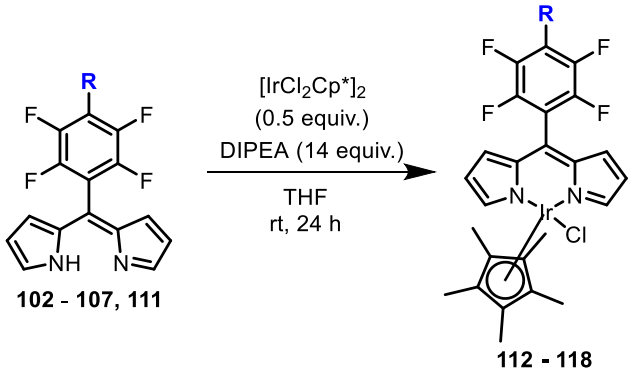

Entry	Starting material	Substituent (R)	Product	Yield [%]
1	**102**		**112**	91
2	**103**	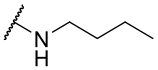	**113**	36
3 [a,b]	**104**	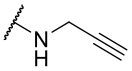	**114**	
4	**105**	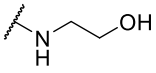	**115**	36
5	**106**	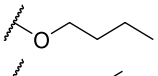	**116**	86
6 [a]	**107**	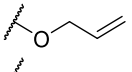	**117**	
7 [a,b]	**111**	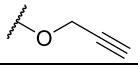	**118**	

[a] no product was isolated, [b] evidence for dealkylation was found.

Dipyrrins **102**, **103**, **105**, and **106** afforded the dipyrrinato complexes in 36% to 91% yields (Table 2). The allyloxy-substituted dipyrrin **111** had been prepared according to the literature.[50b]

The 3-nitrophenyl-substituted dipyrrins (**23** – **27**, **108** – **110**) were also employed for the preparation of chlorido-(dipyrrinato)(pentamethylcyclopentadienyl)iridium(III) complexes. Similar results were

observed for these complexations, again, a synthesis of dipyrrinato iridium(III) complexes was not possible with alkenyl- and alkynyl-substituted dipyrrins (**24** and **109**). The other 3-nitrophenyl-substituted dipyrrins afforded the desired complexes in moderate to good yields (Table 3).

Table 3: Preparation of chlorido(pentamethylcyclopentadienyl)(dipyrrinato)iridium(III) complexes from 3-nitrophenyl-based dipyrrins.

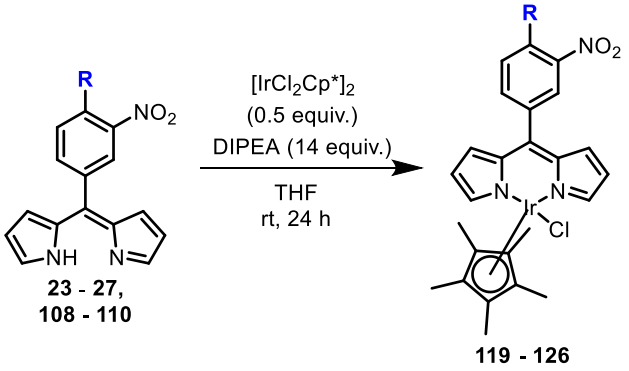

Entry	Starting material	Substituent (R)	Product	Yield [%]
1	**108**		**119**	43
2	**23**	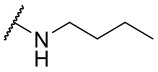	**120**	46
3[a]	**24**	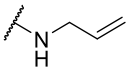	**121**	
4[a]	**109**	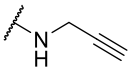	**122**	
5	**25**	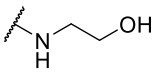	**123**	46
6	**27**	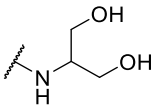	**124**	29
7	**26**	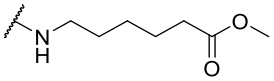	**125**	52
8	**110**	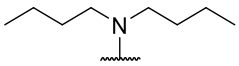	**126**	29

[a] no product was isolated.

In summary, preparations of dipyrrinato complexes were unsuccessful with dipyrrins functionalized with alkene or alkyne groups. In these cases, the desired complexes were not observed and the dipyrrins often seemed to decompose. In some reactions, evidence for a dealkylation of the allyl and propargyl groups was found in the NMR spectra. These observations suggest that the undesired side reactions were caused by the multiple bond in the substituent. The cleavage of propargyl and allyl moieties *via* palladium and ruthenium catalysts is known in the literature.[103] Similarly, an interaction of these multiple bonds with the iridium might have led to the dealkylation and other side reactions.

To obtain dipyrrinato iridium(III) complexes with additional allyl and propargyl groups, the unsubstituted complexes **112** and **119** were tested in the substitution with nucleophiles. For the *post*-

functionalization of complex **112** alcohols and amines were tested, e.g., allyl alcohol, allylamine, propargylamine, and propargyl alcohol, while complex **119** was subjected to the substitution with *n*-butylamine, allyl- and propargyl amine. However, only the substitution of **119** with *n*-butylamine was successful. In the other cases, a formation of the respective complexes was not observed. Again, the dipyrrins appeared to decompose and in the NMR spectra evidence for a dealkylation was found.

Dipyrrins with methyl groups in the 1-,3-,7-, and 9-position were also investigated for the preparation of heteroleptic dipyrrinato iridium(III) complexes. The synthesis of the 1,3,7,9-tetramethyl dipyrrin **129** had already been described in the literature, however, in a one-pot-multi-step sequence.[104] Here instead, the stepwise synthesis of the related dipyrrins was carried out (Scheme 37). The dipyrromethanes **127** and **128** were prepared *via* the acid-catalyzed condensation of 2,4-dimethylpyrrole with the corresponding benzaldehyde. In the next steps, the dipyrromethanes were oxidized with DDQ, followed by the complexation with the iridium half-sandwich complex. This procedure successfully yielded the respective complexes (Scheme 37).

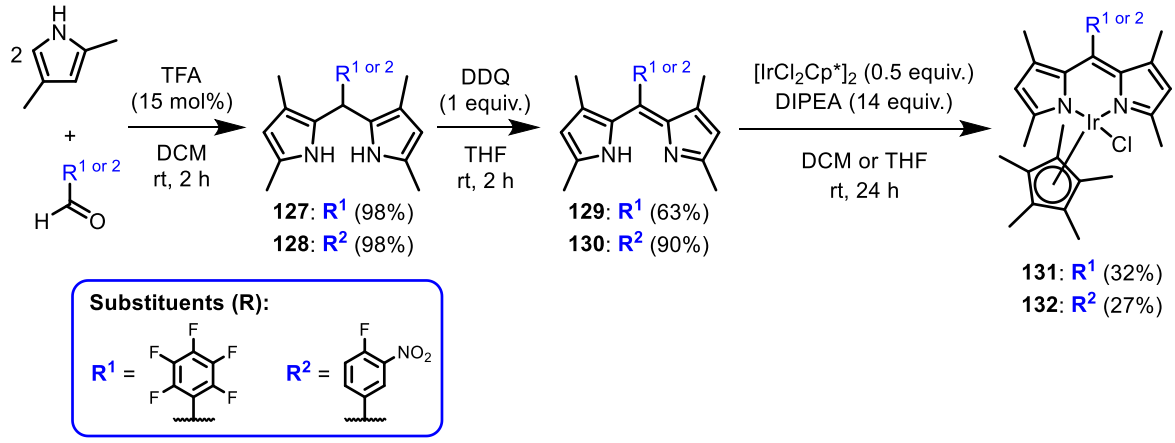

Scheme 37: Preparation of (1,3,7,9-tetramethyldipyrrinato)(cyclopentadienyl)iridium(III) complexes.

The (cyclopentadienyl)(dipyrrinato)iridium(III) complexes were now tested as building blocks for (dipyrrinato)bis(2-phenylpyridyl)iridium(III) complexes. For this, complex **126** was reacted with 2-phenylpyridine under reflux in ethanol. In another experiment, complex **112** was treated with the 2-phenylpyridine in a water/2-methoxyethanol mixture at 120 °C. In both cases, no exchange could be observed, instead, the starting materials were recovered.

Alternatively, the dipyrrins were reacted with DIPEA and a cyclometalated precursor (the dichlorido-bridged (2-phenylpyridyl)iridium(III) complex) to form the desired (dipyrrinato)bis(2-phenylpyridyl)-iridium(III) complexes. With the tested tetrafluorophenyl-substituted dipyrrins, all complexes were obtained in good to high yields, except for the propargyloxy- and propargylamino-substituted compounds (**135** and **139**). In the case of the allylamino-substituted dipyrrin, the respective complex **138** was only obtained in low yields (Table 4). Again, the allyl- and propargyl-substituted dipyrrins appeared to decompose and in the NMR spectra evidence for a dealkylation was found.

Table 4: Preparation of (dipyrrinato)bis(2-phenylpyridyl)iridium(III) complexes *via* tetrafluorophenyl-substituted dipyrrins.

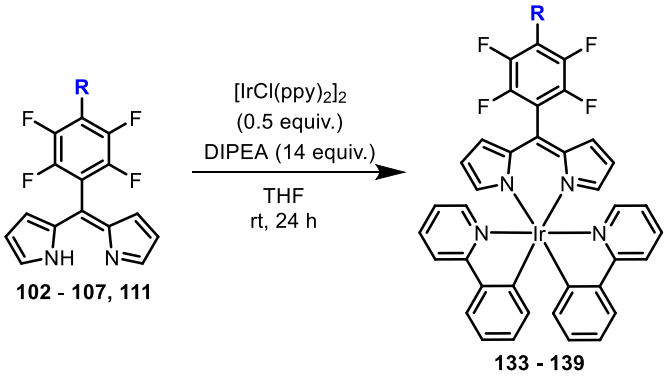

Entry	Starting material	Substituent (R)	Product	Yield [%]
1	**102**		**133**	65
2	**103**	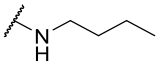	**134**	3
3 [a,b]	**104**	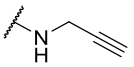	**135**	
4	**105**	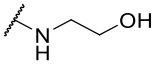	**136**	35
5	**106**	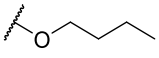	**137**	48
6	**107**	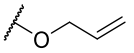	**138**	8
7 [a]	**111**	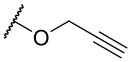	**139**	

[a] no product was isolated, [b] evidence for dealkylation was found.

To finally synthesize the complexes with an allyl or a propargyl moiety, a *post*-functionalization with corresponding amines and alcohols was performed. Using the pentafluorophenyl-substituted complex **133**, a substitution of the related *para*-fluorine position was successfully performed with the tested nucleophiles. High yields were obtained with allylamine, allyl alcohol, and propargyl amine. The substitution with propargylamine still gave the product **135** in good yields (Scheme 38).

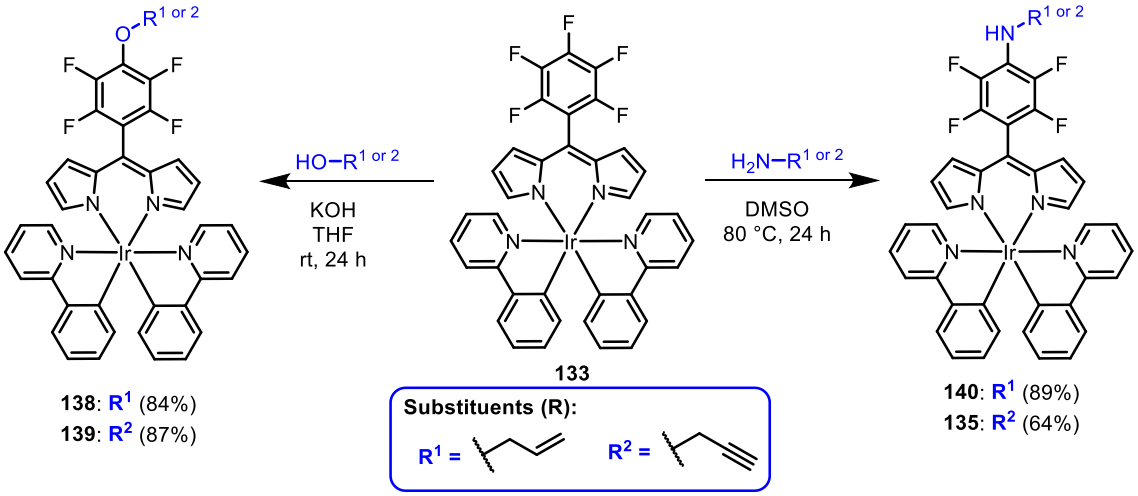

Scheme 38: Nucleophilic substitutions of complex **133** with amines und alcohols.

3-Nitrophenyl-based dipyrrins have as well been studied in the synthesis of (dipyrrinato)-bis(2-phenylpyridyl)iridium(III) complexes. Using the same protocol as already applied for complexation of tetrafluorophenyl-based dipyrrins, almost every reaction led to the (dipyrrinato)bis-(2-phenylpyridyl)iridium(III) complexes. Again, a successful formation of the corresponding complex **143** was not possible with the propargylamino-substituted dipyrrin and the allylamino-substituted complex **137** was achieved only in low yields (Table 5). Also, here, the allyl- and propargyl-substituted dipyrrins appeared to decompose.

Table 5: Preparation of (dipyrrinato)bis(2-phenylpyridyl)iridium(III) complexes *via* 3-nitrophenyl-substituted dipyrrins.

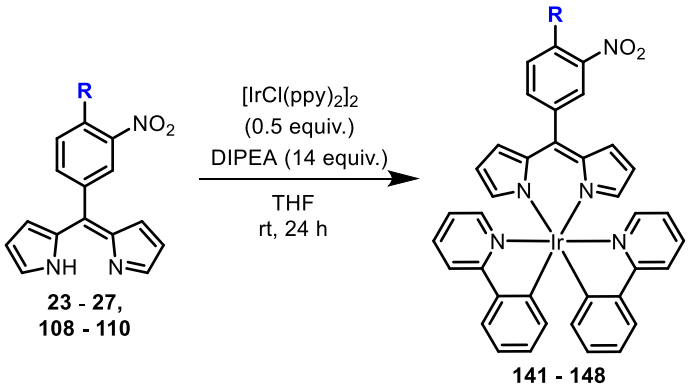

Entry	Starting material	Substituent (R)	Product	Yield [%]
1	**108**		**141**	29
2	**23**	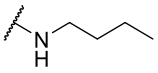	**142**	36
3	**24**	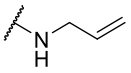	**143**	12
4[a]	**109**	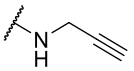	**144**	
5	**25**	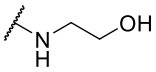	**145**	44
6	**27**	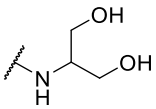	**146**	26
7	**26**	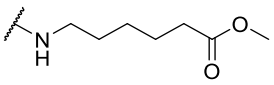	**147**	43
8	**110**	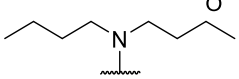	**148**	49

[a] no product was isolated.

The *post*-functionalization was carried out for the 4-fluoro-3-nitrophenyl-substituted complex **141** to obtain complexes with an allylamino or a propargyl moiety. In this case, the nucleophilic substitutions with the allyl and propargyl amine afforded the functionalized complexes as well. The respective complexes **143** and **144** were obtained in 70% and 90%, respectively (Scheme 39).

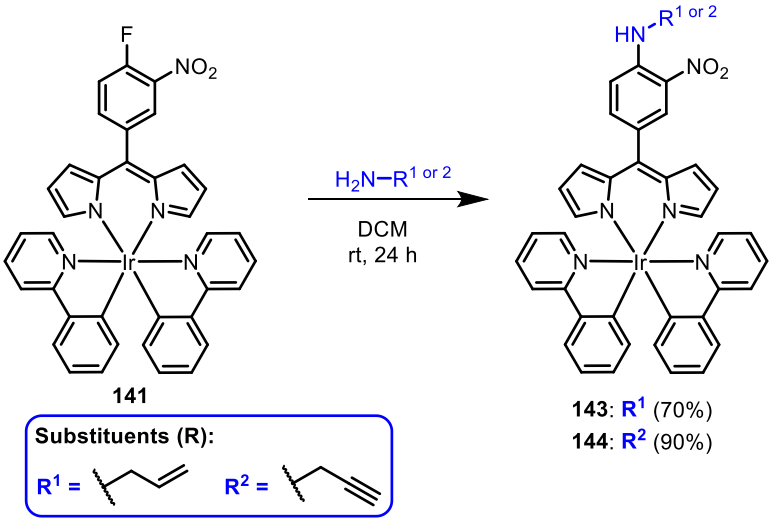

Scheme 39: Nucleophilic substitutions of complex **141** with amines und alcohols.

Furthermore, the glycosylation of the unsubstituted complexes **133** and **141** with thiocarbohydrates was also tested. In analogy to the glycosylation of the BODIPYs, these two complexes could be simply treated with thioglucose and thiogalactose to obtain the glycosylated derivatives in excellent yields within a short reaction time (Scheme 40).

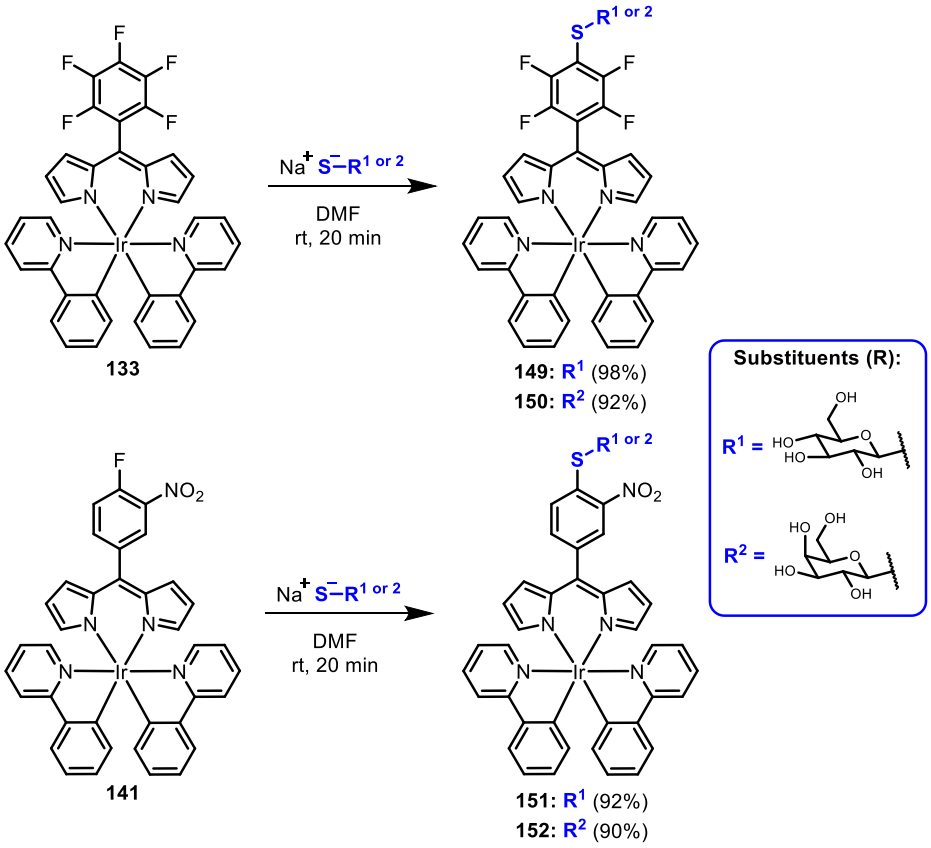

Scheme 40: Glycosylation the (dipyrrinato)bis(2-phenylpyridyl)iridium(III) complexes **133** and **141**.

Finally, a conjugate was prepared from the propargyl-functionalized complex **139** and the azido-substituted BODIPY **153**. The combination of these two molecules was realized *via* the copper(I)-

catalyzed 1,3-dipolar cycloaddition. For this, the complex **139** and BODIPY **153** were dissolved in DMF, then copper sulfate and sodium ascorbate were added. Finally, the desired BODIPY-(dipyrrinato)iridium conjugate could be obtained in a yield of 21% (Scheme 41).

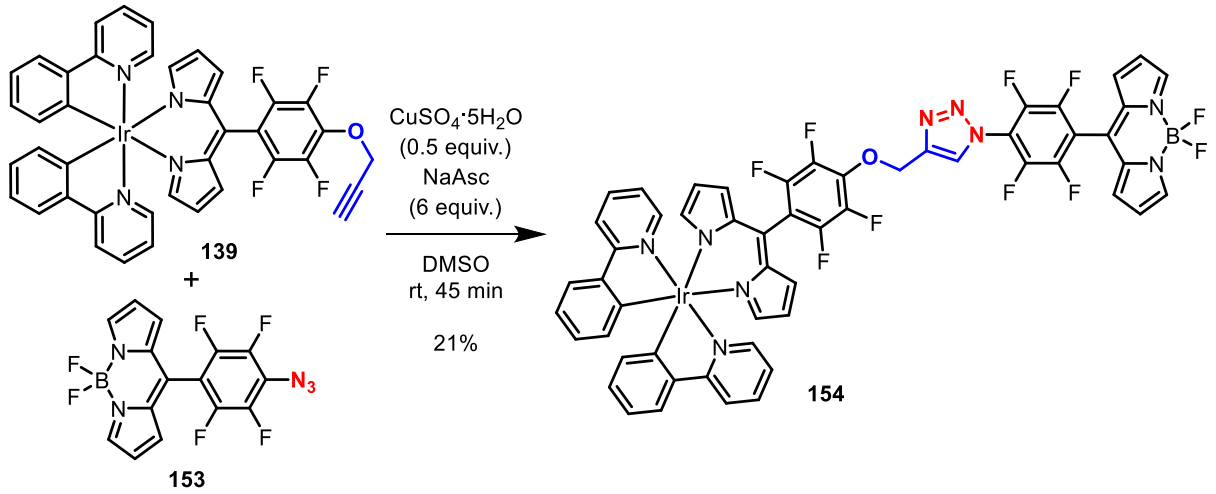

Scheme 41: Preparation of a BODIPY-(dipyrrinato)iridium(III) complex conjugate **154**.

The dark- and phototoxicity of the heteroleptic dipyrrinato iridium(III) complexes was evaluated in assays against bacteria and tumor cells. In addition, the antimicrobial activity was performed with the addition of blood serum, to generate a more realistic testing environment. These tumor cell and bacterial assays were carried out by the biolitec research GmbH.

In general, the heteroleptic dipyrrinato iridium(III) complexes showed only a low dark toxicity against the tested cell lines. In the presence of light certain dipyrrinato iridium(III) complexes were identified with a significant phototoxic activity against the cells. In the case of dipyrrinato complexes with an additional pentamethylcyclopentadienyl ligand, specifically, complexes functionalized with alkyl substituents, e.g., butyl group or the dibutylamino group, exhibited the highest phototoxicity. For the cyclometalated dipyrrinato complexes (equipped with 2-phenylpyridyl ligands), the complexes functionalized with thiocarbohydrates or polar substituents, showed a significant phototoxic effect on the cells. In addition, there was a tendency that the tetrafluorophenyl-substituted dipyrrinato complexes exhibited a more effective phototoxic activity then the nitrophenyl-substituted complexes. In the bacterial assays, a clear dark toxic effect against *S. aureus* was found for the dipyrrinato complexes encompassing a pentamethylcyclopentadienyl ligand. In the presence of light, several complexes were identified, that exhibited a significant phototoxicity even at a low concentration. Interestingly, the respective tetramethyldipyrrinato complexes exclusively showed a significant *phototoxic* activity. Against *P. aeruginos*a, only a limited number of the chlorido(dipyrrinato)-(pentamethylcyclopentadienyl)iridium(III) complexes exhibited dark and phototoxic activity, specifically, the non-functionalized complexes, compounds functionalized with butyl groups, and some complexes with polar groups.

The phototoxic activity decreased significantly on the addition of blood serum, *i.a.,* due to the effects of proteins present in the serum. However, some chlorido(dipyrrinato)(pentamethylcyclopentadienyl) complexes still exhibited a significant phototoxic effect against *S. aureus* in the presence of serum. Remarkably, for the butylamino- and the butyloxy-tetrafluorophenyl-substituted complexes no significant decrease in their phototoxicity was found. As well, a limited phototoxic effect was still found for some of these complexes against *P. aeruginosa* in the presence of serum.

For the (dipyrrinato)bis(2-phenylpyridyl)iridium(III) complexes, a dark and phototoxic activity was exclusively found against *S. aureus*. Here, only the tetrafluorophenyl-based complexes, functionalized with carbohydrate moieties or polar groups, exhibited a phototoxic effect. In the presence of serum, only the glycosylated derivatives kept their high phototoxic activity.

In addition, for the chlorido(dipyrrinato)(pentamethylcyclopentadienyl)iridium(III) complexes **31** and **51** (Fig. 26; a and b) and, as well, for the (dipyrrinato)bis(2-phenylpyridyl)iridium(III) complexes **54**, **60**, and **66** (Fig. 26; c – e) X-ray structure analyses were performed to confirm their structures in the solid state. The molecular structures were measured, solved, and refined by Dr. Keith Flanagan and Dr. Christopher Kingsbury from Prof. Mathias O. Senge's group at Trinity College Dublin. Again, an intermolecular hydrogen bond between the hydrogen of the amine and the related nitro group was found within in the complex **66** (equipped with a 4-amino-3-nitrophenyl moiety).

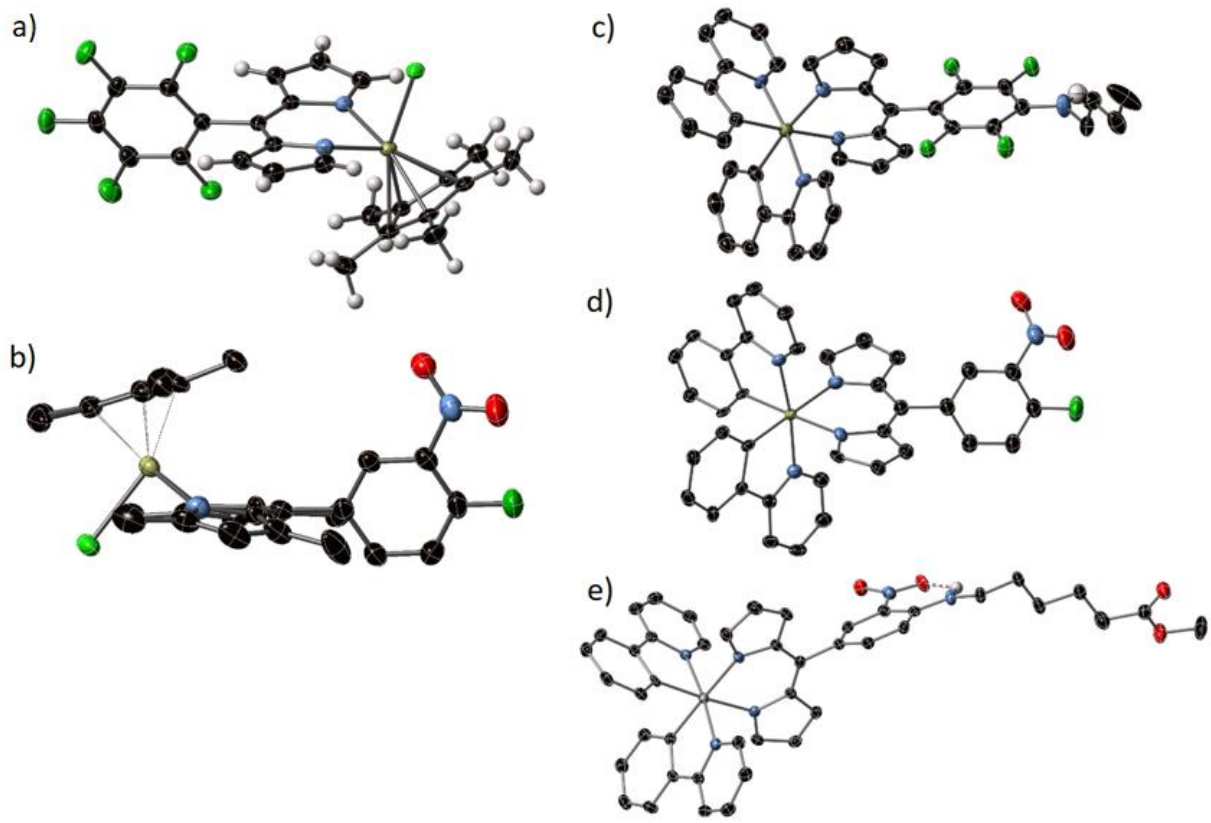

Figure 26: Molecular structures for heteroleptic dipyrrinato iridium complexes: complex **31** (a), complex **51** (b), complex **54** (c), complex **60** (d), and complex **66** (e).

In summary, dipyrrins based on the tetrafluorophenyl and 3-nitrophenyl moiety were successfully applied in the preparation of the respective heteroleptic dipyrrinato iridium(III) complexes. Using these pre-functionalized dipyrrins, dipyrrinato iridium(III) complexes with a wide scope of functional groups were synthesized. However, the *post*-functionalization of the dipyrrinato complexes proved to be more suitable for the introduction of a terminal allyl and terminal propargyl moieties. The concept of *post*-functionalization also enabled an effective functionalization with thiocarbohydrates. Furthermore, tetramethyl core-substituted dipyrrins were also found suitable for the preparation of (1,3,7,9-tetramethyl-dipyrrinato) iridium complexes carrying additional cyclopentadienyl ligands.

In assays against bacteria and tumor cells, several dipyrrinato iridium(III) complexes were identified with a high potential for an application as photosensitizers against tumor cells and bacteria. Especially, the glycosylated derivatives showed a promising efficacy.

3. Unpublished results

3.1 Heteroleptic dipyrrinato ruthenium(II) and iridium(III) complexes

4-Amino-3-nitrophenyl-substituted dipyrrins had already been applied for the synthesis of related chlorido(*p*-cymene)(dipyrrinato)ruthenium(II) complexes (see chapter 2.1). Here, additional dipyrrins (**108** – **110**) were also employed in the syntheses of such types of dipyrrinato ruthenium(II) complexes. Except for dipyrrin **109**, all dipyrrins enabled the synthesis of the corresponding dipyrrinato complexes. The dipyrrins **108** and **110** afforded the complexes **156** and **157** with 58% and 29% yield, respectively (Scheme 42).

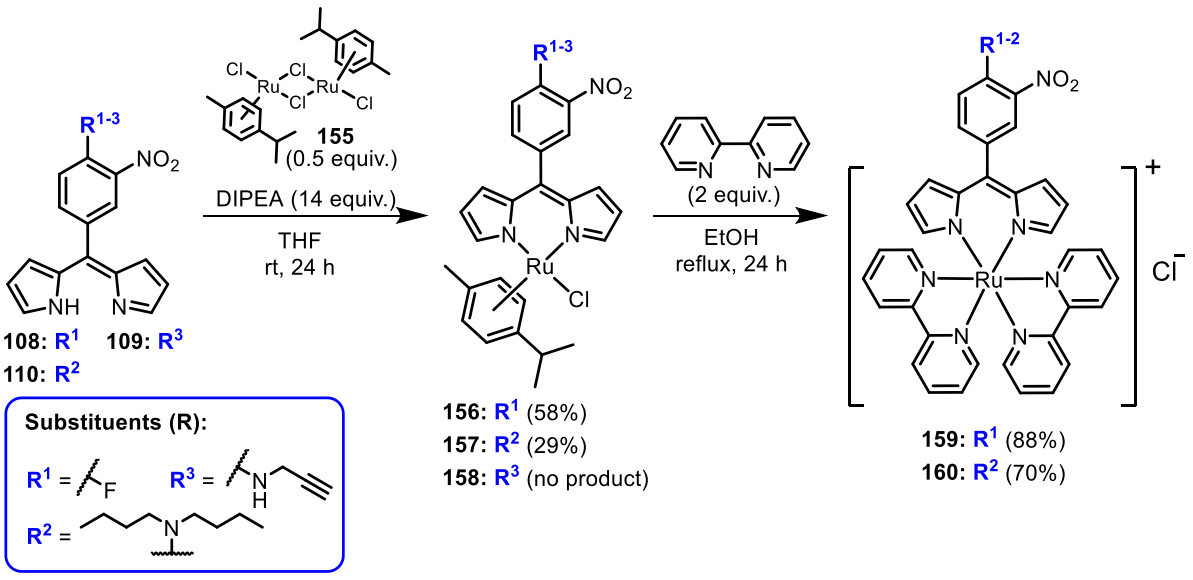

Scheme 42: Preparation of chlorido(*p*-cymene)(dipyrrinato)ruthenium(II) complexes and ligand exchange with 2,2‘-bipyridine.

While the reaction of the propargylamino-substituted dipyrrin **109** and the (*p*-cymene)ruthenium(II) half-sandwich precursor **155** did not result in the complex **158**. Probably, the ruthenium(II) precursor facilitated the decomposition of the propargyl moiety, leading to undesired side products. Similar results had also been observed with the (cyclopentadienyl)iridium(III) precursor (see chapter 2.3). Finally, the ligand exchange was performed with the two dipyrrinato ruthenium complexes **156** and **157**. The reaction with 2,2'-bipyridine could as well be successfully implemented and the respective bis(2,2'-bipyridyl)(dipyrrinato)ruthenium(II) complexes **159** and **160** were obtained in high yields (Scheme 42).

To achieve the chlorido(*p*-cymene)(dipyrrinato)ruthenium(II) complex **158**, equipped with a propargyl moiety, the *post*-functionalization of dipyrrinato complex **156** with propargylamine was performed (Scheme 43). In this case, again no evidence for the successful formation of the desired complex were found. Instead, interactions of the propargyl moiety with the ruthenium center may have led to the decomposition of the complex, as it was found in the substitutions for the dipyrrinato iridium complexes with propargyl amine and propargyl alcohol (see chapter 2.3).

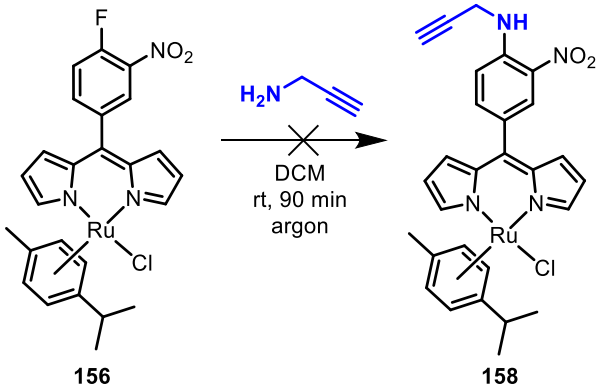

Scheme 43: Attempted *post*-functionalization of complex **156** with propargylamine.

The bis(2,2'-bipyridyl)(dipyrrinato)ruthenium(II) complex **159** was also subjected to *post*-functionalization with propargylamine and ethanolamine (Scheme 44). In contrast to the functionalization of complex **156**, reactions with the tested amines proceeded significantly more effective. Here, no indication for side reactions was found. Both reactions gave the complexes **36** and **161** in high yields (98% and 78%, respectively). The 2-hydroxyethylamino complex **36** was already previously synthesized *via* the complexation of the pre-functionalized dipyrrin. However, the successful *post*-functionalization indicated that this is probably the preferable route of synthesis for functionalized complexes with more labile nucleophiles.

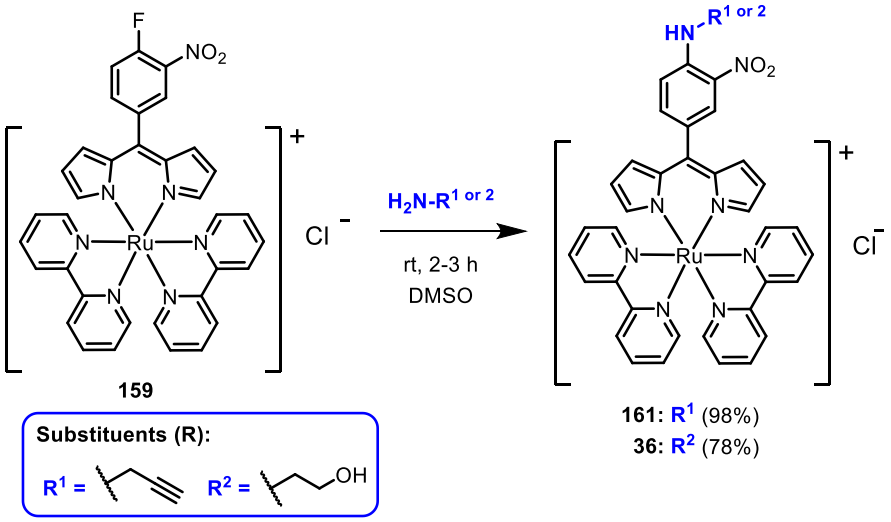

Scheme 44: *post*-Functionalization of complex **159** with amines.

Furthermore, the concept of glycosylation with a thiocarbohydrate was also tested on the dipyrrinato iridium complexes **112** and **119** and to the dipyrrinato ruthenium complex **156**. In analogy to the already applied protocol for the glycosylation of BODIPYs (see chapter 2.2), the complexes were treated with the sodium salt of thioglucose and thiogalactose. In all cases, an introduction of the thiocarbohydrate moieties was not successful, and no evidence of the desired glycosylated derivatives was found (Scheme 45). Perhaps, interactions of the ruthenium center with the thiocarbohydrates induced a decomposition of the corresponding metal complexes.

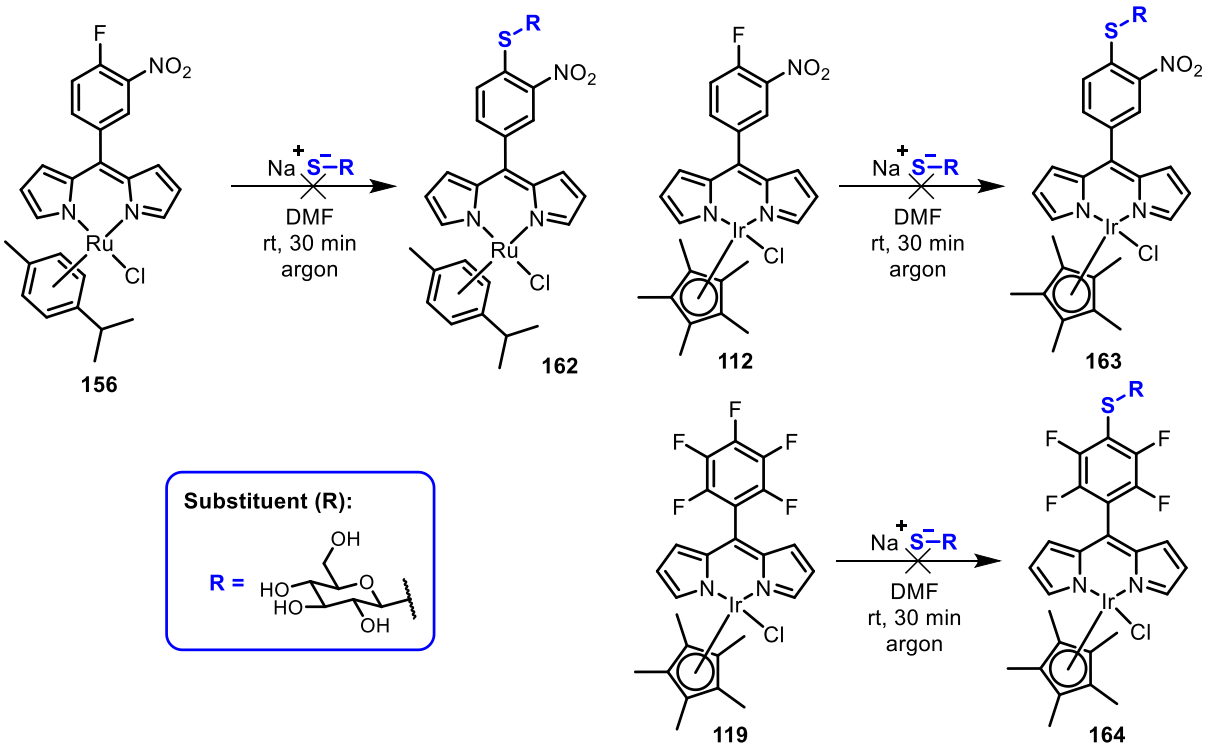

Scheme 45: Attempted substitution of dipyrrinato complexes **112**, **119**, and **156** with thioglucose.

The bis(2,2‘-bipyridyl)(dipyrrinato)ruthenium(II) complex **159** had also been evaluated to glycosylation. For this, complex **159** was treated with the respective thiocarbohydrates. Finally, the glucosyl-substituted derivative **165** and the galactosyl-substituted derivative **166** were obtained in high yields (Scheme 46). No indications for a decomposition of the dipyrrinato ruthenium(II) complex **159** were found, perhaps due to the more shielded metal core within the complex.

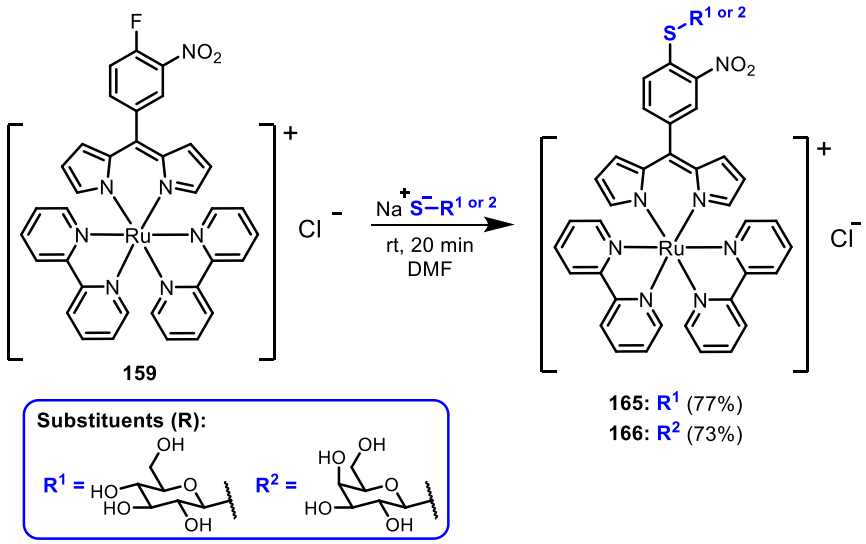

Scheme 46: Glycosylation of complex **159**.

Chlorido(*p*-cymene)(dipyrrinato)ruthenium(II) complexes and bis(2,2’-bipyridyl)(dipyrrinato)-ruthenium(II) complexes were also evaluated in tumor cell and bacterial assays to explore their potential suitability as photosensitizers for PDT and antimicrobial photodynamic inactivation. Selected complexes were studied against several tumor cell lines and against the Gram-positive germ *S. aureus*. In the tumor cell assays the following cell lines were used: human colorectal adenocarcinoma (HT29), human epidermoid carcinoma (A431), submaxillary salivary gland epidermoid carcinoma (A253), and human epithelial tongue squamous cell carcinoma (CAL27). The antibacterial tests were performed in PBS and additionally in the presence of serum to evaluate the antibacterial activity under more realistic conditions. The tumor cell and bacterial assays were carried out by the biolitec research GmbH.

Results for dark and phototoxic activity of the chlorido(*p*-cymene)(dipyrrinato)ruthenium(II) complexes (**28**, **32**, and **156**) against the cell lines and *S*. aureus are shown in Figures 27 and 28. The biological activity of the bis(2,2’-bipyridyl)(dipyrrinato)ruthenium(II) complexes (**33**, **37**, **159**, and **165**) against the tumor cells and *S. aureus* are presented in the Figures 29 and 30.

The chlorido(*p*-cymene)(dipyrrinato)ruthenium(II) complexes **28**, **32**, and **156** exhibited no dark toxicity against all cells. A phototoxic effect was observed exclusively for complexes **28** and **32** against the cell lines A431 and CAL27 (Fig. 27). Compound **28** showed a high phototoxicity on one cell line

(A431) already at a 2 µM. As well, a significant decrease of the viability on the cell line CAL27 was found for **28** at the highest concentration. While for complex **32** a low phototoxic activity at 100 µM against two cell lines (A431 and CAL27) was identified (Fig 27).

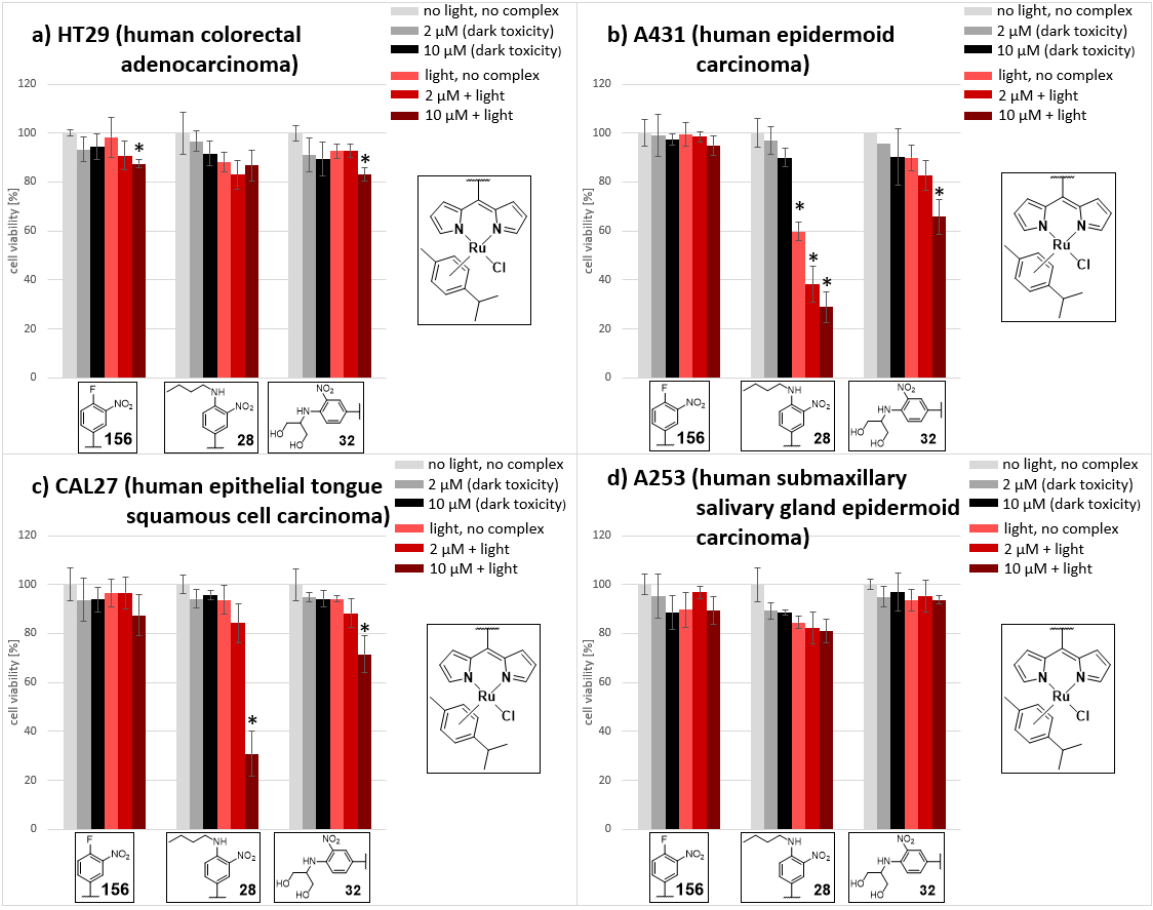

Figure 27: Dark and phototoxicity of chlorido(*p*-cymene)(dipyrrinato)ruthenium(II) complexes in tumor cell assays with the HT29 cell line (**a**) the cell line A431 (**b**), the cell line CAL27 (**c**), and the cell line A253 (**d**).* indicates significant values with $p < 0.005$.

As can be seen from Figure 28, the chlorido(*p*-cymene)(dipyrrinato)ruthenium(II) complexes **28** and **32** showed a significant activity against *S. aureus* in PBS. Both complexes exhibited dark toxicity with a suppression of bacterial growth below the detection limit at a concentration of 100 µM. For complex **28** a strong phototoxic activity was observed, where a complete inactivation of *S. aureus* already at 10 µM was achieved. Compound **32** showed a complete inactivation of bacteria at the highest concentration (100 µM) under light. For the unsubstituted complex **156** no dark and phototoxicity was found in PBS. However, in the presence of serum, dark and phototoxicity of the complexes vanished completely (Fig. 28).

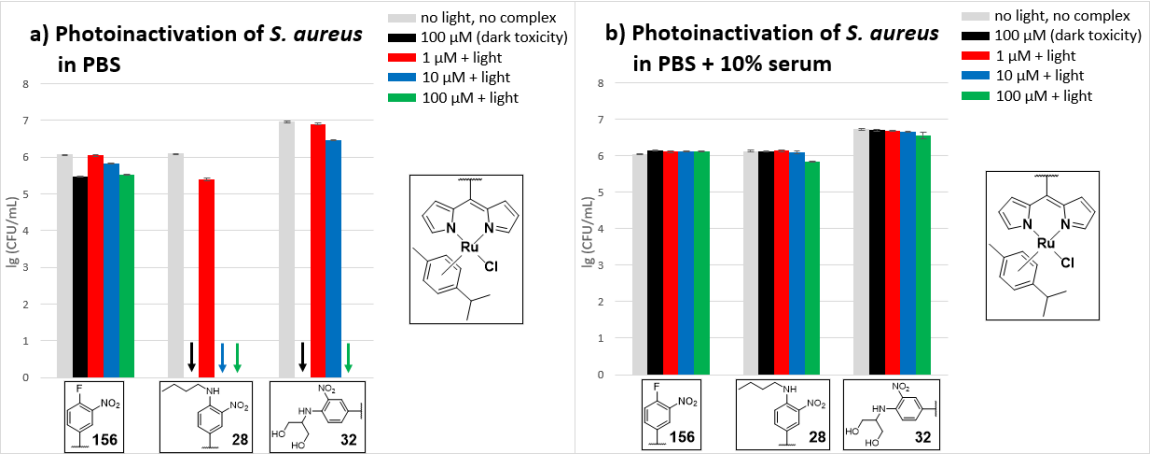

Figure 28: Photoinactivation of *S. aureus* by chlorido(*p*-cymene)(dipyrrinato)ruthenium(II) complexes in PBS (**a**) and in PBS+10% serum (**b**). The antibacterial toxicity is expressed as logarithm of the number of colony-forming units, lg (CFU mL^{-1}). Arrows indicate a suppression of bacterial growth below the detection limit.

In the case of the bis(2,2'-bipyridyl)(dipyrrinato)ruthenium(II) complexes, the unsubstituted complex **159** exhibited a strong phototoxic activity on three cell lines (HT29, A431, and CAL27) at 100 µM, but also high dark toxicity at the same concentration (Fig. 29). Under irradiation with light, complex **33** showed a decrease of the cell viability at the highest concentration on the cell lines A431, CAL27, and A253, while compound **37** showed a phototoxic effect at least at 100 µM against the cell lines A431 and CAL27. In contrast, no significant dark and phototoxicity was observed for the glycosylated complex **165** (Fig. 29).

The bis(2,2'-bipyridyl)(dipyrrinato)ruthenium(II) complexes **33**, **37**, and **159** also showed a high biological activity against *S. aureus* in PBS (Fig. 30). Dark toxic effects were observed for complexes **33** and **159** with a complete inactivation of bacteria at a concentration of 100 µM. The non-functionalized compound **159** exhibited a phototoxic activity already at 10 µM with a suppression of bacterial growth beyond the detection limit. A medium phototoxicity with a three log-stage reduction was also found for **159** at 1 µM. A complete inactivation of *S. aureus* was achieved with complexes **33** and **37** at the highest concentration under light. Notably, both complexes also showed a medium phototoxic activity at a concentration of 10 µM (Fig. 30).

Again, biological activity of the tested BODIPYs decreased in the presence of serum (Fig. 30). The dark toxic activity of complexes **33** and **159** vanished completely. Nevertheless, in the presence of serum, compounds **33**, **37**, and **159** still exhibited a phototoxic activity with a complete inactivation of bacteria at 100 µM. In addition, an inactivation of bacteria of at least two log-stages was observed for complexes **33** and **159** at 10 µM. Again, no dark and phototoxicity was found for the glycosylated complex **169** in PBS and PBS + serum (Fig. 30).

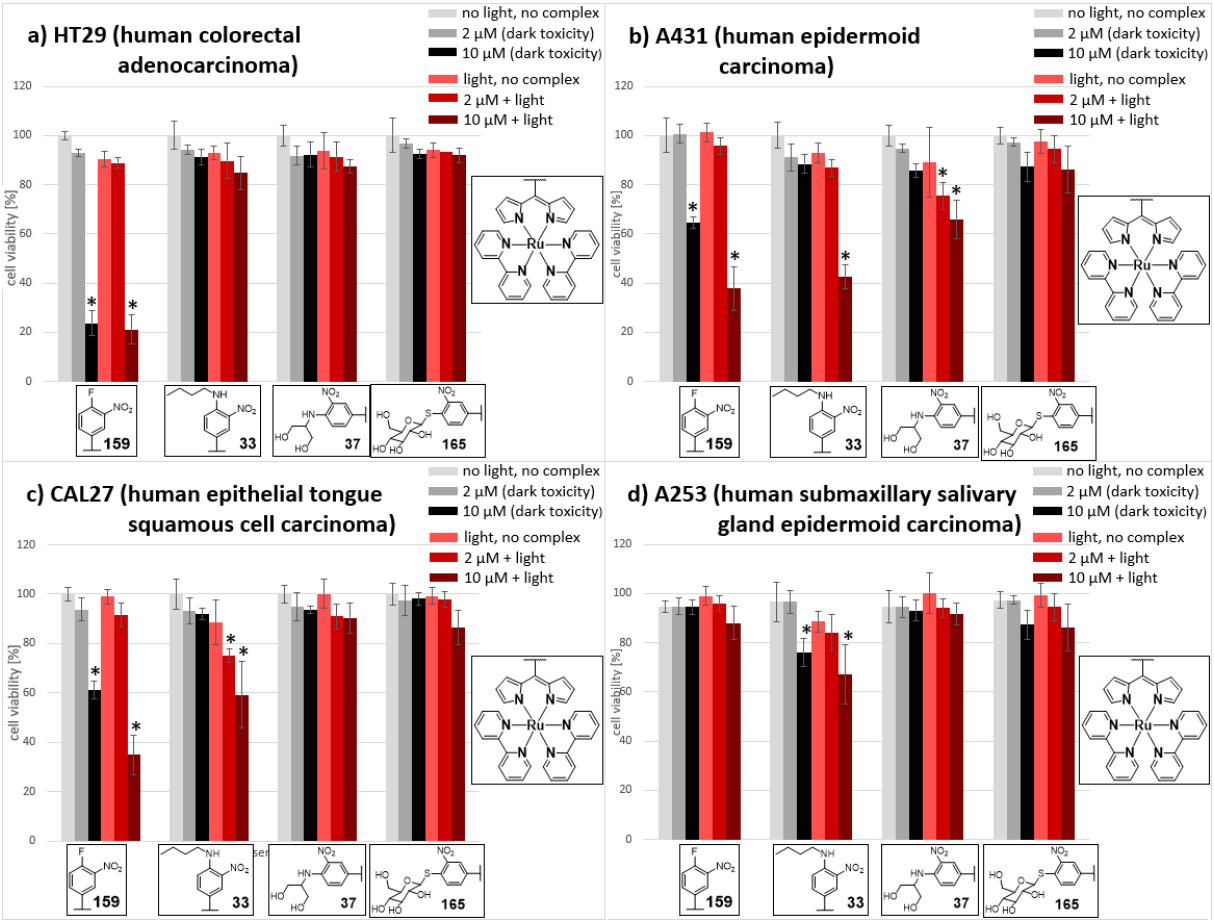

Figure 29: Dark and phototoxicity of bis(2,2'-bipyridyl)(dipyrrinato)ruthenium(II) complexes in tumor cell assays with the HT29 cell line (**a**), the cell line A431 (**b**), the cell line CAL27 (**c**), and the cell line A253 (**d**).* indicates significant values with $p < 0.005$.

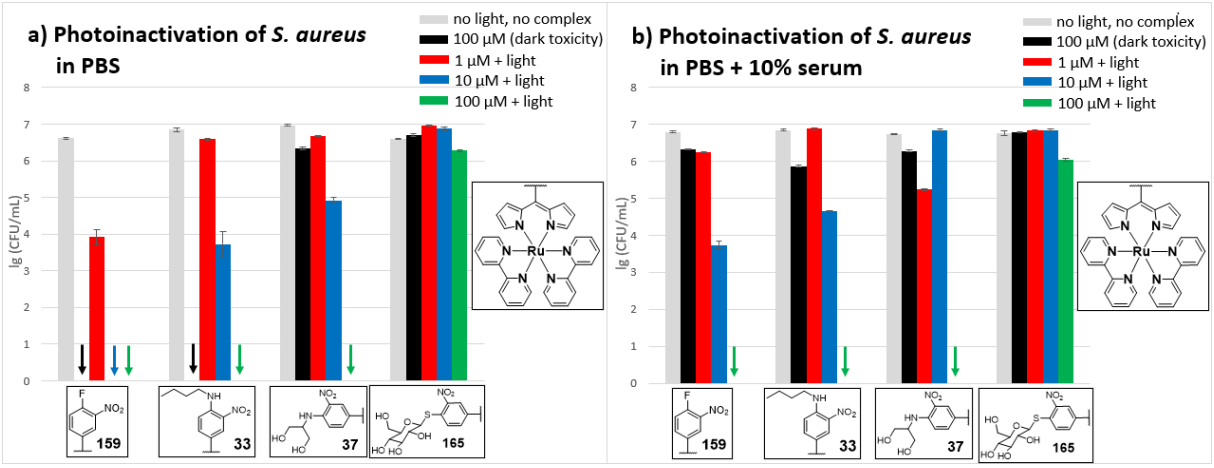

Figure 30: Photoinactivation of *S. aureus* by (2,2'-bipyriyl)(dipyrrinato)ruthenium(II) complexes in PBS (**a**) and in PBS + 10% serum (**b**). The antibacterial toxicity is expressed as logarithm of the number of colony-forming units, lg (CFU mL^{-1}). Arrows indicate a suppression of bacterial growth below the detection limit.

In conclusion, both types of dipyrrinato ruthenium(II) complexes showed a limited activity against tumor cells. In contrast to the related dipyrrinato iridium(III) complexes, the tested dipyrrinato ruthenium(II) complexes only exhibited an activity against two cell lines. For complexes with a polar

substituent or a thioglycosyl moiety no biological activity was found. The chlorido(*p*-cymene)-(dipyrrinato)ruthenium(II) complexes also proved inefficient for inactivation of *S. aureus*, as significant dark and phototoxic activity was observed exclusively in the absence of serum. Nevertheless, bis(2,2'-bipyridyl)(dipyrrinato)ruthenium(II) complexes exhibited pronounced potential for an application in antimicrobial photodynamic inactivation. For many complexes, a high phototoxic effect was detected on *S. aureus* even in the presence of serum. Interestingly, for the glycosylated complex no significant activity against *S. aureus* was identified. However, the high antimicrobial activity exhibited by some bis(2,2'-bipyridyl)(dipyrrinato)ruthenium(II) complexes even in the presence of serum strongly underlines a possible use as photosensitizer for an inactivation of bacteria. In the case of the (dipyrrinato)bis(2-phenylpyridyl)iridium(III) complexes, such efficient antibacterial activity in the presence of serum was observed exclusively for the glycosylated derivatives.

The 1,3,7,9-tetramethyl-substituted dipyrrins **127** and **128** were also applied to the preparation of heteroloeptic (1,3,7,9-tetramethyldipyrrinato)ruthenium(II) complexes. The syntheses were carried out analogously to the already described method for dipyrrinato complexes (treatment with DIPEA and (*p*-cymene)ruthenium(II) precursor, Scheme 47). Finally, both dipyrrins afforded the respective dipyrrinato ruthenium(II) complexes **167** and **168**. The formation of **167** could be performed in DCM, however, the preparation of complex **168** required THF as solvent, due to the low solubility of the starting material **128** in DCM. Compared to the related dipyrrinato ruthenium(II) complexes, the dipyrrins **127** and **128** provided significantly lower yields, here, the ruthenium complexes **167** and **168** were obtained in 4% and 18%, respectively (Scheme 47). Compared to the general yields obtained for the complexation of dipyrrins, here, relative low yields were obtained. The low yields might be the result of a decomposition of the employed tetramethyl-substituted dipyrrins. Similar observations were made during the reaction of corresponding dipyrrins with the iridium(III) precursor (see chapter 2.3).

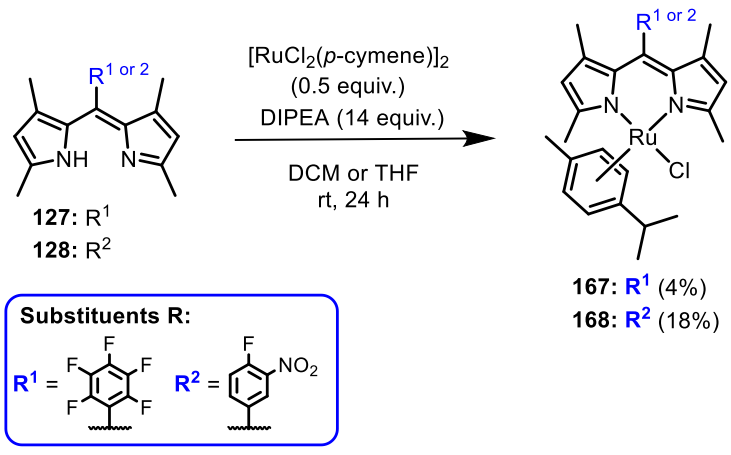

Scheme 47: Preparation of (*p*-cymene)(1,3,7,9-tetramethyldipyrrinato)ruthenium(II) complexes.

Furthermore, the 1,3,7,9-tetramethyl-substituted dipyrromethane **128** was applied in the synthesis of a functionalized chlorido(pentamethylcyclopentadienyl)(1,3,7,9-tetramethyldipyrrinato)iridium(III) complex (Scheme 48).

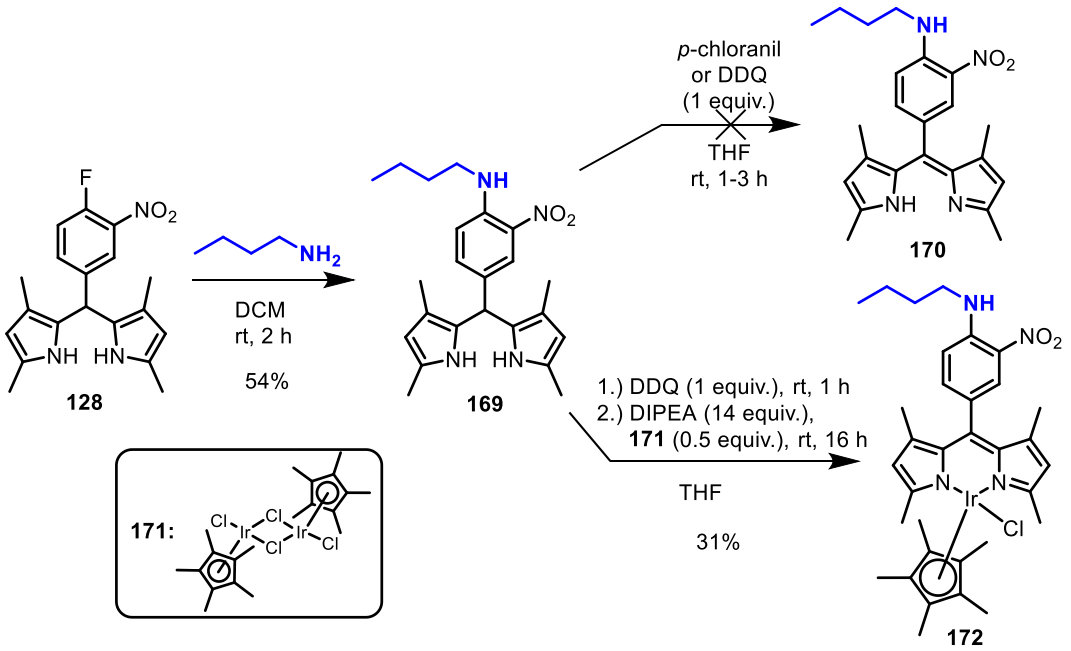

Scheme 48: Synthetic procedure for the (1,3,7,9-tetramethyldipyrrinato)iridium(III) complex **172.**

For the synthesis of this complex, the dipyrromethane **128** was dissolved in DCM and simply treated with *n*-butylamine. This reaction afforded the *n*-butylamino-functionalized dipyrromethane **169** with a yield of 54% (Scheme 48). The final complexation requires the respective dipyrrin, therefore, dipyrromethane **169** was subjected to oxidation with *p*-chloranil and DDQ. However, both reactions did not provide the desired dipyrrin **170**. Although the thin-layer chromatographic control indicated the formation of a single orange fraction with a significantly different R_f compared to the starting material, the purification by column chromatography did not yield the product. Instead, a black-colored fraction appeared during the column chromatography. Perhaps, the dipyrrin decomposed on the adsorbent used (silica gel). To obtain the desired dipyrrinato complex, the pre-functionalized dipyrromethane **128** was therefore again oxidized with DDQ and then, without intermediate isolation of the dipyrrin, treated with DIPEA and the iridium-cyclopentadienyl precursor **171** to directly form the coordination complex **172**. This sequence had already been described in the literature as an alternative procedure for dipyrrinato complexes.[67b,67c] And indeed, *via* this route, the desired functionalized complex **172** was successfully obtained with a yield of 31%.

3.2 Homoleptic dipyrrinato complexes

Beyond an application for the synthesis of heteroleptic dipyrrinato complexes, dipyrrins were also investigated for the preparation of bis(dipyrrinato) and tris(dipyrrinato) complexes. The number of dipyrrins coordinated to the metal center strongly depends on the metal used, resulting in the formation of either bis(dipyrrinato) or tris(dipyrrinato) complexes. Thus, bis(dipyrrinato) complexes are observed with zinc(II), copper(II), or nickel(II), while indium(III), gallium(III), and iron(III) form tris(dipyrrinato) complexes with dipyrrins.[62a,67a,69] The 5-pentafluorophenyldipyrrin and related tetrafluorophenyl-substituted dipyrrins have already applied for the synthesis of the bis(dipyrrinato) and tris(dipyrrinato) complexes.[50b,105]

First, 3-nitrophenyl-substituted dipyrrins **23**, **26**, **108**, and **109** were studied for the preparation of bis(dipyrrinato) complexes (Table 6).

Table 6: Preparation of bis(dipyrrinato) complexes.

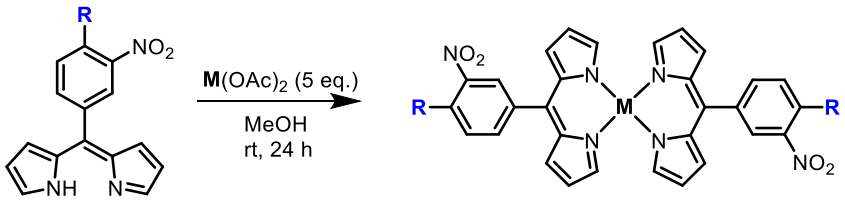

23, 26, 108, 109 **173 - 181**

Entry	Starting material	Substituent (R)	Product	Yield [%]
		Bis(dipyrrinato)zinc(II): M = Zn(II)		
1 [a,b]	**108**		**173**	
2 [a,b]	**23**	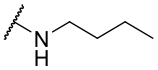	**174**	
3 [a]	**109**	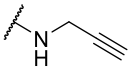	**175**	49
4 [a]	**26**	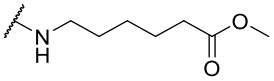	**176**	37
		Bis(dipyrrinato)nickel(II): M = Ni(II)		
5 [a,b]	**108**		**177**	
6 [a,b]	**23**	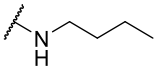	**178**	
7 [a,b]	**109**	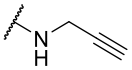	**179**	
		Bis(dipyrrinato)copper(II): M = Cu(II)		
8 [a,b]	**108**		**180**	
9 [a,b]	**23**	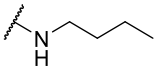	**181**	

[a] evidence for decomposition was found, [b] inseparable mixture of dipyrrin and dipyrrinato complex.

The dipyrrins were reacted with DIPEA and the respective metal(II) acetate. Specifically, zinc(II), nickel(II), and copper(II) acetate were used for the reactions, and DIPEA was used as a base for the deprotonation of the dipyrrin (Table 6). Compared to the synthesis of heteroleptic dipyrrinato complexes, the formation of the bis(dipyrrinato) complexes turned out to be difficult. Only in the case of the dipyrrins **26** and **109** a successful formation of the desired zinc complexes was achieved. Here, the complexes **175** and **176** precipitated as an orange solid during the reaction. Moreover, it was possible to obtain the desired complexes in sufficient purity *via* filtering and subsequent washing with methanol. Thus, the complexes **175** and **176** were obtained with 49% and 37% yield, respectively (Table 6). In the other cases, significantly low amounts of an orange-colored solid were obtained. These isolated solids were identified as a mixture of the desired product and the respective starting material (Table 6). Moreover, the dipyrrins appeared to decompose during the reaction, as large amounts of a black precipitate were observed.

To shift the equilibrium towards the desired complexes the reaction conditions were modified. For this, the reaction temperature was increased for the reaction of **26** with zinc acetate. In an additional experiment, the addition of a further base was tested to improve the reaction of dipyrrin **109** towards the desired bis(dipyrrinato) complex. However, in both cases, an improvement of the complexations was not achieved. Still, mixtures of the complex and the dipyrrin, as well as decomposition of dipyrrins were observed.

The dipyrrins **23**, **26**, **108**, and **109** were also investigated for the synthesis of tris(dipyrrinato) complexes. Metal chlorides were used for the complexations with the dipyrrins. The reactions were carried out analogously to the preparation of the bis(dipyrrinato) complexes, except for higher reaction temperatures, which were required for the formation of the desired complexes (Table 7). Here, more reactions yielded the respective tris(dipyrrinato) complexes. However, in some cases, a successful formation of the complexes could still not be observed. The best results were observed with the dipyrrins **23** and **26**. The tris(dipyrrinato)indium(III) complexes (**183** and **187**) and the tris(dipyrrinato)gallium(III) complexes (**188** and **192**) were synthesized in moderate to good yields. In the case of the dipyrrins **24**, **25**, and **109**, the syntheses were less effective. The tris(dipyrrinato)indium(III) complexes (**184** – **186**) were only isolated in low yields. While the complexation of the allylamino-, propargylamino-, and 2-hydroxyethylamino-substituted dipyrrins (**23**, **24**, and **109**) with gallium(III) chloride did not gave the desired complexes. In the case of the reaction of the unsubstituted dipyrrin **108** and indium(III) chloride, a successful formation of the homoleptic dipyrrinato complex was also not observed. During the performed reactions, decomposition of the dipyrrin was again detected. Side reactions caused by the nitro group may have led to decomposition of the starting material.

Table 7: Preparation of tris(dipyrrinato) complexes.

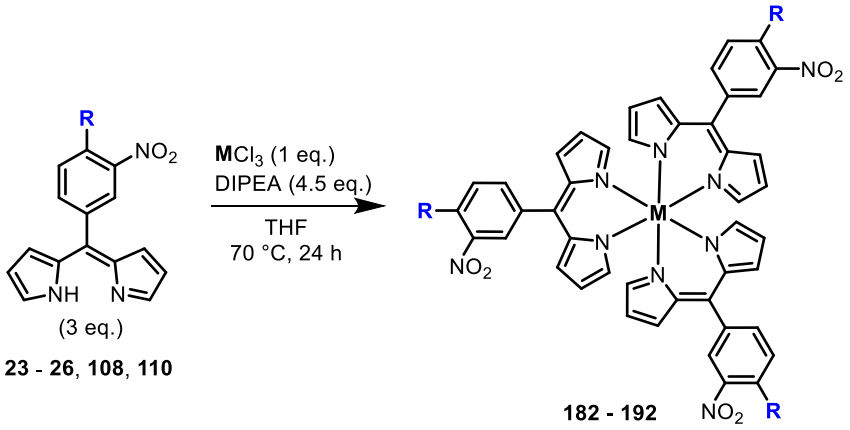

Entry	Starting material	Substituent (R)	Product	Yield [%]
		Tris(dipyrrinato)indium(III): M = In(III)		
1 [a,b]	**108**		**182**	
2 [a]	**23**	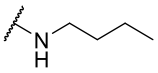	**183**	55
3 [a]	**24**	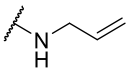	**184**	5
4 [a]	**109**	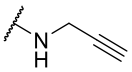	**185**	3
5 [a]	**25**	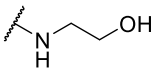	**186**	2
6 [a]	**26**	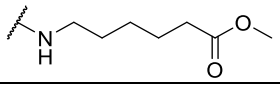	**187**	29
		Tris(dipyrrinato)gallium(III): M = Ga(III)		
7 [a,b]	**23**	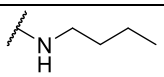	**188**	35
8 [a,b]	**24**	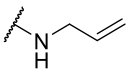	**189**	
8 [a,b]	**109**	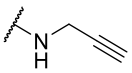	**190**	
9 [a,b]	**25**	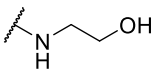	**191**	
10 [a,b]	**26**	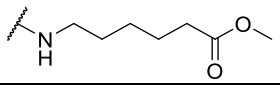	**192**	27

[a] evidence for decomposition was found; [b] no product was isolated.

In an additional set of experiments, selected dipyrrins (**23**, **26**, and **102**) were tested for the preparation of the tris(dipyrrinato)iridium(III) complexes **193** - **195**. The reactions were carried out with the same protocol as used for the other tris(dipyrrinato) complexes (Scheme 49). Again, no indications of the formation of the complexes **193** - **195** were found with iridium(III) chloride and the dipyrrins.

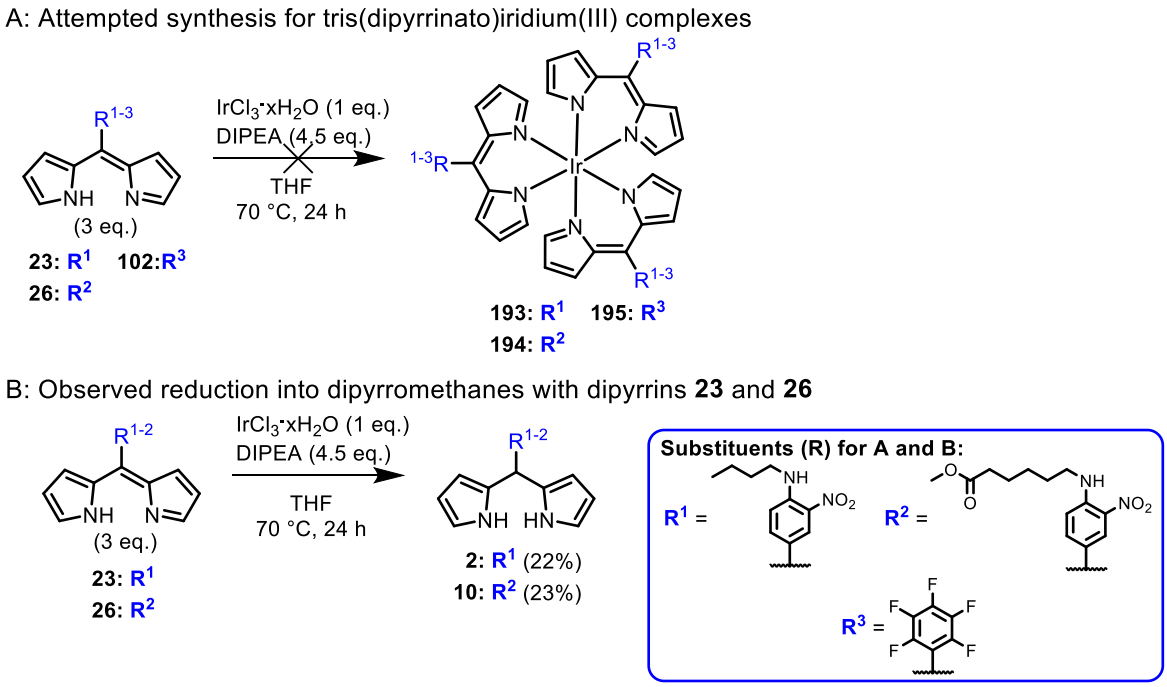

Scheme 49: *meso*-Substituted dipyrrins for the preparation of tris(dipyrrinato)iridium(III) complexes.

In the case of dipyrrin **23** and **26**, however, orange-colored solids could be isolated. Interestingly, NMR and mass spectra proved the formation of the corresponding *dipyrromethanes*. The appearance of dipyrromethanes indicates a reduction of the starting material. In addition, a reduction of dipyrrins to dipyrromethanes is already known in the literature.[105] This observation can also provide an explanation for the difficulty in syntheses of homoleptic dipyrrinato complexes. In general, a reduction of the dipyrrin is also conceivable in other reactions, which can lead to the formation of the dipyrromethanes or other side products.

In conclusion, the 3-nitrophenyl-based dipyrrins are less suitable for the synthesis of the respective homoleptic dipyrrinato complexes, due to the relatively low yields and increased side product formation. The tumor cell and bacterial assays did not provide any evidence of dark and phototoxic activity for the homoleptic dipyrrinato complexes.

3.3 Additional modifications of the BODIPY core structure

In addition to the already described protocol for the combination of the functionalization and targeted halogenation of the 1,3,7,9-tetramethyl BODIPYs (see chapter 2.2), further amines were tested for the nucleophilic substitution of the *para*-phenyl position. Here, BODIPY **65** was functionalized with allylamine and *N*,*N*-dibutylamine (Scheme 50). In the case of the substitution with allylamine, the corresponding product could be obtained in 32% yield. With *N*,*N*-dibutylamine however, no product was observed, instead a dark brown oil was isolated. No spectral evidence for the formation of the product was found.

Finally, the allylamino-functionalized BODIPY **196** was subjected to the halogenation with NBS. Thin-layer chromatographic control showed the formation of the expected product **198**. However, the NMR spectra indicated the formation of additional compounds. Unfortunately, this mixture of BODIPYs could not be separated *via* column chromatography. Probably, halogenation with NBS led to an inseparable mixture of mono- and dibrominated BODIPYs.

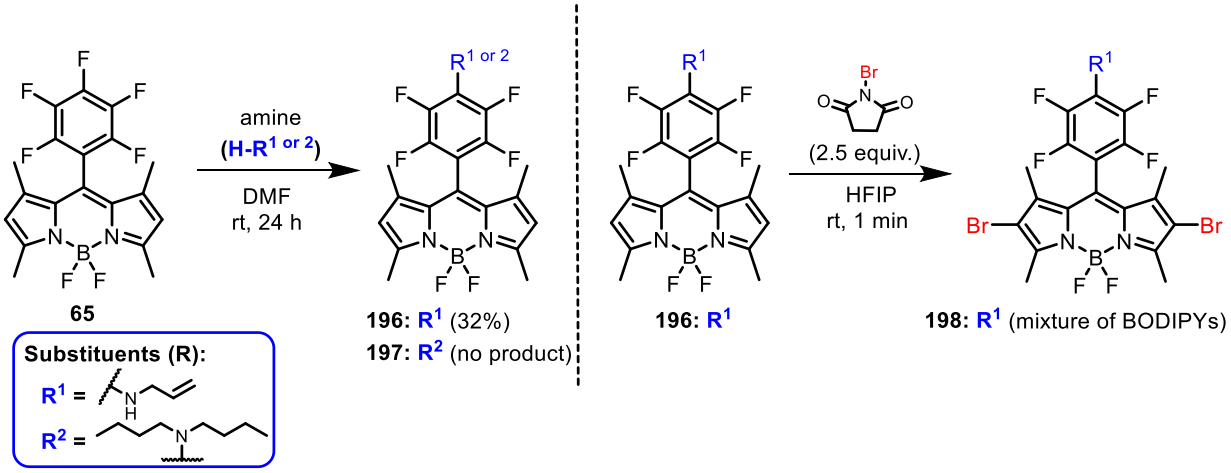

Scheme 50: Nucleophilic substitution of BODIPY **65** with amines and subsequent halogenation of BODIPY **196**.

In the same way, BODIPY **66** was substituted with additional amines. Allylamine, *N*,*N*-dibutylamine, and 6-methyl-6-oxohexylamine were used for this nucleophilic substitution. In all cases, the desired BODIPYs were successfully obtained. The best results were achieved for the functionalization with allylamine (BODIPY **199**; 86% yield). The other two amino-substituted BODIPYs **200** and **201** were obtained in 30% and 35% yield, respectively (Scheme 51).

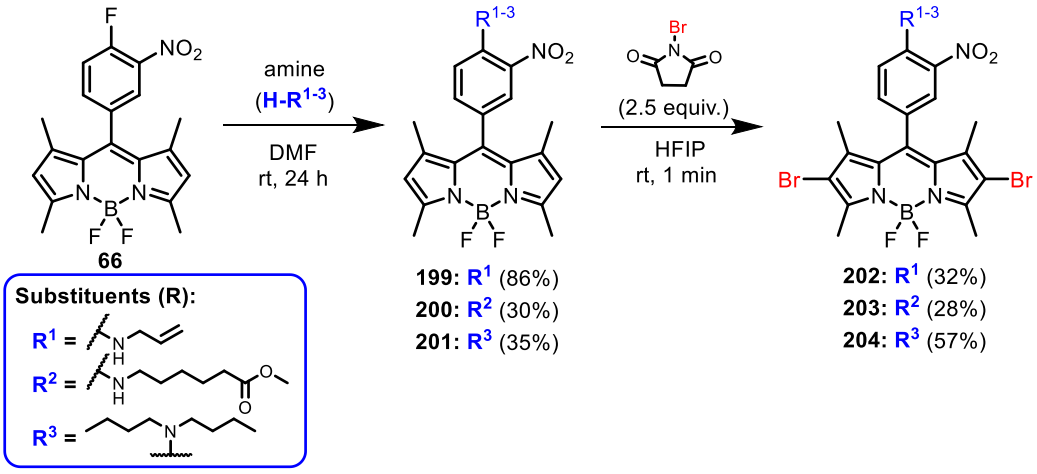

Scheme 51: Nucleophilic substitution of BODIPY **66** with amines and subsequent halogenation.

Subsequently, the halogenation was also performed with the substituted BODIPYs **199** - **201**. Here, all reactions with NBS led to the desired 2,6-dibrominated derivatives (**202** - **204**). Other brominated

BODIPYs were only found in traces. All desired products could be successfully separated from the side products. The halogenated BODIPYs (**202** - **204**) were obtained in moderate to good yields (Scheme 51).

Some BODIPYs were already applied for the targeted halogenation of the related 2-position (see chapter 2.2). Now, 1,3,5,7-tetramethyl-BODIPYs were subjected to the selective substitution of the 2-position with bromine. In analogy to the targeted halogenation of the core-unsubstituted BODIPYs, the tetrafluorophenyl-based BODIPYs **65**, **67**, and **69** were dissolved in DCM and treated with NBS (Scheme 52). Within two hours, full consumption of the starting material was observed *via* thin-layer chromatography. At the same time, the formation of the corresponding 2-bromo-substituted BODIPYs was detected. The halogenation of BODIPY **65** with NBS led to the product **205** in good yield, while significantly higher yields were achieved with the substituted BODIPYs **206** and **207** (78% and 83%, respectively, Scheme 52).

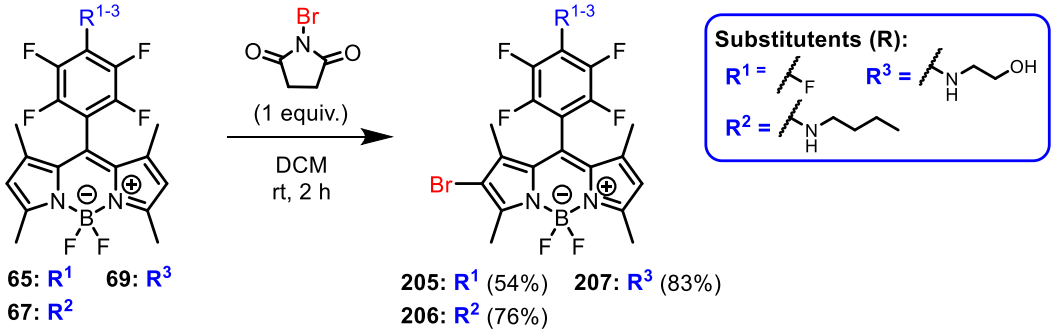

Scheme 52: Targeted bromination of selected 1,3,5,7-tetramethyl-substituted BODIPYs.

Furthermore, the 3-nitrophenyl-substituted BODIPYs (**66**, **71** und **73**) were also tested in the selective monohalogenation. Again, with the functionalized BODIPYs (**71** und **73**) a targeted substitution of the 2-position proved to be possible. However, lower yields were observed in comparison to the tetrafluorophenyl-based BODIPYs (Scheme 53).

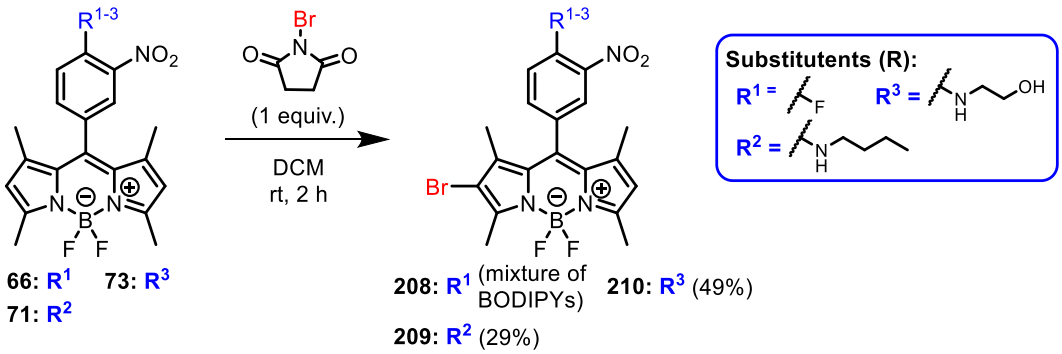

Scheme 53: Targeted bromination of selected 1,3,5,7-tetramethyl-substituted BODIPYs.

In the case of the unsubstituted BODIPY **66**, only a mixture of different BODIPYs with different substitution patterns was obtained (mono- and dihalogenated BODIPYs). A separation of this mixture

was not possible. In general, BODIPYs with two bromine atoms at the core structure could be detected *via* thin-layer chromatography. However, dihalogenated derivatives were only isolated in traces.

The 2-bromo-1,3,5,7-tetrametyl-substituted BODIPYs (**205** – **210**) were also evaluated for their potential suitability in the antimicrobial photodynamic inactivation (Fig. 31). The antibacterial activity was again performed in PBS and PBS supplemented with serum to investigate the activity in a more realistic model. The antimicrobial assays against the Gram-positive germ *S. aureus* were carried out by the biolitec research GmbH.

The BODIPYs (**205** – **210**) exhibited the same high antimicrobial activity as observed for the dibrominated BODIPYs. Except for compounds **205** and **210**, all BODIPYs showed dark toxic effects at a concentration of 100 µM, resulting in a suppression of bacterial growth below the detection limit. For all BODIPYs, a highly effective phototoxicity against *S. aureus* in PBS with a complete inactivation already at 1 µM was also identified (Fig. 31). The antibacterial activity of the tested BODIPYs greatly decreased in the presence of serum. No significant dark toxicity could be found for almost all BODIPYs (**205** and **207** – **210**) anymore.

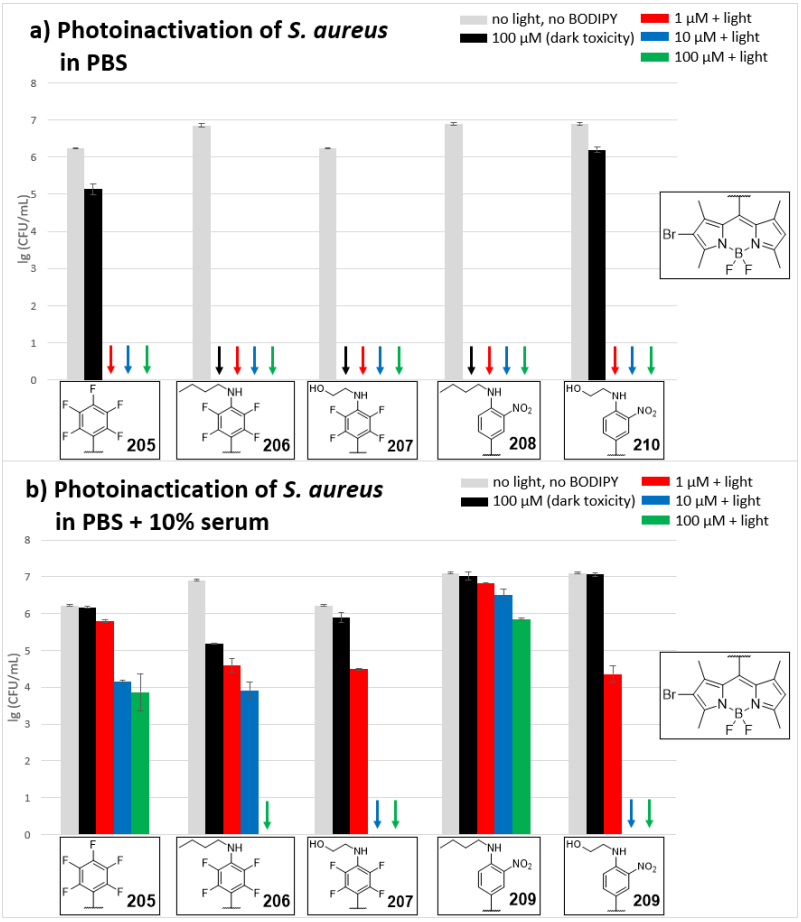

Figure 31: Photoinactivation of *S. aureus* by 2-bromo-1,3,5,7-tetrametyl-BODIPYs in PBS (**a**) and in PBS+10% serum (**b**). The antibacterial toxicity is expressed as logarithm of the number of colony-forming units, lg (CFU mL^{-1}). Arrows indicate a suppression of bacterial growth below the detection limit.

In the case of BODIPY **206**, only a low dark toxicity was observed at 100 µM. Nevertheless, in the presence of serum, BODIPYs **207** and **210** carrying a free hydroxy group, showed a complete inactivation of *S. aureus* already at concentration of 10 µM under light. A medium phototoxicity with a decrease of bacterial viability of approx. two log stages was also found for both complexes at 1 µM. For BODIPY **206** a complete reduction of bacterial growth was detected at the highest concentration under light. While BODIPY **205** only exhibited a reduction of bacterial growth of two log stages. The phototoxic activity of BODIPY **209** decreased significantly in the presence of serum (Fig. 31).
In conclusion, the concept of a mono-bromination of 1,3,5,7-tetrametyl-BODIPYs also resulted in compounds with high potential for an application in antimicrobial photodynamic inactivation.

The absorption and emission spectra indicated a significant difference between the 3-nitrophenyl-based and 2,3,5,6-tetrafluorophenyl-based BODIPYs. These two groups of BODIPYs showed a difference in their absorption and emission maxima of approx. 20 nm. However, the different substituents at the related *para*-phenyl positions exerted no significant influence. Also, no significant influence was exhibited by the methyl substituents on the BODIPY core structure (Fig. 32). The introduction of bromine to the BODIPY on the other hand had a significant impact on the optical properties. Compared to the BODIPYs with an unsubstituted core structure a significant bathochromic shift of the respective absorption maxima (15 – 20 nm) was achieved by the substitution of the 2-position with a bromine atom (Fig. 32). In the case of the dibrominated BODIPYs, an even stronger effect on the optical properties was found. The corresponding absorption and emission maxima of the respective 2,6-dibrominated BODIPYs showed a redshift of about 30 nm (Fig 32).

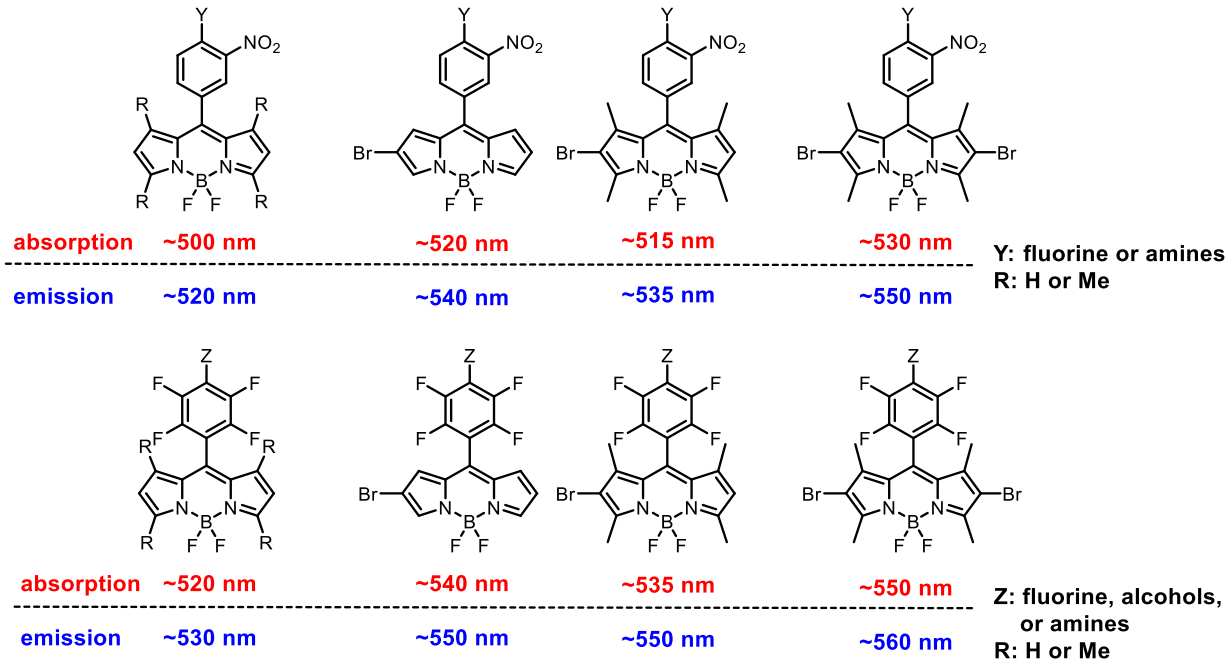

Figure 32: Absorption and emission maxima of different types of BODIPYs.

To investigate the cellular uptake of BODIPYs into cells, confocal laser scanning microscopy (cLSM) was performed. Glycosylated BODIPYs are of particular interest, as the carbohydrate moiety is expected to increase bioavailability and supports the uptake. For this, BODIPYs **92** and **94** carrying a thioglucosyl moiety were evaluated in cellular uptake experiments. The 2-hydroxyethylamino-substituted BODIPY **211**, provided by Claudia Gutsche,[106] was used for comparison with the glycosylated BODIPYs. As well, the respective dibromo-1,3,5,7-tetrametyl-substituted BODIPYs, equipped with a thioglucosyl moiety (**86** and **90**) or a 2-hydroxyethylamino moiety (**78**), were evaluated in cellular uptake experiments. For cLSM, cells (A431 cell line) were seeded in 8-well ibidi μ-slides (13.500 cells/well) in cell culture medium. After one day, the BODIPYs were added at a final test concentration of 10 µM and the cells were grown for another four and 24 hours. After the indicated time, cell nuclei were stained with Hoechst 33342 (1 µg/mL). Cells were washed and confocal images were taken. The cellular uptake experiments were performed in collaboration with the group of Prof. Dr. Rainer Haag, FU Berlin, by Dr. Katharina Achazi and Elisa Quaas. In Figures 33 and 34 the cellular uptake of BODIPYs is shown after four and 24 hours. BODIPY fluorescence is shown in red and the fluorescence of Hoechst 33342 in blue. Transmitted light images were also taken and are shown in gray scale.

As can be seen in Figure 33, the highest uptake was observed with the glucosyl-tetrafluorophenyl BODIPY **92**, as the whole cellular interior exhibits an intense fluorescence even after four hours. Simultaneously, an accumulation of the fluorophore in a specific area located next to the cell nuclei was detected after 24 hours. A slight accumulation of BODIPY **92** was already observed after four hours. BODIPY **210** showed a slower uptake since a clear fluorescence is only visible after 24 hours. A slight accumulation to a specific area near the nucleus was also found for BODIPY **211** after 24 hours. In contrast, for the glucosyl-nitrophenyl-based BODIPY **94** no visible uptake was detected. However, this should be interpreted with caution, this seemingly ‚non-uptake' could be an effect of the lower fluorescence intensity of the nitro-substituted compound. BODIPYs **92**, **94**, and **211** exhibited no influence on the cell viability.

With all halogenated BODIPYs (**78**, **86**, and **90**) a high cellular uptake was achieved, as an intense fluorescence in the cellular interior was found after four hours. After four hours, for the halogenated derivatives no impact on cell viability was found. However, a very high reduction of cell viability was observed by all BODIPYs after 24 hours (Fig. 34).

Experiments confirmed the cellular uptake of the studied BODIPYs. In the case of core-unsubstituted BODIPYs, the glycosylated tetrafluorophenyl-BODIPY **92** proved to be particularly suitable for fluorescence detection of the uptake into cells, at the same time exerting no negative effect on cell viability. The drastically decreased number of cells, as well as the reduced size of the remaining cells, gave evidence for a strong toxic effect of the dibromo-substituted BODIPYs (**78**, **86**, and **90**) on the tumor cells (Fig. 34).

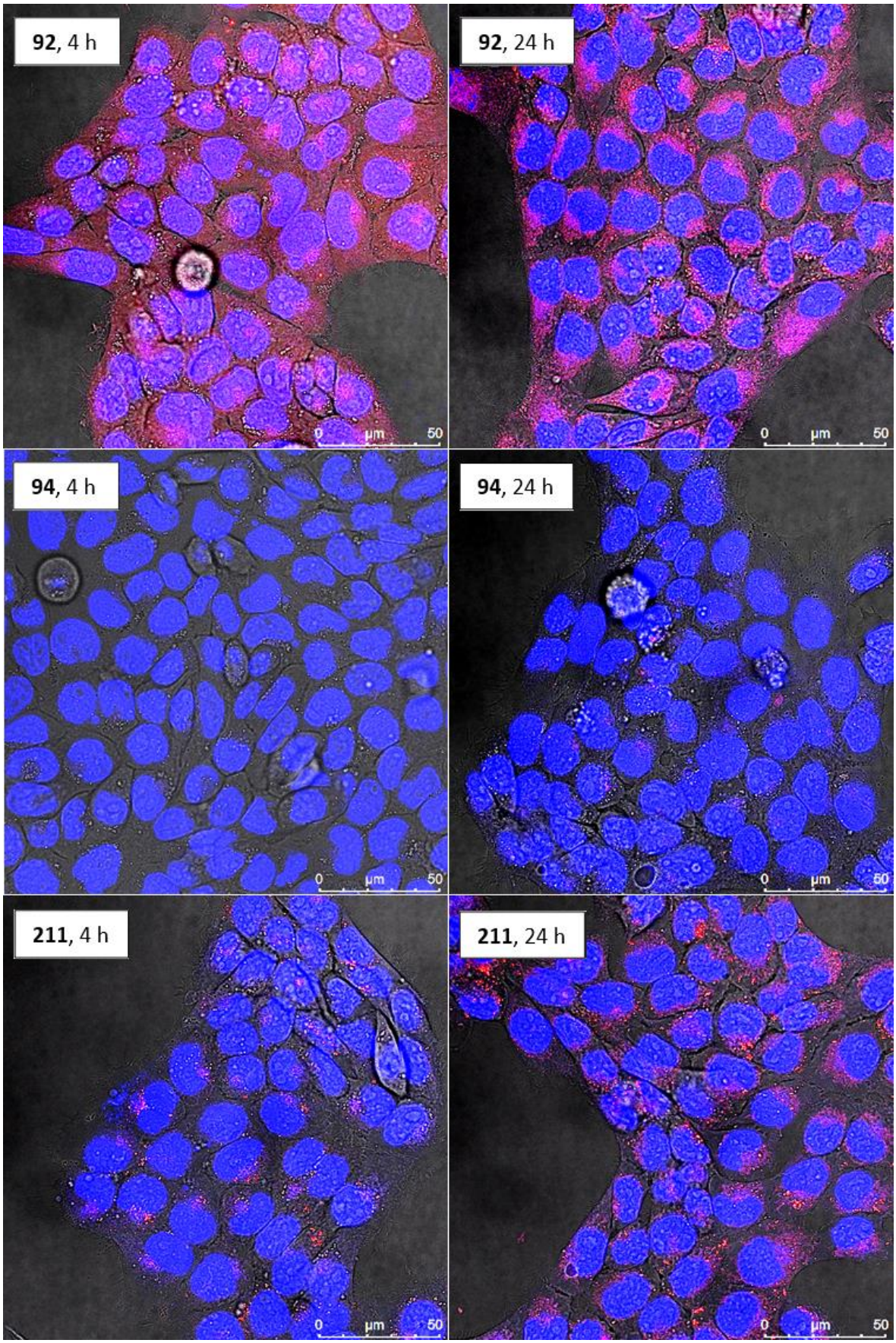

Figure 33: cLSM overlay images of BODIPY **92**, **94**, and **210** for comparison after four and 24 h. BODIPY fluorescence is shown in red and nuclei fluorescence is shown in blue (Hoechst 33342). The transmitted light images are shown in gray scale.

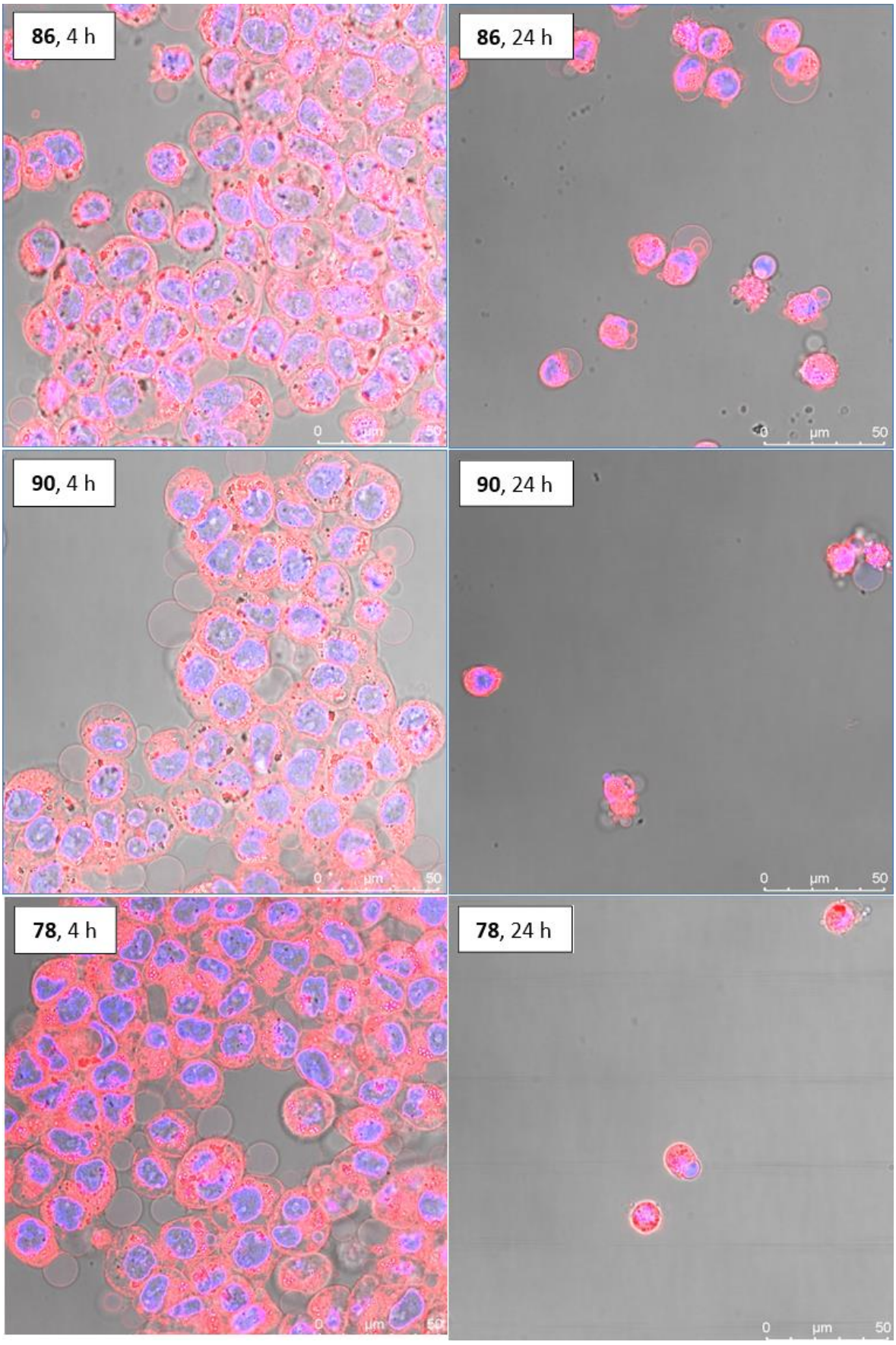

Figure 34: cLSM overlay images of BODIPY **78**, **86**, and **90** after four and 24 h. BODIPY fluorescence is shown in red and nuclei fluorescence is shown in blue (Hoechst 33342). The transmitted light images are shown in gray scale.

3.4 BODIPY-cyclen derivatives

Due to the excellent fluorescence properties, BODIPYs are widely used as fluorescence markers or as theragnostic agents.[27c,107] In addition, derivatives of BODIPYs with macrocyclic molecules are described in the literature, e.g., cyclen or 1,4,7,10-tetraazacyclododecan-1,4,7,10-tetraacetic acid. These types of BODIPY conjugates are specifically interesting for medical imaging.[97a,107a,108] In addition, certain metal-cyclen complexes show promising potential for medical applications, due to their ability to cleave RNA, DNA, peptide-structures, or other biomolecules.[109]

In this project, a direct linking between a BODIPY and a cyclen was performed. This coupling was realized *via* the copper(I)-mediated 1,3-dipolar cycloaddition (click reaction). The coupling of cyclen structures with other molecules or biomolecules through the copper(I)-catalyzed cycloaddition had also been described in the literature.[110] In preparation of the following synthesis of the BODIPY-cyclen derivative, the propargyl-substituted cyclen **212** was prepared (Scheme 54).

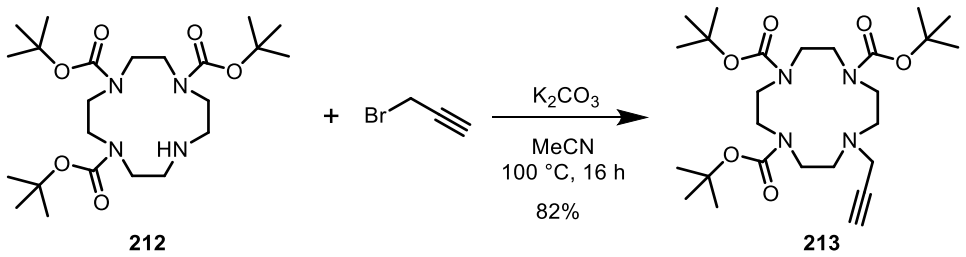

Scheme 54: Preparation of the propargyl-substituted cyclen **213** (compound **212** was provided by the group of Prof. Nora Kulak).

Specifically, to ensure that only one of the amino groups was functionalized with a propargyl moiety, a cyclen was chosen where three amino groups are protected by *tert*-butyloxycarbonyl groups. This functionalization of a *tert*-butyloxycarbonyl protected cyclen with propargyl bromide is known in the literature.[110b,110c] Cyclen **212** was reacted with propargyl bromide and K_2CO_3 (Scheme 54).[110c] Finally, the propargyl-substituted cyclen **213** was successfully obtained in high yields (Scheme 54).

Having the starting materials **153** and **213** at hand, the copper-catalyzed cycloaddition was performed to form the BODIPY-cyclen derivative **214**. Azido-BODIPY **153**, cyclen **213**, $CuSO_4$, and sodium ascorbate were dissolved in DMF (Scheme 55). The cycloaddition progresses through a cyclic reaction mechanism, wherein copper(I) ions catalyze a coupling between the azido group and the alkyne. Finally, the two structural elements (BODIPY and cyclen) are linked *via* a 1,2,3-triazole group.[111]

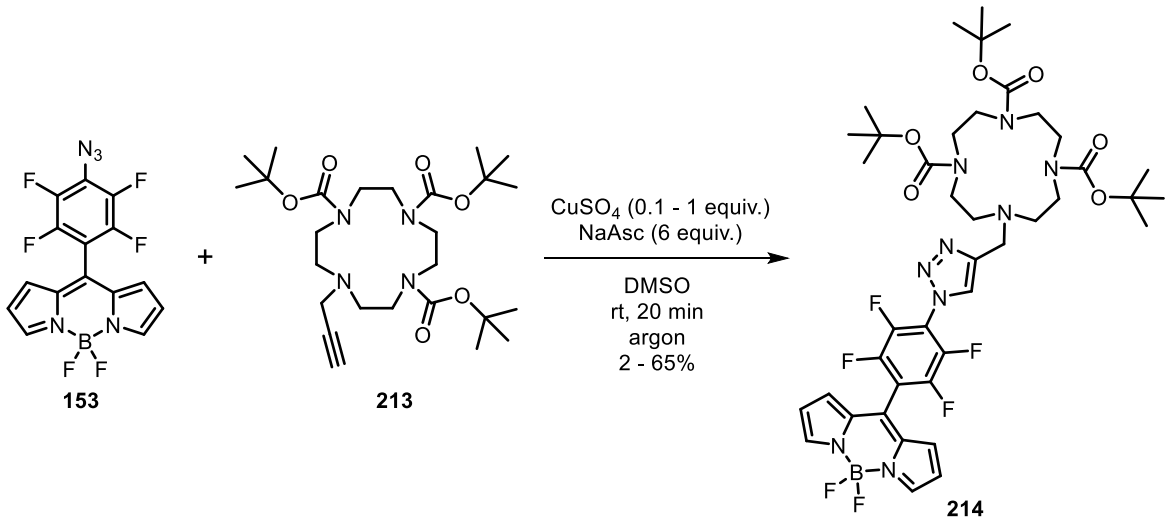

Scheme 55: Copper(I)-catalyzed cycloaddition of BODIPY **153** and cyclen **214**.

For the copper-mediated cycloaddition, typically, catalytic amounts of copper(I) ions are required. Within the reaction mechanism these copper(I) ions are continuously formed, thus, sodium ascorbate is only employed to generate the required copper(I) ions from $CuSO_4$ in the initial step.[111] Interestingly, catalytic amounts of the $CuSO_4$ (10 mol%) only gave small amounts of the desired compound **214**. Instead, evidence for the formation of the 4-amino-2,3,5,6-tetrafluorophenyl substituted BODIPY was identified. Increasing the amount of $CuSO_4$ led into significantly higher yields of the respective product **214**. In the case of 50 mol% of $CuSO_4$, the product was obtained in 55% yield, while increasing the amount of $CuSO_4$ to one equivalent even a yield of 65% was achieved. Simultaneously, quantities of the amino-substituted BODIPY were significantly decreased at higher concentrations of the copper catalyst. In the case of a low $CuSO_4$ concentration, an almost complete coordination of copper(I) ions could be occurred by the cyclen moiety, resulting into an insufficient concentration of the copper catalyst for a successful implementation. In contrast, increased concentrations ensured sufficient quantities of the free copper(I) ions to form of the desired BODIPY-cyclen derivative. No evidence for the occurrence of a copper-cyclen complex was found, instead, the spectroscopic analyses proved the formation of the desired copper-free derivative **214**. Probably, only a temporary complexation of copper ions occurred, giving a possible explanation why larger quantities of copper(II) ions were required and no evidence of a copper complex of **214** was found.

In the next step, the removal of the *tert*-butyloxycarbonyl groups was performed. For this, compound **214** was treated with an excess of trifluoroacetic acid (Scheme 56). Within the first hours, other fluorescent fractions were identified *via* thin-layer chromatography, indicating partial cleavage of the *tert*-butyloxycarbonyl groups. Finally, after 16 hours the starting material was totally consumed and no evidence for products with an incomplete removal of the protecting groups was found.

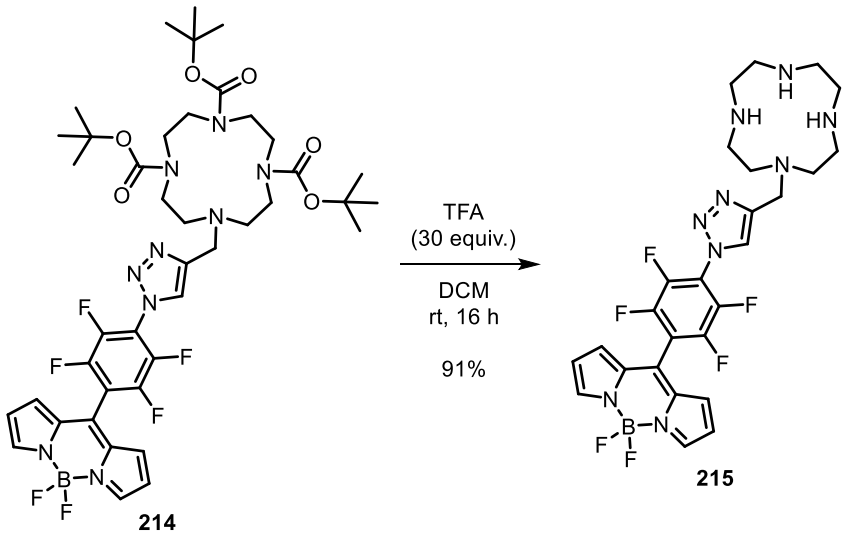

Scheme 56: Acid induced cleavage of the *tert*-butyloxycarbonyl groups.

Instead of a purification by chromatography, a recrystallization was sufficient to achieve the product **215** in pure form. Although a good solubility was obtained in large amounts of methanol, the compound could not be dissolved in typical concentration needed for NMR spectroscopy. The same results were obtained for other solvents tested, e.g., chloroform, DCM, acetone, THF, and DMSO. However, the product could be completely dissolved in water/acetic acid mixture (4/1, v/v), thus, a characterization by NMR spectroscopy was possible. Finally, the NMR and mass spectra confirmed the successful synthesis of the desired product **215** (in 91% yield, see Scheme 56).

Beside the desired product peak, the mass spectrum also showed additional signals. These signals could be assigned to specific BODIPY-cyclen structures, where one fluorine atom, or even both fluorine atoms (of the boron difluoride) were replaced by methoxy groups. As well, evidence for an exchange of a fluorine atom by a hydroxy group was found (Fig. 35).

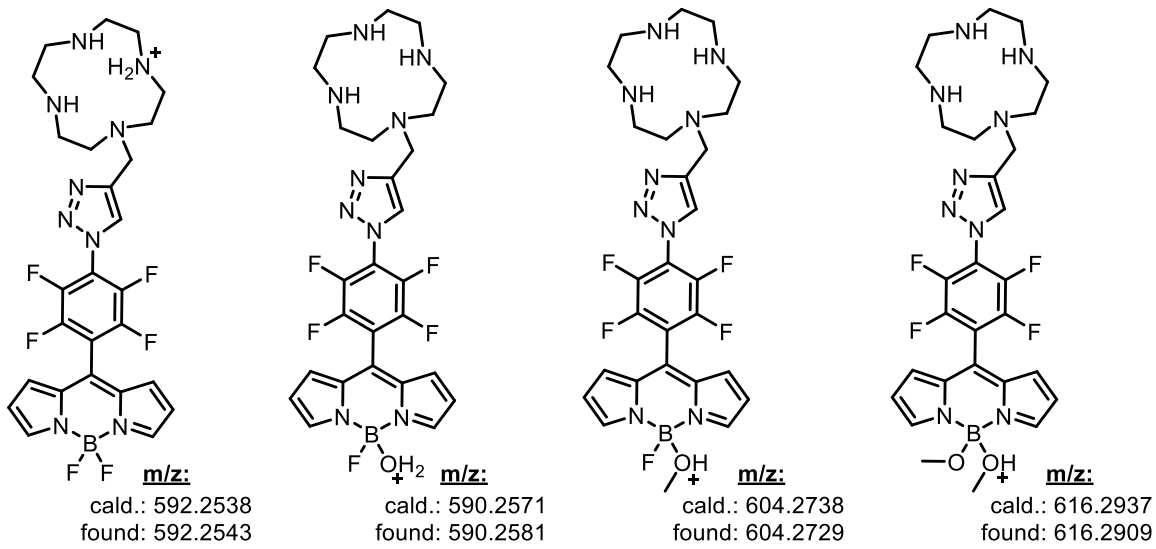

Figure 35: Overview of possible BODIPY structures, corresponding to the respective signals found in the ESI mass spectra.

An exchange of fluorine atoms by methoxy groups was described in the literature only under certain reaction conditions (Methanol/MeONa mixture, increased reaction temperature).[112] The contact of compound **215** with methanol in the synthesis and purification can be excluded, since no methanol was used there. However, methanol was applied to dissolve the substance for mass spectrometric analysis. A replacement of the fluorine atoms is conceivable under the conditions of the measurement. Water (probably present in the methanol) could also cause an exchange of the fluorine atom.

Having the unprotected cyclen-BODIPY derivative **215** at hand, in an additional experiment the complexation with copper(II) ions was investigated. For this, the derivative **215** and $Cu(NO_3)_2$ were dissolved in methanol (Scheme 57). Almost immediately after the addition of the copper nitrate, small amounts of a dark precipitate were observed in the reaction flask. The reaction mixture was heated to reflux for six hours to improve the complexation. After filtration of the suspension and washing with methanol, a dark-blueish solid was obtained.

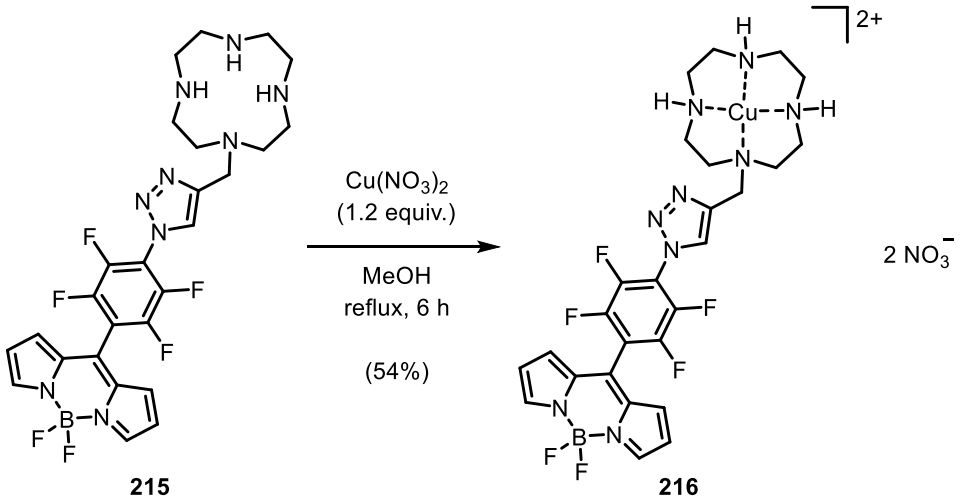

Scheme 57: Complexation of the BODIPY-cyclen derivative **215** with Cu(II) ions.

This compound again showed a poor solubility in all tested solvents, e.g., chloroform, acetone, THF, and DMSO. Moreover, the product was also not soluble in a mixture of water and acetic acid, thus, a characterization of the isolated compound by NMR spectroscopy was not possible. The compound could also not be identified by ESI mass spectrometry, due to the poor solubility/low ionization under these conditions. However, only the EI mass spectrometry gave evidence for the formation of the desired product. Within the (EI-)mass spectrum, two peaks could be assigned, which refers to possible fragments of the derivative **216**. The proposed fragmentation pathway of compound **216** and the associated fragments are shown in Scheme 58. In addition, such a fragmentation mechanism has already been described for cyclens in EI mass spectrometry.[113]

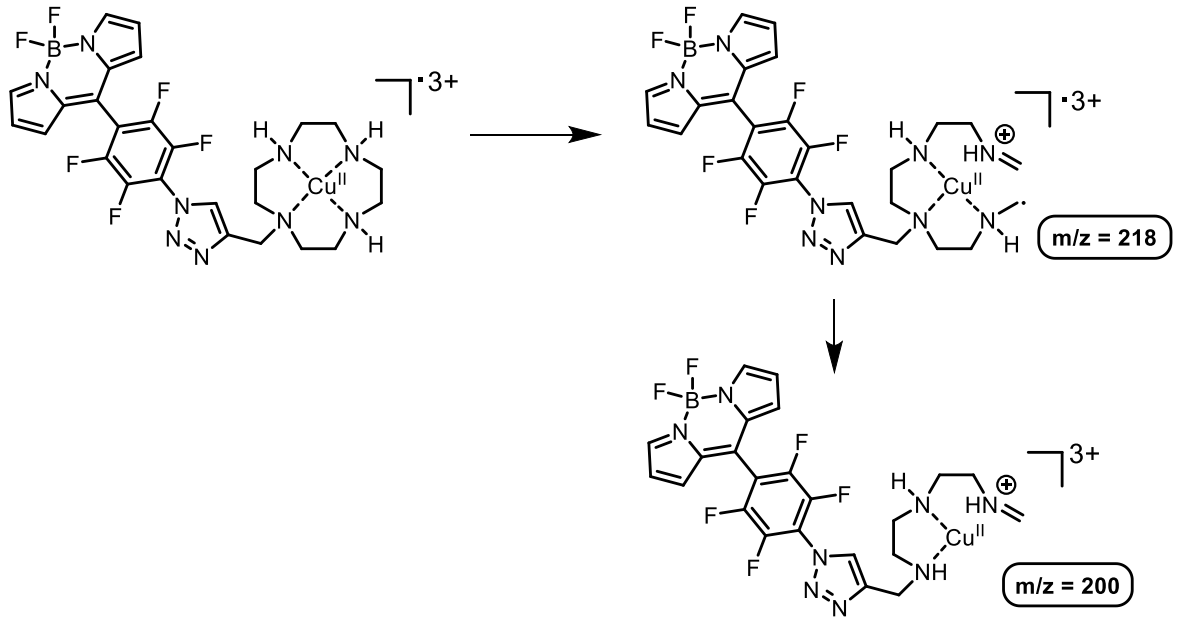

Scheme 58: Proposed mechanism for the fragmentation of compound **216**.

4. Outlook

The work presented in this thesis is focused on the synthesis of functionalized dipyrrinato metal complexes and BODIPYs, as well as on their dipyrrin and dipyrromethane precursors. The target compounds were evaluated for their suitability as potential photosensitizers for an application in PDT and antimicrobial photodynamic inactivation.

The first part discussed the introduction of the 4-fluoro-3-nitrophenyl moiety as a component in dipyrromethanes, dipyrrins, BODIPYs, and dipyrrinato ruthenium(II) complexes. The 4-fluoro-3-nitrophenyl group exhibits high modification potential, as many different amines were utilized for the fluorine exchange reaction to obtain functionalized dipyrromethanes in excellent yields. The scope was not limited to amines, also an azido group enabled an effective substitution. However, alcohols turned out as unsuitable nucleophiles for S_NAr in this case. The pre-functionalized dipyrrins were applied in the synthesis of BODIPYs and dipyrrins. Subsequent reactions with the dipyrrins gave the respective heteroleptic dipyrrinato ruthenium(II) complexes in good to high yields.

In the second part, the combination of the nucleophilic substitution with the modification of the BODIPY core structures with bromine was studied. The combination of these two concepts enabled the synthesis of BODIPY derivatives with a strong phototoxic activity against the Gram-positive germ *S. aureus* and the Gram-negative germ *P. aeruginosa*. Halogenated BODIPYs with additional thiocarbohydrates moieties showed the most effective biological activity under irradiation.

Photoactive heteroleptic dipyrrinato Iridium(III) complexes, based on the 3-nitrophenyl and the 2,3,5,6-tetrafluorophenyl moieties, were synthesized in the third project. Functionalized dipyrrins afforded dipyrrinato(III) complexes in moderate to good yields. The concept of *post*-functionalization was suitable for the introduction of alkenyl, alkynyl, and thiocarbohydrates. In tumor cell and bacterial assays, dipyrrinato iridium(III) complexes with a pronounced potential as possible photosensitizers were identified. Again, compounds with additional thiocarbohydrates exhibited an effective phototoxicity against tumor cells and bacteria.

In a side project homoleptic dipyrrinato complexes were prepared from 3-nitrophenyl-based dipyrrins. The dipyrrins showed a limited efficiency in the syntheses of bis(dipyrrinato) and tris(dipyrrinato) complexes. In many cases, the desired complexes were not obtained, or only in low yields.

In a last project, the synthesis of a BODIPY-cyclen derivative was performed. The copper(I)-mediated cycloaddition allowed the linkage of an azido-BODIPY and a cyclen in high yields. Subsequent transformation (cleavage of the *tert*-butyloxycarbonyl group and complexation of copper(II) ions) yielded in the desired BODIPY-cyclen derivative. However, for this final copper(II) derivative an insufficient solubility in solvents was found which did hindered a suitable characterization.

In future works, the range of possible nucleophiles could be extended to molecules that enable targeted binding to tumor cells. In this context, the introduction of cleavable linkers is also conceivable, since in this way a selective accumulation of the molecule in the tumor tissue is possible. For a potential medical use, the combination of BODIPYs and dipyrrinato complexes with biocompatible carrier systems, e.g., polyglycolides, would also be interesting.

The 1,3,7,9-tetramethyl-substituted dipyrrinato ruthenium(II) and iridium(III) complexes offer the possibility of further functionalization with bromine or iodine. In this way, similar to the modification of the BODIPY core structure with halogens, the phototoxic properties could possibly be significantly enhanced. In addition, the combination of the nucleophilic substitution of the *para*-position with the targeted halogenation of the 1,3,7,9-tetramethyl-substituted dipyrrinato ligand should be also studied in future works.

Finally, other cyclen analogues could also be investigated for the formation of related BODIPY-cyclen derivatives *via* copper(I)-mediated cycloaddition, e.g., oxa- or dioxacyclens.

5. Publications

5.1 meso-(4-Amino-3-nitrophenyl)-substituted dipyrromethanes as building blocks for BODIPYs and dipyrrinato ruthenium(II) complexes

"Synthesis of Porphyrinoids, BODIPYs, and (Dipyrrinato)ruthenium(II) Complexes from Prefunctionalized Dipyrromethanes"

Benjamin F. Hohlfeld, Keith J. Flanagan, Nora Kulak, Mathias O. Senge, Mathias Christmann, and Arno Wiehe, *Eur. J. Org. Chem.* **2019**, 4020-4033. DOI: 10.1002/ejoc.201900530

https://doi.org/10.1002/ejoc.201900530

Author's contribution:

- Synthesis and characterization of dipyrromethanes, dipyrrins, BODIPYs and (dipyrrinato)-ruthenium(II) complexes
- Additional characterization analysis: infrared (IR) spectroscopy and melting point
- Ultraviolet-visible (UV/vis) spectroscopic studies of BODIPYs and (dipyrrinato)ruthenium(II) complexes
- Fluorescence spectroscopic studies of BODIPYs
- Discussion and evaluating of the results
- Preparation and revision of the manuscript and the supporting information

5.2 Modification of the BODIPY structure via the targeted functionalization with bromine and the introduction with additional functional groups

"Exploring the relationship between structure and activity in BODIPYs designed for antimicrobial phototherapy"

Benjamin F. Hohlfeld, Burkhard Gitter, Keith J. Flanagan, Christopher J. Kingsbury, Nora Kulak, Mathias O. Senge and Arno Wiehe, *Org. Biomol. Chem.* **2020**, *18*, 2416-2431. DOI: 10.1039/d0ob00188k

https://doi.org/10.1039/D0OB00188K

Author's contribution:

- Synthesis of pre-functionalized dipyrromethanes
- Synthesis and characterization of BODIPYs and halogenated BODIPYs
- Additional characterization analysis: IR spectroscopy and melting point
- UV/vis and fluorescence spectroscopic studies of BODIPYs
- Discussion and evaluating of the results, including data from bacterial tests
- Preparation and revision of the manuscript and the supporting information

5.3 meso-Substituted dipyrrins as building blocks for photoactive dipyrrinato iridium(III) complexes

"Dipyrrinato-Iridium(III) Complexes for an Application in Photodynamic Therapy and Antimicrobial Photodynamic Inactivation"

Benjamin F. Hohlfeld, Burkhard Gitter, Christopher J. Kingsbury, Keith J. Flanagan, Dorika Steen, Gerhard D. Wieland, Nora Kulak, Mathias O. Senge and Arno Wiehe, *Chem. J. Eur.* **2021**, in press. DOI: 10.1002/ chem.202004776

https://doi.org/10.1002/chem.202004776

Author's contribution:

- Synthesis of pre-functionalized dipyrromethanes
- Synthesis and characterization of dipyrrins and (dipyrrinato)iridium(III) complexes
- Additional characterization analyses: IR spectroscopy and melting point
- UV/vis spectroscopic studies of (dipyrrinato)iridium(III) complexes
- Discussion and evaluating of the results, including data from tumor cell and bacterial tests
- Preparation and revision of the manuscript and the supporting information

6. Synthesis and characterization data for unpublished compounds

General remarks

DCM, *n*-pentane, and methanol were purchased and used as received. Other solvents were purchased and distilled at reduced pressure. Purchased chemicals were used as received without further purification. Reactions were monitored by thin-layer chromatography (Merck, TLC Silica gel 60 F_{254}). Flash column chromatography was performed on silica gel (Fluka silica gel 60M, 40-63µm).

NMR spectra were recorded with JEOL ECX400, JEOL ECP500, Bruker Avance500, and JEOL ECZ600 Instruments. Multiplicity of the signals was assigned as follows: s = singlet, br s = broad singlet, d = doublet, t = triplet, dd = doublet of doublets, dt = doublet of triplets, td = triplet of doublets, ddd = doublet of doublets of doublets, ddt = doublet of doublets of triplets, m = multiplet, m_c = centered multiplet. Chemical shifts are reported relative to $CDCl_3$ (^1H: δ = 7.26 ppm, ^{13}C: δ = 77.2 ppm), CD_2Cl_2 (^1H: δ = 5.32 ppm, ^{13}C: δ = 53.8 ppm), THF-d_8 (^1H: δ = 3.58 ppm, ^{13}C: δ = 67.6 ppm), D_2O (^1H: δ = 4.79 ppm). All ^{13}C NMR spectra are proton-decoupled and coupling constants are given in hertz (Hz). For a detailed peak assignment 2D spectra were measured (COSY, HMBC, and HMQC). Mass spectrometric analyses were carried out on an Agilent Technologies 6210 ESI-TOF (electrospray ionization, time of flight) instrument and on a Waters AutosecPremier, Agilent 7890B GC instrument (electron impact ionization). IR spectra were measured with a JASCO FT/IR 4100 spectrometer equipped with a PIKE MIRacle^{TM} ATR instrument. UV/vis spectra were recorded on a SPECORD S300 UV/vis spectrometer (Analytic Jena) in quartz cuvettes (1 cm length). Specified melting points were recorded on a Reichert Thermovar Apparatus and are not corrected. The ruthenium(II) half-sandwich complex **155**[114] and the iridium(III) half-sandwich complex **171**[115] were prepared according to the literature.

6.1 Heteroleptic dipyrrinato ruthenium(II) and iridium(III) complexes

Di(*µ*-chlorido)bis[chlorido(η^6-*p*-cymene)ruthenium(II)] (**155**):

Rutheniumtrichloride hydrate (2.00 g, 7.62 mmol, 1 equiv.) was dissolved in 75 mL of EtOH, (R)-*α*-phellandrene (9.92 mL, 61.20 mmol, 8 equiv.) was added, and stirred for 4 h at 100°C. The suspension was filtered over a glass frit and washed several times with EtOH. The filtrate was concentrated (approximately to half of the volume) and stored overnight in the freezer. The suspension was again filtered over a glass frit and washed with EtOH. This procedure was repeated twice to increase the yield of the product. The combined solids were dried, and the corresponding ruthenium complex was obtained as a red-brown solid (2.08 g, 89%).

^{1}H-NMR (400 MHz, $CDCl_3$): δ (ppm) = 1.26 (d, *J* = 6.9 Hz, 6H, Me), 2.14 (s, 3H, Me), 2.91 (sept, *J* = 7.0 Hz, 1H, CH), 5.33 (d, *J* = 5.9 Hz, 2H, $CH_{aromat.}$), 5.46 (d, *J* = 6.0 Hz, 1H, $CH_{aromat.}$).

6.1.1 Preparation of chlorido(p-cymene)(dipyrrinato)ruthenium(II) complexes

General synthetic procedure: The dipyrrin (1 equiv.) and **155** (0.5 equiv.) were dissolved in THF. The flask was shielded from ambient light with aluminum foil. DIPEA (14 equiv.) was added, and the mixture was stirred for 24 h at rt. After the indicated time, the mixture was diluted with DCM and saturated NaCl-solution was added. Afterwards, the mixture was extracted with DCM several times. The combined organic layers were dried with Na_2SO_4, filtered, and evaporated to dryness. The crude product was purified by column chromatography; the main fraction was collected and evaporated to dryness. Finally, the obtained solid was recrystallized.

Chlorido(η^6-*p*-cymene)[5-(4-fluoro-3-nitrophenyl)dipyrrinato]ruthenium(II) (**156**):
Complex **156** was prepared according to the general synthetic procedure. Dipyrrin **108** (540 mg, 1.92 mmol), **155** (584 mg, 0.95 mmol), and DIPEA (4.54 mL, 4.94 mmol) were dissolved in 40 mL of THF. After purification (column chromatography, silica gel, DCM/EtOAc = 2/1, v/v) and recrystallization (DCM/*n*-hexane); complex **156** was obtained as a red solid (615 mg, 1.11 mmol, 58%).

^{1}H NMR (500 MHz, $CDCl_3$): δ (ppm) = 1.10 (d, J = 6.8 Hz, 6H, Me_{cymene}), 2.23 (s, 3H, Me_{cymene}), 2.42–2.50 (m, 1H, CH_{cymene}), 5.31 (d, J = 6.1 Hz, 2H, Ar-H_{cymene}), 5.34 (d, J = 6.1 Hz, 2H, Ar-H_{cymene}), 6.46 (s, 2H, $H_{Pyrrole}$), 6.51 (dd, J = 4.4, 1.4 Hz, 2H, $H_{Pyrrole}$), 7.34 (dd, J = 10.5, 8.5 Hz, 1H, Ar-H_{meta}), 7.65 (br s, 1H, Ar-H_{ortho}), 8.06–8.09 (m, 3H, $H_{Pyrrole}$ + Ar-H_{ortho}).
^{13}C NMR (126 MHz, $CDCl_3$): δ (ppm) = 18.8 (Me_{cymene}), 22.2 (Me_{cymene}), 30.8 (CH_{cymene}), 84.7 (Ar-C_{cymene}), 85.1 (Ar-C_{cymene}), 117.9 (Ar-C_{meta}), 119.5 ($C_{Pyrrole}$), 127.3 (Ar-C_{ortho}), 130.5 ($C_{Pyrrole}$), 134.6 ($C_{Pyrrole}$), 137.7 (Ar-C_{ortho}), 141.5 (C_{meso}), 156.0 ($C_{Pyrrole}$).
^{19}F NMR (376 MHz, $CDCl_3$): δ (ppm) = -117.22 (s, 1F, CF).
HRMS (ESI-TOF, DCM/MeOH): *m/z* calcd. for $C_{25}H_{23}FN_3O_2Ru^+$ $[M\text{-}Cl]^+$: 518.0812, found: 518.0851.
IR (ATR): $\tilde{\nu}$ (cm^{-1}) = 3055 [ν(Ar-H)], 2967, [ν(Me)], 2861 [ν(CH)], 1617 [ν(C=N), ν(C=C)], 1553 [$\nu_{as}(NO_2)$], 1344 [$\nu_{sym}(NO_2)$], 726 [δ(HC=CH)].
UV/vis (DCM): λ_{max} (nm) [log (ε/L mol^{-1} cm^{-1})] = 448 [4.29], 497 [4.42].
M.P. (°C): 197-200.

Chlorido(η^6-*p*-cymene){5-[4-(*N,N*-dibutylamino)-3-nitrophenyl]dipyrrinato}ruthenium(II) (**157**):
Complex **157** was prepared according to the general synthetic procedure. Dipyrrin **109** (200 mg, 0.51 mmol), **155** (156 mg, 0.26 mmol), and DIPEA (1.21 mL, 7.13 mmol) were dissolved in 20 mL of THF. After purification (column chromatography, silica gel, DCM/EtOAc = 9/1, v/v) and recrystallization (DCM/*n*-pentane); complex **157** was obtained as a dark red solid (98 mg, 0.15 mmol, 29%).

^{1}H NMR (500 MHz, $CDCl_3$): δ (ppm) = 0.91 (t, *J* = 7.4 Hz, 6H, Me), 1.07 (d, *J* = 6.9 Hz, 6H, Me_{cymene}), 1.28–1.35 (m, 4 H, CH_2), 1.53–1.59 (m, 4 H, CH_2), 2.20 (s, 3H, Me_{cymene}), 2.43 (hept, *J* = 6.8 Hz, 1H, CH_{cymene}), 3.16–3.19 (m, 4 H, CH_2), 5.27 (d, *J* = 6.1 Hz, 2H, Ar-H_{cymene}), 5.30 (d, *J* = 6.3 Hz, 2H, Ar-H_{cymene}), 6.50 (dd, *J* = 4.4, 1.4 Hz, 2H, $H_{Pyrrole}$), 6.65 (dd, *J* = 4.4, 1.3 Hz, 2H, $H_{Pyrrole}$), 7.09 (d, *J* = 8.6 Hz, 1H, Ar-H_{meta}), 7.42 (dd, *J* = 8.6, 2.2 Hz, 1H, Ar-H_{ortho}), 7.75 (d, *J* = 2.2 Hz, 1H, Ar-H_{ortho}), 8.02 (t, *J* = 1.4 Hz, 2H, $H_{Pyrrole}$).

^{13}C NMR (126 MHz, $CDCl_3$): δ (ppm) = 13.96 (Me), 18.7 (Me_{cymene}), 20.3 (CH_2), 22.2 (Me_{cymene}), 29.6 (CH_2), 30.7 (CH_{cymene}), 52.0 (CH_2), 84.7 (Ar-CH_{cymene}), 85.0 (Ar-CH_{cymene}), 100.4 (Ar-C_{cymene}), 118.8 ($C_{Pyrrole}$), 120.1 (Ar-C_{meta}), 128.1*, 128.5 (Ar-C_{ortho}), 130.8 ($C_{Pyrrole}$), 135.1 ($C_{Pyrrole}$ + Ar-C_{ortho}), 140.6*, 144.0 (C_{meso}), 145.3 (Ar-C_{para}), 155.2 ($C_{Pyrrole}$). *These signals could not be assigned exactly to corresponding carbon atoms. They belong to the Ar-C_{ipso} and the Ar-C_{nitro} of the aryl residue.

HRMS (ESI-TOF, MeOH): *m/z* calcd. for $C_{33}H_{41}N_4O_2Ru^+$ $[M\text{-}Cl]^+$: 627.2268, found: 627.2309.

IR (ATR): $\tilde{\nu}$ (cm^{-1}) = 2956, 2926, and 2870 [$\nu(CH_2)$, ν(Me)], 1610 [ν(C=N), ν(C=C)], 1547 [$\nu_{as}(NO_2)$], 1339 [$\nu_{sym}(NO_2)$], 729 [δ(HC=CH)].

UV/vis (DCM): λ_{max} (nm) [log (ε/L mol^{-1} cm^{-1})] = 430 [4.39], 494 [4.42].

M.P. (°C): 125-130.

Attempted synthesis of chlorido(η^6-*p*-cymene){5-[3-nitro-4-(*N*-prop-2-ynylamino)phenyl]-dipyrrinato}ruthenium(II) (**158**):

The reaction was carried out according to the general synthetic procedure. Dipyrrin **110** (100 mg, 0.31 mmol), **155** (96 mg, 0.16 mmol), and DIPEA (0.75 mL, 4.40 mmol) were dissolved in 15 mL of THF. After purification (column chromatography, silica gel, DCM/EtOAc = 1/1, v/v) an orange solid (19 mg) was obtained. However, this fraction could not be assigned to the desired product. The spectra did not allow a meaningful interpretation.

Chlorido(η^6-*p*-cymene)(5-pentafluorophenyl-1,3,7,9-tetramethyldipyrrinato)ruthenium(II) (**167**):

Complex **167** was prepared according to the general synthetic procedure. Dipyrrin **127** (200 mg, 0.55 mmol), **155** (167 mg, 0.27 mmol), and DIPEA (1.30 mL, 7.64 mmol) were dissolved in 10 mL of THF. After purification (column chromatography, silica gel, EtOAc/*n*-hexane = 1/1, v/v) and recrystallization (DCM/*n*-hexane); complex **167** was obtained as an orange solid (16 mg, 20 µmol, 4%). Evidence for a decomposition of the dipyrrin was found, due to the observation of large quantities of a black residue.

^{1}H NMR (500 MHz, $CDCl_3$): δ (ppm) = 1.11 (d, *J* = 6.9 Hz, 6H, Me_{cymene}), 1.54 (s, 6H, Me), 2.03 (s, 1H, CH_{cymene}), 2.11 (s, 3H, Me_{cymene}), 2.75 (s, 6H, Me), 5.15 (d, *J* = 6.1 Hz, 2H, Ar-H_{cymene}), 5.24 (d, *J* = 6.0 Hz, 2H, Ar-H_{cymene}), 6.11 (d, *J* = 1.0 Hz, 2H, $CH_{pyrrole}$).

^{19}F NMR (376 MHz, $CDCl_3$): δ (ppm) = -137.68 (dd, J = 24.0, 8.4 Hz, 1F, CF_{ortho}), -141.12 (dd, J = 24.1, 8.3 Hz, 1F, F_{ortho}), -153.44 (t, J = 20.7 Hz, 1F, CF_{para}), -161.28 - -161.59 (m_c, 2F, CF_{meta}) ppm.
The HRMS and the ^{13}C NMR spectra did not allowed a meaningful interpretation.
M.P. (°C): >250.

Chlorido(η^6-*p*-cymene)[5-(4-fluoro-3-nitrophenyl)-1,3,7,9-tetramethyldipyrrinato]-ruthenium(II) (**168**):
Complex **168** was prepared according to the general synthetic procedure. Dipyrrin **127** (250 mg, 0.74 mmol), **155** (226 mg, 0.37 mmol), and DIPEA (1.80 mL, 10.31 mmol) were dissolved in 20 mL of THF. After purification (column chromatography, silica gel, DCM/EtOAc = 9/1, v/v) and recrystallization (DCM/*n*-hexane); complex **168** was obtained as an orange-reddish solid (79 mg, 0.13 mmol, 13%). Evidence for a decomposition of the dipyrrin was found, due to the observation of large quantities of a black residue.

^{1}H NMR (500 MHz, CD_2Cl_2): δ (ppm) = 1.12–1.17 (d, J = 6.9 Hz, 6H, Me_{cymene}), 1.35 (s, 6H, Me), 2.24 (s, 3H, Me_{cymene}), 2.40–2.48 (s, 1H, CH_{cymene}), 2.71 (s, 6H, Me), 5.20 (br s, 4H, Ar-H_{cymene}), 6.14 (s, 2H, Ar-$CH_{pyrrole}$), 7.41 (ddd, J = 30.8, 10.6, 8.4 Hz, 1H, Ar-H_{meta}), 7.51 – 7.58 (m, 1H, Ar-H_{ortho}), 7.96 (ddd, J = 27.4, 7.3, 2.3 Hz, 1H, Ar-H_{ortho}).
^{13}C NMR (126 MHz, CD_2Cl_2): δ (ppm) = 17.1 (Me), 18.7 (Me_{cymene}), 19.8 (Me), 22.7 (Me_{cymene}), 30.8 (CH_{cymene}), 84.2 (Ar-C_{cymene}), 85.1 (Ar-C_{cymene}), 119.3 (d, J = 7.2 Hz, Ar-C_{meta}), 123.7 ($CH_{Pyrrole}$), 126.6 (Ar-C_{ortho}), 129.2*, 132.64 (d, J = 7.8 Hz, $C_{Pyrrole}$), 136.07 (d, J = 8.4 Hz), 136.5*, 138.5 (C_{meso}), 139.05 (d, J = 8.4 Hz, Ar-C_{ortho}), 142.9 ($C_{Pyrrole}$), 155.88 (d, J = 265.3 Hz, Ar-C_{para}), 163.6 ($C_{Pyrrole}$). *These signals could not be assigned exactly to corresponding carbon atoms. They belong to the Ar-C_{ipso} and the Ar-C_{nitro} of the aryl residue.
^{19}F NMR (376 MHz, CD_2Cl_2): δ (ppm) = -118.60 – -119.31 (m, 1F, CF).
HRMS (ESI-TOF, MeOH): *m/z* calcd. for $C_{29}H_{31}FN_3O_2Ru^+$ $[M\text{-}Cl]^+$: 574.1438, found: 574.1429.
IR (ATR): $\tilde{\nu}$ (cm^{-1}) = 3046 [ν(Ar-H)], 2960 and 2924 [ν(Me)], 2868 [ν(CH)], 1615 [ν(C=N), ν(C=C)], 1535 [$\nu_{as}(NO_2)$], 1345 [$\nu_{sym}(NO_2)$], 734 [δ(HC=CH)].
UV/vis (DCM): λ_{max} (nm) [log (ε/L mol^{-1} cm^{-1})] = 509 [4.64].
M.P. (°C): >250.

6.1.2 Preparation of bis(2,2'-bipyridyl)(dipyrrinato)ruthenium(II) complexes
General synthetic procedure: The chlorido(*p*-cymene)(dipyrrinato)ruthenium(II) complex (1 equiv.) was dissolved in EtOH. 2,2´-bipyridine (2 equiv.) was added and the mixture was heated to reflux for 24 h. The flask was shielded from ambient light with aluminum foil. After the indicated time, the mixture could cool down and was evaporated to dryness. The crude product was purified by column

chromatography; the main fraction was collected and evaporated to dryness. Finally, the obtained solid was recrystallized.

{Bis(2,2´-bipyridyl)[5-(4-fluoro-3-nitrophenyl)dipyrrinato]ruthenium(II)}chloride (**159**):
Complex **159** was prepared according to the general synthetic procedure. Complex **156** (200 mg, 0.36 mmol) and 2,2´-bipyridine (113 mg, 0.72 mmol) were dissolved in 25 mL of EtOH. After purification (column chromatography, silica gel, DCM/MeOH = 9/1, v/v) and recrystallization (DCM/*n*-hexane); complex **159** was obtained as a black solid (233 mg, 0.32 mmol, 88%).

^{1}H NMR (500 MHz, $CDCl_3$): δ (ppm) = 6.28 (dd, *J* = 4.4, 1.5 Hz, 2H, $H_{Pyrrole}$), 6.37–6.38 (m, 2H, $H_{Pyrrole}$), 6.44–6.47 (m, 2H, $H_{Pyrrole}$), 7.29–7.40 (m, 5H, H_{Bipy}, Ar-H_{meta}), 7.64–7.66 (m, 2H, H_{Bipy}), 7.68 (ddd, *J* = 8.5, 4.2, 2.3 Hz, 1H, Ar-H_{ortho}), 7.85 (dd, *J* = 5.7, 1.4 Hz, 1H, H_{Bipy}), 7.88 (dd, *J* = 5.7, 1.4 Hz, 1H, H_{Bipy}), 7.95–8.02 (m, 4H, H_{Bipy}), 8.08 (dd, *J* = 7.0, 2.3 Hz, 1H, Ar-H_{ortho}), 8.74 (t, *J* = 7.3 Hz, 2H, H_{Bipy}), 8.80 (dd, *J* = 8.2, 4.4 Hz, 1H, H_{Bipy}).
^{13}C NMR (126 MHz, $CDCl_3$): δ (ppm) = 117.78 (d, *J* = 20.9 Hz, Ar-C_{meta}), 119.3 ($C_{Pyrrole}$), 124.35 (d, *J* = 8.5 Hz, C_{Bipy}), 124.55 (d, *J* = 10.0 Hz, C_{Bipy}), 126.50 (d, *J* = 3.2 Hz, C_{Bipy}), 126.85 (d, *J* = 6.9 Hz, C_{Bipy}), 127.61 (d, $J_{C,F}$ = 1.9 Hz, Ar-C_{ortho}), 131.1 ($C_{Pyrrole}$), 135.0 ($C_{Pyrrole}$), 135.82 (d, $J_{C,F}$ = 3.8 Hz)*, 136.21 (d, $J_{C,F}$ = 19.0 Hz, C_{Bipy}), 136.52 (d, $J_{C,F}$ = 7.8 Hz)*, 136.80 (d, *J* = 10.0 Hz, C_{Bipy}), 137.37 (d, $J_{C,F}$ = 8.6 Hz, Ar-C_{ortho}), 142.2 (C_{meso}), 150.3 ($C_{Pyrrole}$), 150.57 (d, *J* = 16.4 Hz, C_{Bipy}), 151.60 (d, *J* = 14.9 Hz, C_{Bipy}), 155.40 (d, $J_{C,F}$ = 267.1 Hz, Ar-C_{para}), 157.5 (C_{Bipy}), 158.21 (d, *J* = 7.5 Hz, C_{Bipy}). *These signals could not be assigned exactly to corresponding carbon atoms. They belong to the Ar-C_{ipso} and the Ar-C_{nitro} of the aryl residue.
^{19}F NMR (376 MHz, $CDCl_3$): δ (ppm) = -117.37 (s, 1F, CF).
HRMS (ESI-TOF, MeOH): *m/z* calcd. for $C_{35}H_{25}FN_7O_2Ru^+$ $[M\text{-}Cl]^+$: 696.1092, found: 696.1124.
IR (ATR): $\tilde{\nu}$ (cm^{-1}) = 3066 [ν(Ar-H)], 1615 [ν(C=N) ν(C=C),], 1537 [$\nu_{as}(NO_2)$], 1346 [$\nu_{sym}(NO_2)$], 726 [δ(HC=CH)].
UV/vis (DCM): λ_{max} (nm) [log (ε/L mol^{-1} cm^{-1})] = 464 [4.76], 520 [4.25].
M.P. (°C): >250.

{Bis(2,2´-bipyridyl){5-[4-(*N*,*N*-dibutylamino)-3-nitrophenyl]dipyrrinato}ruthenium(II)}-chloride (**160**):
Complex **160** was prepared according to the general synthetic procedure. Complex **157** (130 mg, 0.20 mmol) and 2,2´-bipyridine (62 mg, 0.39 mmol) were dissolved in 15 mL of EtOH. After purification (column chromatography, silica gel, DCM/MeOH = 9/1, v/v) and recrystallization (DCM/*n*-pentane); complex **160** was obtained as a black solid (116 mg, 0.14 mmol, 70%).

^{1}H NMR (500 MHz, $CDCl_3$): δ (ppm) = 0.88 (t, J = 7.3 Hz, 3H, Me), 1.26–1.33 (m_c, 2H, CH_2), 1.52–1.58 (m_c, 2H, CH_2), 3.16–3.18 (m_c, 2H, CH_2), 6.28 (d, J = 4.5, 2H, $H_{Pyrrole}$), 6.35 (s, 2H, $H_{Pyrrole}$), 6.66–6.67 (m, 2H, $H_{Pyrrole}$), 7.11 (d, J = 8.6 Hz, 1H, Ar-H_{meta}), 7.29 (t, J = 6.4 Hz, 4H, H_{Bipy}), 7.44 (dd, J = 8.6, 2.2 Hz, 1H, Ar-H_{ortho}), 7.63–7.66 (m, 2H, H_{Bipy}), 7.76 (d, J = 2.2 Hz, 1H, Ar-H_{ortho}), 7.83 (s, 2H, H_{Bipy}), 7.90–8.00 (m, 4H, H_{Bipy}), 8.66 (t, J = 9.5 Hz, 2H, H_{Bipy}), 8.78 (d, J = 7.9 Hz, 2H, H_{Bipy}).

^{13}C NMR (126 MHz, $CDCl_3$): δ (ppm) = 14.2 (Me), 20.5 (CH_2), 29.9 (CH_2), 52.2 (CH_2), 118.9 ($C_{Pyrrole}$), 120.3 (Ar-C_{meta}), 124.4 (C_{Bipy}), 124.7 (C_{Bipy}), 126.1*, 126.7 (C_{Bipy}), 127.1 (C_{Bipy}), 128.6 (Ar-C_{ortho}), 131.7 ($C_{Pyrrole}$), 135.3 (Ar-C_{ortho}), 135.8 ($C_{Pyrrole}$), 136.8 (C_{Bipy}), 136.3*, 136.9 (C_{Bipy}), 144.9 (C_{meso}), 145.5 (Ar-C_{para}), 149.6 ($C_{Pyrrole}$), 150.9 (C_{Bipy}), 152.1 (C_{Bipy}), 157.8 (C_{Bipy}), 158.5 (C_{Bipy}). *These signals could not be assigned exactly to corresponding carbon atoms. They belong to the Ar-C_{ipso} and the Ar-C_{nitro} of the aryl residue.

HRMS (ESI-TOF, MeOH): *m/z* calcd. for $C_{43}H_{43}N_8O_2Ru^+$ $[M\text{-}Cl]^+$: 805.2547, found: 805.2587.

IR (ATR): $\tilde{\nu}$ (cm^{-1}) = 3062 [ν(Ar-H)], 2958, 2929, and 2869 [ν(CH_2, ν(Me)], 1610 [ν(C=N), ν(C=C)], 1543 [ν_{as}(NO_2)], 1345 [ν_{sym}(NO_2)], 726 [δ(HC=CH)].

UV/vis (DCM): λ_{max} (nm) [log (ε/L mol^{-1} cm^{-1})] = 388 [4.34], 463 [4.75], 524 (shoulder).

M.P. (°C): 190-195.

6.1.3 Nucleophilic substitution of dipyrrinato ruthenium(II) and iridium(III) complexes

Attempted nucleophilic substitution of complex **156** with propargylamine:

Complex **156** (100 mg, 0.18 mmol, 1 equiv.) and propargylamine (0.23 mL, 3.62 mmol, 20 equiv.) were dissolved in 1 mL of DCM. The mixture was stirred for 4 h at rt. After the indicted time, the mixture was diluted with EtOAc and washed with water several times. The organic layer was dried with Na_2SO_4, filtered, and evaporated to dryness. After purification by column chromatography (silica gel, DCM/MeOH = 8/1, v/v) an orange solid (22 mg) was obtained. However, this fraction could not be assigned to the desired product **158**. The spectra did not allow a meaningful interpretation.

{Bis(2,2'-bipyridyl){5-[3-nitro-4-(*N*-prop-2-ynylamino)phenyl]dipyrrinato}ruthenium(II)}chloride (**161**):

Complex **159** (80 mg, 0.11 mmol, 1 equiv.) and propargylamine (0.14 mL, 2.19 mmol, 20 equiv.) were dissolved in 1 mL of DMSO. The mixture was stirred for 2 h at rt. After the indicted time, the mixture was diluted with EtOAc and washed with water several times. The organic layer was dried with Na_2SO_4, filtered, and evaporated to dryness. After purification by column chromatography (silica gel, DCM/MeOH = 9/1, v/v); complex **161** was obtained as a black solid (82 mg, 0.10 mmol, 98%).

^{1}H NMR (500 MHz, $CDCl_3$): δ (ppm) = 2.33 (t, J = 2.5 Hz, 1H, CH), 4.16 (d, J = 2.5 Hz, 2H, CH_2), 6.24–6.25 (2H, $H_{Pyrrole}$), 6.31 (s, 2H, $H_{Pyrrole}$), 6.60 (d, J = 4.9 Hz, 2H, $H_{Pyrrole}$), 6.99 (d, J = 8.8 Hz, 1H, Ar-H_{meta}), 7.27–7.33 (m, 4H, H_{Bipy}), 7.53 (dd, J = 8.8, 2.1 Hz, 1H, Ar-H_{ortho}), 7.65 (d, J = 5.6 Hz, 2H, H_{Bipy}), 7.84 (t, J = 6.1 Hz,

2H, H_{Bipy}), 7.97–7.94 (m, 4H, H_{Bipy}), 8.20 (d, *J* = 2.1 Hz, 1H, Ar-H_{ortho}), 8.41 (d, *J* = 7.3 Hz, 2H, H_{Bipy}), 8.46 (d, *J* = 8.2 Hz, 2H, H_{Bipy}).

^{13}C NMR (126 MHz, $CDCl_3$): δ (ppm) = 32.6 (CH_2), 72.7 (CH), 78.7 (C), 113.1 (Ar-C_{meta}), 118.5 ($C_{Pyrrole}$), 123.5 (d, *J* = 3.4 Hz, C_{Bipy}), 123.7 (d, *J* = 10.1 Hz, C_{Bipy}), 126.4 (d, *J* = 14.0 Hz, C_{Bipy}), 126.7 (C_{Bipy}), 127.1*,128.4 (Ar-C_{ortho}), 131.7 ($C_{Pyrrole}$), 131.7*, 135.8 ($C_{Pyrrole}$), 135.8 (C_{Bipy}), 136.5 (C_{Bipy}), 138.3 (Ar-C_{ortho}), 144.5 (Ar-C_{para}), 146.6 (C_{meso}), 149.4 ($C_{Pyrrole}$), 150.7 (d, *J* = 13.1 Hz, C_{Bipy}), 151.8 (C_{Bipy}), 157.3 (C_{Bipy}), 158.1 (C_{Bipy}). *These signals could not be assigned exactly to corresponding carbon atoms. They belong to the Ar-C_{ipso} and the Ar-C_{nitro} of the aryl residue.

HRMS (ESI-TOF, MeOH): *m/z* calcd. for $C_{38}H_{29}N_8O_2Ru^+$ $[M\text{-}Cl]^+$: 731.1451, found: 731.1446.

IR (ATR): $\tilde{\nu}$ (cm^{-1}) = 3296 [ν(C≡CH)], 3069 [ν(Ar-H)], 1624 [ν(C=N), ν(C=C)], 1537 [$\nu_{as}(NO_2)$], 1346 [$\nu_{sym}(NO_2)$], 728 [δ(HC=CH)].

UV/vis (DCM): λ_{max} (nm) [log (ε/L mol^{-1} cm^{-1})] = 376 [4.38], 463 [4.71], 524 [4.26].

M.P. (°C): >250.

Preparation of {bis(2,2'-bipyridyl){5-[4-(*N*-2-hydroxyethylamino)-3-nitrophenyl]dipyrrinato}-ruthenium(II)} chloride *via* post-functionalization (**36**):

Complex **159** (90 mg, 0.12 mmol, 1 equiv.) and ethanolamine (0.15 mL, 2.46 mmol, 20 equiv.) were dissolved in 1 mL of DMSO. The mixture was stirred for 3 h at rt. Due to the high polarity of the product, the mixture was directly evaporated to dryness with a rotary evaporator. The crude product was purified by column chromatography (silica gel, DCM/MeOH = 9/1, v/v); complex **36** was obtained as a black solid (69 mg, 88 µmol, 73%).

^{1}H NMR (500 MHz, DMSO-d_6): δ = 3.49–3.50 (m, 2H, CH_2), 3.70–3.72 (m, 2H, CH_2), 6.34–6.35 (m, 4H, $H_{pyrrole}$), 6.64 (d, *J* = 4.0 Hz, 2H, $H_{pyrrole}$), 7.18 (d, *J* = 9.0 Hz, 1H, Ar-H_{meta}), 7.43– (m, 2H, H_{bipy}), 7.57–7.55 (m, 3H, H_{bipy} + Ar-H_{ortho}), 7.75 (br s, 2H, H_{bipy}), 7.83 (s, 2H, H_{bipy}), 8.02–8.06 (m, 5H, H_{bipy} + Ar-H_{ortho}), 8.43–8.45 (m, 1H, NH), 8.76 (d, *J* = 7.3 Hz, 4H, H_{bipy}) ppm.

General synthetic procedure for glycosylation of dipyrrinato metal complexes: The corresponding complex (1 equiv.) and the related 1'-thio-β-D-carbohydrate sodium salt (1.2 equiv.) were dissolved in 5 mL of DMF. The mixture was stirred for the indicated time at rt. Afterwards, 5 ml of water was added and stirred for additional 5 min at rt. Due to the high polarity of the product, the mixture was directly evaporated to dryness with a rotary evaporator. The crude product was purified by column chromatography; the main fraction was collected and evaporated to dryness.

Attempted synthesis of chlorido(η^6-*p*-cymene){5-[3-nitro-4-(1'-thio-β-D-glucosyl)phenyl]dipyrrinato}-ruthenium(II) (**162**):

The reaction was carried out according to the general synthetic procedure. Complex **156** (100 mg, 0.18 mmol) and 1'-thio-β-D-glucose sodium salt (47 mg, 0.22 mmol) were dissolved in DMF. The mixture was stirred for 20 min. After purification (column chromatography, silica gel, DCM/MeOH = 8/1, v/v, then DCM/MeOH = 6/1, v/v) an orange solid (68 mg) was obtained. However, this fraction could not be assigned to the desired product. The spectra did not allow a meaningful interpretation.

Attempted synthesis of chlorido(pentamethyl-η^5-cyclopentadienyl){5-[4-(1'-thio-β-D-glucosyl)-2,3,5,6-tetrafluorophenyl]dipyrrinato}iridium(III) (**163**):

The reaction was carried out according to the general synthetic procedure. Complex **112** (100 mg, 0.15 mmol) and 1'-thio-β-D-glucose sodium salt (39 mg, 0.18 mmol) were dissolved in DMF. The mixture was stirred for 30 min. After purification (column chromatography, silica gel, DCM/MeOH = 8/1, v/v) an orange solid (26 mg) was obtained. However, this fraction could not be assigned to the desired product. The spectra did not allow a meaningful interpretation.

Attempted synthesis of chlorido{5-[3-nitro-4-(1'-thio-β-D-glucosyl)phenyl]dipyrrinato}(pentamethyl-η^5-cyclopentadienyl)iridium(III) (**164**):

The reaction was carried out according to the general synthetic procedure. Complex **119** (100 mg, 0.16 mmol) and 1'-thio-β-D-glucose sodium salt (41 mg, 0.19 mmol) were dissolved in DMF. The mixture was stirred for 30 min. After purification (column chromatography, silica gel, DCM/MeOH = 8/1, v/v) an orange solid (68 mg) was obtained. However, this fraction could not be assigned to the desired product. The spectra did not allow a meaningful interpretation.

{Bis(2,2'-bipyridyl){5-[3-nitro-4-(1'-thio-β-D-glucosyl)phenyl]dipyrrinato}ruthenium(II)}-chloride (**165**):

Complex **165** was prepared according to the general synthetic procedure. Complex **159** (100 mg, 0.14 mmol) and 1'-thio-β-D-glucose sodium salt (35 mg, 0.16 mmol) were dissolved in DMF. The mixture was stirred for 20 min. After purification (column chromatography, silica gel, DCM/MeOH = 4/1, v/v) and recrystallization (DCM + MeOH/*n*-hexane); complex **165** was obtained as a black solid (97 mg, 0.11 mmol, 77%).

^{1}H NMR (500 MHz, $CDCl_3$/CD_3OD = 9/1): δ (ppm) = 3.32–3.39 (m, 4H, 2´-H + 3´-H + 4´-H + 5´-H), 3.59 (dt, *J* = 12.1, 3.8 Hz, 1H, 6´-H), 3.75 (dd, *J* = 11.4, 5.5 Hz, 1H, 6´-H), 4.73 (d, *J* = 8.7 Hz, 1H, 1´-H), 6.13 (d, *J* = 5.6 Hz, 2H, $H_{Pyrrole}$), 6.20–6.22 (m, 2H, $H_{Pyrrole}$), 6.36 (s, 2H, $H_{Pyrrole}$), 7.17 (t, *J* = 6.6 Hz, 2H, H_{Bipy}), 7.23–7.26 (m, 2H, H_{Bipy}), 7.48 (d, *J* = 7.3 Hz, 1H, H_{meta}), 7.57 (d, *J* = 5.5 Hz, 2H, H_{Bipy}), 7.68 (dd, *J* = 8.3, 1.7 Hz, 1H, H_{ortho}), 7.75–7.83 (m, 6H, H_{Bipy}), 8.02 (d, *J* = 1.9 Hz, 1H, H_{ortho}), 8.29 (d, *J* = 8.3 Hz, 4H, H_{Bipy}).

^{13}C NMR (126 MHz, CD_2Cl_2/CD_3OD = 9:1): δ (ppm) = 60.6 (6´-C), 69.7 (4´-C), 72.1 (2´-C), 74.7 (3´-C), 78.2 (5´-C), 80.2 (1´-C), 118.6 ($C_{Pyrrole}$), 123.3 (C_{Bipy}), 126.6 (Ar-C_{ortho}), 129.8 (Ar-C_{meta}), 130.98 ($C_{Pyrrole}$), 134.9*, 135.4 (Ar-C_{ortho}), 135.7 (C_{Bipy}), 136.2 (C_{Bipy}), 150.6 $C_{Pyrrole}$), 151.7 (C_{Bipy}), 153.1 (C_{Bipy}), 157.1 (C_{Bipy}), 158.1 (C_{Bipy}). *This signal could not be assigned exactly to corresponding carbon atom. It belongs to the Ar-C_{ipso} or the Ar-C_{nitro} of the aryl residue.

HRMS (ESI-TOF, MeOH): *m/z* calcd. for $C_{41}H_{36}N_7O_7RuS^+$ $[M\text{-}Cl]^+$: 872.1435, found: 872.1449.

IR (ATR): $\tilde{\nu}$ (cm^{-1}) = 3306 [ν(OH)], 3071 [ν(Ar-H)], 1601 [ν(C=N), ν(C=C)], 1547 [$\nu_{as}(NO_2)$]], 1346 [$\nu_{sym}(NO_2)$], 724 [δ(HC=CH)].

UV/vis (MeOH): λ_{max} (nm) [log (ε/L mol^{-1} cm^{-1})] = 462 [4.62], 515 [4.04].

M.P. (°C): >250.

{Bis(2,2'-bipyridyl){5-[3-nitro-4-(1'-thio-β-D-galactosyl)phenyl]dipyrrinato}ruthenium(II)}chloride (**166**):

Complex **166** was prepared according to the general synthetic procedure. Complex **159** (90 mg, 0.12 mmol) and 1'-thio-β-D-glucose sodium salt (32 mg, 0.15 mmol) were dissolved in 5 mL of DMF. The mixture was stirred for 30 min. After purification (column chromatography, silica gel, DCM/MeOH = 4/1, v/v) and recrystallization (DCM + MeOH/*n*-hexane); complex **166** was obtained as a black solid (81 mg, 88 µmol, 73%).

^{1}H NMR (500 MHz, $CDCl_3$/CD_3OD = 9/1): δ (ppm) = 3.53 (dd, *J* = 9.0, 1.9 Hz, 1H, 3´-H), 3.63 (dd, *J* = 5.9, 5.0 Hz, 1H, 5´-H), 3.67–3.70 (m, 2H, 6´-H), 3.72–3.77 (m, 1H, 2´-H), 3.88–3.93 (m, 1H, 4´-H), 4.75 (d, *J* = 9.9 Hz, 1H, 1´-H), 6.15–6.18 (m, 2H, $H_{Pyrrole}$), 6.24 (dd, *J* = 6.7, 2.2 Hz, 2H, $H_{Pyrrole}$), 6.40 (d, *J* = 2.9 Hz, 2H, $H_{Pyrrole}$), 7.19–7.22 (m, 2H, H_{Bipy}), 7.27–7.31 (m, 2H, H_{Bipy}), 7.51 (d, *J* = 8.7 Hz, 1H, H_{meta}), 7.60 (d, *J* = 5.0 Hz, 2H, H_{Bipy}), 7.78–7.88 (m, 7H, H_{ortho} + H_{Bipy}), 8.05 (d, *J* = 1.9 Hz, 1H, H_{ortho}), 8.34 (d, *J* = 7.1 Hz, 4H, H_{Bipy}).

^{13}C NMR (126 MHz, CD_2Cl_2/CD_3OD = 9:1): δ (ppm) = 61.1 (6´-C), 68.5 (4´-C), 69.1 (2´-C), 74.8 (3´-C), 78.9 (5´-C), 85.8 (1´-C), 118.6 ($C_{Pyrrole}$), 123.2 (C_{Bipy}), 123.3 (C_{Bipy}), 126.4 (C_{Bipy}), 126.5 (Ar-C_{ortho}), 126.7 (C_{Bipy}), 127.5 (Ar-C_{meta}), 130.98 ($C_{Pyrrole}$), 134.8*, 135.3 (Ar-C_{ortho}), 135.6 (C_{Bipy}), 136.2 (C_{Bipy}), 142.99*, 145.3 (Ar-C_{para}), 149.5 ($C_{Pyrrole}$), 150.6 (C_{Bipy}), 151.8 (C_{Bipy}), 157.1 (C_{Bipy}), 157.99 (C_{Bipy}). *These signals could not be assigned exactly to corresponding carbon atom. It belongs to the Ar-C_{ipso} or the Ar-C_{nitro} of the aryl residue.

HRMS (ESI-TOF, MeOH): *m/z* calcd. for $C_{41}H_{36}N_7O_7RuS^+$ $[M\text{-}Cl]^+$: 872.1435, found: 872.1440.

IR (ATR): $\tilde{\nu}$ (cm^{-1}) = 3351 [ν(OH)], 3098 [ν(Ar-H)], 1602 [ν(C=N), ν(C=C)], 1549 [$\nu_{as}(NO_2)$]], 1346 [$\nu_{sym}(NO_2)$], 725 [δ(HC=CH)].

UV/vis (MeOH): λ_{max} (nm) [log (ε/L mol^{-1} cm^{-1})] = 462 [4.60], 515 [4.03].

M.P. (°C): >250.

6.1.4 Preparation of the 1,3,7,9-tetramethyl-dipyrrinato iridium complex

5-[4-(*N*-Butylamino)-3-nitrophenyl]-1,3,7,9-tetramethyldipyrromethane (**169**):

Dipyrromethane **128** (486 mg, 1.42 mmol, 1 equiv.) and *n*-butylamine (6.00 mL, 60.70 mmol, 40 equiv.) were dissolved in 5 mL of DCM. The mixture was stirred for 2 h at rt. Afterwards, the mixture was diluted in EtOAc and washed with water several times. The organic layer was dried with Na_2SO_4, filtered, and evaporated to dryness. After purification (column chromatography (silica gel, DCM/*n*-hexane, 3:1, v/v); dipyrromethane **169** was obtained as a yellow-orange solid (303 mg, 0.77 mmol, 54%).

^{1}H NMR (600 MHz, $CDCl_3$): δ (ppm) = 0.98 (td, *J* = 7.4, 2.1 Hz, 3H, Me_{butyl}), 1.44–1.50 (m, 2H, CH_2), 1.68–1.73 (m, 2H, CH_2), 1.82 (s, 6H, Me), 2.15 (s, 6 H, Me), 3.28 (td, *J* = 7.1, 5.1 Hz, 2H, CH_2), 5.33 (s, 1H, CH), 5.70 (d, *J* = 2.8 Hz, 2H, $H_{pyrrole}$), 6.80 (d, *J* = 8.9 Hz, 1H, Ar-H_{meta}), 7.25 (t, *J* = 2.2 Hz, 1H, Ar-H_{ortho}), 7.93 (d, *J* = 2.2 Hz, 1H, Ar-H_{ortho}), 8.02 (t, *J* = 5. Hz, 1H, NH)

^{13}C NMR (151 MHz, $CDCl_3$): δ (ppm) = 11.2 (Me_{butyl}), 13.1 (Me), 13.5 (Me), 20.3 (CH_2), 31.2 (CH_2), 39.5 (CH_2), 42.9 (CH), 108.9 ($C_{pyrrole}$), 114.4 (Ar-C_{meta}), 115.3 ($C_{pyrrole}$), 125.3 (Ar-C_{ortho}), 125.7*, 125.9 ($C_{pyrrole}$), 129.4 ($C_{pyrrole}$), 131.7*, 136.8 (Ar-C_{ortho}), 144.7 (Ar-C_{para}).

HRMS (ESI-TOF, DCM/MeOH): *m/z* calcd. for $C_{23}H_{29}N_4O_2^+$ [dipyrrin+H]$^+$: 393.2258, found: 393.2302.

Attempted synthesis of 5-[4-(*N*-butylamino)-3-nitrophenyl]-1,3,7,9-tetramethyldipyrrin (**170**):

Oxidation with *p*-chloranil: Dipyrromethane **169** (430 mg, 1.09 mmol, 1 equiv.) was dissolved in 10 mL of THF. *p*-Chloranil (270 mg, 1.09 mmol, 1 equiv., suspended in 5 mL of THF) was added and the reaction mixture was stirred for 3 h at rt. Afterwards, the solvent was evaporated at reduced pressure, the remaining solid was dissolved (EtOAc) and filtered over a silica gel filled glass frit. The filtrate was again evaporated to dryness. After purification (silica gel, column chromatography, EtOAc/*n*-hexane, 3:1, v/v, then EtOAc, then MeOH) no product could be observed. Instead, a dark colored fraction remained at the starting point of the column. However, thin-layer chromatographic control gave evidence of a fraction that could be assigned to the desired product.

Oxidation with DDQ: Dipyrromethane **169** (176 mg, 0.45 mmol, 1 equiv.) was dissolved in 5 mL of THF. DDQ (101 mg, 0.45 mmol, 1 equiv., suspended in 5 mL of THF) was added and the reaction mixture was stirred for 1 h at rt. Afterwards, the solvent was evaporated at reduced pressure, the remaining solid was dissolved (EtOAc) and filtered over a silica gel filled glass frit. The filtrate was again evaporated to dryness. After purification (silica gel, column chromatography, EtOAc/*n*-hexane, 3:1, v/v, then EtOAc, then MeOH) no product could be observed. Instead, a dark colored fraction remained at the starting point of the column. However, thin-layer chromatographic control gave evidence of a fraction that could be assigned to the desired product.

Di(μ-chlorido)bis[chlorido(η^5-pentamethylcyclopendienyl)iridium(III)] (**171**)

Under an argon atmosphere iridiumtrichloride hydrate (2.00 g, 5.66 mmol, 1 equiv.) was dissolved in 50 mL of MeOH, pentamethylcyclopentadiene (1.28 mL, 7.94 mmol, 1.4 equiv.) was added, and stirred for 40 h at 75°C. The suspension was filtered over a glass frit and washed several times with MeOH. The filtrate was concentrated (approximately to half of the volume) and stored overnight in the freezer (to increase the yield of the product). The suspension was again filtered over a glass frit and washed with MeOH. The combined solids were dried, and the corresponding iridium complex was obtained as an orange solid (1.51 g, 67%).

^{1}H-NMR (400 MHz, $CDCl_3$): δ (ppm) = 1.58 (s, Me).

The NMR spectroscopic data are in accordance to the literature.[116]

Preparation of the {5-[4-(*N*-butylamino)-3-nitrophenyl]-1,3,7,9-tetramethyldipyrrinato}chlorido-(pentamethyl-η^5-yclopentdienyl)iridium(III) *via* dipyrromethane (**172**):

Dipyrromethane **169** (321 mg, 0.81 mmol, 1 equiv.) was dissolved in 5 mL of THF. DDQ (184 mg, 0.81 mmol, 1 equiv.) was added and the mixture was stirred for 1 h at rt. Afterwards, DIPEA (0.96 mL, 5.67 mmol, 7 equiv.) and **171** (323 mg, 0.41 mmol, 0.5 equiv.) were added and stirred for additional 16 h. After the indicated time, the reaction mixture was diluted with DCM. Water was added and the mixture was extracted with DCM several times. The combined organic layers were dried with Na_2SO_4, filtered, and evaporated to dryness. After purification (column chromatography (silica gel, DCM/EtOAc, 4:1, v/v); complex **172** was obtained as an orange solid (188 mg, 0.25 mmol, 31%)

^{1}H NMR (600 MHz, $CDCl_3$): *δ* (ppm) = 1.01 (t, *J* = 7.4 Hz, 3H, Me_{butyl}), 1.41 (s, 1H, Me_{cp*}), 1.50–1.53 (m, 2H, CH_2), 1.63 (s, 6H, Me), 1.74–1.78 (m, 2H, CH_2), 2.59 (s, 6H, Me), 3.38 (td, *J* = 7.1, 5.4 Hz, 1H, CH_2), 6.11 (s, 2H, $H_{pyrrole}$), 6.97–7.01 (Ar-H_{meta}), 7.23–7.32 (Ar-H_{ortho}), 8.02–8.04 (Ar-H_{ortho}), 8.13 (br s, 1H, NH).

^{13}C NMR (151 MHz, $CDCl_3$): *δ* (ppm) = 8.99 (Me_{cp*}), 13.99 (Me_{butyl}), 16.9 (Me), 18.7 (Me), 20.7 (CH_2), 31.4 (CH_2), 43.4 (CH_2), 86.5 (C_{cp*}), 114.7 (Ar-C_{meta}), 122.6 ($CH_{pyrrole}$), 126.1 (Ar-C_{ortho}), 131.8 ($C_{pyrrole}$), 132.2*, 136.8*, 139.4 (Ar-C_{ortho}), 141.2 (C_{meso}), 143.8 ($C_{pyrrole}$), 145.9 (Ar-C_{para}), 161.2 ($C_{pyrrole}$).

HRMS (ESI-TOF, DCM/MeOH): *m/z* calcd. for $C_{33}H_{42}N_4O_2Ir^+$ [M-Cl]$^+$: 719.2932, found: 719.2967.

6.2 Homoleptic dipyrrinato complexes

6.2.1 Preparation of bis(dipyrrinato)metal complexes

General synthetic procedure: The corresponding dipyrrin (1 equiv.) was dissolved in 10 mL of MeOH, and the related metal acetate (5 equiv.) was added. The mixture was stirred for 24 h at rt. After the indicated time, the reaction mixture was diluted with EtOAc and washed with water several times. The

organic layer was dried with Na_2SO_4, filtered, and evaporated to dryness. The crude product was purified by column chromatography; the main fraction was collected and evaporated to dryness.
Except for complex **175** and complex **176**, here, the mixture was filtered over a glass frit and the resulting solid was washed with MeOH. Afterwards, the obtained solid was dried in the exicator.

Attempted synthesis of bis[5-(4-fluoro-3-nitrophenyl)dipyrrinato]zinc(II) (**173**):
The reaction was carried out according to the general synthetic procedure. Dipyrrin **108** (128 mg, 0.45 mmol) and zinc acetate dihydrate (464 mg, 2.25 mmol) were dissolved in MeOH. After purification (column chromatography, silica gel, EtOAc/n-hexane = 4/1, v/v) an orange solid (12 mg) was obtained. However, evidence for a mixture of the desired complex and the corresponding starting material were found in the NMR spectra. Evidence for a decomposition of the dipyrrin was found, due to the observation of large quantities of a black residue.

Attempted synthesis of bis{5-[4-(*N*-butylamino)-3-nitrophenyl]dipyrrinato}zinc(II) (**174**):
The reaction was carried out according to the general synthetic procedure. Dipyrrin **23** (150 mg, 0.45 mmol) and zinc acetate dihydrate (489 mg, 2.23 mmol) were dissolved in MeOH. After purification (column chromatography, silica gel, EtOAc/n-hexane = 4/1, v/v) an orange solid (89 mg) was obtained. However, evidence for a mixture of the desired complex and the corresponding starting material were found in the NMR spectra. Evidence for a decomposition of the dipyrrin was found, due to the observation of large quantities of a black residue.

Bis{5-[3-nitro-4-(*N*-prop-2-ynylamino)phenyl]dipyrrinato}zinc(II) (**175**):
Complex **175** was prepared according to the general synthetic procedure. Dipyrrin **109** (200 mg, 0.63 mmol) and zinc acetate dihydrate (690 mg, 3.15 mmol) were dissolved in MeOH. The reaction mixture was filtered over a glass frit and the resulting orange solid was washed with MeOH. The product **175** was obtained as an orange solid (108 mg, 0.15 mmol, 49%).

^{1}H NMR (500 MHz, THF-d_8): δ (ppm) = 2.78 (t, *J* = 2.4 Hz, 2H, CH), 4.32 (dd, *J* = 5.9, 2.5 Hz, 4H, CH_2), 6.42 (s, 4H, $H_{Pyrrole}$), 6.78 (d, *J* = 4.1 Hz, 4H, $H_{Pyrrole}$), 7.26 (d, *J* = 8.8 Hz, 2H, Ar-H_{meta}), 7.52 (d, *J* = 25.7 Hz, 4H, $H_{Pyrrole}$), 7.74 (dd, *J* = 8.8, 2.2 Hz, 2H, Ar-H_{ortho}), 8.36 (d, *J* = 2.2 Hz, 2H, Ar-H_{ortho}), 8.46 (t, *J* = 5.9 Hz, 2H, NH).
^{13}C NMR (126 MHz, THF-d_8): δ (ppm) = 33.2 (CH_2), 73.4 (CH), 80.6 (C), 114.5 (Ar-C_{meta}), 118.3 (d, *J* = 34.6 Hz, $C_{Pyrrole}$), 127.9*, 129.7 (Ar-C_{ortho}), 133.0*, 133.4 (d, *J* = 23.6 Hz, $C_{Pyrrole}$), 139.1 (Ar-C_{ortho}), 141.7 ($C_{Pyrrole}$), 145.6 (Ar-C_{para}), 147.6 (C_{meso}), 150.84 (d, *J* = 74.8 Hz, $C_{Pyrrole}$). *These signals could not be assigned exactly to corresponding carbon atoms. They belong to the Ar-C_{ipso} and the Ar-C_{nitro} of the aryl residue.

HRMS (ESI-TOF, DCM/MeOH): *m/z* calcd. for $C_{36}H_{27}N_8O_4Zn^+$ $[M+H]^+$: 699.1441, found: 699.1441, *m/z* calcd. for $C_{36}H_{26}N_8O_4NaZn^+$ $[M+Na]^+$: 721.1261, found: 721.1260, *m/z* calcd. for $C_{36}H_{26}N_8O_4KZn^+$ $[M+K]^+$: 737.1000, found: 737.1013, *m/z* calcd. for $C_{18}H_{15}N_4O_2^+$ [ligand+H]$^+$: 319.1190, found: 319.1211.
IR (ATR): $\tilde{\nu}$ (cm^{-1}) = 3383 [ν(NH)], 3291 [ν(C≡CH)], 3094 [ν(Ar-H)], 1621 [ν(C=N), ν(C=C)], 1528 [ν_{as}(NO_2)], 1332 [ν_{sym}(NO_2)], 734 [δ(HC=CH)].
UV/vis (acetone): λ_{max} (nm) [log (ε/L mol^{-1} cm^{-1})] = 369 [4.26], 462 (shoulder), 483 [4.82].
M.P. (°C): 224-226.

Bis{5-[4-(*N*-6-methoxy-6-oxohexylamino)-3-nitrophenyl]dipyrrinato}zinc(II) (**176**):
Complex **176** was prepared according to the general synthetic procedure. Dipyrrin **26** (150 mg, 0.37 mmol) and zinc acetate dihydrate (403 mg, 3.84 mmol) were dissolved in MeOH. The reaction mixture was filtered over a glass frit and the resulting orange solid was washed with MeOH. The product **176** was obtained as an orange solid (54 mg, 68 µmol, 37%).

^{1}H NMR (500 MHz, THF-d_8): δ (ppm) = 1.51–1.57 (m, 4H, CH_2), 1.69–1.75 (m, 4H, CH_2), 1.79–1.85 (m, 4H, CH_2), 2.35 (t, *J* = 7.4 Hz, 4H, CH_2), 3.47–3.51 (m, 4H, CH_2), 3.61 (s, 6H, Me), 6.42 (s, 4H, $H_{Pyrrole}$), 6.79 (d, *J* = 3.9 Hz, 4H, $H_{Pyrrole}$), 7.15 (d, *J* = 8.9 Hz, 2H, Ar-H_{meta}), 7.51 (d, *J* = 26.5 Hz, 4H, $H_{Pyrrole}$), 7.68 (dd, *J* = 8.8, 2.2 Hz, 2H, Ar-H_{ortho}), 8.31 (t, *J* = 5.4 Hz, 2H, NH), 8.33 (d, *J* = 2.2 Hz, 2H, Ar-H_{ortho}).
^{13}C NMR (126 MHz, THF-d_8): δ (ppm) = 25.98 (CH_2), 27.6 (CH_2), 29.8 (CH_2), 34.4 (CH_2), 43.8 (CH_2), 51.5 (Me), 114.0 (Ar-C_{meta}), 118.2 ($C_{Pyrrole}$), 126.9*, 129.9 (Ar-C_{ortho}), 132.2*, 133.4 ($C_{Pyrrole}$), 139.4 (Ar-C_{ortho}), 141.7 ($C_{Pyrrole}$), 146.7 (Ar-C_{para}), 147.8 (C_{meso}), 150.7 ($C_{Pyrrole}$), 173.8 (CO). *These signals could not be assigned exactly to corresponding carbon atoms. They belong to the Ar-C_{ipso} and the Ar-C_{nitro} of the aryl residue.
HRMS (ESI-TOF, DCM/MeOH): *m/z* calcd. for $C_{22}H_{25}N_4O_4^+$ [ligand+H]$^+$: 409.1870, found: 409.1880.
IR (ATR): $\tilde{\nu}$ (cm^{-1}) = 3375 [ν(NH)], 3089 [ν(Ar-H)], 2942 [ν(CH_2)], 1732 [ν(COOMe)], 1621 [ν(C=N), ν(C=C)], 1528 [ν_{as}(NO_2)], 1333 [ν_{sym}(NO_2)], 732 [δ(HC=CH)].
UV/vis (DCM): λ_{max} (nm) [log (ε/L mol^{-1} cm^{-1})] = 385 [4.54], 483 [5.06].
M.P. (°C): 127-130.

Attempted synthesis of bis[5-(4-fluoro-3-nitrophenyl)dipyrrinato]nickel(II) (**177**):
The reaction was carried out according to the general synthetic procedure. Dipyrrin **108** (128 mg, 0.45 mmol) and zinc acetate tetrahydrate (562 mg, 2.25 mmol) were dissolved in MeOH. After purification (column chromatography, silica gel, DCM/MeOH = 4/1, v/v) an orange solid (31 mg) was obtained. However, evidence for a mixture of the desired complex and the corresponding starting material were found in the NMR spectra. Evidence for a decomposition of the dipyrrin was found, due to the observation of large quantities of a black residue.

Attempted synthesis of bis{5-[4-(*N*-butylamino)-3-nitrophenyl]dipyrrinato}nickel(II) (**178**):
The reaction was carried out according to the general synthetic procedure. Dipyrrin **23** (150 mg, 0.45 mmol) and nickel acetate tetrahydrate (555 mg, 2.23 mmol) were dissolved in MeOH. After purification (column chromatography, silica gel, DCM/MeOH = 4/1, v/v) no evidence for the corresponding product was found. Evidence for a decomposition of the dipyrrin was found, due to the observation of large quantities of a black residue.

Attempted synthesis of bis{5-[3-nitro-4-(*N*-prop-2-ynylamino)phenyl]dipyrrinato}nickel(II) (**179**):
The reaction was carried out according to the general synthetic procedure. Dipyrrin **109** (200 mg, 0.63 mmol) and nickel acetate tetrahydrate (782 mg, 3.15 mmol) were dissolved in MeOH. After purification (column chromatography, silica gel, DCM/MeOH = 4/1, v/v) an orange solid (76 mg) was obtained. However, evidence for a mixture of the desired complex and the corresponding starting material were found in the NMR spectra. Evidence for a decomposition of the dipyrrin was found, due to the observation of large quantities of a black residue.

Attempted synthesis of bis[5-(4-fluoro-3-nitrophenyl)dipyrrinato]copper(II) (**180**):
The reaction was carried out according to the general synthetic procedure. Dipyrrin **108** (128 mg, 0.45 mmol) and copper acetate monohydrate (451 mg, 2.25 mmol) were dissolved in MeOH. After purification (column chromatography, silica gel, DCM/MeOH = 4/1, v/v) an orange solid (25 mg) was obtained. However, evidence for a mixture of the desired complex and the corresponding starting material were found in the NMR spectra. Evidence for a decomposition of the dipyrrin was found, due to the observation of large quantities of a black residue.

Attempted synthesis of bis{5-[4-(*N*-butylamino)-3-nitrophenyl]dipyrrinato}copper(II) (**181**):
The reaction was carried out according to the general synthetic procedure. Dipyrrin **23** (110 mg, 0.33 mmol) and copper acetate monohydrate (329 mg, 1.65 mmol) were dissolved in 10 mL of MeOH. After purification (column chromatography, silica gel, DCM/MeOH = 4/1, v/v) no evidence for the corresponding product was found. Evidence for a decomposition of the dipyrrin was found, due to the observation of large quantities of a black residue.

Attempted synthesis of bis[5-(4-fluoro-3-nitrophenyl)dipyrrinato]zinc(II) (**173**) with an additional base:
Dipyrrin **108** (100 mg, 0.35 mmol, 1 equiv.), zinc acetate dihydrate (387 mg, 1.77 mmol, 5 equiv.), and NaOAc trihydrate (223 mg, 1.77 mmol, 5 equiv.) were dissolved in 10 mL of THF. The mixture was stirred for 24 h at rt. Afterwards, the reaction mixture was diluted with EtOAc and washed with water several times. The organic layer was dried with Na_2SO_4, filtered, and evaporated to dryness. After

purification (column chromatography, silica gel, DCM/MeOH = 4/1, v/v) no evidence for the corresponding product was found. Evidence for a decomposition of the dipyrrin was found, due to the observation of large quantities of a black residue.

Attempted synthesis of bis{5-[3-nitro-4-(*N*-prop-2-ynylamino)phenyl]dipyrrinato}zinc(II) with increased temperature (**175**):
Dipyrrin **109** (80 mg, 0.31 mmol, 1 equiv.) and zinc acetate dihydrate (276 mg, 1.57 mmol, 5 equiv.) were dissolved in 10 mL of THF. The mixture was stirred for 24 h at 70°. After the indicated time, the reaction mixture was diluted with EtOAc and washed with water several times. The organic layer was dried with Na_2SO_4, filtered, and evaporated to dryness. After purification (column chromatography, silica gel, DCM/MeOH = 4/1, v/v) an orange solid (14 mg) was obtained. Again, Evidence for a decomposition of the dipyrrin was found, due to the observation of large quantities of a black residue.

6.2.2 Preparation of tris(dipyrrinato)metal complexes

General synthetic procedure: The corresponding dipyrrin (3 equiv.), DIPEA (15 equiv.), and the related metal chloride (1 equiv.) were dissolved in 15 mL of THF. The mixture was stirred for 24 h at 70°. After the indicated time, the reaction mixture was diluted with DCM. Water was added and the mixture was extracted with DCM several times. The combined organic layers were dried with Na_2SO_4, filtered, and evaporated to dryness. The crude product was purified by column chromatography; the main fraction was collected and evaporated to dryness.

Attempted synthesis of tris{5-[3-nitro-4-(*N*-prop-2-ynylamino)phenyl]dipyrrinato}indium(III) (**182**):
The reaction was carried out according to the general synthetic procedure. Dipyrrin **108** (500 mg, 1.57 mmol), $GaCl_3$·pentane (1.05 mL, 0.52 mmol), and DIPEA (1.34 mL, 7.85 mmol) were dissolved in 15 mL of THF. After column purification (chromatography, silica gel, DCM/EtOAc = 1/1, v/v) no evidence for the corresponding product was found. Evidence for a decomposition of the dipyrrin was found, due to the observation of large quantities of a black residue.

Tris{5-[4-(*N*-butylamino)-3-nitrophenyl]dipyrrinato}indium(III) (**183**):
Complex **183** was prepared according to the general synthetic procedure. Dipyrrin **23** (200 mg, 0.60 mmol), $InCl_3$ (44 mg, 0.20 mmol), and DIPEA (0.50 mL, 2.97 mmol) were dissolved in THF. After purification (column chromatography, silica gel, DCM/EtOAc = 9/1, v/v); complex **183** was obtained as an orange-red solid (122 mg, 0.11 mmol, 55%).

^{1}H NMR (500 MHz, CD_2Cl_2): δ (ppm) = 1.02 (t, *J* = 7.4 Hz, 9H, Me), 1.49–1.52 (m, 6H, CH_2), 1.75–1.81 (m, 6H, CH_2), 3.38–3.42 (m, 6H, CH_2), 6.39 (dd, *J* = 10.1, 6.1 Hz, 6H, $H_{Pyrrole}$), 6.77 (s, 6H, $H_{Pyrrole}$), 6.94 (d, *J* = 8.9 Hz, 3H, Ar-H_{meta}), 7.13 (d, *J* = 14.7 Hz, 6H, $H_{Pyrrole}$), 7.56 (ddd, *J* = 8.5, 4.2, 1.8 Hz, 3H, Ar-H_{ortho}), 8.19 (t, *J* = 5.3 Hz, 3H, NH), 8.24 (dd, *J* = 3.7, 2.2 Hz, 3H, Ar-H_{ortho}).

^{13}C NMR (126 MHz, CD_2Cl_2): δ (ppm) = 13.96 (Me), 20.7 (CH_2), 31.4 (CH_2), 43.4 (CH_2), 113.1 (Ar-C_{meta}), 117.7 ($C_{Pyrrole}$), 126.5*, 129.3 (Ar-C_{ortho}), 131.1*, 134.3 ($C_{Pyrrole}$), 138.98 (Ar-C_{ortho}), 141.3 ($C_{Pyrrole}$), 146.1 (Ar-C_{para}), 147.0 (C_{meso}), 150.0 ($C_{Pyrrole}$). *These signals could not be assigned exactly to corresponding carbon atoms. They belong to the Ar-C_{ipso} or the Ar-C_{nitro} of the aryl residue.

HRMS (ESI-TOF, DCM/MeOH): *m/z* calcd. for $C_{57}H_{57}N_{12}O_6InNa^+$ $[M+Na]^+$: 1143.3455, found: 1143.3518, *m/z* calcd. for $C_{57}H_{57}N_{12}O_6InK^+$ $[M+K]^+$: 1159.3194, found: 1159.3257, *m/z* calcd. for $C_{38}H_{38}N_8O_4In^+$ [M-ligand]$^+$: 785.2049, found: 785.2092, *m/z* calcd. for $C_{19}H_{21}N_4O_2^+$ [ligand+H]$^+$: 337.1659, found: 337.1679.

IR (ATR): $\tilde{\nu}$ (cm^{-1}) = 3376 [*ν*(NH)], 3098 [*ν*(Ar-H)], 2956, 2927, and 2862 [*ν*(CH_2, *ν*(Me)], 1621 [*ν*(C=N), *ν*(C=C)], 1526 [$\nu_{as}(NO_2)$], 1333 [$\nu_{sym}(NO_2)$], 732 [*δ*(HC=CH)].

UV/vis (DCM): λ_{max} (nm) [log (ε/L mol^{-1} cm^{-1})] = 445 [4.82], 483 [4.50].

M.P. (°C): 145-149.

Tris{5-[3-nitro-4-(*N*-prop-2-enylamino)phenyl]dipyrrinato}indium(III) (**184**):

Complex **184** was prepared according to the general synthetic procedure. Dipyrrin **24** (500 mg, 1.56 mmol), $InCl_3$ (115 mg, 0.52 mmol), and DIPEA (1.33 mL, 7.80 mmol) were dissolved in THF. After purification (column chromatography, silica gel, DCM/EtOAc = 4/1, v/v); complex **184** was obtained as an orange solid (30 mg, 26 µmol, 5%). Evidence for a decomposition of the dipyrrin was found, due to the observation of large quantities of a black residue.

^{1}H NMR (500 MHz, CD_2Cl_2): δ (ppm) = 4.08 (t, *J* = 4.4 Hz, 2H, CH_2), 5.30 (d, *J* = 11.5 Hz, 1H, -CH=**CH_2**), 5.38 (d, *J* = 17.2 Hz, 1H, -CH=**CH_2**), 6.02 (ddt, *J* = 17.2, 10.0, 5.0 Hz, 1H, -**CH**=CH_2), 6.40 (dt, *J* = 17.6, 3.8 Hz, 2H, $H_{pyrrole}$), 6.75 (d, *J* = 5.1 Hz, 2H, $H_{pyrrole}$), 6.92 (d, *J* = 8.8 Hz, 1H, Ar-H_{meta}), 7.13 (d, *J* = 17.7 Hz, 2H, $H_{pyrrole}$), 7.55 (dt, *J* = 6.2, 3.7 Hz, 1H, Ar-H_{ortho}), 8.26 (d, *J* = 2.7 Hz, 1H, Ar-H_{ortho}), 8.31 (t, *J* = 5.8 Hz, 1H, NH).

^{13}C NMR (126 MHz, CD_2Cl_2): δ (ppm) = 45.9 (CH_2), 113.4 (Ar-C_{meta}), 117.3 ($C_{pyrrole}$ + -CH=**CH_2**), 127.0*, 129.2 (Ar-C_{ortho}), 131.5*, 133.7 (-**CH**=CH_2), 134.4 ($C_{pyrrole}$), 138.8 (Ar-C_{ortho}), 141.1 ($C_{pyrrole}$), 145.8 (C_{meso}), 146.8 ($C_{pyrrole}$), 149.8 ($C_{pyrrole}$ + Ar-C_{para}). *These signals could not be assigned exactly to corresponding carbon atoms. They belong to the Ar-C_{ipso} and the Ar-C_{nitro} of the aryl residue.

IR (ATR): $\tilde{\nu}$ (cm^{-1}) = 3379 [*ν*(NH)], 3083 [*ν*(Ar-H)], 2981 [*ν*(CH_2)], 1625 [*ν*(C=N-), *ν*(C=C)], 1525 [$\nu_{as}(NO_2)$], 1334 [$\nu_{sym}(NO_2)$], 991 [*δ*(-CH=CH_2)], 735 [*δ*(HC=CH)].

UV/vis (DCM): λ_{max} (nm) [log (ε/L mol^{-1} cm^{-1})] = 446 [4.42], 495 [4.09].
M.P. (°C): 150-156.

Tris{5-[3-nitro-4-(*N*-prop-2-ynylamino)phenyl]dipyrrinato}indium(III) (**185**):
Complex **185** was prepared according to the general synthetic procedure. Dipyrrin **109** (500 mg, 1.57 mmol), $InCl_3$ (116 mg, 0.52 mmol), and DIPEA (1.34 mL, 7.85 mmol) were dissolved in THF. After purification (column chromatography, silica gel, DCM/EtOAc = 4/1, v/v); complex **185** was obtained as an orange solid (15 mg, 16 µmol, 3%). Evidence for a decomposition of the dipyrrin was found, due to the observation of large quantities of a black residue.

^{1}H NMR (500 MHz, $CDCl_3$/$(CD_3)_2CO$ = 2/1): δ (ppm) = 2.39 (t, *J* = 2.3 Hz, 1H, CH), 4.22 (d, *J* = 2.2 Hz, 2H, CH_2), 6.68 (dd, *J* = 4.1, 2.0 Hz, 2H, $H_{pyrrole}$), 6.97 (br s, 2H, $H_{pyrrole}$), 7.14 (d, *J* = 9.0 Hz, 1H, Ar-H_{meta}), 7.70 (dd, *J* = 9.0, 2.0 Hz, 1H, Ar-H_{ortho}), 8.00 (s, 2H, $H_{pyrrole}$), 8.38 (d, *J* = 1.7 Hz, 1H, Ar-H_{meta}), 8.64–8.67 (m, 1H, NH).
The ^{13}C NMR spectrum did not allowed a meaningful interpretation, due to the low quantities.
HRMS (ESI-TOF, acetone): *m/z* calcd. for $C_{54}H_{40}N_{12}O_6In^+$ $[M+H]^+$: 1067.2227, found: 1067.2227, *m/z* calcd. for $C_{54}H_{39}N_{12}O_6InNa^+$ $[M+Na]^+$: 1089.2047, found: 1089.2057, *m/z* calcd. for $C_{54}H_{39}N_{12}O_6InK^+$ $[M+K]^+$: 1105.1786, found: 1105.1795, *m/z* calcd. for $C_{36}H_{26}N_8O_4In^+$ [M-ligand]$^+$: 749.1110, found: 749.1132, *m/z* calcd. for $C_{18}H_{15}N_4O_2^+$ [ligand+H]$^+$: 319.1190, found: 319.1195.
UV/vis (acetone): λ_{max} (nm) [log (ε/L mol^{-1} cm^{-1})] = 443 [4.63], 497 [4.35].
M.P. (°C): 170-175.

Tris{5-[4-(*N*-2-hydroxyethylamino)-3-nitrophenyl]dipyrrinato}indium(III) (**186**):
Complex **186** was prepared according to the general synthetic procedure. Dipyrrin **25** (500 mg, 1.54 mmol), $InCl_3$ (114 mg, 0.51 mmol), and DIPEA (1.31 mL, 7.71 mmol) were dissolved in THF. After purification (column chromatography, silica gel, DCM/EtOAc = 1/2, v/v); complex **186** was obtained as an orange solid (11 mg, 10 µmol, 2%). Evidence for a decomposition of the dipyrrin was found, due to the observation of large quantities of a black residue.

^{1}H NMR (500 MHz, THF-d_8): δ (ppm) = 3.52–3.53 (m, 2H, CH_2), 3.79–3.81 (m, 2H, CH_2), 6.25 (s, 2H, $H_{pyrrole}$), 6.85 (s, 2H, $H_{pyrrole}$), 7.10 – 7.14 (m, 3H, $H_{pyrrole}$ + Ar-H_{meta}), 8.04 (d, *J* = 8.4 Hz, 1H, Ar-H_{ortho}), 8.60 (br s, 1H, NH), 8.81 (br s, 1H, Ar-H_{ortho}).
^{13}C NMR (126 MHz, THF-d_8): δ (ppm) = 46.4 (CH_2), 60.9 (CH_2), 110.9 ($C_{pyrrole}$), 115.1 (Ar-C_{meta}), 118.1 ($C_{pyrrole}$), 121.1 ($C_{pyrrole}$), 125.7 ($C_{pyrrole}$), 126.7*, 129.3 (Ar-C_{ortho}), 132.0*, 132.3 (C_{meso}), 132.5 (Ar-C_{para}), 136.7 (Ar-C_{ortho}). *These signals could not be assigned exactly to corresponding carbon atoms. They belong to the Ar-C_{ipso} and the Ar-C_{nitro} of the aryl residue.

IR (ATR): $\tilde{\nu}$ (cm^{-1}) = 3367 [ν(NH), ν(OH)], 2939 [$\nu(CH_2)$], 2878 [ν(CH)], 1565 [$\nu_{as}(NO_2)$], 1523 [ν(Ar-C)], 1353 [$\nu_{sym}(NO_2)$], 732 [δ(HC=CH)]..

UV/vis (MeOH): λ_{max} (nm) [log (ε/L mol^{-1} cm^{-1})] = 448 [4.84], 495 [4.64].

M.P. (°C): 105-110.

Tris{5-[4-(*N*-6-methoxy-6-oxohexylamino)-3-nitrophenyl]dipyrrinato}indium(III) (**187**):

Complex **187** was prepared according to the general synthetic procedure. Dipyrrin **26** (100 mg, 0.25 mmol), $InCl_3$ (18 mg, 82 µmol), and DIPEA (0.21 mL, 1.23 mmol) were dissolved in THF. After purification (column chromatography, silica gel, DCM/EtOAc = 1/1, v/v); complex **187** was obtained as an orange solid (32 mg, 24 µmol, 29%).

^{1}H NMR (500 MHz, CD_2Cl_2): δ (ppm) = 1.49–1.55 (m, 6H, CH_2), 1.69–1.75 (m, 6H, CH_2), 1.78–1.84 (m, 6H, CH_2), 2.36 (t, *J* = 7.4 Hz, 6H, CH_2), 3.39–3.43 (m, 6H, CH_2), 3.36 (s, 9H, Me), 6.39 (dd, *J* = 10.7, 6.2 Hz, 6H, $H_{Pyrrole}$), 6.76 (s, 6H, $H_{Pyrrole}$), 6.93 (d, *J* = 8.9 Hz, 3H, Ar-H_{meta}), 7.13 (d, *J* = 14.7 Hz, 6H, $H_{Pyrrole}$), 7.54–7.57 (m, 3H, Ar-H_{ortho}), 8.18 (t, *J* = 5.3 Hz, 3H, NH), 8.24 (s, 3H, Ar-H_{ortho}).

^{13}C NMR (126 MHz, CD_2Cl_2): δ (ppm) = 24.99 (CH_2), 26.9 (CH_2), 29.1 (CH_2), 34.2 (CH_2), 43.4 (CH_2), 51.7 (Me), 113.1 (Ar-C_{meta}), 117.6 ($C_{Pyrrole}$), 126.6*, 129.3 (Ar-C_{ortho}), 131.2*, 134.3 ($C_{Pyrrole}$), 138.9 (Ar-C_{ortho}), 141.2 ($C_{Pyrrole}$), 146.0 (Ar-C_{para}), 146.9 (C_{meso}), 150.2 ($C_{Pyrrole}$), 174.1 (CO). *This signal could not be assigned exactly to corresponding carbon atom. It belongs to the Ar-C_{ipso} or the Ar-C_{nitro} of the aryl residue.

HRMS (ESI-TOF, MeOH): *m/z* calcd. for $C_{54}H_{40}N_{12}O_6In^+$ $[M+H]^+$: 1067.2227, found: 1067.2227, *m/z* calcd. for $C_{54}H_{39}N_{12}O_6InNa^+$ $[M+Na]^+$: 1089.2047, found: 1089.2057, *m/z* calcd. for $C_{54}H_{39}N_{12}O_6InK^+$ $[M+K]^+$: 1105.1786, found: 1105.1795, *m/z* calcd. for $C_{36}H_{26}N_8O_4In^+$ [M-ligand]$^+$: 749.1110, found: 749.1132, *m/z* calcd. for $C_{18}H_{15}N_4O_2^+$ [ligand+H]$^+$: 319.1190, found: 319.1195.

IR (ATR): $\tilde{\nu}$ (cm^{-1}) = 3375 [ν(NH)], 3098 [ν(Ar-H)], 2942 [$\nu(CH_2)$], 1732 [ν(COOMe)], 1621 [ν(C=N), ν(C=C)], 1528 [$\nu_{as}(NO_2)$], 1333 [$\nu_{sym}(NO_2)$], 733 [δ(HC=CH)].

UV/vis (DCM): λ_{max} (nm) [log (ε/L mol^{-1} cm^{-1})] = 446 [4.84], 498 [4.51].

M.P. (°C): 170-175.

Tris{5-[4-(*N*-butylamino)-3-nitrophenyl]dipyrrinato}gallium(III) (**188**):

Complex **188** was prepared according to the general synthetic procedure. Dipyrrin **23** (500 mg, 1.49 mmol), $GaCl_3$·pentane (1.00 mL, 0.50 mmol), and DIPEA (1.26 mL, 7.43 mmol) were dissolved in THF. After purification (column chromatography, silica gel, DCM/EtOAc = 1/1, v/v); complex **188** was obtained as an orange solid (185 mg, 0.18 mmol, 35%).

^{1}H NMR (500 MHz, CD_2Cl_2): δ (ppm) = 1.02 (t, J = 7.4 Hz, 9H, Me), 1.49–1.57 (m, 6H, CH_2), 1.75–1.81 (m, 6H, CH_2), 3.41 (td, J = 7.1, 5.3 Hz, 6H, CH_2), 6.33 (d, J = 16.8 Hz, 6H, $H_{Pyrrole}$), 6.74–6.76 (m, 3H, $H_{Pyrrole}$), 6.85–6.91 (m, 3H, $H_{Pyrrole}$), 6.96 (d, J = 8.9 Hz, 3H, Ar-H_{meta}), 7.57 (t, J = 7.3 Hz, 3H, Ar-H_{ortho}), 8.20 (t, J = 5.2 Hz, 3H, NH), 8.27 (d, J = 5.1 Hz, 3H, Ar-H_{ortho}).

^{13}C NMR (126 MHz, CD_2Cl_2): δ (ppm) = 13.96 (Me), 20.7 (CH_2), 31.4 (CH_2), 43.4 (CH_2), 113.3 (Ar-C_{meta}), 117.2 (dd, J = 35.1, 21.3 Hz, $C_{Pyrrole}$), 126.7*, 129.2 (Ar-C_{ortho}), 131.3*, 132.7–133.1 (m, $C_{Pyrrole}$), 138.8 (Ar-C_{ortho}), 139.7 ($C_{Pyrrole}$), 145.9 (Ar-C_{para}), 146.1 (C_{meso}), 148.9–149.6 (m, $C_{Pyrrole}$). *These signals could not be assigned exactly to corresponding carbon atoms. They belong to the Ar-C_{ipso} or the Ar-C_{nitro} of the aryl residue.

HRMS (ESI-TOF, DCM/MeOH): *m/z* calcd. for $C_{57}H_{57}GaN_{12}O_6K^+$ $[M+K]^+$: 1113.3411, found: 1113.3443, *m/z* calcd. for $C_{38}H_{38}GaN_8O_4^+$ [M-ligand]$^+$: 739.2266, found: 739.2294, *m/z* calcd. for $C_{19}H_{21}N_4O_2^+$ [ligand+H]$^+$: 337.1659, found: 337.1679.

IR (ATR): $\tilde{\nu}$ (cm^{-1}) = 3376 [ν(NH)], 3097 [ν(Ar-H)], 2956, 2928, and 2869 [ν(CH_2, ν(Me)], 1622 [ν(C=N), ν(C=C)], 1529 [ν_{as}(NO_2)], 1336 [ν_{sym}(NO_2)], 731 [δ(HC=CH)].

UV/vis (DCM): λ_{max} (nm) [log (ε/L mol^{-1} cm^{-1})] = 447 [4.73], 498 [4.53].

M.P. (°C): 156-160.

Attempted synthesis of tris{5-[3-nitro-4-(*N*-prop-2-enylamino)phenyl]dipyrrinato}gallium(III) (**189**):
The reaction was carried out according to the general synthetic procedure. Dipyrrin **24** (500 mg, 1.56 mmol), $GaCl_3$·pentane (1.04 mL, 0.52 mmol), and DIPEA (1.33 mL, 7.80 mmol) were dissolved in THF. After purification (column chromatography, silica gel, DCM/EtOAc = 4/1, v/v); an orange solid (92 mg) was obtained. However, this fraction could not be assigned to the desired product. The spectra did not allow a meaningful interpretation. Evidence for a decomposition of the dipyrrin was found, due to the observation of large quantities of a black residue.

Attempted synthesis of tris{5-[3-nitro-4-(*N*-prop-2-ynylamino)phenyl]dipyrrinato}gallium(III) (**190**):
The reaction was carried out according to the general synthetic procedure. Dipyrrin **109** (500 mg, 1.57 mmol), $GaCl_3$·pentane (1.05 mL, 0.52 mmol), and DIPEA (1.34 mL, 7.85 mmol) were dissolved in THF. After purification (column chromatography, silica gel, DCM/EtOAc = 1/1, v/v) an orange solid (41 mg) was obtained. However, this fraction could not be assigned to the desired product. The spectra did not allow a meaningful interpretation. Evidence for a decomposition of the dipyrrin was found, due to the observation of large quantities of a black residue.

Attempted synthesis of tris{5-[4-(*N*-2-hydroxyethylamino)-3-nitrophenyl]dipyrrinato}gallium(III) (**191**): The reaction was carried out according to the general synthetic procedure. Dipyrrin **25** (500 mg, 1.54 mmol), $GaCl_3$·pentane (1.03 mL, 0.51 mmol), and DIPEA (1.31 mL, 7.71 mmol) were dissolved in 15 mL of THF. After column purification (chromatography, silica gel, DCM/EtOAc = 1/2, v/v) an orange solid (53 mg) was obtained. However, this fraction could not be assigned to the desired product. The spectra did not allow a meaningful interpretation. Evidence for a decomposition of the dipyrrin was found, due to the observation of large quantities of a black residue.

Tris{5-[4-(*N*-6-methoxy-6-oxohexylamino)-3-nitrophenyl]dipyrrinato}gallium(III) (**192**):
Complex **192** was prepared according to the general synthetic procedure. Dipyrrin **26** (500 mg, 1.22 mmol), $GaCl_3$·pentane (0.82 mL, 0.41 mmol), and DIPEA (1.04 mL, 6.12 mmol) were dissolved in 10 mL of THF. After purification (column chromatography, silica gel, DCM/EtOAc = 1/1, v/v); complex **191** was obtained as orange solid (135 mg, 0.11 mmol, 27%).

^{1}H NMR (500 MHz, CD_2Cl_2): δ (ppm) = 1.47–1.53 (m, 2H, CH_2), 1.67–1.73 (m, 2H, CH_2), 1.76–1.82 (m, 2H, CH_2), 2.35 (t, *J* = 7.4 Hz, 2H, CH_2), 3.38–3.42 (m, 2H, CH_2), 3.65 (s, 3H, Me), 6.31 (d, *J* = 15.1 Hz, 2H, $H_{pyrrole}$), 6.73 (t, *J* = 4.9 Hz, 2H, $H_{pyrrole}$), 6.83–6.89 (m, 2H, $H_{pyrrole}$), 6.94 (d, *J* = 8.9 Hz, 1H, Ar-H_{meta}), 7.54–7.57 (m, 1H, Ar-H_{ortho}), 8.18 (t, *J* = 5.3 Hz, 1H, NH), 8.24 (d, *J* = 4.5 Hz, 1H, Ar-H_{ortho})
^{13}C NMR (126 MHz, CD_2Cl_2): δ (ppm) = 24.98 (CH_2), 26.9 (CH_2), 29.0 (CH_2), 34.2 (CH_2), 43.4 (CH_2), 51.9 (Me), 113.3 (Ar-C_{meta}), 117.2 ($C_{pyrrole}$), 125.9*, 129.2 (Ar-C_{ortho}), 131.2*, 132.9 ($C_{pyrrole}$), 138.9 (Ar-C_{ortho}), 139.8 ($C_{pyrrole}$), 145.9 (C_{meso}), 146.0 (Ar-C_{para}), 149.3 ($C_{pyrrole}$), 174.7 (CO). *These signals could not be assigned exactly to corresponding carbon atoms. They belong to the Ar-C_{ipso} and the Ar-C_{nitro} of the aryl residue.
HRMS (ESI-TOF, MeOH): *m/z* calcd. for $C_{66}H_{69}GaN_{12}O_{12}Na^+$ $[M+Na]^+$: 1313.4306, found: 1313.4267, *m/z* calcd. for $C_{66}H_{69}GaN_{12}O_{12}K^+$ $[M+K]^+$: 1329.4045, found: 1329.4010, *m/z* calcd. for $C_{44}H_{46}GaN_8O_8^+$ $[M\text{-ligand}]^+$: 883.2689, found: 883.2667.
IR (ATR): $\tilde{\nu}$ (cm^{-1}) = 3377 [ν(NH)], 3100 [ν(Ar-H)], 2944 [$\nu(CH_2)$], 1736 [ν(COOMe)], 1621 [ν(C=N), ν(C=C)], 1540 [$\nu_{as}(NO_2)$], 1337 [$\nu_{sym}(NO_2)$], 737 [δ(HC=CH)].
UV/vis (DCM): λ_{max} (nm) [log (ε/L mol^{-1} cm^{-1})] = 448 [4.75], 498 [4.56].
M.P. (°C): 200-208.

Attempted synthesis of tris{5-[4-(*N*-butylamino)-3-nitrophenyl]dipyrrinato}iridium(III) (**193**):
The reaction was carried out according to the general synthetic procedure. Dipyrrin **23** (275 mg, 0.82 mmol), $IrCl_3$·xH_2O (96 mg, 0.27 mmol), and DIPEA (0.70 mL, 4.09 mmol) were dissolved in THF. After purification (column chromatography, silica gel, DCM/EtOAc = 1/1, v/v) an orange solid was

obtained and this fraction was assigned to the corresponding 5-[4-(*N*-butylamino)-3-nitrophenyl]-dipyrromethane (60 mg, 0.18 mmol, 22%).

^{1}H NMR (500 MHz, CD_2Cl_2): δ (ppm) = 0.96 (t, *J* = 7.4 Hz, 3H, Me), 1.40–1.50 (m_c, 2H, CH_2), 1.65–1.72 (m_c, 2H, CH_2), 3.26–3.31 (m_c, 2H, CH_2), 5.36 (s, 1H, H_{meso}), 5.85 (br s, 2H, $H_{pyrrole}$), 6.10–6.12 (m, 2H, $H_{pyrrole}$), 6.68–6.70 (m, 2H, $H_{pyrrole}$), 6.83 (d, *J* = 8.9 Hz, 1H, Ar-H_{meta}), 7.31 (dd, *J* = 8.9, 2.2 Hz, 1H, Ar-H_{ortho}), 7.93 (d, *J* = 2.2 Hz, 1H, Ar-H_{ortho}), 8.01–8.06 (m, 3H, NH).
HRMS (ESI-TOF, MeOH): *m/z* calcd. for $C_{19}H_{22}N_4O_2Na^+$ $[M+Na]^+$: 361.1635, found: 361.1652.

Attempted synthesis of tris{5-[4-*N*-6-methoxy-6-oxohexylamino)-3-nitrophenyl]dipyrrinato}-iridium(III) (**194**):
The reaction was carried out according to the general synthetic procedure. Dipyrrin **26** (300 mg, 0.73 mmol), $IrCl_3 \cdot xH_2O$ (86 mg, 0.25 mmol), and DIPEA (0.60 mL, 3.67 mmol) were dissolved in THF. After purification (column chromatography, silica gel, DCM/EtOAc = 1/1, v/v) an orange solid was obtained and this fraction was assigned to the corresponding 5-[4-*N*-6-methoxy-6-oxohexylamino)-3-nitrophenyl]dipyrromethane (70 mg, 0.17 mmol, 23%).

^{1}H NMR (500 MHz, CD_2Cl_2): δ (ppm) = 1.42–1.49 (m_c, 2H, CH_2), 1.63–1.76 (m_c, 4H, CH_2), 2.32 (t, *J* = 7.4 Hz, 2H, CH_2), 3.28–3.33 (m_c, 2H, CH_2), 3.63 (s, 3H, Me), 5.38 (s, 1H, H_{meso}), 5.86–5.87 (m, 2H, $H_{pyrrole}$), 6.11–6.13 (m, 2H, $H_{pyrrole}$), 6.70–6.72 (m, 2H, $H_{pyrrole}$), 6.84 (d, *J* = 8.9 Hz, 1H, Ar-H_{meta}), 7.33 (dd, *J* = 8.9, 2.2 Hz, 1H, Ar-H_{ortho}), 7.94 (d, *J* = 2.2 Hz, 1H, Ar-H_{ortho}), 8.02 (t, *J* = 5.2 Hz, 1H, NH), 8.17 (br s, 2H, NH).
HRMS (ESI-TOF, DCM/MeOH): *m/z* calcd. for $C_{22}H_{26}N_4O_4Na$+ $[M+Na]^+$: 433.1852, found: 433.1860.

Attempted synthesis of tris(5-pentafluorophenyldipyrrinato)iridium(III) (**195**):
The reaction was carried out according to the general synthetic procedure. Dipyrrin **102** (250 mg, 0.81 mmol), $IrCl_3 \cdot xH_2O$ (95 mg, 0.27 mmol), and DIPEA (0.70 mL, 4.03 mmol) were dissolved in THF. After purification (column chromatography, silica gel, DCM/*n*-hexane = 1/1, v/v) an orange solid (129 mg) was obtained. However, this fraction could not be assigned to the desired product. The spectra did not allow a meaningful interpretation. Evidence for a decomposition of the dipyrrin was found, due to the observation of large quantities of a black residue.

6.3 Modification of the 1,3,5,7-BODIPY structure

6.3.1 Nucleophilic substitution

General synthetic procedure: The BODIPY (1 equiv.) was dissolved in DMF or DCM and the related amine (10 – 20 equiv.) was added. The mixture was stirred for the indicated time at rt. Afterwards, the

mixture was diluted with EtOAc and washed with water several times. The organic layer was dried with Na_2SO_4, filtered, and evaporated to dryness. The organic layer was dried with Na_2SO_4, filtered, and evaporated to dryness. The crude product was purified by column chromatography; the main fraction was collected and evaporated to dryness.

8-[4-(*N*-Prop-2-enylamino)-2,3,5,6-tetrafluoro-phenyl]-1,3,5,7-tetramethyl-4,4-difluoro-4-bora-3a,4a-diaza-*s*-indacene (**196**):

BODIPY **196** was prepared according to the general synthetic procedure. BODIPY **65** (200 mg, 0.48 mmol) and allylamine (0.36 mL, 4.83 mmol, 10 equiv.) were dissolved in 5 mL of DMF. After purification (column chromatography, silica gel, EtOAc/*n*-hexane = 1/9, v/v); BODIPY **196** was obtained as an orange solid (74 mg, 0.16 mmol, 32%).

^{1}H NMR (500 MHz, $CDCl_3$): δ (ppm) = 1.65 (s, 6H, Me), 2.54 (s, 6H, Me), 4.06 (dt, *J* = 5.7, 1.5 Hz, 2H, CH_2), 5.20 (dq, *J* = 10.3, 1.3 Hz, 1H, -CH=**CH_2**), 5.25 (dq, *J* = 17.1, 1.5 Hz, 1H, -CH=**CH_2**), 5.93 (ddt, *J* = 17.2, 10.3, 5.7 Hz, 1H, -**CH**=CH_2), 6.02 (s, 2H, $H_{Pyrrole}$).

^{13}C NMR (126 MHz, $CDCl_3$): δ (ppm) = 13.6 (Me), 14.8 (Me), 47.96 (CH_2), 101.0 (Ar-C_{ipso}), 117.3 (-CH=**CH_2**), 121.8 ($CH_{Pyrrole}$), 127.8 (C_{meso}), 131.9 ($C_{Pyrrole}$), 132.3 (-**CH**=CH_2), 134.6 (Ar-C_{para}), 142.1 ($C_{Pyrrole}$), 156.9 ($C_{Pyrrole}$).

^{19}F NMR (376 MHz, $CDCl_3$): δ (ppm) = -143.00 (d, *J* = 18.0 Hz, 2F, CF_{meta}), -145.92 – -146.18 (m_C, 2F, BF_2), -158.61 (d, *J* = 18.9 Hz, 2F, CF_{ortho}).

HRMS (ESI-TOF, MeOH): *m/z* calcd. for $C_{22}H_{20}BF_6N_3Na^+$ $[M+Na]^+$: 474.1547, found: 474.1542, *m/z* calcd. for $C_{22}H_{20}BF_6N_3K^+$ $[M+K]^+$: 490.1286, found: 490.1281, *m/z* calcd. for $C_{44}H_{40}B_2F_{12}N_6Na^+$ $[2M+Na]^+$: 925.3201, found: 925.3185.

IR (ATR): $\tilde{\nu}$ (cm^{-1}) = 3406 [ν(NH)], 2958 and 2931 [ν(CH_2), ν(Me)], 2867 [ν(CH)], 1658 [ν(C=N), ν(C=C)], 1495 [δ(CH_2), δ(Me)], 1153 [ν(BF)], 768 [δ(-HC=CH-)].

UV/vis (DCM): λ_{max} (nm) [log (ε/L mol^{-1} cm^{-1})] = 515 [4.83].

Fluorescence (DCM): λ_{max} (nm) = 527 at $\lambda_{Excitation}$ (nm) = 500.

M.P. (°C): 165-169.

Attempted synthesis of 8-[4-(*N,N*-dibutylamino)-2,3,5,6-tetrafluorophenyl]-1,3,5,7-tetramethyl-4,4-difluoro-4-bora-3a,4a-diaza-*s*-indacene (**197**):

The reaction was carried out according to the general synthetic procedure. BODIPY **65** (200 mg, 0.48 mmol) and *N*,*N*-dibutylamine (1.64 mL, 9.66 mmol, 20 equiv.) were dissolved in 10 mL of DMF. After purification (column chromatography, silica gel, DCM) a dark oil (100 mg) was obtained. However, this fraction could not be assigned to the desired product. The spectra did not allow a meaningful interpretation.

8-[3-Nitro-4-(*N*-2-prop-2-enylamino)phenyl]-1,3,5,7-tetramethyl-4,4-difluoro-4-bora-3a,4a-diaza-*s*-indacene (**199**):

BODIPY **199** was prepared according to the general synthetic procedure. BODIPY **66** (132 mg, 0.34 mmol) and allylamine (0.3 mL, 3.40 mmol, 10 equiv.) were dissolved in 10 mL of DCM. After column purification (chromatography, silica gel, *n*-hexane/EtOAc = 9/1, v/v); BODIPY **199** was obtained as an orange solid (124 mg, 0.29 mmol, 86%).

^{1}H NMR (500 MHz, $CDCl_3$): δ (ppm) = 1.53 (s, 6H, Me), 2.54 (s, 6H, Me), 4.05 (t, *J* = 5.0 Hz, 2H, CH_2), 5.29–5.36 (m, 2H, **H_2C**=CH-), 5.95–6.02 (m, 3H, $H_{Pyrrole}$ + H_2C=**CH**-), 6.98 (d, *J* = 8.8 Hz, 1H, Ar-H_{meta}), 7.30 (dd, *J* = 8.8, 2.2 Hz, 1H, Ar-H_{ortho}), 8.14 (d, *J* = 2.1 Hz, 1H, Ar-H_{ortho}), 8.28 (t, *J* = 5.8 Hz, 1H, NH).

^{13}C NMR (126 MHz, $CDCl_3$): δ (ppm) = 14.7 (Me), 15.3 (Me), 45.6 (CH_2), 115.2 (Ar-C_{meta}), 117.7 (**H_2C**=CH), 121.6 ($CH_{Pyrrole}$), 121.8*, 126.8 (Ar-C_{ortho}), 131.9 ($C_{Pyrrole}$), 132.1 (C_{meso}), 132.7 (H_2C=**CH**-), 136.0 (Ar-C_{ortho}), 139.2*, 142.7 ($C_{Pyrrole}$), 145.3 (Ar-C_{para}), 156.1 ($C_{Pyrrole}$). *These signals could not be assigned exactly to corresponding carbon atoms. They belong to the Ar-C_{ipso} and the Ar-C_{nitro} of the aryl residue.

^{19}F NMR (376 MHz, $CDCl_3$): δ (ppm) = -145.57 – -146.59 (m_c, 2F, BF_2).

HRMS (ESI-TOF, MeOH): *m/z* calcd. for $C_{22}H_{23}BF_2N_4O_2Na^+$ $[M+Na]^+$: 447.1774, found: 447.1796 , *m/z* calcd. for $C_{22}H_{23}BF_2N_4O_2K^+$ $[M+K]^+$: 463.1514, found: 463.1543, *m/z* calcd. for $C_{44}H_{46}B_2F_4N_8O_4Na^+$ $[2M+Na]^+$: 871.3656, found: 871.3699, *m/z* calcd. for $C_{44}H_{46}B_2F_4N_8O_4K^+$ $[2M+K]^+$: 887.3396, found: 887.3442.

IR (ATR): $\tilde{\nu}$ (cm^{-1}) = 3590 [ν(NH)], 2920 [ν(CH_2)], 1628 [ν(C=N), ν(C=C)], 1543 [ν_{as}(NO_2)], 1527 [δ(Ar-C)], 1466 [δ(CH_2), δ(Me)], 1349 [ν_{sym}(NO_2)], 1061 [ν(BF)], 758 [δ(HC=CH)].

UV/vis (DCM): λ_{max} (nm) [log (ε/L mol^{-1} cm^{-1})] = 504 [4.83].

Fluorescence (DCM): λ_{max} (nm) = 517 at $\lambda_{Excitation}$ (nm) 490.

M.P. (°C): 176-179.

8-[4-(*N*-6-Methoxy-6-oxohexylamino)-3-nitrophenyl]-1,3,5,7-tetramethyl-4,4-difluoro-4-bora-3a,4a-diaza-*s*-indacene (**200**):

BODIPY **200** was prepared according to the general synthetic procedure. BODIPY **66** (200 mg, 0.52 mmol), DIPEA (1.8 mL, 10.33 mmol, 20 equiv.), and methyl-6-aminohexanoate hydrochloride (939 mg, 5.17 mmol, 10 equiv.) were dissolved in 20 mL of DCM. After purification (column chromatography, silica gel, *n*-hexane/EtOAc = 9/1, v/v, then *n*-hexane/EtOAc = 4/1, v/v); BODIPY **200** was obtained as an orange solid (80 mg, 0.16 mmol, 30%).

^{1}H NMR (500 MHz, $CDCl_3$): δ (ppm) = 1.49–1.57 (m, 8H, Me + CH_2), 1.70–1.76 (m, 2H, CH_2), 1.77–1.83 (m, 2H, CH_2), 2.36 (t, *J* = 7.4 Hz, 2H, CH_2), 2.54 (s, 6H, Me), 3.36 (td, *J* = 7.1, 5.0 Hz, 2H, CH_2), 3.67 (s, 3H,

Me_{COOMe}), 5.99 (s, 2H, $H_{Pyrrole}$), 6.98 (d, *J* = 8.8 Hz, 1H, Ar-H_{meta}), 7.31 (dd, *J* = 8.7, 2.2 Hz, 1H, Ar-H_{ortho}), 8.11–8.14 (m, 2H, Ar-H_{ortho} + NH).

^{13}C NMR (126 MHz, $CDCl_3$): δ (ppm) = 14.7 (Me), 15.3 (Me), 24.6 (CH_2), 26.7 (CH_2), 28.7 (CH_2), 33.9 (CH_2), 43.1 (CH_2), 51.7 (Me_{COOMe}), 114.8 (Ar-C_{meta}), 121.5*, 121.6 ($CH_{Pyrrole}$), 126.9 (Ar-C_{ortho}), 131.9 ($C_{Pyrrole}$), 131.9 (C_{meso}), 136.1 (Ar-C_{ortho}), 139.3*, 142.7 ($C_{Pyrrole}$), 145.5 (Ar-C_{para}), 156.1 ($C_{Pyrrole}$), 173.95 (CO). *These signals could not be assigned exactly to corresponding carbon atoms. They belong to the Ar-C_{ipso} and the Ar-C_{nitro} of the aryl residue.

^{19}F NMR (376 MHz, $CDCl_3$): δ (ppm) = -145.57 – -146.63 (m_c, 2F, BF_2).

HRMS (ESI-TOF, MeOH): *m/z* calcd. for $C_{26}H_{31}BFN_4O_4^+$ $[M-F]^+$: 493.2417, found: 493.2410, *m/z* calcd. for $C_{26}H_{31}BF_2N_4O_4Na^+$ $[M+Na]^+$: 535.2299, found: 535.2298.

IR (ATR): $\tilde{\nu}$ (cm^{-1}) = 3377 [ν(NH)], 2929 [ν(CH_2), ν(Me)], 2858 [ν(CH)], 1734 [ν(COOMe)], 1626 [ν(C=N), ν(C=C)], 1542 [ν_{as}(NO_2)], 1526 [δ(Ar-C)], 1468 [δ(CH_2), δ(Me)], 1304 [ν_{sym}(NO_2)], 1075 [ν(BF)], 758 [δ(HC=CH)]. **UV/vis (DCM):** λ_{max} (nm) [log (ε/L mol^{-1} cm^{-1})] = 504 [4.66].

Fluorescence (DCM): λ_{max} (nm) = 518 at $\lambda_{Excitation}$ (nm) 490.

M.P. (°C): 123-125.

8-[4-(*N*,*N*-Dibutylamino)-3-nitrophenyl]-1,3,5,7-tetramethyl-4,4-difluoro-4-bora-3a,4a-diaza-*s*-indacene (**201**):

BODIPY **201** was prepared according to the general synthetic procedure. BODIPY **66** (200 mg, 0.52 mmol) and *N*,*N*-dibutylamine (1.60 mL, 9.66 mmol, 15 equiv.) were dissolved in 10 mL of DCM. After column purification (chromatography, silica gel, *n*-hexane/EtOAc = 9/1, v/v); BODIPY **201** was obtained as an orange solid (90 mg, 0.18 mmol, 35%).

^{1}H NMR (500 MHz, $CDCl_3$): δ (ppm) = 0.87 (t, *J* = 7.4 Hz, 6H, Me_{Butyl}), 1.25–1.32 (m, 4H, CH_2), 1.50–1.56 (m, 10H, CH_2 + Me) , 2.55 (s, 6H, Me), 3.20 (t, *J* = 7.3 Hz, 1H, CH_2), 6.00 (s, 2H, $H_{Pyrrole}$), 7.28 (br s, 2H, Ar-H_{meta} + Ar-H_{ortho}), 7.65 (t, *J* = 1.2 Hz, 1H, Ar-H_{ortho}).

^{13}C NMR (126 MHz, $CDCl_3$): δ (ppm) = 13.9 (Me_{Butyl}), 14.8 (Me), 14.99 (Me), 20.2 (CH_2), 29.5 (CH_2), 52.2 (CH_2), 121.7 ($CH_{Pyrrole}$), 122.6 (Ar-C_{meta}), 126.3 (Ar-C_{ortho}), 131.7 ($C_{Pyrrole}$), 132.7 (Ar-C_{ortho}), 138.96*, 142.1*, 142.8 ($C_{Pyrrole}$), 144.9 (Ar-C_{para}), 156.2 ($C_{Pyrrole}$). *These signals could not be assigned exactly to corresponding carbon atoms. They belong to the Ar-C_{ipso} and the Ar-C_{nitro} of the aryl residue.

^{19}F NMR (376 MHz, $CDCl_3$): δ (ppm) = -145.61 – -146.64 (m_c, 2F, BF_2).

HRMS (ESI-TOF, MeOH): *m/z* calcd. for $C_{27}H_{35}BF_2N_4O_2Na^+$ $[M+Na]^+$: 519.2713, found: 519.2713.

IR (ATR): $\tilde{\nu}$ (cm^{-1}) = 2957 and 2929 [ν(CH_2), ν(Me)], 2871 [ν(CH)], 1613 [ν(C=N), ν(C=C)], 1545 [ν_{as}(NO_2)], 1512 [δ(Ar-C)], 1467 [δ(CH_2), δ(Me)], 1348 [ν_{sym}(NO_2)], 1082 [ν(BF)], 760 [δ(HC=CH)].

UV/vis (DCM): λ_{max} (nm) [log (ε/L mol^{-1} cm^{-1})] = 505 [4.62].

Fluorescence (DCM): λ_{max} (nm) = 515 at $\lambda_{Excitation}$ (nm) 490.

M.P. (°C): 95-99.

6.3.2 Substitution of the 2- and 6-position with NBS

General synthetic procedure: The BODIPY (1 equiv.) was dissolved in 2 mL of HFIP, NBS (2.5 equiv.) was added, and the mixture was stirred for the indicated time at rt. Afterwards, the reaction mixture was diluted with EtOAc and washed with water several times. The organic layer was dried with Na_2SO_4, filtered, and evaporated to dryness. The crude product was purified by column chromatography; the main fraction was collected and evaporated to dryness.

Attempted synthesis of 2,6-dibromo-8-[4-(*N*-prop-2-enylamino)-2,3,5,6-tetrafluorophenyl]-1,3,5,7-tetramethyl-4,4-difluoro-4-bora-3a,4a-diaza-*s*-indacene (**198**):

The reaction was carried out according to the general synthetic procedure. BODIPY **196** (90 mg, 0.20 mmol) and NBS (88 mg, 0.50 mmol) were dissolved in HFIP. After purification (column chromatography, silica gel, EtOAc/*n*-hexane = 1/9, v/v) a red solid (66 mg) was obtained. However, evidence for the formation of mixture of BODIPYs was found in the NMR spectra.

2,6-Dibromo-8-[3-nitro-4-(*N*-2-prop-2-enylamino)phenyl]-1,3,5,7-tetramethyl-4,4-difluoro-4-bora-3a,4a-diaza-*s*-indacene (**202**):

BODIPY **202** was prepared according to the general synthetic procedure. BODIPY **199** (87 mg, 0.21 mmol) and NBS (91 mg, 0.51 mmol) were dissolved in HFIP. The mixture was stirred for 1 min. After purification (column chromatography, silica gel, EtOAc/*n*-hexane = 1/9, v/v); BODIPY **202** was obtained as a red solid (53 mg, 92 µmol, 44%).

^{1}H NMR (500 MHz, THF-d_8): δ (ppm) = 1.58 (m, 6H, Me), 2.56 (s, 6H, Me), 4.12–4.15 (m, 2H, CH_2), 5.23 (ddd, *J* = 10.4, 1.5 Hz, 1H, **H_2C**=CH-), 5.31 (ddd, *J* = 17.2, 1.6 Hz, 1H, **H_2C**=CH-), 6.01 (ddt, *J* = 17.2, 10.1, 4.9 Hz, 1H, H_2C=**CH**-), 7.20 (d, *J* = 8.8 Hz, 1H, Ar-H_{meta}), 7.41 (dd, *J* = 8.8, 2.1 Hz, 1H, Ar-H_{ortho}), 8.19 (d, *J* = 2.2 Hz, 1H, Ar-H_{ortho}), 8.45 (t, *J* = 5.9 Hz, 1H, NH).

^{13}C NMR (126 MHz, THF-d_8): δ (ppm) = 13.9 (Me), 14.8 (Me), 46.1 (CH_2), 112.3 (C_{Br}), 116.9 (**H_2C**=CH-), 117.0 (Ar-C_{meta}), 121.5*, 127.7 (Ar-C_{ortho}), 131.99 ($C_{Pyrrole}$), 133.5*, 134.9 (H_2C=**CH**-), 136.4 (Ar-C_{ortho}), 141.1 ($C_{Pyrrole}$), 142.1 (C_{meso}), 146.8 (Ar-C_{para}), 154.9 ($C_{Pyrrole}$). *These signals could not be assigned exactly to corresponding carbon atoms. They belong to the Ar-C_{ipso} and the Ar-C_{nitro} of the aryl residue.

^{19}F NMR (376 MHz, THF-d_8): δ (ppm) = -146.56 – -146.27 (m_c, 2F, BF_2).

HRMS (ESI-TOF, MeOH): *m/z* calcd. for $C_{22}H_{21}BBr_2FN_4O_2^+$ $[M-F]^+$: 563.0082, found: 563.0083, *m/z* calcd. for $C_{22}H_{21}BBr_2F_2N_4O_2Na^+$ $[M+Na]^+$: 604.9964, found: 604.9968, *m/z* calcd. for $C_{22}H_{21}BBr_2F_2N_4O_2K^+$

[M+K]$^+$: 620.9703, found: 620.9707, *m/z* calcd. for $C_{44}H_{42}B_2Br_4F_4N_8O_4Na^+$ [2M+Na]$^+$: 1187.0036, found: 1187.0044.

IR (ATR): $\tilde{\nu}$ (cm^{-1}) = 3358 [ν(NH)], 2925 [ν(CH_2)], 2847 [ν(CH)], 1631 [ν(C=N), ν(C=C)], 1535 [ν_{as}(NO_2)], 1460 [δ(CH_2), δ(Me)], 1346 [ν_{sym}(NO_2)], 1170 and 1119 [ν(BF), ν(CBr)], 755 [δ(HC=CH)].

UV/vis (DCM): λ_{max} (nm) [log (ε/L mol^{-1} cm^{-1})] = 399 [4.17], 528 [4.85].

Fluorescence (DCM): λ_{max} (nm) = 550 at $\lambda_{Excitation}$ (nm) = 380, 510

M.P.(°C): 209-214.

2,6-Dibromo-8-[4-(*N*-6-methoxy-6-oxohexylamino)-3-nitrophenyl]-1,3,5,7-tetramethyl-4,4-difluoro-4-bora-3a,4a-diaza-*s*-indacene (**203**):

BODIPY **203** was prepared according to the general synthetic procedure. BODIPY **200** (95 mg, 0.19 mmol) and NBS (83 mg, 0.46 mmol) were dissolved in HFIP. The mixture was stirred for 1 min. After purification (column chromatography, silica gel, EtOAc/*n*-hexane = 1/9, v/v); BODIPY **203** was obtained as a red solid (67 mg, 0.10 mmol, 54%).

^{1}H NMR (500 MHz, THF-d$_8$): δ (ppm) = 1.48–1.54 (m, 2H, CH_2), 1.59 (s, 6H, Me), 1.67–1.71 (m, 2H, CH_2), 1.76–1.82 (m, 2H, CH_2), 2.33 (t, *J* = 7.3 Hz, 2H, CH_2), 2.56 (s, 6H, Me), 3.46 (td, *J* = 7.3, 5.6 Hz, 2H, CH_2), 3.60 (s, 3H, Me_{COOMe}), 7.27 (d, *J* = 8.8 Hz, 1H, Ar-H$_{meta}$), 7.43 (dd, *J* = 8.8, 2.2 Hz, 1H, Ar-H$_{ortho}$), 8.18 (d, *J* = 2.1 Hz, 1H, Ar-H$_{ortho}$), 8.27 (t, *J* = 5.5 Hz, 1H, NH).

^{13}C NMR (126 MHz, THF-d$_8$): δ (ppm) = 13.9 (Me), 14.9 (Me), 25.98 (CH_2), 27.6 (CH_2), 29.4 (CH_2), 34.3 (CH_2), 43.9 (CH_2), 51.5 (Me_{COOMe}), 112.6 (C_{Br}), 116.5 (Ar-C$_{meta}$), 121.2*, 127.9 (Ar-C$_{ortho}$), 132.0 ($C_{Pyrrole}$), 133.2*, 136.6 (Ar-C$_{ortho}$), 141.1 ($C_{Pyrrole}$), 142.1 (C_{meso}), 146.9 (Ar-C$_{para}$), 154.9 ($C_{Pyrrole}$), 173.8 (CO). *These signals could not be assigned exactly to corresponding carbon atoms. They belong to the Ar-C$_{ipso}$ and the Ar-C$_{nitro}$ of the aryl residue.

^{19}F NMR (376 MHz, THF-d$_8$): δ (ppm) = -146.56 – -146.25 (m_c, 2F, BF_2).

HRMS (ESI-TOF, MeOH): *m/z* calcd. for $C_{26}H_{29}BBr_2F_2N_4O_4Na^+$ [M+Na]$^+$: 693.0488, found: 693.0503, *m/z* calcd. for $C_{26}H_{29}BBr_2F_2N_4O_4K^+$ [M+K]$^+$: 709.0228, found: 709.0235, *m/z* calcd. for $C_{52}H_{58}B_2Br_4F_4N_8O_8Na^+$ [2M+Na]$^+$: 1363.1085, found: 1363.1112.

IR (ATR): $\tilde{\nu}$ (cm^{-1}) = 3379 [ν(NH)], 2926 [ν(CH_2), ν(Me)], 2860 [ν(CH)], 1733 [ν(COOMe)], 1632 [ν(C=N), ν(C=C)], 1532 [ν_{as}(NO_2)], 1457 [δ(CH_2), δ(Me)], 1346 [ν_{sym}(NO_2)], 1163 and 1118 [ν(BF), ν(CBr)], 755 [δ(HC=CH)].

UV/vis (DCM): λ_{max} (nm) [log (ε/L mol^{-1} cm^{-1})] = 404 [4.19], 532 [4.87].

Fluorescence (DCM): λ_{max} (nm) = 550 at $\lambda_{Excitation}$ (nm) = 390, 520.

M.P.(°C): 152-155.

2,6-Dibromo-8-[4-(*N,N*-dibutylamino)-3-nitrophenyl]-1,3,5,7-tetramethyl-4,4-difluoro-4-bora-3a,4a-diaza-*s*-indacene (**204**):

BODIPY **204** was prepared according to the general synthetic procedure. BODIPY **202** (90 mg, 0.18 mmol) and NBS (80 mg, 0.45 mmol) were dissolved in HFIP. The mixture was stirred for 1 min. After purification (column chromatography, silica gel, EtOAc/*n*-hexane = 1/9, v/v); BODIPY **204** was obtained as a red solid (68 mg, 0.10 mmol, 57%).

^{1}H NMR (500 MHz, THF-d$_8$): δ (ppm) = 0.89 (t, J = 7.3 Hz, 6H, Me_{Butyl}), 1.28–1.35 (m, 4H, CH_2), 1.53–1.59 (m, 10H, Me + CH_2), 2.56 (s, 6H, Me), 3.25 (t, J = 7.1 Hz, 4H, CH_2), 7.39 (dd, J = 8.7, 2.0 Hz, 1H, Ar-H_{meta}), 7.46 (dd, J = 8.7, 1.4 Hz, 1H, Ar-H_{ortho}), 7.77 (d, J = 2.0 Hz, 1H, Ar-H_{ortho}).

^{13}C NMR (126 MHz, THF-d$_8$): δ (ppm) = 13.99 (Me_{Butyl}), 14.3 (Me), 14.6 (Me), 21.0 (CH_2), 30.6 (CH_2), 52.8 (CH_2), 112.3–112.4 (m, C_{Br}), 123.7 (Ar-C_{meta}), 125.4*, 127.2 (Ar-C_{ortho}), 131.8 ($C_{Pyrrole}$), 133.2 (Ar-C_{ortho}), 141.1 ($C_{Pyrrole}$), 141.7 (C_{meso}), 143.9*, 146.4 (Ar-C_{para}), 154.97 ($C_{Pyrrole}$). *These signals could not be assigned exactly to corresponding carbon atoms. They belong to the Ar-C_{ipso} and the Ar-C_{nitro} of the aryl residue.

^{19}F NMR (376 MHz, THF-d$_8$): δ (ppm) = -146.52 – -146.31 (m_c, 2F, BF_2).

HRMS (ESI-TOF, MeOH): *m/z* calcd. for $C_{27}H_{34}BBr_2F_2N_4O_2^+$ $[M+H]^+$: 655.1084, found: 655.1087, *m/z* calcd. for $C_{27}H_{33}BBr_2F_2N_4O_2Na^+$ $[M+Na]^+$: 677.0903, found: 677.0899, *m/z* calcd. for $C_{54}H_{66}B_2Br_4F_4N_8O_4Na^+$ $[2M+Na]^+$: 1331.1914, found: 1331.1930.

IR (ATR): $\tilde{\nu}$ (cm^{-1}) = 2957 and 2929 [ν(CH_2), ν(Me)], 2871 [ν(CH)], 1615 [ν(C=N), ν(C=C)], 1533 [ν_{as}(NO_2)], 1461 [δ(CH_2), δ(Me)], 1346 [ν_{sym}(NO_2)], 1171 and 1118 [ν(BF), ν(CBr)], 756 [δ(HC=CH)].

UV/vis (DCM): λ_{max} (nm) [log (ε/L mol^{-1} cm^{-1})] = 389 [4.03], 533 [4.86].

Fluorescence (DCM): λ_{max} (nm) = 551 at $\lambda_{Excitation}$ (nm) = 360, 520.

M.P.(°C): 157-159.

6.3.3 Selective substitution of the 2-position with NBS

General synthetic procedure: The corresponding BODIPY (1 equiv.) was dissolved in 5 mL of DCM, NBS (1 equiv., dissolved in 2 mL of DCM) was added dropwise. The mixture was stirred for 2 h at rt. Afterwards, the reaction mixture was diluted with EtOAc and washed with water several times. The organic layer was dried with Na_2SO_4, filtered, and evaporated to dryness. The crude product was purified by column chromatography; the main fraction was collected and evaporated to dryness.

2-Bromo-8-pentafluorophenyl-1,3,5,7-tetramethyl-4,4-difluoro-4-bora-3a,4a-diaza-*s*-indacene (**205**):

BODIPY **205** was prepared according to the general synthetic procedure. BODIPY **65** (200 mg, 0.48 mmol) was dissolved in DCM and NBS (86 mg, 0.48 mmol) was added. After column purification

(chromatography, silica gel, EtOAc/*n*-hexane = 1/9, v/v); BODIPY **205** was obtained as an orange solid (140 mg, 0.23 mmol, 54%).

^{1}H NMR (500 MHz, THF-d_8): δ (ppm) = 1.67 (s, 3H, Me), 1.68 (s, 3H, Me), 2.55 (s, 6H, Me), 6.26 (s, 2H, $H_{pyrrole}$).

^{13}C NMR (126 MHz, THF-d_8): δ (ppm) = 12.9 (Me), 13.8 (Me), 13.9 (Me), 15.1 (Me), 109.9–110.2 (m, Ar-C_{ipso}), 111.96 (C_{Br}), 123.98 (Ar-C_{para}), 124.5 ($CH_{pyrrole}$), 130.0 ($C_{pyrrole}$), 133.2 ($C_{pyrrole}$), 138.0 ($C_{pyrrole}$), 145.2 ($C_{pyrrole}$), 154.1 ($C_{pyrrole}$), 162.3 ($C_{pyrrole}$).

^{19}F NMR (376 MHz, THF-d_8): δ (ppm) = -141.77 (d, J = 21.1 Hz, 2F, CF_{meta}), -146.27 – -146.52 (m_C, 2F, BF_2), -152.19 (t, J = 20.8 Hz, 1F, CF_{para}), -161.29 (t, J = 20.9 Hz, 2F, CF_{ortho}).

HRMS (ESI-TOF, MeOH): *m/z* calcd. for $C_{19}H_{14}BBrF_7N_2^+$ $[M+H]^+$: 493.0316, found: 493.0347, *m/z* calcd. for $C_{19}H_{13}BBrF_7N_2Na^+$ $[M+Na]^+$: 515.0136, found: 515.0166, *m/z* calcd. for $C_{19}H_{13}BBrF_7N_2K^+$ $[M+K]^+$: 530.9875, found: 530.9906, *m/z* calcd. for $C_{38}H_{26}B_2Br_2F_{14}N_4Na^+$ $[2M+Na]^+$: 1009.0359, found: 1009.0406

IR (ATR): $\tilde{\nu}$ (cm^{-1}) = 2981 and 2928 [ν(Me)], 1656 [ν(C=N), *ν*(C=C)], 1497 [*δ*(Me)], 1184 and 1091 [ν(BF), *ν*(CBr)].

UV/vis (DCM): λ_{max} (nm) [log (ε/L mol^{-1} cm^{-1})] = 532 [4.78].

Fluorescence (DCM): λ_{max} (nm) = 550 at $\lambda_{Excitation}$ (nm) = 520.

M.P. (°C): 197-200.

2-Bromo-8-[4-(*N*-butylamino)-2,3,5,6-tetrafluoophenyl]-1,3,5,7-tetramethyl-4,4-difluoro-4-bora-3a,4a-diaza-*s*-indacene (**206**):

BODIPY **206** was prepared according to the general synthetic procedure. BODIPY **67** (150 mg, 0.32 mmol) was dissolved in DCM and NBS (57 mg, 0.32 mmol) was added. After column purification (chromatography, silica gel, EtOAc/*n*-hexane = 1/9, v/v); BODIPY **206** was obtained as an orange solid (134 mg, 0,25 mmol, 76%).

^{1}H NMR (500 MHz, THF-d_8): δ (ppm) = 0.96 (t, J = 7.4 Hz, 3H, Me), 1.39–1.45 (m, 2H, CH_2), 1.61–1.66 (m, 2H, CH_2), 1.73 (s, 6H, Me), 2.53 (s, 6H, Me), 3.45–3.48 (m, 2H, CH_2), 5.72 (br s, 1H, NH), 6.20 (s, 2H, $H_{pyrrole}$).

^{13}C NMR (126 MHz, THF-d_8): δ (ppm) = 12.8 (Me), 13.7 (Me), 13.96 (Me_{butyl}), 14.3 (Me), 15.0 (Me), 99.2 (Ar-C_{ipso}), 111.3–114.0 (m, C_{Br}), 121.1 (C_{meso}), 123.9 ($CH_{pyrrole}$), 126.9 (Ar-C_{para}), 131.0 ($C_{pyrrole}$), 134.1 ($C_{pyrrole}$), 138.1 ($C_{pyrrole}$), 145.3 ($C_{pyrrole}$), 152.95 ($C_{pyrrole}$), 161.2 ($C_{pyrrole}$).

^{19}F NMR (376 MHz, THF-d_8): δ (ppm) = -145.67 – -145.75 (m, 2F, CF_{meta}), -146.43 – -146.60 (m_C, 2F, BF_2), -161.32 (d, J = 16.3 Hz, 2F, CF_{ortho}).

HRMS (ESI-TOF, DCM/MeOH): *m/z* calcd. for $C_{23}H_{23}BBrF_5N_3^+$ [M-F]$^+$: 526.1083, found: 526.1085, *m/z* calcd. for $C_{23}H_{24}BBrF_6N_3^+$ [M+H]$^+$: 546.1145, found: 546.1152, *m/z* calcd. for $C_{46}H_{46}B_2Br_2F_{12}N_6Na^+$ [2M+H]$^+$: 1115.2017, found: 1115.2020.

IR (ATR): $\tilde{\nu}$ (cm^{-1}) = 3408 [*ν*(NH)], 2959 and 2929 [*ν*(CH_2), *ν*(Me)], 2872 [*ν*(CH)], 1656 [*ν*(C=N), *ν*(C=C)], 1183 and 1119 [*ν*(BF), *ν*(CBr))].

UV/vis (DCM): λ_{max} (nm) [log (ε/L mol^{-1} cm^{-1})] = 387 [3.70], 528 [4.68].

Fluorescence (DCM): λ_{max} (nm) = 545 at $\lambda_{Excitation}$ (nm) = 370, 510.

M.P. (°C): 101-104.

2-Bromo-8-[4-(*N*-2-hydroxyethylamino)-2,3,5,6-tetraflourophenyl]-1,3,5,7-tetramethyl-4,4-difluoro-4-bora-3a,4a-diaza-*s*-indacene (**207**):

BODIPY **207** was prepared according to the general synthetic procedure. BODIPY **69** (147 mg, 0.32 mmol) was dissolved in DCM and NBS (57 mg, 0.32 mmol) was added. The mixture was stirred for 2 h. After purification (column chromatography, silica gel, EtOAc/*n*-hexane = 1/1, v/v); BODIPY **207** was obtained as an orange solid (144 mg, 0.21 mmol, 83%).

^{1}H NMR (500 MHz, THF-d$_8$): δ (ppm) 1.73 (s, 6H, Me), 2.53 (s, 6H, Me), 3.53–3.57 (m, 2H, CH_2), 3.68–3.71 (m, 2H, CH_2), 4.03 (t, *J* = 5.2 Hz, 1H, OH), 5.65 (br s, 1H, NH), 6.21 (s, 2H, $H_{pyrrole}$).

^{13}C NMR (126 MHz, THF-d$_8$): δ (ppm) = 12.9 (Me), 13.7 (Me), 14.0 (Me), 15.3 (Me), 48.7 (CH_2), 62.2 (CH_2), 99.2–99.6 (m, Ar-C_{ipso}), 111.3 (m, C_{Br}), 123.9 ($CH_{pyrrole}$), 126.9 (Ar-C_{para}), 130.96 ($C_{pyrrole}$), 134.1 ($C_{pyrrole}$), 138.1 ($C_{pyrrole}$), 145.4 ($C_{pyrrole}$), 152.95 ($C_{pyrrole}$), 161.2 ($C_{pyrrole}$).

^{19}F NMR (376 MHz, THF-d$_8$): δ (ppm) = -145.76 – -145.87 (m, 2F, CF_{meta}), -146.38 – -146.63 (m_C, 2F, BF_2), -160.87 (d, *J* = 16.3 Hz, 2F, CF_{ortho}).

HRMS (ESI-TOF, DCM/MeOH): *m/z* calcd. for $C_{21}H_{19}BBrF_6N_3ONa^+$ [M+Na]$^+$: 556.0601, found: 556.0616, *m/z* calcd. for $C_{21}H_{19}BBrF_6N_3OK^+$ [M+K]$^+$: 574.0340, found: 574.0388.

IR (ATR): $\tilde{\nu}$ (cm^{-1}) = 3403 [*ν*(OH), *ν*(NH)], 2957 and 2929 [*ν*(CH_2), *ν*(Me)], 1656 [*ν*(C=N), *ν*(C=C)], 1496 [δ(CH_2), δ(Me)], 1184 and 1119 [*ν*(BF), *ν*(CBr)].

UV/vis (DCM): λ_{max} (nm) [log (ε/L mol^{-1} cm^{-1})] = 382 [4.00], 528 [4.84].

Fluorescence (DCM): λ_{max} (nm) = 544 at $\lambda_{Excitation}$ (nm) = 370, 510.

M.P. (°C): 148-150.

Attempted synthesis of 2-bromo-8-[4-fluor-3-nitrophenyl]-1,3,5,7-tetramethyl-4,4-difluoro-4-bora-3a,4a-diaza-*s*-indacene (**208**):

The reaction was carried out according to the general synthetic procedure. BODIPY **66** (150 mg, 0.39 mmol) was dissolved in DCM and NBS (69 mg, 0.39 mmol) was added. After column purification

(chromatography, silica gel, EtOAc/*n*-hexane = 1/4, v/v) an orange solid (98 mg) was obtained. However, evidence for the formation of mixture of BODIPYs was found in the NMR spectra.

2-Bromo-8-[4-(*N*-butylamino)-3-nitrophenyl]-1,3,5,7-tetramethyl-4,4-difluoro-4-bora-3a,4a-diaza-*s*-indacene (**209**):

BODIPY **209** was prepared according to the general synthetic procedure. BODIPY **71** (118 mg, 0.27 mmol) was dissolved in DCM and NBS (47 mg, 0.27 mmol) was added. After column purification (chromatography, silica gel, EtOAc/*n*-hexane = 1/9, v/v); BODIPY **209** was obtained as an orange solid (41 mg, 78 µmol, 29%).

^{1}H NMR (500 MHz, THF-d_8): δ (ppm) = 1.01 (t, *J* = 7.4 Hz, 3H, Me_{Butyl}), 1.47–1.55 (m, 2H, CH_2), 1.57 (s, 3H, Me), 1.59 (s, 3H, Me), 1.74–1.79 (m, 2H, CH_2), 2.52 (s, 3H, Me), 2.53 (s, 3H, Me), 3.42–3.46 (m, 2H, CH_2), 6.14 (s, 1H, $H_{Pyrrole}$), 7.24 (d, *J* = 8.8 Hz, 1H, Ar-H_{meta}), 7.43 (dd, *J* = 8.8, 2.1 Hz, 1H, Ar-H_{ortho}), 8.16 (d, *J* = 2.1 Hz, 1H, Ar-H_{ortho}), 8.22 (t, *J* = 4.7 Hz, 1H, NH).

^{13}C NMR (126 MHz, THF-d_8): δ (ppm) = 13.6 (Me), 14.3 (Me_{Butyl}), 14.5 (Me), 14.9 (Me), 15.7 (Me), 21.3 (CH_2), 32.1 (CH_2), 43.8 (CH_2), 110.8–110.9 (m, C_{Br}), 116.3 (Ar-C_{meta}), 121.7*, 123.3 ($CH_{Pyrrole}$), 127.8 (Ar-C_{ortho}), 131.2 ($C_{Pyrrole}$), 133.1* 133.8 ($C_{Pyrrole}$), 136.8 (Ar-C_{ortho}), 138.7 ($C_{Pyrrole}$), 141.5 ($C_{Pyrrole}$), 145.9 (C_{meso}), 146.8 (Ar-C_{para}), 151.9 ($C_{Pyrrole}$), 154.7 ($C_{Pyrrole}$). *These signals could not be assigned exactly to corresponding carbon atoms. They belong to the Ar-C_{ipso} and the Ar-C_{nitro} of the aryl residue.

^{19}F NMR (376 MHz, THF-d_8): δ (ppm) = -146.53 – -146.77 (m_c, 2F, BF_2).

HRMS (ESI-TOF, MeOH): *m/z* calcd. for $C_{23}H_{26}BBrF_2N_4O_2Na^+$ $[M+Na]^+$: 541.1192, found: 541.1222, *m/z* calcd. for $C_{23}H_{26}BBrF_2N_4O_2K^+$ $[M+K]^+$: 559.0911, found: 559.0948 *m/z* calcd. for $C_{46}H_{52}B_2Br_2F_4N_8O_4Na^+$ $[2M+Na]^+$: 1061.2472, found: 1061.2518.

IR (ATR): $\tilde{\nu}$ (cm^{-1}) = 3381 [ν(NH)], 2958 and 2928 [ν(CH_2), ν(Me)], 2866 [ν(CH)], 1628 [ν(C=N), ν(C=C)], 1541 [ν_{as}(NO_2)], 1354 [ν_{sym}(NO_2)], 1186 and 1087 [ν(BF), ν(CBr)].

UV/vis (DCM): λ_{max} (nm) [log (ε/L mol^{-1} cm^{-1})] = 395 [4.09], 516 [4.88].

Fluorescence (DCM): λ_{max} (nm) = 534 at $\lambda_{Excitation}$ (nm) = 380, 500.

M.P. (°C): 140-142.

2-Bromo-8-[4-(*N*-2-hydroxyethylamino)-3-nitrophenyl]-1,3,5,7-tetramethyl-4,4-difluoro-4-bora-3a,4a-diaza-*s*-indacene (**210**):

BODIPY **210** was prepared according to the general synthetic procedure. BODIPY **73** (120 mg, 0.28 mmol) was dissolved in DCM and NBS (50 mg, 0.28 mmol) was added. After purification (column chromatography, silica gel, EtOAc/*n*-hexane = 1/1, v/v); BODIPY **210** was obtained as an orange solid (69 mg, 0.14 mmol, 49%).

^{1}H NMR (500 MHz, THF-d_8): δ (ppm) = 1.57 (s, 3H, Me), 1.59 (s, 3H, Me), 2.52 (s, 3H, Me), 2.53 (s, 3H, Me), 3.49–3.52 (m, 2H, CH_2), 3.81–3.84 (m, 2H, CH_2), 4.26 (t, *J* = 5.0 Hz, 1H, OH), 6.14 (s, 1H, $H_{Pyrrole}$), 7.27 (d, *J* = 8.8 Hz, 1H, Ar-H_{meta}), 7.42 (dd, *J* = 8.8, 2.1 Hz, 1H, Ar-H_{ortho}), 8.16 (d, *J* = 2.1 Hz, 1H, Ar-H_{ortho}), 8.45 (t, *J* = 4.9 Hz, 1H, NH).

^{13}C NMR (126 MHz, THF-d_8): δ (ppm) = 13.6 (Me), 14.5 (Me), 14.9 (Me), 15.7 (Me), 46.4 (CH_2), 60.9 (CH_2), 110.8 (C_{Br}), 116.3 (Ar-C_{meta}), 121.7*, 123.3 ($CH_{Pyrrole}$), 127.7 (Ar-C_{ortho}), 131.8 ($C_{Pyrrole}$), 133.3* 133.8 ($C_{Pyrrole}$), 136.7 (Ar-C_{ortho}), 138.7 ($C_{Pyrrole}$), 141.5 ($C_{Pyrrole}$), 145.9 (C_{meso}), 145.98 (Ar-C_{para}), 151.8 ($C_{Pyrrole}$), 159.7 ($C_{Pyrrole}$). *These signals could not be assigned exactly to corresponding carbon atoms. They belong to the Ar-C_{ipso} and the Ar-C_{nitro} of the aryl residue.

^{19}F NMR (376 MHz, THF-d_8): δ (ppm) = -146.32 – -146.94 (m_c, 2F, BF_2).

HRMS (ESI-TOF, MeOH): *m/z* calcd. for $C_{21}H_{22}BBrF_2N_4O_3Na^+$ $[M+Na]^+$: 529.0829, found: 529.0820, *m/z* calcd. for $C_{21}H_{22}BBrF_2N_4O_3K^+$ $[M+K]^+$: 547.0548, found: 547.0554 *m/z* calcd. for $C_{42}H_{44}B_2Br_2F_4N_8O_6Na^+$ $[2M+Na]^+$: 1037.1745, found: 1037.1703.

IR (ATR): $\tilde{\nu}$ (cm^{-1}) = 3374 [ν(OH), ν(NH)], 2925 [ν(CH_2), ν(Me)], 1627 [ν(C=N), ν(C=C)], 1524 [ν_{as}(NO_2)], 1460 [δ(CH_2), δ(Me)], 1352 [ν_{sym}(NO_2)], 1185 and 1082 [ν(BF), ν(CBr)].

UV/vis (DCM): λ_{max} (nm) [log (ε/L mol^{-1} cm^{-1})] = 395 [4.12], 516 [4.88].

Fluorescence (DCM): λ_{max} (nm) = 534 at $\lambda_{Excitation}$ (nm) = 380, 500.

M.P. (°C): 196-204.

6.4 Preparation of BODIPY-cyclen derivatives

*6.4.1 1,4,7-Tris(tert-butoxycarbonyl)-10-(prop-2-ynyl)-1,4,7,10-tetraazacyclododecane (**213**):*

1,4,7-Tris(*tert*-butoxycarbonyl)-1,4,7,10-tetraazacyclododecane **212** (500 mg, 1.06 mmol, 1 equiv.) and potassium carbonate (585 mg, 4.23 mmol, 4 equiv.) were dissolved in 10 mL of MeCN. Afterwards, propargyl bromide (1.38 mL, 1.06 mmol, 1 equiv.) was added and stirred for 16 h at 100°C. After the indicated time, the reaction mixture was cool down to rt. The suspension was filtered and washed with MeCN. The filtrate was evaporated to dryness and purified by column chromatography; the main fraction was collected and evaporated to dryness. After column chromatography (silica gel, EtOAc/*n*-hexane = 7/3, v/v); product **213** was obtained as a colorless solid (442 mg, 82%).

^{1}H NMR (400 MHz, $CDCl_3$): δ (ppm) = 1.44–1.49 (m, 27H, Me), 2.17 (s, 1H, CH), 2.77 (br s, 4H, $CH_{2,\ cyclen}$), 3.29–3.51 (m, 14H, $CH_{2,\ cyclen}$).

HRMS (ESI-TOF, DCM/MeOH): *m/z* calcd. for $C_{26}H_{47}N_4O_6^+$ $[M+H]^+$: 511.3490, found: 511.3528, *m/z* calcd. for $C_{26}H_{46}N_4O_6Na^+$ $[M+Na]^+$: 533.3310, found: 533.3352.

The spectroscopic data were in accordance with the literature.[110c]

*6.4.2 Preparation of the BODIPY-cyclen derivative via copper(I)-mediated cycloaddition (**214**):*

Under argon atmosphere, compound **213** (1 equiv.), BODIPY **153** (0.66 – 1 equiv.), $CuSO_4 \cdot 5H_2O$ (0.1 – 1 equiv.), and sodium ascorbate (4 – 6 equiv.) were dissolved in 10 mL of DMSO. The mixture was stirred for 20 min at rt. After the indicated time, the reaction mixture was diluted with 10 mL of water and extracted with DCM several times. The combined organic layers were dried with Na_2SO_4, filtered, and evaporated to dryness. The crude product was purified by column chromatography (EtOAc/*n*-hexane = 1/1, v/v) and recrystallization (DCM/*n*-pentane).

Variant A: 10 mol% of $CuSO_4$

Compound **213** (200 mg, 0.39 mmol), BODIPY-N_3 (150 mg, 0.39 mmol), $CuSO_4 \cdot 5H_2O$ (10 mg, 39 µmol), and sodium ascorbate (234 mg, 1.18 mmol) were dissolved in DMSO. After column purification, product **214** was obtained as an orange solid (8 mg, 9 µmol, 2 %). In addition, the corresponding 4-amino-2,3,5,6-tetrafluorophenyl-substituted BODIPY were obtained in larger quantities (110 mg, 0.31 mmol, 79%).

Variant B: 50 mol% of $CuSO_4$

Compound **213** (89 mg, 0.17 mmol), BODIPY-N_3 (100 mg, 0.26 mmol), $CuSO_4 \cdot 5H_2O$ (22 mg, 0.09 mmol), and sodium ascorbate (207 mg, 1.05 mmol) were dissolved in DMSO. After column purification, product **214** was obtained as an orange solid (85 mg, 95 µmol, 55 %). The corresponding 4-amino-2,3,5,6-tetrafluorophenyl-substituted BODIPY were obtained in lower quantities (31 mg, 9 µmol, 38%).

Variant C: 1 equiv. of $CuSO_4$

Compound **213** (89 mg, 0.17 mmol), BODIPY-N_3 (100 mg, 0.26 mmol), $CuSO_4 \cdot 5H_2O$ (44 mg, 0.17 mmol), and sodium ascorbate (207 mg, 1.05 mmol) were dissolved in DMSO. After column purification, product **214** was obtained as an orange solid (101 mg, 0.11 mmol, 65 %). The corresponding 4-amino-2,3,5,6-tetrafluorophenyl-substituted BODIPY were obtained in traces.

^{1}H NMR (500 MHz, $CDCl_3$): δ (ppm) = 1.41–1.50 (m, 27 H, Me), 2.73 (br s, 2H, $CH_{2,cyclen}$), 2.80 (br s, 2H, $CH_{2,cyclen}$), 3.66–3.44 (m, 8H, $CH_{2,cyclen}$), 3.58 (br s, 4H, $CH_{2,cyclen}$), 4.07 (s, 2H, CH_2), 6.61 (d, *J* = 4.2 Hz, 2H, $H_{pyrrole}$), 6.87 (d, *J* = 4.2 Hz, 2H, $H_{pyrrole}$), 7.92 (s, 1H, CH), 8.01 (s, 2H, $H_{pyrrole}$).

^{13}C NMR (151 MHz, $CDCl_3$): δ (ppm) = 28.6 (Me), 28.9 (Me), 48.1 ($CH_{2,cyclen}$), 50.1 ($CH_{2,cyclen}$), 53.7 ($CH_{2,cyclen}$), 54.8 ($CH_{2,cyclen}$), 54.7 (CH_2), 79.5 (-**C**$(Me)_3$), 79.9 (-**C**$(Me)_3$), 120.2 ($C_{pyrrole}$), 125.4 (C_{meso}), 128.9 (CH), 130.5 ($C_{pyrrole}$), 134.7 ($C_{pyrrole}$), 147.2 ($C_{pyrrole}$).

^{19}F NMR (376 MHz, $CDCl_3$): δ (ppm) =-134.71 – -134.80 (m, 2F, CF_{meta}), -144.10 (dd, *J* = 21.8, 10.1 Hz, 2F, CF_{ortho}), -144.60 – -144.82 (m_C, 2F, BF_2).

HRMS (ESI-TOF, MeOH): *m/z* calcd. for $C_{41}H_{52}BF_6N_9O_6Na^+$ $[M+Na]^+$: 914.3930, found: 914.3952, *m/z* calcd. for $C_{41}H_{52}BF_6N_9O_6K^+$ $[M+K]^+$: 930.3669, found: 930.3677.

IR (ATR): $\tilde{\nu}$ (cm^{-1}) = 3111 [ν(Ar-H)], 2975 and 2931 [$\nu(CH_2)$, ν(CH)], 1678 [ν(C=N), ν(C=C), ν(R-O-CO-NR_2),], 1458 [$\delta(CH_2)$, δ(CH)], 1389 [ν(-$C(Me)_3$)], 1079 [ν(BF)].

UV/vis (MeOH): λ_{max} (nm) [log (ε/L mol^{-1} cm^{-1})] = 520 [4.50].

Fluorescence (MeOH): λ_{max} (nm) = 500 at $\lambda_{Excitation}$ (nm) = 544.

M.P. (°C): 125-130.

*6.4.3 Cleavage of the tert-butyloxycarbonyl groups (**215**):*

Compound **214** (90 mg, 0.10 mmol, 1 equiv.) and trifluoroacetic acid (0.26 mL, 3.36 mmol, 34 equiv.) were dissolved in 4 mL of DCM. The mixture was stirred for 16h at rt. After the indicated time, the reaction mixture was diluted with EtOAc and was washed with 5 mL of a saturated $NaHCO_3$ solution, then with 10 mL of a saturated NaCl-solution. The organic layer was dried with Na_2SO_4, filtered, and evaporated to dryness. The crude product was purified by recrystallization (DCM/*n*-hexane). The product **215** was obtained as a dark green solid (55 mg, 0.93 µmol, 92%)

^{1}H NMR (500 MHz, D_2O/acetic acid-d_4 = 4/1): δ (ppm) = 2.79 (br s, 6H, $CH_{2,cyclen}$), 3.00 (br s, 6H, $CH_{2,cyclen}$), 3.18 (br s, 2H, CH_2), 3.90 (br s, 4H, $CH_{2,cyclen}$), 6.70 (br s, 2H, $H_{pyrrole}$), 7.85–7.88 (m, 3H, $H_{pyrrole}$ + CH), 8.34 (br s, 2H, $H_{pyrrole}$).

^{19}F NMR (376 MHz, D_2O/acetic acid-d_4 = 4/1): δ (ppm) =-129.12 – -129.55 (m, 2F, CF_{meta}), -146.38 – -146.45 (m_C, 2F, BF_2). -150.55 (br s, 2F, CF_{ortho}),

The ^{13}C NMR spectrum did not allowed a meaningful interpretation.

HRMS (ESI-TOF, MeOH): *m/z* calcd. for $C_{26}H_{29}BF_6N_9^+$ $[M+H]^+$: 592.2538, found: 592.2543.

Evidence was found for an exchange of the fluorine atoms for methoxy or hydroxy groups.

Exchange of the fluorine atom for OMe: *m/z* calcd. for $C_{27}H_{32}BF_5N_9O^+$ $[M-F+MeOH]^+$: 604.2738, found: 604.2729, exchange of both fluorine atoms for OMe: *m/z* calcd. for $C_{28}H_{35}BF_4N_9O_2^+$ $[M+H]^+$: 616.2937, found: 616.2909.

Exchange of the fluorine atom for OH: *m/z* calcd. for $C_{26}H_{30}BF_5N_9O^+$ $[M-F+H_2O]^+$: 590.2571, found: 590.2581.

UV/vis (MeOH): λ_{max} (nm) [log (ε/L mol^{-1} cm^{-1})] = 515 [4.09].

Fluorescence (MeOH): λ_{max} (nm) = 500 at $\lambda_{Excitation}$ (nm) = 540.

M.P. (°C): >250.

*6.4.4 Preparation of the BODIPY-Cu(II)-cyclen derivative (**216**):*

Compound **215** (22 mg, 37 µmol, 1 equiv.) was dissolved in 5 mL of MeOH and was heated until a gently boil was observed. Then, $Cu(NO_3)_2$ (11 mg, 45 µmol, 1.2 equiv.; solved in 5 mL of MeOH) was added to the solution *via* the reflux condenser. The solution was heated to reflux for 6 h, afterwards, the mixture could cool down slowly. The mixture was filtered over a glass frit, the obtained solid was washed with

MeOH and was dried in the exicator. The filtrate was concentrated at the rotary evaporator, approximately to the half of the volume and stored at the refrigerator overnight (to increase the amount of the product). The resulting mixture was again filtered, washed, and the solid was dried. Finally, a dark blueish solid (14 mg, 20 µmol, 54%) was obtained.

A meaningful interpretation *via* NMR spectroscopy and ESI mass spectrometry was not possible, due to the low solubility. EI mass spectrometry provided a mass spectrum and evidence for fragments (m/z= 200 and 218) that could be associated to compound **216** was found.

EI-MS (rel. Int. %): m/z 68 (46), 118 (19), 130 (25), 168 (16), 180 (18), 200 (5) $[M - \cdot CH_2\text{-}NH\text{-}CH\text{-}CH_2]^{3+}$, 218 (9) $[M]^{3+}$, 458 (100), 624 (6).

7. References

[1] a) J. M. Berg, J. L. Tymoczko, G. J. Gatto, jr., L. Stryer, *Stryer Biochemie*, 8. Auflage, Springer-Verlag GmbH Deutschland, **2018**, 257-258; b) C. E. Valdez, Q. A. Smith, M. R. Nechay, A. N. Alexandrova, *Acc. Chem. Res.* **2014**, *47*, 3110-3117; c) K. A. McCall, C.-C. Huang, C. A. Fierke, *J. Nutr.* **2000**, *130*, 1437S-1446S; d) Y. Nicolet, B. R. Lemon, J. C. Fontecilla-Camps, *Trends Biochem. Sci.* **2000**, *25*, 138-143; e) J. L. Boer, S. B. Mulrooney, R. P. Hausinger, *Arch. Biochem. Biophys.* **2014**, *544*, 142-152; f) K. J. Waldron, N. J. Robinson, *Nat. Rev. Microbiol.* **2009**, *7*, 25-35; g) K. J. Waldron, J. C. Rutherford, D. Ford, N. J. Robinson, *Nature* **2009**, *460*, 823-830.

[2] a) F.-P. Montforts, B. Gerlach, F. Höper, *Chem. Rev.* **1994**, *94*, 327-347; b) D. V. Vavilin, W. F. J. Vermaas, *Physiol. Plant.* **2002**, *115*, 9-24; c) B. Meunier, S. P. de Visser, S. Shaik, *Chem. Rev.* **2004**, *104*, 3947-3980.

[3] R. W. Hay, chapter 5: Plant Metalloenzymes, *Plants and the Chemical Elements: Biochemistry, Uptake, Tolerance and Toxicity*, edited by E. Farago, VCH Verlagsgesellschaft: Weinheim Germany, **1994**, pp. 107-148.

[4] a) B. Shane, *Food Nutr. Bull. Suppl.* **2008**, *29*, S5-S16; b) J.-H. Martens, H. Barg., M. Warren, D. Jahn, *Appl. Microbiol. Biotechnol.* **2002**, *58*, 275-285.

[5] a) D. Mauzerall, *Phil. Trans. R. Soc. Lend. B.* **1976**, *273*, 287-294, R. Tanaka und A. Tanaka, *Annu. Rev. Plant Biol.* **2007**, *58*, 321-346.

[6] a) R. Goericke, *Limnol. Oceanogr.* **2002**, *47*, 290-295; b) H. Scheer, W. A. Svec, B. T. Cope, M. H. Studier, R. G. Scott, J. J. Katz, *J. Am. Chem. Soc.* **1974**, *96*, 3714-3716.

[7] a) G. Schwarz, R. R. Mendel, M. W. Ribbe, *Nature* **2009**, *460*, 839-847; b) R. R. Mendel, R. Hänsch, *J. Exp. Bot.* **2002**, *53*, 1689-1698; c) C. Kisker, H. Schindelin, D. C. Rees, *Annu. Rev. Biochem.* **1997**, *66*, 233-267.

[8] a) D. Niks, R. Hill, *Protein Sci.* **2019**, *28*, 111-122; b) J. L. Johnson, K. V. Rajagopalan, S. Mukund, M. W. W. Adams, *J. Biol. Chem.* **1993**, *268*, 4848-4852.

[9] a) P. J. Sadler, Z. Guo, *Pure & Appl. Chem.* **1998**, *70*, 863-871; b) S. M. Cohan, S. J. Lippert, *Prog. Nucleic. Acid. Res. Mol. Biol.* **2001**, *67*, 93-130; c) K. Barabas, R. Milner, D. Lurie, C. Adin, *Vet. Comp. Oncol.* **2008**, *6*, 1-18.

[10] I. Arany, R. L. Safirstein, *Semin. Nephro.* **2003**, *23*, 460-464.

[11] a) L. Galluzzi, L. Senovilla, I. Vitale, J. Michels, O. Keep, M. Castedo, K. Kroemer, *Oncogene* **2012**, *31*, 1869-1883; b) J. Zhou, Y. Kang, L. Chen, H. Wang, J. Liu, S. Zeng L., Yu, *Front. Pharmacol.* **2020**, *11*, 343.

[12] a) L. Galluzzi, I. Vitale, J. Michels, C. Brenner, G. Szabadkai, A. Harel-Bellan, M. Castedo. G. Kroemer, *Cell Death Dis.* **2014**, *5*, 1-18; b) L. R. Kelland, S. Y. Sharp, C. F. O'Neill, F. I. Raynaud, P. J. Beale, I. R. Judson, *J. Inorg. Biochem.* **1999**, *77*, 111-115.

[13] a) G. Gasser, *Chimia* **2015**, *69*, 442-446, b) G. Jaouen, A. Vessières, S. Top, Chem. Soc. Rev. **2015**, *44*, 8802-8817; c) D. Dive, C. Biot, *ChemMedChem* **2008**, *3*, 383-391.

[14] a) C. Roder, M. J. Thompson, *Drugs R&D* **2015**, *15*, 13-20; b) E. Erdogan, T. Lamark, M. Stallings-Mann, L. Jamieson, M. Pellechia, E. A. Thompson, T. Johansen, A. P. Fields, *J. Biol. Chem.* **2006**, *281*, 28450-28459.

[15] a) N. Cutillas, G. S. Yellol, C. de Haro, C. Vicente, V, Rodríguez, J. Ruiz, *Coord. Chem. Rev.* **2013**, *257*, 2784-2797; b) I. Ott, R. Gust, *Arch. Pharm. Chem. Life Sci.* **2007**, *340*, 117-126; c) U. Jungwirth, C. R. Kowol, B. K. Keppler, C. G. Hartinger, W. Berger, P. Heffeter, *Antioxid. Redox Signaling* **2011**, *15*, 1085-1127; d) S. K. Nandarwar, H. J. Kim, *ChemistrySelect* **2019**, *4*, 1706-1721.

[16] a) J. Li, L. Zeng, K. Xiong, T. W. Rees, C. Jin, W. Wu, Y. Chen, L. Ji, H. Chao, *Chem. Commun.* **2019**, *55*, 10972-10975; b) R. P. Paitandi, R. K. Gupta, R. S. Singh, G. Sharma, B. Koch, D. S. Pandey, *Eur. J. Med. Chem.* **2014**, *84*, 17-29; c) C. Mari, V. Pierroz, S. Ferrari, G. Gasser, *Chem. Sci.* **2015**, *6*, 2660-2686; d) C. Imberti, P. Zhang, H. Huang, P. J. Sadler, *Angew. Chem. Int. Ed.* **2020**, *59*, 61-73, *Angew. Chem.* **2020**, *132*, 61-73; e) W. H. Ang, P. J. Dyson, *Eur. J. Inorg. Chem.* **2006**, 4003-4018; f) C.-M. Che, F.-M. Siu, *Curr. Opin. Chem. Biol.* **2010**, *14*, 255-261; g) R. Guan, L. Xie, L. Ji, H. Chao, *Eur. J. Inorg. Chem.* **2020**, *42*, 3978-3986; h) A. Levina, A. Mitra, P. A. Lay, *Metallomics* **2009**, *1*, 458-470.

[17] a) S. Leijen, S. A. Burgers, P. Baas, M. Tibben, E. van Werkhoven, E. Alessio, G. Sava, J. H. Beijnen, J. H. M. Schallens, *Invest. New Drugs* **2015**, *33*, 201-214; b) C. G. Hartinger, M. A. Jakupec, S. Zorbas-Seifried, M. Groessi, A. Egger, W. Berger, H. Zorbas, P. J. Dyson, B. K. Keppler, *Chem. Biodiversity* **2008**, *5*, 2140-2155.

[18] a) A. R. Timerbaev, C. G. Hartinger, S. S. Aleksenko, B. K. Keppler, *Chem. Rev.* **2006**, *106*, 2224-2248; b) O. Mazuryk, K. Kurpiewska, K. Lewiński, G. Stochel, M. Brindell, *J. Inorg. Biochem.* **2012**, *116*, 11-18; c) W. Guo, W. Zheng, X. Li, Y. Zhao, S. Xiong, F. Wang, *Inorg. Chem.* **2013**, *52*, 5328-5338.

[19] H. Huang, S. Banerjee, P. J. Sadler, *ChemBioChem* **2018**, *19*, 1574-1589.

[20] A. Frei, *Antibiotics* **2020**, *9*, 90.

[21] a) L. Zaffiri, J. Gardner, L. H. Toledo-Pereyra, *J. Invest. Surg.* **2012**, *25*, 67-77; b) N. Lloyd, H. W. Morgan, B. K. Nicholson, R. S. Ronimus, *Angew. Chem. Int. Ed.* **2005**, *44*, 941-944.

[22] R. Sethi, R. K. Kesharwani, S. Haroon, J. D. Pandey, K. Misra, *Proc. Natl. Acad. Sci., India, Sect. A Phys. Sci.* **2013**, *83*, 97-103.

[23] a) M. S. Masoud, E. A. Ali, N. M. Nasr, *J. Chem. Pharm. Res.* **2015**, *7*, 64-90; b) A. S. Hassan, T. S. Hafez, *J. Appl. Pharm. Sci.* **2018**, *8*, 156-165; c) A. M. Malik, O. A. Dar, P. Gull, M. Y. Wani, A. A. Hashmi, *Med. Chem. Commun.* **2018**, *9*, 409-436; d) S. A. Patil, S. A. Patil, R Patil, R. S. Keri, S. Budagumoi, G. R. Balakrishna, M. Tacke, *Future Med. Chem.* **2015**, *7*, 1305-1333; e) C. S. Allardyce, P. J. Dyson, *Platinum Metals Rev*. **2001**, *45*, 62-69.

[24] a) F. Li, J. G. Collins, F. R. Kenne, *Chem. Soc. Rev.* **2015**, *44*, 2529-2542; b) Y. Yang, G. Liao, C. Fu, *Polymers* **2018**, *10*, 650; c) J. M. Hearn, G. M. Hughes, I. Romero-Canelón, A. F. Munro, B. Rubio-Ruiz, Z. Liu, N. O Carragher, P. J. Sadler, *Metallomics* **2018**, *10*, 93–107; d) F. Chen, J. Moat, D, McFeely, G. Clarkson, I. J. Hands-Portman, J. P. Furner-Pardoe, F. Harrison, C. G. Dowson, P. J. Sadler, *J. Med. Chem.* **2018**, *61*, 7330-7344.

[25] a) O. J. Stacey, S. J. A. Pope, *RSC Adv.* **2013**, *3*, 25550-25564; b) S. Monro, K. L. Colón, H. Yin, J. Roque III, P. Konda, S. Gujar, R. P. Thummel, L. Lilge, C. G. Cameron, S. A. McFarland, *Chem. Rev.* **2019**, *119*, 797-828; c) L. K. McKinzie, I. V. Sazanovich, E. Baggaley, M. Bonneau, V. Guerchais, J. A. G. Williams, J. A. Weinstein, H. E. Bryant, *Chem. Eur. J.* **2017**, *23*, 234-238; d) H. Abrahamse, M. R. Hamblin, *Biochem. J.* **2016**, *473*, 347-364; e) S. A. McFarland, A. Mandel, R. Dumoulin-White, G. Gasser, *Curr. Opin. Chem. Biol.* **2020**, *56*, 23-27.

[26] a) Z. Zhou, Z.-R. Lu, *WIREs Nanomed. Nanobiotechnol.* **2013**, *5*, 1-18; b) S. Aime, P. Caravan, *J. Magn. Reson. Imaging* **2009**, *30*, 1259-1267; c) C. Bolzati, F. Refosco, P. Ruzza, *Curr. Med. Chem.* **2010**, *17*, 2656-2683; d) C. Bolzati, D. Carta, N. Salvaese, F. Refosco, *Anti-Cancer Agents Med. Chem.* **2012**, *12*, 428-461; e) Z. Liu, Y. Yan, D. Liu, F. Wang, X. Chen, *Bioconjugate Chem.* **2009**, *20*, 1016-1025.

[27] a) N. Boens, V. Leen, W. Dahaen, *Chem. Soc. Rev.* **2012**, *41*, 1130-1172; b) B. Brizet, V. Goncalves, C. Bernhard, P. D. Harvey, F. Denat, C. Goze, *Chem. Eur. J.* **2014**, *20*, 12933-12944; c) T. Kowada, H. Maeda, K. Kikuchi, *Chem. Soc. Rev.* **2015**, *44*, 4953-4972.

[28] a) D. E. De Vos, M. Dams, B. F. Sels, P. A. Jacobs, *Chem. Rev.* **2002**, *102*, 3615-3640; b) W. Shi, C. Liu, A. Lei, *Chem. Soc. Rev.* **2011**, *40*, 2761-2776.

[29] a) M. Ohff, A. Ohff, M. E. van der Boom, D. Milstein, *J. Am. Chem. Soc.* **1997**, *119*, 11687-11688; b) M. Ohff, A. Ohff, D. Milstein, *Chem. Commun.* **1999**, 357-358; c) R. B. Bedford, S. M. Draper, P- N. Scully, S. L. Welch, *New J. Chem.* **2000**, *24*, 745-747.

[30] a) J. Jarupatrakorn, T. D. Tilley, *J. Am. Chem. Soc.* **2002**, *124*, 8380-8388; b) D. Hoegaerts, B. F. Sels, D. E. De Vos, F. Verpoort, P. A. Jacobs, *Catal. Today* **2000**, *60,* 209-218; c) T. S. Reger, K. D. Janda, *J. Am. Chem. Soc.* **2000**, *122*, 6929-6934; d) J.-L. Zhang, C.-M. Che, *Org. Lett.* **2002**, *4*, 1911-1914.

[31] a) M. P. Doyle, B. D. Brandes, A. P. Kazala, R. J. Pieters, M. B. Jarstfer, L. M. Watkins, C. T. Eagle, Tetrahedron Lett., 1990, 31, 6613-6616; b) W. Sun, C.-G. Xia, H.-W. Wang, *New J. Chem.* **2002**, *26*, 755-758; c) J. M. Fraile, J. I. Garćia, J. A. Mayoral, T. Tarnai, *Tetrahedron: Asymmetry* **1998**, *9*, 3997-4008.

[32] a) R. R. Schrock, C. Czekelius, *Adv. Synth. Catal.* **2007**, *349*, 55-77; b) A. Fürster, M. Liebl, C. W. Lehmann, M. Picquet, R. Kunz, C. Bruneau, D. Touchard, P. H. Dixneuf, *Chem. Eur. J.* **2000**, *6*, 1847-1857; c) M. Scholl, T. M. Trnak, J. P. Morgan, R. H. Grupps, *Tetrahedron Lett.* **1999**, *40*, 2247-2250; d) S. H. Pine, G. S. Shen, H. Hoang, *Synthesis* **1991**, *2*, 165-166.

[33] a) K. A. Burdett, L. D. Harris, P. Margl, B. R. Maughon, T. Mokhtar-Zadeh, P. C. Saucier, E. P. Wasserman, *Organometallics* **2004**, *23*, 2027-2047; b) F. N. Tebbe, G. W. Parshall, D. W. Ovenall, J*. Am. Chem. Soc.* **1979**, *101*, 17, 5074-5075.

[34] a) M. K. Nazeeruddin, E. Baranoff, M. Grätzel, *Sol. Energy* **2011**, *85*, 1172-1178; b) C.-Y.Chen, H.-C. Lu, C.-G. Wu, J.-G. Chen, K.-C. Ho, *Adv. Funct. Mater.* **2007**, *17*, 29-36; c) M. K. Nazeeruddin, M. Grätzel, *Struct. Bond.* **2007**, *123*, 113-175; d) B. Bozic-Weber, E. C. Canstable, C. E. Housecroft, *Coord. Chem. Rev.* **2013**, *257*, 3089-3106, e) D. Kumaresan, R. P. Thummel, T. Bura, G. Ulrich, R. Ziessel, *Chem. Eur. J.* **2009**, *15*, 6335-6339; f) S. Erten-Ela, M. D. Yilmaz, B. Lcli, Y. Dede, S, Lcli, W. U. Akkaya, *Org. Lett.* **2008**, 10, 3299-3302.

[35] a) D.-L. Ma, V. P.-Y. Ma, D. S.-H. Chan, K.-H. Leung, H.-Z. He, C.-H. Leung, *Coord. Chem. Rev.* **2012**, *256*, 3087-3113; b) C. W. Rogers, M. O. Wolf, *Coord. Chem. Rev.* **2002**, *233-234*, 341-350.

[36] a) A. Zampetti, A, Minotto, B. M. Squeo, V. G. Gregoriou, S. Allard, U. Scherf, C. L. Chochos, F. Cacialli, *Sci. Rep.* **2017**, article number: 1611; b) S. Baysec, A. Minotto, P. Klein, S. Poddi, A. Zampetti, S. Allard, F, Cocialli, U. Scherf, *Sci. China: Chemistry* **2018**, *61*, 932-939.

[37] a) R. J. Kuppler, D. J. Timmons, Q.-R. Fang, J.-R. Li, T. A. Makal, M. D. Young, D. Yuan, D, Zhao, W. Zhuang, H.-C. Zhou, *Coord. Chem. Rev.* **2009**, *253*, 3042-3066; b) H.-C. Zhou, J. R. Long, O. M. Yaghi, *Chem. Rev.* **2012**, *112*, 673-674.

[38] a) A. Ackroyd, C. Keity, N. Brown, M. Reed, *Photochem. Photobiol.* **2001**, *74*, 656-669; b) D. E. J. G. Dolmans, D. Fukumura, R. K. Jain, *Nat. Rev. Cancer* **2003**, *3*, 380-387; c) D. Kessel, *J. Clin. Med.* **2019**, *8*, 1581.

[39] a) K. Kalka, H. Merh, H. Muktar, *J. Am. Acad. Dermatol.* **2000**, *42*, 389-413; b) N. C. Zeitouni, A. R. Oseroff, S. Shieh, *Mol. Immunol.* **2003**, *39*, 1133-1136; c) H. Huang, *Technol. Cancer Res. Treat.* **2005**, *4*, 283-293; d) C. M. Moore, D: Pensde, M. Emberton, *Nat. Clin. Pract. Urol.* **2009**, *6*, 18-30; e) S. B. Brown, E. A. Brown, I. Walker, *Lancet Oncol.* **2004**, *5*, 497-508.

[40} a) F. Cieplik, D. Deng, W. Crielaard, *Crit. Rev. Microbiol.* **2018**, *44*, 571-589; b) M. Wainwright, *Int. J. Antimicrob. Agents* **2003**, 510-520; c) T. Maisch, R. M. Szeimies, N. Lehn, C. Abels, *Hautarzt* **2002**, *56*, 1048-1055; d) L. Costa, M. A. F. Faustino, M. G. P. M. S. Neves, A. Cunha, A. Almeida, *Viruses* **2012**, *4*, 1034-1074; e) A. Wiehe, J. M. O'Brien, M. O. Senge, *Photochem. Photobiol. Sci.* **2019**, *18*, 2565-2612; f) R. F. Donnely, P. A. McCarron, M. M. Tunney, *Microbiol. Res.* **2008**, *163*, 1-12.

[41] a) F. H. Sakamoto, L. Torezan, R. R. Anderson, *J. Am. Acad. Dermatol.* **2010**, *63*, 195-211; b) C. Queirós, P. M. Garrido, J. M. Silva, P. Filipe, *Dermatologic Therapy.* **2020**, *33*, e13997.

[42] K. Page, M. Wilson, I. P. Parkin, *J. Mater. Chem.* **2009**, *19*, 3819-3831.

[43] a) P. Agostinis, K. Berg, K. A. Cengel, T. H. Foster, A. W. Girotti, S. O. Gollnick, S. M. Hahn, M. R. Hamblin, A. Juzeniene, D. Kessel, M. Korbelik, J. Moan, P. Mroz, D. Nowis, J. Piette, B. C. Wilson, J. Golab MD, *CA: Cancer. J. Clin.* **2011**, *61*, 250-281; b) A. P. Castano, P. Mroz, M. R. Hamblin, *Nat. Rev. Cancer* **2006**, *6*, 535-545; c) Á. Juarranz, P. Jaén, F. Sanz-Rodríuez, J. Cuevas, S. González, *Clin. Transl. Oncol.* **2008**, *10*, 148-154; d) A. P. Castano, T. N. Demidova, M. R. Hamblin, Photodiagn. Photodyn. Ther. 2004, 1, 279-293; e) C. A. Robertson, D. H. Evans, H. Abrahamse, *J. Photochem. Photobiol., B* **2009**, *96*, 1-8.

[44] T. Maisch, J. Photochem. Photobiol. B, 2015, 150, 2-10.

[45] a) S. Hatz, J. D. C. Lambert, P. R. Ogilby, *Photochem. Photobiol. Sci.* **2007**, *6*, 1106-1116; b) S. Hackbarth, J. Schlothauer, A. Preuß, B. Röder, *J. Photochem. Photobiol., B* **2010**, *98*, 173-179; c) M. C. DeRosa, R. J. Crutchley, *Coord. Chem. Rev.* **2002**, *233-234*, 351-371; d) E. Skovsen, J. W. Snyder, J. D. C. Lambert, P. C. Ogilby, *J. Phys. Chem. B* **2005**, *109*, 8570-8573.

[46] A. B. Ormond, H. S. Freeman, *Materials* **2013**, *6*, 817-840.

[47] a) A. F. Olea, F. Wilkinson, *J. Phys. Chem.* **1995**, *99*, 4518-4524; b) C. Pierlot, S. Hajjam, C. Barthélémy, J.-M. Aubry, *J. Photochem. Photobiol., B* **1996**, *36*, 31-39.

[48] a) H. Shi, P. J. Sadler, *Br. J. Cancer* **2020**, *123*, 871-873; b) L. K. Mckinzie, H. E. Bryant, J. A. Weinstein, *Coord. Chem. Rev.* **2018**, *379*, 2-29.

[49] a) P. I. Djurovich, D. Murphy, M. E. Thompson, B. Hernandez, R. Gao, P. L. Hunt, M. Selke, *Dalton Trans.* **2007**, 3763–3770; b) C. Mari, H. Huang, R. Rubbiani, M. Schulze, F. Würthner, H. Chao, G. Gasser, *Eur. J. Inorg. Chem.* **2017**, 1745–1752.

[50] a) S. Swavey, K. Morford, M. Tsao, K. Comfort, M. K. Kilroy, *J. Inorg. Biochem.* **2017**, *175*, 101-109, b) C. S. Gutsche, S. Gräfe, B. Gitter, K. J. Flanagan, M. O. Senge, N. Kulak, A. Wiehe, *Dalton Trans.* **2018**, *47*, 12373-12384.

[51] a) B. F. O. Nascimento, S. M. M. Lopes, M. Pinero, T. M. V. D. Pino e Melo, *Molecules* **2019**, *24*, 4348; b) C. Brückner, J. J. Posakony, C. K. Johnson, R. W. Boyle, B. R. Boyle, B. R. James, D. Dolphin, *J. Porphyrins Phthalocyanines* **1998**, *2*, 455-465; c) C.-H. Lee, S. J. Lindsey, *Tetrahedron* **1994**, *50*, 11427-11440.

[52] H. R. A. Golf, H.-U. Reissig, A. Wiehe, *Org. Lett.* **2015**, *17*, 982-985.

[53] J. P. Nargakatti, K. R. Ashley, *Synthesis* **1974**, 186-187.

[54] N. A. M. Pereira, T. M. V. D. Pino e Melo, *Org. Prep. Proced. Int.* **2014**, *46*, 183-213.

[55] B. J. Littler, M. A. Miller, C.-H. Hung, R. W. Wagner, D. F. O'Shea, P. D. Boyle, J. S. Lindsey, *J. Org. Chem.* **1999**, *64*, 1391-1396.

[56] a) J. S. Lindsey, *Acc Chem. Rev.* **2010**, *43*, 300-311; b) B. Temelli, C. Unaleroglu, *Tetrahedron* **2006**, *62*, 10130-10135; c) P. Thamyongkit, A. D. Bhise, M. Taniguchi, J. S. Lindsey, *J. Org. Chem.* **2006**, *71*, 903-910.

[57] R. Naik, P. Joshi, S. P. Kaiwar (nee Vakil), R. K. Deshpande, *Tetrahedron* **2003**, *59*, 2207-2213.

[58] A. Singhal, S. Singh, S. M. S. Chauhan, *ARKIVOC* **2016**, *6*, 144-151.

[59] J. K. Laha, S. Dhanalekshmi, M. Taniguchi, A. Ambrosie, J. S. Lindsey, *Org. Process Res. Dev.* **2003**, *7*, 799-812.

[60] a) R. Sakamoto, T. Iwashima, M. Tsuchiya, R. Toyoda, R. Matsuoka, J. F. Kögel, S. Kusaka, K. Hoshiko, T. Yagi, T. Nagayama, H. Nishihara, *J. Mater. Chem. A* **2015**, *3*, 15357-15371; b) C. Brückner, Y. Zhang, S. J. Rettig, D. Dolphin, *Inorg. Chim. Acta* **1997**, *263*, 279-286; c) R. S. Shikha, R. P. Paitandi, R. K. Gupta, D. S. Pandey, *Coord. Chem. Rev.* **2020**, *414*, 213269.

[61] S. A. Baudron, *Dalton Trans.* **2020,** *49*, 6161-6175.

[62] a) C. Brückner, V. Karunaratne, S. J. Rettig, D. Dolphin, *Can. J. Chem.* **1996**, *74*, 2182-2193; T. E. Wood, A. Thompson, *Chem. Rev.* **2007**, *10*, 1831-1861; b) A. Thompson, S. Bennett, H. M. Gillis, T. E. Wood, *J. Porphyrins Phthalocyanines* **2008**, *12*, 918-931; c) A. Ikezaki, M. Nakamura, S. Neya, Tetrahedron, 2019, 75, 1563-1568; d) N. Boens, B. Verbelen, M. J. Ortiz, L. Jiao, W. Dahaen, *Coord. Chem. Rev.* **2019**, *399*, 213024.

[63] a) S. R. Halper, S. M. Cohan, *Chem. Eur. J.* **2003**, *9*, 4661-4669; b) A. A.-S Ali, J. Cipot-Wechsler, S. M. Crawford, O. Selim, R. L. Stoddard, S. T. Cameron, A, Thompson, *Can. J. Chem.* **2010**, *88*, 725-735.

[64] a) R. Beckert, E. Fänghanel, W. Habicher, H.-J. Knölker, P. Metz, K. Schwetlick, *Organikum*, Wiley-VCH: Weinheim Germany, **2009**, 445-446; b) M. T. Huynh, C. W. Anson, A. C. Cavell, S. S. Stahl, S. Hammes-Schiffer, *J. Am. Chem. Soc.* **2016**, *138*, 15903-15910; c) A. E. Wendlandt, S. S. Stahl, *Angew. Chem. Int. Ed.* **2015**, *49*, 14638-14658, *Angew. Chem.* **2015**, *127*, 14848-14868; d) J. H. P. Utley, G. G. Rozenberg, *J. Appl. Electrochem.* **2003**, *33*, 525-532.

[65] a) D. Walker, J. D. Hiebert, *Chem. Rev.* **1967**, *67*, 153-195; b) H. H. Jung. P. E. Floreancig, *Tetrahedron* **2009**, *65*, 10830-10836; c) P. P. Fu, R. G. Harvey, *Chem. Rev.* **1978**, *78*, 317-361.

[66] H. Fischer, M. Schubert, *Ber. Dtsch. Chem. Ges.* **1924**, *57*, 610-617.

[67] a) J. R. Storck, V. S. Thoi, S. M. Cohen, *Inorg. Chem.* **2007**, *46*, 11213-11223; b) R. P. Paitandi, R. S. Singh, S. Mukhopadhyay, G. Sharma, B. Koch, P. Vishnoi, D. S. Pandey, *Inorg. Chim. Acta* **2017**, *454*, 117-127; c) K. Hanson, A. Tamayo, V. V. Diev, M. T. Whited, P. I. Djurovich, M. E. Thompson, *Inorg. Chem.* **2010**, *49*, 6077-6084; d) A. Loudet, K. Burgess, *Chem. Rev.* **2007**, *107*, 4891-4932.

[68] a) F. C. March, D. A. Couch, K. Emerson, J. E. Fergusson, W. T. Robinson, *J. Chem. Soc. A* **1971**, 440-448; b) M. Elder, B. R. Penfold, *J. Chem. Soc. A* **1969**, 2556-2559; c) A. Béziau, S. A. Baudron, A. Fluck, M. W. Hosseini, *Inorg. Chem.* **2013**, *52*, 14439-14448.

[69] S. M. Cohan, S. R. Halper, *Inorg. Chim. Acta* **2002**, *341*, 12-16.

[70] a) D. Ramlot, M. Rebarz, L. Volker, M. Ovaere, D. Beljonne, W. Dahaen, L. Van Meervelt, C. Moucheron, A. K.-De Mesmaeker, *Eur. J. Inorg. Chem.* **2013**, 2031-2040; b) M. Yadav, A. K. Singh, B. Maiti, D. S. Pandey, *Inorg. Chem.* **2009**, *48*, 7593-7603; c) M. Yadav, A. K. Singh, D. S. Pandey, *Organometallics* **2009**, *28*, 4713-4723; d) S. J. Smalley, M. R. Waterland, S. G. Telfer, *Inorg. Chem.* **2009**, *48*, 13-15.

[71] R. Sakamoto, T. Iwashima, J. F. Kögel, S. Kusaka, M. Tsuchiya, Y. Kitagawa, H, Nishihara, *J. Am. Chem. Soc.* **2016**, *138*, 5666−5677.

[72] G. Li, L. Ray, E. N. Glass, K. Kovnir, A. Khoroshutin, S. I. Gorelsky, M. Shatruk, *Inorg. Chem.* **2012**, *51*, 1614–1624.

[73] a) A. Kochem, L. Chiang, B. Baptiste, C, Philouze, N. Leconte, O. Jarjayes, T, Storr, F. Thomas, *Chem. Eur. J.* **2012**, *18*, 14590-14593; b) L. Lecarme, L. Chiang, J. Moutet, N. Leconte, O. Jarjayes, T, Storr, F. Thomas, *Dalton Trans.* **2016**, *45*, 16325-16334; c) Y. Baek, T. A. Betley, *J. Am. Chem. Soc.* **2019**, *141*, 7797-7806; d) C. Kleinlein, S.-L. Zheng, T. A. Betley, *Inorg. Chem.* **2017**, *56*, 5892-5901; e) M. Saikawa, M. Diacho, T. Nakamura, J. Uchida, M. Yamamura, T. Nabeshima, *Chem. Commun.* **2016**, *52*, 4014-4017.

{74] a) N. Sakamoto, C. Ikeda, M. Yamamura, T. Nabeshima, *J. Am. Chem. Soc.* **2011**, *133*, 4726-4729; b) M. Yamamura, M. Albrecht, M. Albrecht, Y. Nishimura, T. Arai, T. Nabeshima, *Inorg. Chem.* **2014**, *53*, 1355-1360.

[75] a) C. Bronner, S. A. Baudron, M. W. Hosseini, *Inorg. Chem.* **2010**, *49*, 8659-8661; b) R. Matsuoka, T. Nabeshima, *Front. Chem.* **2018**, *6*, 349; c) N. Singh, J.-H. Jo, Y. H. Song, H. Kim, M. S. Lah, K.-W. Chi, *Chem. Commun.* **2015**, *51*, 4492-4495; d) R. P. Paitandi, S. Mukhopadhyay, R. P. Singh, V. Sharma, S. M. Mobin, D. S. Pandey, *Inorg. Chem.* **2017**, *56*, 12232-12247; d) C. Bronner, M. Veiga, A.Guenet, L. De Cola, M. W. Hosseini, C. A. Strassert, S. A. Baudron, *Chem. Eur. J.* **2012**, *18*, 4041-4050; e) M. Pernot, T. Bastogne, N. P. E. Barry, B. Therrien, G. Koellenspergere, S. Hann, V. Reshetov, M. Barberi-Heyob, *J. Photochem. Photobiol., B* **2012**, *117*, 80-89; f) J. Zhao, X. Zhang, L. Fang, C. Gao, C. Xu, S. Gou, *Small* **2020**, *16*, 2000363; g) J. Karges, O. Blacque, H. Chao, G. Gasser, *Inorg. Chem.* **2019**, *58*, 12422-12432.

[76] J. Sun, W. Wu, J. Zhao, *Eur. J. Inorg. Chem.* **2011**, 3165-3173.

[77] a) R. K. Gupta, A. Kumar, R. P. Paitandi, R. S. Singh, S. Mukhopadhyay, S. P. Verma, P. Das, D. S. Pandey, *Dalton Trans.* **2016**, *45*, 7163-7177; b) R. K. Gupta, G. Sharma, R. Pandey, A. Kumar, B. Koch, P.-Z. Li, Q. Xu, D. S. Pandey, *Inorg. Chem.* **2013**, *52*, 13984-13996.

[78] J. Karges, U. Basu, O. Blacque, H. Chao, G. Gasser, *Angew. Chem. Int. Ed.* **2019**, *58*, 14334-14340, *Angew. Chem.* **2019**, *131*, 14472-14478.

[79] G. Ulrich, R. Ziessel, A. Harriman, *Angew. Chem. Int. Ed.* **2008**, *47*, 1184-1201, *Angew. Chem.* **2008**, *120*, 1202-1219.

[80] H. Lu, J. Mack, Z. Chen, *Chem. Soc. Rev.* **2014**, *43*, 4778-4823.

[81] L. Wang, B. Verbelen, C. Tonnelé, D. Beljonne, R. Lazzaroni, V. Leen, W. Dahaen, N. Boens, *Photochem. Photobiol. Sci.* **2013**, *12*, 835-847.

[82] A. Treibs, F. H. Kreuzer, *Liebigs Ann. Chem.* **1968**, *718*, 208-223.

[83] J. S. Lindsey, R. W. Wagner, *Pure & Appl. Chem.* **1996**, *68*, 1373-1380.

[84] B. Guo, X. Peng, A. Cui, Y. Wu, M. Tian, L. Zhang, X. Chen, Y. Gao, *Dyes and Pigm.* **2007**, *73*, 206-210.

[85] Y. Ni, J. Wu, *Org. Biomol. Chem.* **2014**, *12*, 3774-3791.

[86] S. A. Baudron, *CrystEngComm* **2016**, *18*, 4671-4680.

[87] A. Bessette, G. S. Hanan, *Chem. Soc. Rev.* **2014**, *43*, 3342-3405.

[88] M. Benstead, G. H. Mehl, R. W. Boyle, *Tetrahedron* **2011**, *67*, 3573-3601.

[89] a) A. Kamkaew, S. H. Lim, H. B. Lee, L. V. Kiew, L. Y. Chung, K. Burgess, *Chem. Soc. Rev.* **2013**, *42*, 77-88; b) S.G. Awuah, Y, You, *RSC Adv.* **2012**, *2*, 11169-11183.

[90] a) E. Fron, E. Coutiño-Gonzalez, L. Pandey, M. Sliwa, M. Van der Auweraer, F. C. De Schryver, J. Thomas, Z. Dong, V. Leen, M. Smet, W. Dehaen, T. Vosch, *New J. Chem.* **2009**, *33*, 1490-1496; b) N. Epelde-Elezcano, V. Martínez-Martínez, E. Peña-Cabrera, C. F. A. Gómez-Durán, I. López-Arbeloa, S. Lacombe, *RSC Adv.* **2016**, *6*, 41991-41998.

[91] a) X.-F. Zhang, X. Yang, *J. Phys. Chem. B* **2013**, *117*, 5533–5539; b) J. Zou, Z. Yin, K. Ding, Q. Tang, J. Li, W. Si, J. Shao, Q. Zhang, W. Huang, X. Dong, *ACS Appl. Mater Interfaces* **2017**, *9*, 32475-32481; c) M. J. Ortiz, A. R. Agarrabeitia, G. Duran-Sampedro, J. B. Prieto, T. A. Lopez, W. A. Massad, H. A. Montejano, N. A.García, I. López-Arbeloab, *Tetrahedron* **2012**, *68*, 1153-1162; d) S. R. Martinez, Y. B. Palacios, D. A. Heredia, M. L. Maximiliano, A. M. Durantini, *ACS Infect. Dis.* **2019**, *5*, 1624-1633.

[92] a) M. A. Filatov, S. Karuthedath, P. M. Polestshuk, S. Callaghan, K. J. Flanagan, T. Wiesner, F. Laquai, M. O. Senge, *ChemPhotoChem* **2018**, *2*, 606-615; b) W. Hu, X.-F. Zhang, X. Lu, S. Lan, D. Tian, T. Li, L. Wang, S. Zhao, M. Feng, J. Zhang, *Dyes Pigm.* **2018**, *149*, 306-314; Y. Yang, Q. Guo, H. Chen, Z. Zhou, Z. Guo, Z. Shen, *Chem. Commun.* **2013**, *49*, 3940-3942.

[93] a) M. Makosza, *Russ. Chem. Bull.* **1996**, *45*, 491-504; b) F. Pietra, *Q. Rev., Chem. Soc.* **1969**, *23*, 504-521.

[94] O. N. Chupakhin, V. N. Charushin, *Tetrahedron Lett.* **2016**, *57*, 2665-2672.

[95] J. Kvíčala, M. Beneš, O. Paleta, V. Král, *J. Fluorine Chem.* **2010**, *131*, 1327-1337.

[96] a) H. R. A. Golf, H.-U. Reissig, A, Wiehe, *Eur. J. Org. Chem.* **2015**, 1548-1568; b) T, Bříza, R. Kaplánek, M. Havlík, B. Dolenský, Z. Kejík, P. Martásek, V. Král, *Supramol. Chem.* **2008**, *20*, 237-242; c) M. H. Beyzavi, D. Lentz, H.-U. Reissig, A. Wiehe, *Chem. Eur. J.* **2013**, *19*, 6203-6208; d) S. J. Shaw, K. J. Elgie, C. Edwards, R. W. Boyle, *Tetrahedron Lett.* **1999**, *40*, 1595-1596; e) Y. Tian, B. R. Shumway, D. R. Meldrum, *Chem. Mater.* **2010**, *22*, 2069-2078.

[97] a) Y. Volkova, B. Brizet, P. D. Harvey, F. Denat, C. Goze, *Eur. J. Org. Chem.* **2014**, 2268-2274; b) B. Chandrakantha, A. M. Isloor, P. Shetty, H. K. Fun, G. Hedge, *Eur. J. Med. Chem.* **2014**, *7*, 316-323.

[98] a) E. E. Kwan, Y. Zeng, H. A. Besser, E. N. Jacobsen, *Nat. Chem.* **2018**, *10***,** 917-923; b) J. H. Stenlid, T. Brinck, *J. Org. Chem.* **2017**, *82*, 3072-3083.

[99] B. F. Hohlfeld, Master Thesis, Freie Universität Berlin, 2015.

[100] a) F. Lv, B. Tang, E. Hao, Q, Liu, H. Wang, L. jiao, *Chem. Commun.* **2019**, *55*, 1639-1642; b) G. F. A. Gómez-Durán, I. Esnal, I. Valois-Escamilla, A. Urias-Benavidas, J. Bañuelos, I. López-Arbeloa, I. Garcia-Moreno, E. Peña-Cabrera, *Chem. Eur. J.* **2016**, *22*, 1048-1061; c) V. Lakshmi, M. R. Rao, M. Ravikanth, *Org. Biomol. Chem.* **2015**, *13*, 2501-2517; d) T. Rohand, M. Buruah, W. Qin, N. Boens, W. Dahaen, *Chem. Commun.* **2006**, 266-268; e) J. Wang, Q. Wu, Q, Gong, K. Cheng, Q. Liu, C. Yu, E, Hao, L. Jiao, *Adv. Synth. Catal.* **2019**, *361*, 769-777.

[101] V. Leen, V. Z. Gonzalvo, W. M. Deborggraeve, N. Boens, W. Dehaen, *Chem. Commun.* **2010**, *46*, 4908-4910.

[102] G. Vives, C. Giansante, R. Bofinger, G. Raffy, A. Del Guerzo, B. Kauffmann, P. Batat, G. Jonusauskas, N. D. McClenaghan, *Chem. Commun.* **2011**, *47*, 10425-10427.

[103] a) M. Pal, K. Parasuraman, K. R. Yeleswarapu, *Org. Lett.* **2003**, *5*, 349-352; b) S. Chandrasekhar, C.R. Reddy, R. J. Rao, *Tetrahedron* **2001**, 3435-3438; c) J. Wang, F. Li, W. Pei, M. Yang, Y. Wu, D. Ma, F. Zhang, J. Wang, *Tetrahedron Lett.* **2018**, *59*, 1902-1905.

[104] X. Liu, H. Nan, W. Sun, Q. Zhang, M. Zhan, L. Zou, Z. Xie, X. Li, C. Lu, Y. Cheng, *Dalton Trans.* **2012**, *41*, 10199-10210.

[105] J. A. Melanson, D. A. Smithen, T. S. Cameron. A. Thompson, *Can. J. Chem.* **2014**, *92*, 688-694.

[106] C. S. Gutsche, Doctoral Thesis, Freie Universität Berlin, **2018**.

[107] a) B. Bertrand, K. Passador, C. Goze, F. Denat, E. Bodio, M. Selmain, *Coord. Chem. Rev.* **2018**, *358*, 108-124; b) N. Zhao, T. M. Williams, Z. Zhou, F. R. Fronczek, M. Sibrian-Vazquez, S. D. Jois, M. G. H. Vicente, *Bioconjugate Chem.* **2017**, *28*, 1566-1579; c) C. Uriel, C. Permingeat, J. Ventura, E. Avellanal-Zaballa, J Bañuelos, I. García-Moreno, A. M. Gómez, J. C. Lopez, *Chem. Eur. J.* **2020**, *26*, 5388-5399; d) J. Jiménez, R. Prieto-Montero, B. L. Maroto, F. Moreno, M. J. Ortiz, A. Oliden-Sánchez, I. López-Arbeloa, V. Martínez-Martínez, S. de la Moya, *Chem. Eur. J.* **2020**, *26*, 601-605.

[108] N. Maindron, M. Ipuy, C. Bernhard, D. Lhenry, M. Moreau, S. Carme, A. Oudot, B. Collin, J.-M. Vrigneaud, P. Provent, F. Brunotte, F. Denat , C. Goze, *Chem. Eur. J.* **2016**, *22*, 12670-12674.

[109] a) J. Shu, W. S. Chei, *Curr. Opin. Chem. Biol.* **2008**, *12*, 207-213; b) C.S. Rossiter, R. A. Mathews, J. R. Morrow, *Inorg. Chem.* **2005**, *44*, 9397-9404; c) J. Hormann, C. Perera, N. Deibel, D. Lentz, B. Sarkar, N. Kulak, *Dalton Trans.* **2013**, *42*, 4357-4360; d) T. Zhang, X. Zhu, R. Prabhakar, *Organometallics* **2014**, *33*, 1925-1935; e) J. Hormann, M. van der Meer, B. Sarkar, N. Kulak, *Eur. J. Inorg. Chem.* **2015**, 4722-4730.

[110] a) J. K. Molly, O. Kotova, R. D. Peacock, T. Gunnlaugson, *Org. Biomol. Chem.* **2012**, *10*, 314-322; b) M. Jauregui, W. S. Perry, C. Allain, L. R. Vidler, M. C. Willis, A. M. Kenwright, J. S. Snaith, G. J. Stasiuk, M. P. Lowe, S. Faulkner, *Dalton Trans.* **2009**, 6283-6285; c) L. M. Seebald, C. M. DeMott, S. Ranganathan, P. N. A. Okai, A. Glazunova, A. Chen, A. Shekhtman, M. Royzen, *Inorg. Chem.* **2017**, *56*, 3773-3780; d) A. K. R. Junker, M. Tropiano, S. Faulkner, T. J. Sørensen, *Inorg. Chem.* **2016**, *55*, 12299-12308.

[111] a) R. Berg, B. F. Straub, *Beilstein J. Org. Chem.* **2013**, *9*, 2715-2750; b) B. Schulze, U. S. Schubert, *Chem. Soc. Rev.* **2014**, *43*, 2522-2571.

[112] Y. Gabe, T. Ueno, Y. Urano, H. Kijima, T. Nagano, *Anal. Bioanal. Chem.* **2006**, *386*, 621-626.

[113] A. K. Mishra, J.-F. Chatal, *New J. Chem.* **2001**, 25, 336-339.

[114] M. A. Bennett, T. N. Huang, T. W. Matheson, A. K. Smith, S. Ittel, W. Nickeerson, *Inorg. Synth.* **1982**, *21*, 74-78.

[115] C. White, A. Yates, P. M, Maitlis, D. M. Heinekey, *Inorg. Synth.* **1992**, *29*, 228-234.

[116] S. Chen, X. Liu, X. Ge, Q. Wang, Y. Xie, Y. Hao, Y. Zhang, L. Zhang, W. Shang, Z. Liu, *Inorg. Chem. Front.* **2020**, *7*, 91-100.

Curriculum Vitae

For reasons of data protection, not included in the online version.